

APC/C Activity during the Cell Cycle

Shifting gears in protein degradation

Michiel Boekhout

COVER

The cover shows the cassette and chain of a bicycle, which allow for shifting gears, so that even uphill or cycling against the wind, you can keep moving forward. As this thesis describes part of the cell cycle, the comparison to a bicycle is easily made, and this also fits to the different speeds, or different gears if you will, at which proteins are degraded throughout the cell cycle.

The research described in this thesis was performed at the division of Molecular Carcinogenesis and the division of Cell Biology I of the Netherlands Cancer Institute – Antoni van Leeuwenhoek (NKI-AvL), Amsterdam, the Netherlands. The layout and printing of this book were financially supported by the Netherlands Cancer Institute.

ISBN: **XXXX**

Printed & Lay Out by: Proefschriftmaken.nl || Uitgeverij BOXPress
Published by: Uitgeverij BOXPress, 's-Hertogenbosch

Copyright 2015, Michiel Boekhout

APC/C Activity during the Cell Cycle

Shifting gears in protein degradation

Activiteit van de APC/C tijdens de cel cyclus

Snelheidsveranderingen in eiwit afbraak

(met een samenvatting in het Nederlands)

Proefschrift

ter verkrijging van de graad van doctor aan de Universiteit Utrecht op gezag van de rector magnificus, prof. dr. G.J. van der Zwaan, ingevolge het besluit van het college voor promoties in het openbaar te verdedigen op maandag 14 september 2015 des middags te 2.30 uur

door

Michiel Boekhout

geboren op 24 maart 1985 te Leiden

Promotor: Prof.dr. R.A. Bernards

Copromotor: Dr. R.M.F. Wolthuis

TABLE OF CONTENTS

| | | |
|------------------|--|-----|
| Chapter 1 | General Introduction | 7 |
| Chapter 2 | Nek2A destruction marks APC/C activation at the prophase-to prometaphase transition by spindle-checkpoint-restricted Cdc20 | 29 |
| Chapter 3 | Dynamic Instability of Nek2A in G2 Phase Requires APC/CCdh1 | 59 |
| Chapter 4 | Feedback regulation between atypical E2Fs and APC/CCdh1 controls the G1/S phase transition | 77 |
| Chapter 5 | Cyclostop, a non-degradable APC/C-binding Emi1 fragment that blocks cells in mitosis independently of the mitotic checkpoint | 101 |
| Chapter 6 | General Discussion | 125 |
| Appendix | References | 142 |
| | Nederlandse Samenvatting | 163 |
| | English Summary | 167 |
| | Dankwoord | 171 |
| | Curriculum Vitae | 177 |
| | List of Publications | 178 |

CHAPTER 1

The Anaphase Promoting Complex, the behemoth of ubiquitination

Michiel Boekhout & Rob Wolthuis

INTRODUCTION

For successful propagation of life, each cell need to divide and correctly duplicate, leading to the creation of two identical daughter cells. To this end, all the genetic material has to be replicated flawlessly, as well as the intracellular organelles and cellular contents including mRNA, proteins and all other macro-molecular complexes that need to be distributed to both daughter cells. This can be divided in several stages, namely **G1** (gap1 phase), in which cells prepare for **S-phase** (DNA synthesis phase) during which the chromosomes are duplicated so that there are two identical chromosome sisters for each chromosome, followed by **G2** (gap2 phase). After G2 the cells enter the **M-phase** (mitosis), a short but dramatic phase, during which cells hyper-condense their DNA into their characteristic chromosomal shape and breakdown the nucleus. The cell completely rounds up, and all chromosomes line up in the middle of the cell and become correctly attached to the mitotic spindle. The mitotic spindle is constructed from microtubule polymers, which connect to a structure known as the kinetochore in middle of the chromosomes, to the spindle poles at opposite sides of the mitotic cell. The spindle poles are the structure from which the microtubules radiate, and of which the microtubules that become correctly attached to the kinetochore are stabilized. After all pairs of identical sister chromatids, together forming the chromosome, are both attached to the microtubules originating from the opposite spindle poles, the proteins that keep them together are dissolved and the chromatids are separated through the pulling forces exerted by the mitotic spindle. The single sisters become incorporated in the forming nucleus establishing the full genome of the new daughter cell. Mitosis is finalized by cytokinesis in which the outer membrane of the mother cell is constricted, followed by abscission, leading to the creation of two genetically identical daughter cells.

To ensure effective and safe continuation of the cell cycle, multiple sophisticated checkpoints have evolved. Cells have to move from one phase to the next without the risk of going back or becoming stuck. One mechanism to ensure this is to eliminate the factors responsible for these transitions, after the transition has taken place. A simplified view identifies proteins, encoded for by genes on the DNA, as one of the major executors, as well as regulators, of cell cycle progression. To get rid of proteins, in a regulated manner, an intricate system is in place, in which they are modified by the addition of ubiquitin marks, signaling their destruction. More specifically, polyubiquitin chains are formed: as on ubiquitin itself there are multiple sites for the addition of yet another ubiquitin, giving rise to the possibility of multibranching destruction signals. Ubiquitin is transferred unto a target protein by a series of specialized enzymes, which act consecutively. These are the E1-activating, E2-conjugating enzymes and the E3 ubiquitin ligases (**Fig. 1**). While there are only two E1 enzymes¹, several dozen of E2 enzymes exist, while several hundred E3 enzymes are encoded in the genome².

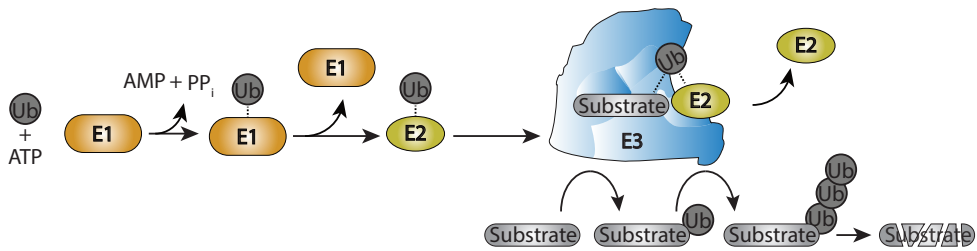


Figure 1 Ubiquitination pathway of RING E3 ubiquitin ligases

In a first ATP dependent step, ubiquitin is activated and bound to the E1 enzyme. Subsequently, the E1 ubiquitin activating enzyme transfers ubiquitin in a trans thiol reaction to the active site cysteine of an E2 conjugating enzyme. The E2 enzyme binds to the E3 RING ubiquitin ligase, serving as a platform between E2 and substrate. The E3 RING domain directs the ubiquitin from the E2 to a lysine in the substrate protein. Although only a single ubiquitin site is depicted, substrates are likely to receive ubiquitin moieties on separate lysines. Multiple ubiquitination reactions on the same substrate lead to the formation of polyubiquitin chains.

This thesis centers around one particular E3 enzyme, the Anaphase-Promoting Complex/Cyclosome (APC/C), responsible for the rapid destruction of a plethora of different proteins at specific times, which is essential for cell cycle progression.

THE ANAPHASE PROMOTING COMPLEX / CYCLOSOME

The APC/C is a huge E3 ubiquitin ligase composed of 19 subunits, consisting of 14 distinct proteins, creating a 1.2 mDa complex³ (**Fig. 2**). While named for its requirement to help cells to progress from metaphase to anaphase^{4,5}, it has become clear that the APC/C targets a multitude of proteins for destruction also during other phases of the cell cycle. While (cryo)EM studies of endogenous APC/C gave initial insight into its structure^{6,7}, recently developed systems that allow for recombinant expression of clusters of subunits have been developed⁸, which show in detail the APC/C composition and conformational changes it undergoes upon activation^{9–12}. Clearly, recent contributions made by structural biologists have greatly increased insight into regulation and functioning. The fascination for the APC/C is reflected by the numerous reviews in the past decade that discuss it^{13–22}. Here, we will follow the general nomenclature to describe its different forms, in the compositions in which they are thought to be present in the cell. The bare complex itself is known as the ‘apo-APC/C’, but when bound to an activator (discussed below) the complex is referred to as APC/C^{Cdc20} or APC/C^{Cdh1}. The APC/C can also be bound by inhibitors, indicated as APC/C^{MCC} and APC/C^{Emi1}.

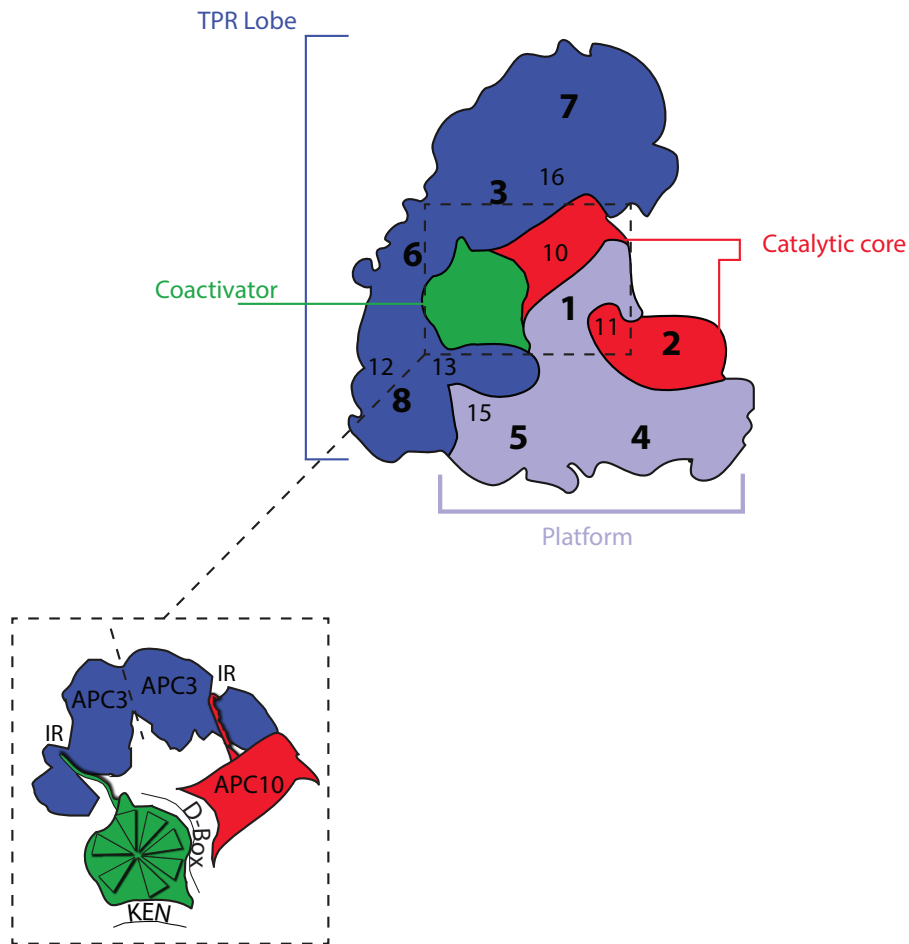


Figure 2 Overview of APC/C structural organization of APC/C bound to activator.

In dark blue the TPR lobe, in light blue the APC/C platform and the catalytic core is depicted in red. The activator shown in green. The inset shows zoom-in of current understanding of the IR tails of the activator and APC10, binding to separate APC3 subunits which are present as a dimer in the complex. The D-box is recognized by the receptor formed between APC10 and the activator, while the KEN box is recognized separately.

Adapted from Barford 2011²³ and Chang and Barford 2014³.

Probably the two most famous substrates targeted for destruction by the APC/C are securin and cyclin B. Securin is an inhibitor of anaphase, that must be degraded to allow activation of separase, an enzyme that cleaves cohesion which holds the sister chromatids together, and Cyclin B1, when in an active complex with Cdk1, is an inhibitor of mitotic exit. Cyclin B1 must be degraded to synchronize sister chromatid separation with cytokinesis. However, many more APC/C substrates have been discovered, and the list is probably not yet complete.

STRUCTURE AND FUNCTION

The size and complexity of the APC/C made it difficult to study the role and nature of individual subunits. However, while the specific role of the different subunits is not always clear, the complex can roughly be divided in three sub-complexes^{3,23}; i) the platform, ii) the TPR lobe (or “arc lamp”) and iii) the catalytic core (**Fig. 2** and **Table 1**). The platform consists of subunits APC1, APC4, APC5 and the smaller subunit APC15. The TPR lobe is named after the TPR (34 residue tetra-tricopeptide repeats) domains found in multiple of its subunits and is made up of: APC7, APC3, APC6, APC8 and the smaller subunits APC16, APC13 and Cdc26 (also called APC12). Of these, at least APC3, APC6 and APC8 are incorporated in the APC/C as homodimers. Finally, the catalytic core consists of the APC2 cullin like subunit, the APC11 RING containing subunit and APC10. These are at the apex of the complex²⁴, and are the subunits responsible for conferring enzymatic E3 ubiquitin ligase activity.

Indeed, APC2 recruits APC11 as part of the APC/C⁷. Together, APC2 and APC11 are sufficient to drive ubiquitination *in vitro*, if E1 and E2 enzymes are provided, although they show no substrate specificity^{24–26}. APC2 and APC11 are flexible proteins in terms of their structures, making it difficult to analyze them by crystallography, and this likely reflects their adaptability to different substrates¹². APC10 contacts APC2 on the C-terminal domain (CTD)^{7,10}, and plays a pivotal role in recognizing substrates by their APC/C specific motifs (described below).

The APC/C itself is subject to regulation, as it is phosphorylated when active²⁷. These phosphorylations probably act twofold; they enhance intrinsic activity^{28–30}, but surely also enhance recruitment of certain substrates, at the very least cyclin B, via recognition of phosphorylations on the APC3 subunit mediated by Cks1^{31,32}.

Table 1 APC/C subunits and sub complexes

| Sub complex | Large APC/C subunits | Small APC/C subunits |
|---|----------------------|----------------------|
| Platform | 1, 4, 5 | 15 |
| TPR Lobe | 3, 6, 7, 8 | 12, 13, 16 |
| Catalytic Core | 2 | 10, 11 |
| Adapted from Frye <i>et al.</i> 2013, Chang <i>et al.</i> 2014. | | |

Depicted are the 3 sub-complexes of the APC/C and the subunits they consist of. The large subunits are 65kD or more, Apc1 is exceptionally large at 216kD, the smaller subunits are smaller than 15kD, except APC10 (21kD). See also Chang and Barford 2014³.

THE ACTIVATORS, ENABLING ANNIHILATION

Regardless of its large size, the APC/C is critically dependent on either one of two activator proteins Cdc20 or Cdh1 in cells for activity^{27,33}. It has become clear that the role of these activators is at least twofold; they recognize motifs in substrates and thereby play a role in recruiting or retaining them on the APC/C, but secondly they can also directly activate the APC/C, by inducing a conformational change^{6,12}. This is probably also brought about by enabling the E2 enzymes access to the substrate³³⁻³⁷.

Cdh1 and Cdc20 are homologues and thus they have an overall similar protein composition: N-terminally they contain a C-Box [DR X/F IP X R]³⁸ followed by 7 WD-40 repeats, forming a circularized beta-propeller structure³⁹⁻⁴², and they both finish on the extreme C-terminus with an IR dipeptide as tail, shown to be important for binding to the APC/C^{43,44}. Specific for Cdc20 are the KEN box, MIM/KILR motif [KR][IV][LV]...[P] and the CRY box (**Fig. 3**).

The IR tail is required for both activators to allow functional binding to the APC/C. For Cdh1 multiple studies show that the IR tail binds to the Cdc27/APC3 subunit^{43,44}, between TPR8 and TPR9^{12,45}. Furthermore, Cdh1 becomes essential when *SIC1* (yeast homologue of Cdk1 inhibitor) is deleted^{133,34}, dependent on the presence of the IR tail⁴¹. Mutational analysis in budding yeast identified both APC8 (Cdc23) and APC3 (Cdc27) as direct interacting subunits of Cdh1, and the same APC/C mutants shows less induced activity by Cdc20 in vitro as well⁴⁶. Direct binding of the same site in APC8 was verified for Cdc20 in human cells⁴⁷, indicating that Cdc20 and Cdh1 in this respect are seemingly indistinguishable. Likely this represents binding via the C-box, which according to multiple lines of evidence plays a role in mediating direct binding

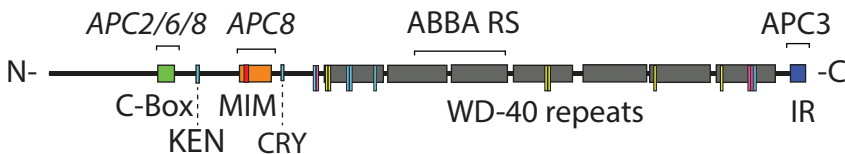


Figure 3 Cdc20 protein overview

Depicted are the known motifs interacting with the APC/C, the mitotic checkpoint proteins or motifs of the substrate. In green the C-box (77-83), the KEN motif (97-99), in orange the MIM (126-147) (Mad2 Interacting Motif), containing the KILR (129-132) motif. The CRY motif (165-167), the ABBA recognition site (ABBA RS) (240-300) at the second and third WD-40 repeat. Cdc20 ends in an IR tail (498-499). Amino acids indicated to recognize motifs in the substrate are depicted as follows: in yellow the amino acids for the KEN motif, in pink the amino acids recognizing the arginine (R) of the D-box motif, in cyan the amino acids recognizing leucine (L) of the D-box motif. Based on Chao *et al.* 2014⁵⁸ and He *et al.* 2013²³¹. See also table 2.

to the APC/C^{45,48–50}, although the APC/C subunit to which the C-box binds has not been identified beyond dispute. Binding assays in *Xenopus* egg extracts as well as with purified APC/C subunits from insect cells, and Cdc20 mutants, indicate that the C-box associates with APC6 and APC8⁵¹. Studies in yeast however suggest that the C-box does not bind APC8⁴⁵. APC3 has also been indicated to bind to the C-box⁴¹, while EM data suggests the Cdc20 binding partner could be APC2^{7,10}.

Functionally the C-box (which is identical in Cdc20 and Cdh1), may be able to activate the APC/C directly^{35,51}. It plays a role in retaining Cdc20 on the APC/C, when bound by checkpoint proteins⁴⁹. In vitro experiments using purified components show that the C-box greatly enhances the catalytic efficiency of Ube2S, approximately 175 fold, when measuring the resulting ubiquitination on substrates^{37,52}. Interestingly, mutational analysis shows that the C-box does not play a role in the recruitment of the E2 enzymes³⁷, but more likely is responsible for the conformational changes in the APC/C facilitating efficient polyubiquitination¹².

Besides catalyzing the activity of the APC/C, the WD-40 domains also may play a role in recognizing and retaining (ubiquitinated) substrates on the APC/C, to allow for further proteasomal targeting⁵³. Indeed, while substrates are able to bind either the activator or APC10 via a D-box motif, more detailed analysis shows that these are both required to form a bipartite D-box receptor^{41,45,54–58}.

Both activators are subject to phosphorylation, which prevents their activation of the APC/C. For Cdh1 this is mediated by CyclinE /Cdk2⁵⁹ and cyclin B1-Cdk1⁶⁰. Cdk-mediated phosphorylation prevents recruitment of Cdh1 to the APC/C. Similarly, inhibitory phosphorylations are placed on Cdc20 by Cdk1, or MAPK, leading to increased binding to Mad2^{61–63}. Indeed, dephosphorylation of activators is also a crucially regulated step required for full APC/C activity. Data from yeast shows that Cdc14 is a crucial phosphatase activated after checkpoint satisfaction to relieve Cdh1 phosphorylations and leading to full APC/C^{Cdh1} activity^{33,64}. More recently also dephosphorylation of Cdc20 has been shown to be necessary to activate the APC/C⁵¹.

While Cdc20 and Cdh1 overlap in both structure and function, they current dogma dictates they act exclusively on the APC/C. While Cdc20 is responsible for APC/C activation from the beginning of mitosis at least until the onset of anaphase, Cdh1 takes credit for destruction of APC/C substrates in all other phases of the cell cycle.

Cdh1

Cdh1 associates with the APC/C throughout the cell cycle, except for the beginning of mitosis, when it is held inactive via Cdk1 mediated phosphorylation, and replaced

by Cdc20. However, Cdh1 becomes active again shortly after metaphase, until the end of G1. In vitro Cdh1 shows no clear substrate specificity, however via its regulation, in cells, it is responsible for the destruction of a subset of proteins.

Cdh1 is not essential in either budding or fission yeast^{33,65}, but more recent work shows that Cdh1 loss leads to gross chromosomal rearrangements in budding yeast⁶⁶. Loss of Cdh1 leads to stabilization of Aurora kinases in mitotic exit⁶⁷⁻⁷⁰ and knockout of *Fzr1* is lethal in mice, due to genomic instability⁷¹. In the absence of Cdh1, it can be functionally replaced during mitotic exit by Cdc20, but Cdh1 is essential to allow for sufficient time in G1, so it can prevent premature entry into S-phase in certain cells^{72,73}. Multiple studies show indeed that Cdh1 plays a role not only during unperturbed cell cycle progression, but also in regulating the DNA damage response throughout interphase⁷³⁻⁷⁷ and in the prevention of replications stress⁷⁸.

Besides phosphorylations restraining Cdh1 activity, the protein Mad2L2 sequesters Cdh1 during prometaphase as an additional measure to prevent precocious APC/C activation, which could lead to unfaithful chromosome segregation⁷⁹. During mitosis, after the mitotic checkpoint is satisfied, loss of cyclin B-Cdk1 activity and simultaneous rise of phosphatase activity induce Cdh1 dephosphorylation^{41,80}, which unleashes Cdh1 to form an APC/C^{Cdh1} complex.

Cdc20

Cdc20 is the APC/C activator that is more confined in both its substrate specificity as well as in its temporal control. The gene encoding Cdc20 was already identified through yeast genetic screens 3 decades ago by mutants that arrest in mitosis and are defective of entering anaphase⁸¹ (and references therein). Cdc20 activates the APC/C from the earliest moment of prometaphase for a subset of substrates^{35,82,83} and degrades checkpoint-controlled substrates during and beyond metaphase after checkpoint satisfaction. The *Drosophila* homologue of Cdc20, *Fizzy*, is required for destruction of cyclins A and B⁸⁴, which also holds true for vertebrates, as loss of Cdc20 causes mitotic arrest in two cell mouse embryos⁸⁵. Depletion of Cdc20 by RNAi in human cells shows that it is essential for mitotic exit but also reveal that very low levels of Cdc20 protein are still sufficient for progression through mitosis^{86,87}. Part of the Cdc20 regulation comes from Cdk1-directed phosphorylation of TPR containing APC/C subunits^{27,88-91}, which stimulate Cdc20 recruitment. Conversely, phosphorylation of Cdc20 itself by Bub1^{92,93} and Cdk1⁶¹ plays an inhibitory role²⁷ as it has been implicated in increased binding to checkpoint proteins⁶¹, and prevents association to the APC/C^{51,92}.

A motif found exclusively in Cdc20 is the KILR motif, which is required to interact with Mad2 as well as the APC/C, and is therefore subject to competition between binding

partners⁴⁸. It is not clear where the KILR site directly binds, but data from human cells as well as from yeast point towards APC8^{45,47,48}.

Cdc20 protein levels are regulated in a complex manner. Both the KEN box⁹⁴ and the CRY box⁹⁵ (**Fig. 3**) are found in Cdc20, but not Cdh1, and are responsible for its degradation, mediated by the APC/C itself. While Cdc20 is captured in the MCC, it is constantly ejected from the APC/C by the Mnd2/APC15 subunit, which promotes autoubiquitination and checkpoint inactivation⁹⁶. Indeed, checkpoint proteins are required for Cdc20 degradation during mitotic delay, and ubiquitination of Cdc20 occurs via an intramolecular mechanism^{96–101}. Excess of Cdc20 can overcome the checkpoint, and prevents normal checkpoint functioning^{96,98}. This was also elegantly shown in fission yeast by doubling the small amount of Cdc20 that is normally present, which impaired the mitotic checkpoint¹⁰². Further strengthening the argument that Cdc20 needs to be turned over for a normal checkpoint response is the fact that lysine less Cdc20 overrides the checkpoint¹⁰³. Thus proteolysis of Cdc20 likely partially enforces checkpoint potency. The turnover of Cdc20, and also other checkpoint proteins is reviewed in more detail in several reviews^{21,104–106}.

THE INHIBITORS, CAGING THE BEAST

To ensure that the APC/C is only active at the right place and at the right time, at least two different inhibitory mechanisms are in place. From the end of G1 to the end of G2, Emi1 is expressed, a singular 50 kD protein, of which only the C-terminal 143 amino acids seem to be essential for APC/C inhibition. From the onset of mitosis to metaphase, the SAC (spindle assembly checkpoint), or mitotic checkpoint, is actively present, a 200 kD complex, termed the MCC, of which the formation, regulation and interactions are clearly very dynamic. Emi1 inhibits the APC/C^{Cdh1}, while the MCC inhibits APC/C^{Cdc20}.

Emi1

During S-phase and subsequent G2-phase the APC/C needs to be restrained to allow normal cell cycle progression. A specific F-box containing protein called Emi1 (early mitotic inhibitor) is responsible for blocking the APC/C during this time. Its transcription is driven by E2F¹⁰⁷ at the end of G1. Emi1 inhibits Cdh1, which is the APC/C activator during these cell cycle phases. While work in *Xenopus* showed potent inhibition of APC/C^{Cdc20}¹⁰⁸, in *Drosophila* Emi1/RCA1 specifically inhibits APC/C^{Cdh1}, and not APC/C^{Cdc20}^{109,110}. One possible explanation for this difference is that *Xenopus* eggs lack the Cdh1 protein, which may have resulted in subtle evolutionary changes and thus loss of Cdc20 inhibition. At this point, it remains controversial whether Emi1 can inhibit Cdc20^{108,111}, but its potent inhibition of Cdh1 is undisputed^{111,112}. Emi1

binds to the APC/C independently of activator^{112,113}, but also forms complexes with the activators^{107,108,114}, dependent on the D-box in Emi1.

Misregulation of Emi1 leads to multiple problems, including DNA re-replication, as cells will degrade Geminin and cyclin A forcing them to reenter S-phase^{111,115}. Mitotic defects have also been reported¹¹⁶, and are shown to be dependent on the failure to inhibit the APC/C¹¹⁷. Interestingly, remaining Emi1 is present at the spindle poles during mitosis, and this is suggested to lead to local inhibition of the APC/C¹¹⁸, although spatial regulation of APC/C functioning is not well characterized. A role for Emi1 in inhibiting the APC/C is well conserved among metazoans, as it was discovered in *Drosophila* to act as a regulator of cyclin A (RCA1)^{109,110}. Also loss of *harpy*, the zebrafish homologue of Emi1, leads to re-replication of the DNA in a manner that is dependent on APC/C activity, which is lethal early during gastrulation^{119,120}.

Three domains in the Emi1 protein play separate but cooperative roles in APC/C inhibition: a D-box, a zinc binding region (ZBR) domain and the C-terminal tail, that consists of an LRRL motif^{108,112,121}. These domains are also conserved in Emi2, an Emi1 homologue which plays a specific role in inhibiting the APC/C during meiosis^{122,123}. The role of the LRRL tail was first discovered for Emi2 for its role in APC/C inhibition during meiosis^{124,125}, but this small domain was also shown to be essential for the function of Emi1. The tail of Emi1 specifically targets the catalytic function of Ube2S, independently of blocking D-box mediated substrate recognition by APC10^{121,123} and thus interferes with ubiquitin chain elongation¹²⁶. However, it should be noted that in *in vitro* reactions, also the chain elongation preformed by UbcH10 was reduced, while monoubiquitination was not hampered¹²⁶. Furthermore, significant depletion of Ube2S by RNAi did not lead to any detectable mitotic defects (data not shown), indicating that eviction of Ube2S from the APC/C is not the main mechanism by which Emi1 inhibits the APC/C.

To alleviate Emi1 inhibition prior to mitosis, at least two mechanisms are in place. Phosphorylation by Plk1 on both serines in the DSGxxS motif^{127,128}, lead to recognition and ubiquitination of Emi1 by the the SCF ^{β -TRCP} E3 ubiquitin ligase¹¹⁷. SCF (Skp1-cullin-F box) is a ubiquitin ligase that depends on substrate recruitment by an F-box containing protein (such as β -TRCP), a process which often takes place in phosphorylation dependent manner. In mice, the two adaptor F-box proteins required for recognition by the SCF, β -TRCP1 and β -TRCP2, play non-redundant roles in Emi1 destruction¹¹⁶. Besides direct degradation, phosphorylation on Emi1 is also directly implicated in preventing it from inhibiting the APC/C¹²⁹, which could also explain why stabilizing Emi1 in prometaphase does not prevent cyclin A degradation¹³⁰.

In conclusion, multiple weak interactions between Emi1 and the APC/C synergize, which culminate in potent APC/C inhibition. Inhibitory proteins that use destruction motifs to function as ‘pseudo-substrates’, are likely a universal theme, because also non-homologous genes encoding for APC/C inhibitors employ KEN and D-boxes, such as Mes1 in fission yeast³⁵ or GIG1/OSD1 in Arabidopsis¹³¹. Mes1 and Gig1/OSD1 also both flaunt a C-terminal MR tail, and the latter also has been shown functional for APC/C binding.

The mitotic checkpoint

The checkpoint inhibits the onset of anaphase until all sister chromatids are correctly bi-orientated and attached with both their kinetochores to the mitotic spindle. In this manner genomic stability is ensured and two genetically identical daughter cells can be formed. The mitotic checkpoint was discovered in yeast by genetic screening^{132,133}, identifying the core components, the mitotic arrest deficient (Mad) and budding uninhibited by benomyl (Bub) proteins. Like the APC/C, the mode of action of the mitotic checkpoint has been extensively reviewed^{106,134,135}. While yeast strains deficient for checkpoint proteins are able to divide until they are challenged with spindle poisons, mice with a similar defect are not viable^{136,137}. The checkpoint complex in humans is a heterotetramer consisting of BubR1 (Mad3), Bub3, Mad2 and Cdc20. Cdc20 was originally identified as the target of the MCC^{138–140}. Mad2 interacts with the ‘Mad2 interaction motif’ (MIM) on Cdc20, that also encompasses the KILR motif^{148,141–143} (**Fig. 3**). BubR1 relies on two KEN boxes (KEN1 and KEN2), which are both required for Cdc20 binding and to form a functional checkpoint^{144–146}. Many other genes that are required for a functional mitotic checkpoint, rather play a role in the generation of the MCC, (Bub1, Mad1, RZZ complex), while not being part of the complex itself. These are often components of, or at least present at, kinetochores during mitosis, and are required for recruiting either upstream players or MCC proteins themselves. Certainly, an intimate relationship between kinetochores and the checkpoint exists. Classic laser ablation experiments indicated that the unattached kinetochores produce the “wait” signal delaying cell division, with a single unattached kinetochore being sufficient to delay the onset of anaphase¹⁴⁷. Moreover, recent experiments show that this response is not binary but continuous. While a single unattached kinetochore is sufficient to elicit checkpoint signaling, the checkpoint does not exert an ‘all or nothing’ response, but the strength of the signal is directly correlated to the amount of unattached kinetochores^{148,149}.

The kinetochores themselves are large protein complexes, consisting of more than 80 different proteins assembled on the centromeres. Centromeres are characterized by being enriched for the specialized histone variant CENP-A¹⁵⁰. Within the kinetochore several functional and structural sub-components have been identified^{151,152}. Briefly, the constitutive centromere associated network (CCAN)¹⁵³, recruits the KMN network¹⁵⁴,

which consists of KNL1, Mis12 and NDC80 complexes. Together, these form the outer kinetochore and are essential for microtubule attachments¹⁵⁵. This network on its turn recruits the RZZ complex¹⁵⁶, which is responsible for recruiting the dynein/dynactin complex, which finally links to the microtubules of the mitotic spindle.

One of the most upstream kinases responsible for establishing the checkpoint is Mps1¹⁵⁷ which phosphorylates the kinetochore protein KNL1 on 'MELT' repeats. Subsequently, Mps phosphorylation allows for the recruitment of the Bub proteins (Bub1, Bub3 and BubR1)¹⁵⁸⁻¹⁶¹, and in turn the Mad1-Mad2 complexes. Inhibition of Mps1 thus prevents MCC assembly¹⁶²⁻¹⁶⁴. Mps1 plays a more intricate role than only phosphorylating KNL1, and is itself regulated by Aurora B kinase, while also feeding in on Aurora B or Cdk1 activity. Some controversy remains, as Aurora B also plays a role in sensing incorrectly attached kinetochore microtubules and therefore it has been difficult to discriminate between its role in generating versus maintaining the checkpoint^{165,166}. To complicate matters further, MPS1 activity is also responsible for its own turnover at the kinetochore, as MPS1 inhibition leads to increased recruitment^{162,167,168}, putting a feed forward loop in place.

The unattached kinetochore is the scaffold for the 'Bub-hub'. Bub3 is required to recruit both Bub1 and BubR1 at the kinetochore¹⁶⁹⁻¹⁷². While Bub3 is not required for BubR1 and Mad2 to inhibit APC/C^{Cdc20} *in vitro*^{24,146,173}, Bub3 is required for an efficient checkpoint response in a cellular context^{145,146}. This is corroborated by the fact that BubR1 mutants which are unable to bind Bub3, also have a greatly diminished checkpoint response^{145,146}. Indeed, BubR1 requires Bub1 for its recruitment, but Bub1 recruitment is not dependent on BubR1^{159,171,174-178}. The 'Bub-hub' is ultimately responsible for supplying an efficient site of Mad1-Mad2 dimers, which catalyze the actual formation of the MCC.

Setting up the checkpoint hinges on Mad2 existing in either an 'open' (O-Mad2) state or 'closed' (C-Mad2), respectively. Open Mad2 is inactive, while closed Mad2 actively inhibits Cdc20^{142,143} (**Figure 4**). Conversion of O-Mad2 is enabled by dimerization with Mad1 at the unattached kinetochore, so the Mad1-Mad2 dimer acts as a catalyst. They capture O-Mad2, convert and subsequently release this as C-Mad2, which acts as cytoplasmic soluble inhibitor^{179,180}. This is known as the 'template' model, in which the newly produced C-Mad2 binds to Cdc20 and prevent it from activating the APC/C^{181,182}. Not only does Mad2 capture Cdc20 in the MCC, it is also shown to bind the same location on Cdc20, the KILR motif, as the APC/C and therefore directly competes for binding⁴⁸. Indeed, Mad2 was one of the first players to be identified to inhibit APC/C^{Cdc20} *in vitro*^{29,183}, but the mechanistic details of how Mad2 is temporally, spatially and mechanistically responsible for this inhibition have been uncovered more recently.

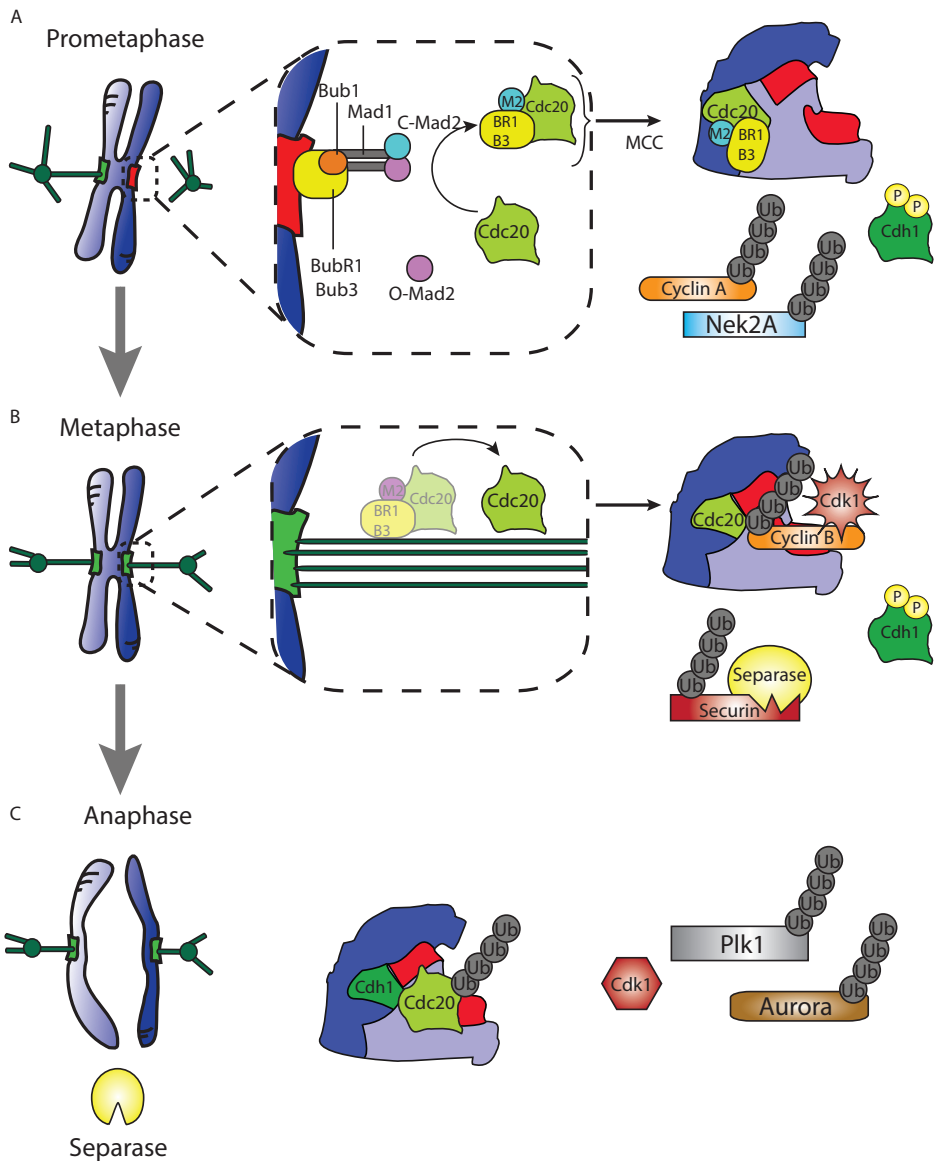


Figure 4 The mitotic checkpoint

A) In prometaphase unattached kinetochores (red) at the middle the chromosome, recruit the Bub proteins, which in turn recruit Mad1 dimers. The Mad1 dimers are able to convert 'open-Mad2' (O-Mad2) to 'closed-Mad2' (C-Mad2). The C-Mad2, BubR1 (BR1) and Bub3(B3) together bind Cdc20 forming the MCC. Only prometaphase substrates such as Nek2A and CyclinA are efficiently degraded. **B)** At metaphase, when the chromosomes are correctly biorientated, no new MCC is formed, and free Cdc20 is able to bind the APC/C, which leads to efficient ubiquitination of D-box containing substrates. Destruction of cyclin B leads to a decrease in Cdk1 activity, while destruction of securin frees separase. **C)** Free separase cleaves cohesin, leading to the separation of sister chromatids. Cdh1 is responsible for the destruction of Cdc20 and takes over the activator role, efficiently targeting the remaining KEN motif containing substrates for destruction. Figure adapted from Lara-Gonzalez and Taylor 2012¹⁰⁶, Overlack *et al.* 2015¹⁵⁹.

Even more so, while the checkpoint is clearly generated from kinetochores in mitosis, already before NEBD the nuclear pores act as checkpoint generating sites, required to build up a buffer of inhibitory signal before mitotic entry^{167,184,185}.

While it is clear that Cdc20 is continuously ubiquitinated and degraded, there is evidence that the first is already sufficient for MCC disassembly⁹⁹: as even in the presence of proteasome inhibitor the MCC can still disassemble^{11,103,186–188}. But besides ubiquitination, it is clear that kinases are also essential for maintaining the checkpoint, because inhibition of either MPS1 or Aurora B also lead to MCC disassembly even when the proteasome is inhibited^{158,189,190}.

Turning off the checkpoint after correct biorientation is less well understood compared to its assembly. It is clear however that extracting the MCC from the APC/C is dependent on the APC/C subunit APC15^{96,189,191}, while free MCC is tempered by the protein p31comet. Depletion of p31comet also results in increased MCC levels^{189,190,192}. The exact mechanism is unclear: p31Comet either prevents binding of BubR1 to C-Mad2-Cdc20¹⁹³ or extracts Mad2 from the MCC¹⁹². At the very least, p31Comet is a binding partner of C-Mad2^{194,195}, thus preventing Cdc20 inhibition.

ProTAME / APCin

Recently chemical inhibitors of the APC/C have been developed. Firstly Tosyl-L-Arginine Methyl Ester (TAME), that *in vitro* is sufficient to inhibit APC/C^{Cdc20} and APC/C^{Cdh1} *in vitro*, and ProTAME, a cell permeable derivative¹⁹⁶. Its chemical structure resembles the IR tail found in both activators, and thus it also prevents binding of the activator IR tail to the APC/C. Interestingly, APC10 binding is not affected by ProTAME¹⁹⁷. Indeed, a second mode of action is inducing the loss of prebound Cdc20, shown by the observation that TAME increases the autoubiquitination of Cdc20¹⁹⁷. Notably, treatment with ProTAME did not prevent Cdc20 from associating to the APC/C, likely due to the IR-independent mediated binding of Cdc20, that is amplified by the use of spindle poisons¹⁹⁶. In the presence of ProTAME APC/C substrates are not ubiquitinated to their full extent. Specifically, cyclin B1 ubiquitination, can be rescued by adding additional Ube2S to the reaction¹⁹⁷. While ProTAME clearly inhibits APC/C activity, it does not fully prevent its ubiquitinating capacity, also evident from the fact that Cdc20 is still auto-ubiquitinated in the presence of ProTAME. The mitotic arrest induced by ProTAME does not inhibit turnover of the MCC even in the presence of proteasome inhibitor, strengthening the argument that ubiquitination, in case it leads to checkpoint turnover, is independent of proteolysis¹⁹⁸. Very recently, a second inhibitor was developed named ‘apcin’. This inhibitor binds directly to the D-box receptor formed by the WD-40 domains and synergizes with ProTAME¹⁹⁹. Interestingly, the inhibitory potential of apcin is substrate specific, reinforcing the notion that activators are able to

direct destruction in a substrate specific manner. Cyclin B1, which is strongly dependent on the recognition of its D-box to be degraded, can already be stabilized at least partially by apcin alone, while CyclinA and Nek2A are degraded even at high concentrations of apcin *in vitro*.

The Helpers, assisting in destruction

E3 ubiquitin ligases require E2 enzymes to transfer ubiquitin to target substrates. There are several E2 enzymes that help the APC/C to transfer the first mono-ubiquitin to its substrates, likely without much specificity for particular lysines in the substrates^{200,201}. However, a second E2 is responsible for elongating and branching the ubiquitin chains on substrates to ensure their rapid recognition by the proteasome and subsequent degradation^{202,203}. In mammalian cells, the E2 responsible for the priming mono-ubiquitination is UbcH10, (also known as UbcX and E2-C in other species) and *in vitro*, at least also UbcH5 (or Ubc4) can also perform this function^{4,201,204–208}. The singular identified ubiquitin chain extender is Ube2S (or E2-EPF), and this function is performed by Ubc1 in budding yeast²⁰⁹.

In vitro work shed light on the interaction between various APC/C subunits and the E2 proteins, however, how and when the E2s are recruited, and what their precise contributions are to APC/C mediated destruction is still not very clear. In fission yeast, the orthologues of these mammalian E2 enzymes are essential for normal mitotic progression²¹⁰. Interestingly, while proteasomal degradation for most proteins occurs via ubiquitin chains that become linked to lysine 48 (K48 chains) of the conjugated ubiquitin, the APC/C almost exclusively delivers K11-linked polyubiquitin chains in humans^{64,211}. This is due to the preference of both UbcH10 as well Ube2S for the formation of K11 linked poly-ubiquitin chains^{64,212,213}. K11 linked poly-ubiquitination seems to preferentially form during mitosis in an APC/C dependent manner and is therefore also seen as the cell cycle specific form of poly-ubiquitination^{214,215}. However, it should be noted that in budding yeast, Ubc1 synthesizes K48 linked chains mediated by the APC/C. The reason of this discrepancy is unclear at present.

Recent data on how the APC/C actually confers K11 polyubiquitin chains to substrates support the model that single ubiquitin molecules are added in succession on the distal side of the ubiquitin chain^{52,216}. Interestingly, the same work shows direct binding between Cdc20 and Ube2S, which presents an attractive model for locally confining the proteins that are required for APC/C mediated degradation. The RING domain of APC11 and Ube2S cooperate in an unprecedented manner: the RING domain of APC11 lowers the K_M of the donor ubiquitin, already attached to the substrate, which leads to enhanced catalytic activity of Ube2S. Intriguingly, possibly not only the type of linkage matters for the speed of destruction, but rather also the amount of poly-ubiquitin

branches that are created on a chain, because an increasing number of branches leads to a stronger signal for proteasomal degradation^{217,218}.

So, UbcH10 and Ube2S tightly collaborate to provide the APC/C with ubiquitinating potential. Simultaneous depletion of UbcH10 and Ube2S can impair APC/C activity, while their separate knockdown shows only minor defects^{123,211,215}. Also in vitro, it is clear that Ube2S cooperates with either UbcH10 or UbcH5, to form longer polyubiquitin chains²¹⁹. While only absence of both leads to deficiencies, overexpressing of either one alone can play a role in disrupting normal cell division. UbcH10 over-expression might lead to erroneous cell division or promote tumorigenesis²²⁰ and misregulation of Ube2S is also implicated in increased tumor growth²²¹, as well as modulating drug sensitivity when overexpressed in breast cancer²²².

UbcH10

UbcH10 depletion in *Drosophila* causes mitotic defects, and stabilization of APC/C targets²⁰⁶, but in mammalian cells gives only minor defects^{211,215}. It has been suggested that self-inactivation of UbcH10 by the APC/C allows for autonomous downregulation at the G1 to S border^{212,223}. There is some controversy here, as it has also been reported that UbcH10 plays a specific role in G1, and specifically does not play a role in autonomous regulation of APC/C activity during mitosis²²⁴. UbcH10 can, at least in vitro, also be sufficient to lead to cyclin B degradation²⁰¹. UbcH10 binds both the RING subunit of APC11, as well as to the cullin domain in APC2^{212,225}. The APC11 RING domain activates UbcH5 and UbcH10 in a canonical RING mechanism⁵², meaning that mutations in the RING domain hinder placing of the primary mono-ubiquitins on substrates. Ubc4 (the UbcH10 orthologue in yeast) is also dependent on the presence of an activator, as it stimulates its activity over a hundred fold³⁷. The same study also shows that APC10 is required for efficient and processive ubiquitination of substrates. To place the first ubiquitin on a substrate, it may be that a specific initiation motif on the substrate is required, to facilitate a nearby lysine to be conjugated by UbcH10²¹¹. Interestingly, UbcH10 when present at sufficient levels seems to be able to override the checkpoint^{99,212}. Very recent experiments that measure as precise as a single ubiquitin moiety, via fluorescent TIRF microscopy, on purified components, or on cellular extracts, show that UbcH10 indeed places up to the first three ubiquitins highly processive. Ube2S works at a much slower rate, but is more efficient in elongation of the ubiquitin chain²²⁶. Intriguingly, the authors discovered that a single encounter between the APC/C and the substrate leads to short ubiquitin chain, which increases affinity for the APC/C. This leads to a feed forward loop, which they named “processive affinity amplification”. The same study showed that multiple shorter ubiquitin chains, rather than a single longer chain, provide a higher affinity signal of the substrate for the APC/C. This mode of action allows the APC/C to dynamically target its substrates, as

the final degradation signal is the sum of many low affinity interactions, resulting in high affinity binding between the enzyme and the substrate.

Ube2S

Ube2S is responsible for chain elongation and branching of ubiquitin chains^{214,219}. It specifically forms K11 chains in conjunction with the APC/C^{214,215}. Interestingly, it is dispensable for normal mitotic progression, but it might be required for recovering from a mitotic delay²¹⁹. Ube2S mediates polyubiquitin chain formation on substrates with a priming ubiquitin without further requirement of UbcH10, also *in vitro*²¹⁴. In an attempt to determine the exact location of Ube2S binding to the APC/C, two laboratories independently identified both APC2 and APC11, via either cryo-EM, or crosslinking and biochemical analysis. However, cryo-EM also identified APC4 and APC5 as interacting subunits⁵², while biochemical analysis additionally identified Cdc20²¹⁶. Using separately translated APC subunits, APC10 has also been identified as a C-terminal tail-dependent binding partner of Ube2S¹²³. Previously, direct APC/C independent binding to the WD-40 domains of Cdh1 has also been identified²²⁷. Ube2S does not require Cdh1 for binding⁵², but others show greatly diminished binding between Ube2S and the APC/C when the activator is lacking²¹⁶. However, there is consensus that the presence of an activator greatly enhances ubiquitin chain formation. Recent kinetic studies confirm that the presence of an activator increases the catalytic rate of the E2 enzymes several hundred fold, but that this is still dependent on a substrate interacting with the activator via a degron motif³⁷. This is dubbed a “substrate-assisted catalytic mechanism”. Even with mutations in the APC11 RING domain Ube2S binding is largely retained, and dependent on the combined APC2-APC4 region⁵². While the RING domain is not required for Ube2S binding, *in vitro* kinetic assays do show it is crucial for Ube2S function. Ube2S is dependent on its LRRL tail to bind to the APC/C, and directly competes with Emi1 for binding¹²⁶. The LRRL tail is required for APC/C binding, and probably mediates binding to the cullin domain of APC2 via electrostatic interactions.

THE TARGETS, THE VICTIMS

Targeting and Motifs

Several recurring motifs are found in APC/C targets, often (but not solely) in unstructured regions, and are crucial for their recruitment and destruction. Typically, these motifs do not exceed a length of 10 amino acids, and mediate a low specificity and affinity binding, to allow for a highly dynamic interaction. While the D-box^{228,229} and KEN-box⁹⁴ were originally discovered as motifs for destruction, it is now clear that these motifs play a role in APC/C activators and regulators as well. There are clear differences

between the two; the D-box binds both APC10 and the activator, between blades 1 and 7^{55,230,231}, while the KEN box is single-handedly recognized by the activator²³⁰ (**Table 2** and **Figure 5**). While the D-box is more specifically recognized by Cdc20, the KEN box is the preferred motif for Cdh1²³. Indeed, the role of the activator as ‘adaptor’ for either of these motifs is well established^{94,232–234}. However, the KEN box and D-Box also play an essential role for inhibitors of the APC/C, as they are present and functional in ACM1²³¹ and Emi1¹¹². Interestingly many substrates containing a D-box additionally possess a KEN box²³³. However, if both motifs generally play a redundant or additional role, as found for Securin⁸⁰, is not well characterized.

The most recently discovered motif is the ABBA motif, which is also found conserved in both targets and regulators of the APC/C. The name is derived from the proteins which possess the motif; Cyclin A, Bub1, BubR1 and ACM1^{144,235}. It should be noted that the ABBA motif was also separately found in ACM1 and was referred to as the A-motif²³¹. This ABBA motif binds between blades 2 and 3 of the WD40 domain, and for ACM1 mediates inhibition, while for Cyclin A is crucial for its prometaphase destruction.

Several non-prominent, possibly degenerate motifs have also been discovered, such as the A-box for Aurora A⁶⁸ and the O-box for Orc1²³⁶ (see also Barford²³). Also the role for the TEK box, a region found in ubiquitin and Securin, is thought to facilitate K11 linkages has been suggested to be present in other substrates^{64,237}. Interestingly, even degenerate motifs have been proposed (e.g. the NEN box for the KEN box) and shown to be functional, allowing for a further substantial increase of potential interacting proteins⁴². Another layer of regulation through post-translational modifications of motifs has been discovered, although this does not seem to be a general rule for motif

Table 2 Amino acids in the activators involved in motif recognition

Cdc20 / Cdh1

| | | | | | | | | |
|------------|----------|-----------------|-----------------|----------|----------|----------|-----------------|----------|
| KEN | D 184 | Y 185 | F 329 | N 331 | N 331 | T 377 | Q 401 | R 445 |
| R | D 177 | D 464 | E 465 | | | | | |
| L | R 174 | K 176 | L 176 | L 198 | V 200 | I 216 | V 216 | L 467 |

Indicated in numbers are the amino acids corresponding to the Cdc20 protein. Based on alignment between Cdc20 and Cdh1 amino acids are compared. Standard BLAST alignment shows conservation between Cdc20 and Cdh1 starts at 160 of Cdc20, which corresponds to amino acid 163 in Cdh1. Please note however, that the C-box (77-83, see Figure 2) is present in both activators. If the corresponding amino acid in Cdh1 is not conserved the alternative amino acid is depicted in red, otherwise a single amino acid is shown in black. Based on Chao *et al.* 2014⁵⁸ and He *et al.* 2013²³¹.

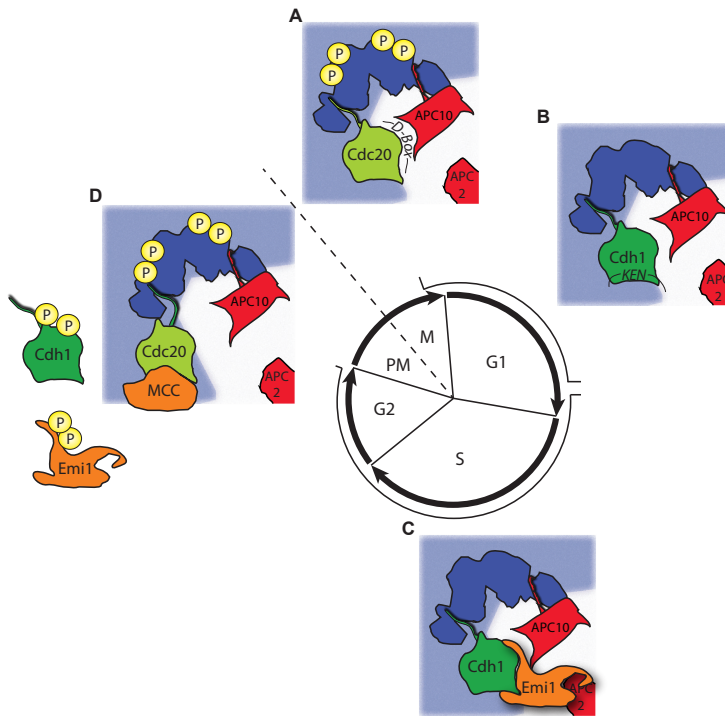


Figure 5 Regulation of substrate recognition by the APC/C and activator throughout the cell cycle.

A) After the mitotic checkpoint has been satisfied, Cdc20 and APC10 are in perfect proximity to recognize D-box motifs and are prioritized to target cyclin B and securin for proteasomal degradation. The D-box receptor is formed by APC10 and Cdc20. **B)** At the end of mitosis is responsible for degrading Cdc20 and assumes its role in recognizing and substrates containing either a D-box or KEN box. Note that the APC/C no longer is phosphorylated in G1, which is also not required for Cdh1 recruitment. Note that the KEN motif is recognized by Cdh1 separately of APC10. **C)** Rising levels of Emi1 due to E2F transcription at the end of G1 are responsible for inhibiting Cdh1, through binding tail dependently to APC/C, and several other motifs, directly in the catalytic core of the APC/C. **D)** At the onset of mitosis, the Emi1 is phosphorylated and degraded, while Cdh1 is kept in check by rising Cdk1 activity which prevent APC/C association. APC/C phosphorylation on the other hand stimulate Cdc20 recruitment, which is kept inhibited by binding of the checkpoint proteins, distancing Cdc20 from APC10.

recognition. For Pds1 (yeast Securin), Cdc6²³⁸ and Skp2 phosphorylation of the D-box prevents recognition^{239–241}.

Tails

Another intriguing recruitment motif is the C-terminal APC/C targeting tail. This completely C-terminal motif is currently defined as [ILM]R²⁴², and is present in both activators, several specific yeast meiotic activators and at least the substrates Nek2A²⁴³ and Kif18A⁸², but also in the APC10 subunit. The IR tail of the activators and APC10 have been clearly pinpointed to principally interact with APC3^{41,44,45}. However, under

conditions when Cdc20 is bound to the checkpoint, point mutations in the TPR domain of APC8 revealed that APC8 is the principal subunit that Cdc20 binds to when the mitotic checkpoint is active²⁴⁴. Likely, the [ILM]R tail binds to several TPR repeats, depending on the APC/C state, and possibly confirmation of the substrate in question. At least there is a striking difference between the MCC and Nek2A, as the mutation in APC8 that leads to loss of 90% of checkpoint binding to the APC/C does not lead to loss of Nek2A binding to the same extent⁸².

The above-mentioned definition does not encompass the C-terminal tails (LRRL) that are found in Emi1/Emi2 and Ube2S¹²⁶, which are required for APC/C targeting¹²³. Indeed, LRRL tails do not prevent Cdc20 binding¹²⁴, and do not bind TPR repeats, but are more likely directed to the APC2 subunit¹²⁶, although no exact location has been determined.

CONCLUSION

The emerging picture shows an intricate interplay of all players involved (**Fig. 5**). At the very end of G2, phosphorylation of Emi1 leads to its destruction, removing its inhibitory potential on APC/C^{Cdh1}. Concurrently, Cdh1 is phosphorylated to inactivate it. Upon entering mitosis the APC/C becomes hyper phosphorylated, leading to increased affinity for Cdc20. Just before mitotic entry, mitotic checkpoint complexes are formed at nuclear pores, which take over APC/C inhibition as soon as Emi1 disappears. The loss of Emi1, and recruitment of Cdc20, either bound to the other checkpoint proteins or not, also allows for recruitment of Ube2s, and already primes the APC/C for activation. At each unattached kinetochore the Bub proteins and conversion of O-Mad2 to C-Mad2, drive catalytic formation of the MCC, which inhibits Cdc20. APC/C^{MCC} or APC/C^{Cdc20} displays some activity, which leads to slow degradation of substrates that are stabilized by the mitotic checkpoint, and rapid degradation of spindle checkpoint independent APC/C^{Cdc20} substrates. When the mitotic checkpoint is satisfied, and Cdc20 is free of checkpoint proteins, it binds the APC/C and cooperates with APC10 to recognize the D-box motif in substrates. Priming ubiquitins are placed on the substrate by UbcH10, the WD-40 domain of the activator interacts either with degron motifs or these priming ubiquitins, to ensure retention of the substrate. Priming ubiquitins are rapidly followed up by Ube2S which to ensure swift addition of distal ubiquitins in a K11 linked manner, leading to a compact polyubiquinated substrate, which will be subsequently recognized and destroyed by the proteasome.

Chapter 2

Nek2A destruction marks APC/C activation at the prophase-to-prometaphase transition by spindle-checkpoint restricted Cdc20

Michiel Boekhout¹ and Rob Wolthuis^{1,2}

Affiliations:

1: Division of Cell Biology I (B5) and Division of Molecular Carcinogenesis (B7), The Netherlands Cancer Institute (NKI-AvL), 1066 CX Amsterdam;

2: Department of Clinical Genetics (Division of Oncogenetics), VUmc and VUmc Cancer Center Amsterdam, CCA/V-ICI Research Program Oncogenesis, VUmc Medical Faculty, The Netherlands.

Published in Journal of Cell Science, 2015, 128: 1639-53

ABSTRACT

Nek2A is a presumed APC/C^{Cdc20} substrate, which, like cyclin A, is degraded in mitosis while the spindle checkpoint is active. Cyclin A prevents spindle checkpoint proteins from binding to Cdc20 and is recruited to the APC/C in prometaphase. We found that Nek2A and cyclin A avoid stabilization by the spindle checkpoint in different ways. First, enhancing mitotic checkpoint complex (MCC) formation by nocodazole treatment inhibited the degradation of geminin and cyclin A while Nek2A disappeared at normal rate. Secondly, depleting Cdc20 effectively stabilized cyclin A but not Nek2A. Nevertheless, Nek2A destruction critically depended on Cdc20 binding to the APC/C. Thirdly, in contrast to cyclin A, Nek2A was recruited to the APC/C before the start of mitosis. Interestingly, the spindle checkpoint very effectively stabilized an APC/C-binding mutant of Nek2A, which required the Nek2A KEN box. Apparently, in cells, the spindle checkpoint primarily prevents Cdc20 from binding destruction motifs. Nek2A disappearance marks the prophase-to-prometaphase transition, when Cdc20, regardless of the spindle checkpoint, activates the APC/C. However, Mad2 depletion accelerated Nek2A destruction, indicating that spindle checkpoint release further increases APC/C^{Cdc20} catalytic activity.

Keywords: APC/C; Cdc20; cyclin A; Nek2A; spindle checkpoint

INTRODUCTION

The Anaphase-Promoting Complex/Cyclosome (APC/C) is an E3 ubiquitin ligase that, together with either one of its regulatory co-activators, Cdc20 or Cdh1, targets multiple mitotic regulators for proteasomal degradation. These include cyclin B1, securin and geminin, making APC/C^{Cdc20} a major factor in directing cell division, sister chromatid separation and DNA replication licensing^{13,20,245}. Several questions remain about how the activity of APC/C^{Cdc20} is controlled in mitosis. Phosphorylation of the APC/C by mitotic kinases at the end of prophase leads to increased affinity for Cdc20^{27,61}. Complex formation of the APC/C with co-activator probably induces a conformational change that activates the APC/C^{6,35}, perhaps by facilitating the recruitment of the E2 enzyme UbcH10^{12,37}. Cdc20 also acts as an APC/C substrate recruitment factor that binds directly to degradation motifs in APC/C substrates, such as the D-box and the KEN box^{41,56}. At the point in the cell cycle when APC/C^{Cdc20} complexes are formed, however, the spindle checkpoint also becomes active and blocks Cdc20. Spindle checkpoint proteins, including Mad2 and BubR1, capture Cdc20 into the inhibitory mitotic checkpoint complex (MCC)²⁴⁶. Cdc20 remains inhibited by the spindle checkpoint until the chromosomes are bi-oriented on the mitotic spindle^{18,106,134}. Once the spindle checkpoint is satisfied, APC/C^{Cdc20} becomes active and sends cyclin B1, securin and geminin for proteasomal degradation^{80,245,247}. Interestingly however, the APC/C^{Cdc20} substrate cyclin A2 disappears shortly after nuclear envelope breakdown, regardless of the inhibitory effect of the spindle checkpoint^{248,249}.

The mechanism by which cyclin A destruction evades the spindle checkpoint has largely been solved. The N-terminus of cyclin A associates strongly with Cdc20 and thereby competes off spindle checkpoint proteins^{250–252}. Thus, cyclin A, by its N-terminus, binds a specific fraction of Cdc20 that cannot be blocked by Mad2 and BubR1. In addition, the Cdc20-cyclin A complex, bound to Cdk1 and Cks, is exclusively recruited to the APC/C in prometaphase, when the APC/C becomes phosphorylated²⁵⁰. Recently, it was shown that cyclin A destruction early in mitosis serves progressive stabilization of the mitotic spindle, promoting proper attachments to kinetochores and formation of the metaphase plate³.

Nek2A is a centrosomal kinase that is highly expressed in G2 phase but rapidly disappears in prometaphase. Nek2A phosphorylates, for instance, C-Nap and Rootletin, which are involved in centrosome separation and bipolar spindle formation^{254–257}, but more recently has also been implicated in the Hippo signalling pathway²⁵⁸. Although Nek2A is an APC/C substrate, conclusive evidence that its destruction in mammalian cells depends only on APC/C^{Cdc20}, or that a different proteasomal targeting pathway contributes to its degradation, too, is lacking. Furthermore, the role of Cdc20 in directing APC/C-mediated Nek2A degradation is under debate^{35,82}. In contrast to cyclin A, even at high

levels Nek2A was not found to interfere with the ability of BubR1 to bind Cdc20⁸², indicating that Nek2A and cyclin A may differ in the way their destruction escapes control by the spindle checkpoint. Because the spindle checkpoint may block the recruitment of substrates to the APC/C by Cdc20, an attractive model explaining the timing of Nek2A degradation is that its destruction depends only on the APC/C, not on Cdc20. An observation in support of this model is that Nek2A has a C-terminal MR tail that binds directly to TPR motifs of APC/C subunits^{82,243,259}. However, in such a model, Nek2A binding to the APC/C would be expected to be cell cycle regulated, to explain its timely destruction. Furthermore, a TPR-binding tail is, for instance, also present in the stable APC/C component APC10, showing that this motif alone is insufficient to turn a protein into an APC/C substrate^{44,260,261}. Nek2A forms dimers which facilitate Nek2A binding to the APC/C⁸², but dimerization is also not cell cycle-regulated¹²⁶². Altogether therefore, it is unclear which mechanism ensures that Nek2A is degraded at the right time in mitosis and what the role of Cdc20 is in this process. Here, we tried to address this by asking the following questions: does Nek2A turn-over rely exclusively on the APC/C and Cdc20? And, how does Nek2A degradation escape control by the spindle checkpoint? We analyzed Nek2A degradation in live cells, in relation to two well-characterized APC/C^{Cdc20} substrates: geminin, which is stabilized in response to the spindle checkpoint, and cyclin A, which is degraded independently of the spindle checkpoint.

RESULTS

Nek2A is degraded in mitosis regardless of enforced spindle checkpoint activation

As detected by Western blot, Nek2A is degraded when cells are arrested in mitosis by taxol treatment (**Fig. 1A**). We wanted to know whether, as was reported recently for cyclin A, Nek2A may be partially stabilized by increasing the formation of the Cdc20-inhibitory MCC, a consequence of treating mitotic cells with spindle poisons^{148,192}. To follow detailed changes in protein stability over time, we used time lapse fluorescence microscopy of U2OS cells expressing geminin-Cherry, a validated checkpoint-controlled APC/C^{Cdc20} substrate²⁴⁵, together with an N-terminally tagged Venus-Nek2A fusion, during G2 phase and mitosis (**Fig. 1B**). Upon nocodazole treatment, geminin-Cherry remained stable as long as cells delayed in mitosis (**Fig. 1C**). However, fluorescent Nek2A was destroyed right at the prophase-to-prometaphase transition, regardless of whether cells were left untreated or blocked in either nocodazole or taxol (**Fig. 1C, D**; **Supplemental Fig. 1A** shows expression levels of the fluorescent Nek2; also see Fig. 3B, below). We conclude therefore that Nek2A differs from other APC/C^{Cdc20} substrates, including cyclin A, in that its degradation is not delayed at all by increasing spindle checkpoint activity. These results indicate that Nek2A is either not exclusively degraded

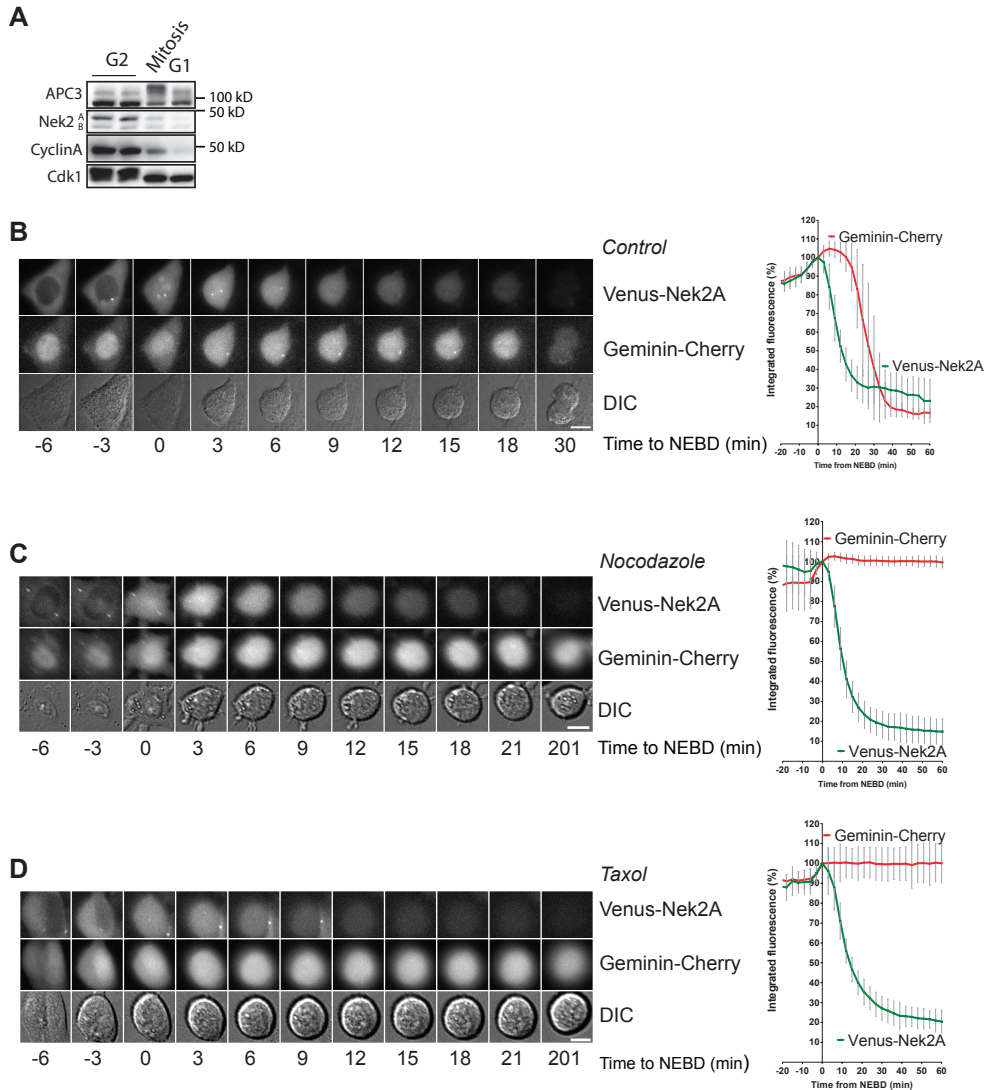


Figure 1. Nek2A destruction does not respond to super-activation of the spindle checkpoint.

(A) U2OS cells were synchronized in G2-phase by 8h thymidine release, or released into taxol after 24h thymidine block and collected after 16h by mitotic shake off. Mitotic cells were treated for 1h with roscovitine to force them out of mitosis into a G1-like state ⁷⁵. (B) U2OS cells stably transduced with retroviral Venus-Nek2A and Geminin-Cherry constructs were imaged by fluorescence and DIC time lapse microscopy at 3 minute intervals. Panel shows degradation of Nek2A and Geminin during a normal mitosis. (C) nocodazole treated cells and (D) taxol treated cells degraded Nek2A at rates normal for mitosis, showing Nek2A degradation does not respond to the increased spindle checkpoint activity under conditions of treatment with spindle poisons. Integrated fluorescence of the cells was measured and normalized to 100% for the intensities in the frame when NEBD started, as determined by the first detection of cytoplasmic dispersal of nuclear Geminin-Cherry. Graphs shown are mean \pm s.d.. Scale bar = 10 μ m.

via APC/C^{Cdc20}, or that Nek2A destruction occurs regardless of whether Cdc20 is blocked by spindle checkpoint proteins or not.

Nek2A degradation after inhibiting APC/C^{Cdc20}

To resolve this matter, we first investigated whether Nek2A degradation exclusively depended on Cdc20. We used time-lapse fluorescence microscopy to follow cells stably expressing both geminin-Cherry and Venus-Nek2A, after treatment with RNAi directed against Cdc20. In control cells, Venus-Nek2A destruction started right at NEBD (**Fig. 2A, upper panel, Fig. 2B**; fluorescent Nek2A protein levels reached 50% of their NEBD levels within 15.6 minutes \pm 6.1 s.d., n=25, in 3 independent experiments). Although the mitotic delay after Cdc20 RNAi varied between cells, we found that cells arresting in mitosis for two hours or more did not degrade geminin-Cherry. Remarkably however, fluorescent Nek2A was degraded only slightly more slowly (**Fig. 2A, middle panel, Fig. 2C**). In these cells, the point when 50% of fluorescent Nek2A had disappeared was delayed to 28.5 minutes \pm 12.0 s.d. (n=51, 5 independent experiments, **Fig. 2C**). We then investigated the effect of the APC/C inhibitor ProTAME, which blocks normal binding of Cdc20 to the APC/C^{197,263}. While treatment with 20 μ M of ProTAME almost completely stabilized geminin-Cherry, we observed only modest stabilization of Venus-Nek2A, roughly similar to the partial stabilization of Venus-Nek2A following Cdc20 RNAi (half-life 41 minutes \pm 12.6 s.d., n=15 from 2 independent experiments, **Fig. 2A lowest panel and Fig. 2D**). When depleting the cullin-like subunit APC2, NEBD to anaphase lasted 489.1 minutes \pm 200 (n=13 from 3 independent experiments). Also in these cells, geminin-Cherry was clearly stabilized, confirming efficient depletion of the APC2 subunit (**Fig. 2E**, Western blot included). Nevertheless, Venus-Nek2A was still degraded effectively (**Fig. 2E**; time to 50% of the Venus-Nek2A levels at NEBD was 17.8 minutes \pm 3.6 s.d.). Significant stabilization of Venus-Nek2A was not observed in APC3 RNAi cells or after the combined knockdown of Ube2S and UbcH10, even though geminin-Cherry was largely stable in these cells (**Supplemental Fig. 1B, C**, respectively). Endogenous Nek2A disappeared despite depletion of APC subunits or the APC/C-directed E2 enzyme Ube2S, too (**Supplemental Fig. 1D**). So, Nek2A degradation proceeds even when the function of APC/C^{Cdc20} is significantly impaired. This may indicate that a second, APC/C^{Cdc20} -independent pathway targets Nek2A under these conditions. Alternatively, a catalytic amount of APC/C^{Cdc20}, remaining after either APC subunit or Cdc20 depletion by RNAi, or after pharmacological inhibition of APC/C^{Cdc20}, is sufficient to effectively process Nek2A.

Cyclin A destruction is more dependent on Cdc20 than Nek2A destruction

We then directly compared the degradation of Nek2A to that of the spindle checkpoint-independent APC/C^{Cdc20} substrate cyclin A in live cells. We made use of tetracyclin-inducible cyclin A-Venus U2OS cells stably expressing Cherry-Nek2A. During

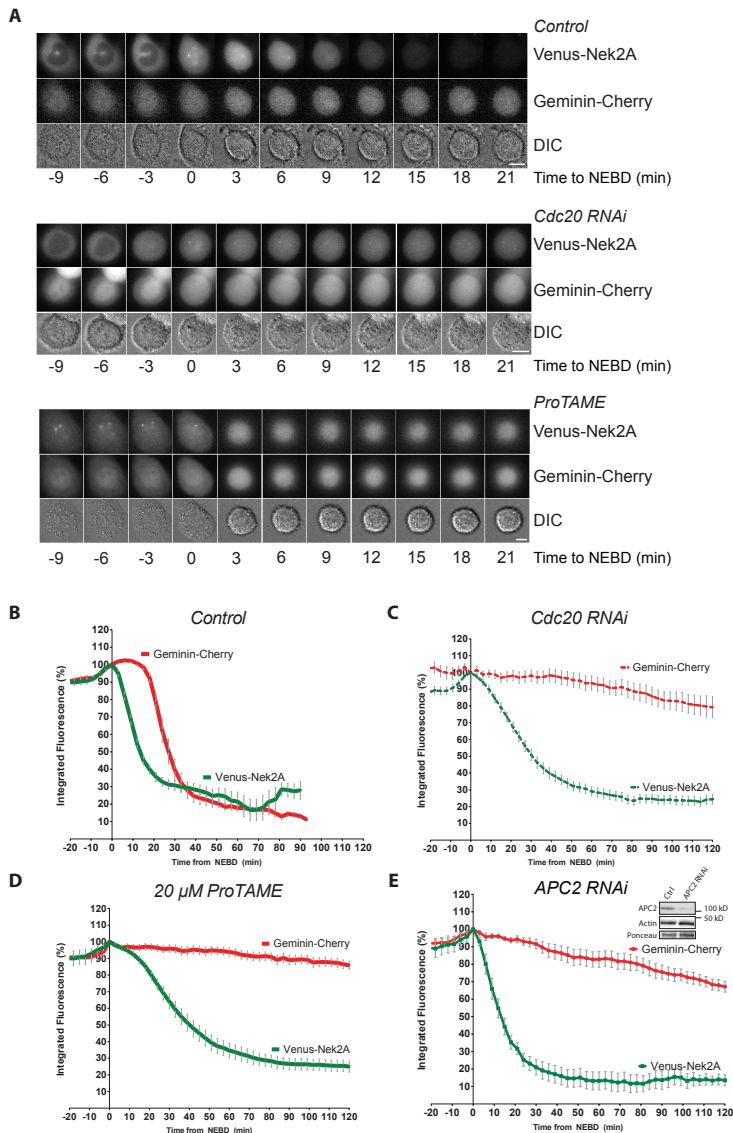


Figure 2. Compared to the spindle checkpoint-dependent APC/C^{Cdc20} substrate Geminin, Nek2A is not efficiently stabilized by direct inhibition of APC/C^{Cdc20}.

(A) U2OS cells were imaged by fluorescent and DIC microscopy at 3 minute intervals, after treatment with RNAi oligos or ProTAME as indicated. Time on the X-axis was set to 0 at the onset of NEBD, as explained in the Legend to Figure 1. (B) Averages of multiple single cells are shown, which were normalized to 100% fluorescence for $t=0$. Mean fluorescence is plotted \pm s.e.m. Control cells, combined $n=20$, 3 separate experiments; (C) U2OS cells treated with Cdc20 RNAi combined $n=47$ from 4 separate experiments; (D) U2OS Cells treated 20 μ M ProTame were imaged $n=15$ from 2 independent experiment. Scale bar=10 μ M; (E) U2OS cells stably expressing indicated fusion proteins were transfected with APC2 RNAi and split either for imaging or lysed and analysed by westernblot. Graph depicts mean values $n=11 \pm$ s.e.m. 2 separate experiments;

unperturbed mitosis, or after nocodazole treatment, Nek2A degradation started several minutes before that of cyclin A, exactly at the point of nuclear envelope breakdown, as determined by the abrupt appearance of cytoplasmic cyclin A (Fig 3A, top panel, Fig 3A, B, destruction plots). Nek2A degradation progressed more rapidly than that of cyclin A (Fig. 3A, destruction plot). Typically, we had found that Cdc20 needs to be depleted below 5% of its normal cellular levels for cyclin A stabilization²⁵⁰. In a Cdc20 RNAi experiment where the time from NEBD to anaphase was 183 minutes \pm 72.9 s.d., and 50% of cyclin A-Venus remained after 74 minutes of mitotic delay, Cherry-Nek2A was only minimally stabilized (**Fig. 3C, Supplemental Fig. 2A**). In another experiment that led to more severe Cdc20 depletion, NEBD to anaphase lasted more than 12 hours (766.5 min \pm 152.3 s.d., **Supplemental Fig. 2B**). However, although these Cdc20 RNAi cells failed to degrade cyclin A for the first 120 minutes of mitosis, Nek2A still declined rapidly (**Fig. 3D**). Apparently, depleting Cdc20 affects cyclin A destruction much more than Nek2A destruction (**Fig. 3C,D, Supplemental Fig. 2A,B**). Nevertheless, the degree to which Nek2A was stabilized correlated to the degree of cyclin A stabilization upon Cdc20 depletion. Similar results were obtained when we followed cells depleted for either APC2 or the combination of E2 enzymes, Ube2S and UbcH10 (**Supplemental Fig. 2C,D**). These results again suggest that Nek2A can either be processed independently of the APC/C or Cdc20, or that a very small amount of Cdc20, remaining after RNAi treatment, is sufficient to support Nek2A degradation. To fully block the function of Cdc20, we then combined Cdc20 RNAi with proTAME, which act synergistically²⁶³. Interestingly, both cyclin A-Venus and Cherry-Nek2A became completely stable during prometaphase now (Compare **Fig. 3E**, proTAME alone, with **3F**, proTAME plus Cdc20 RNAi). ProTAME, a cell-permeable compound that resembles an IR tail, did not interfere with the recruitment of Nek2A to the APC/C (**Supplemental Fig. 3A,B**, and see below). This shows that Nek2A destruction in mitosis fully depends on binding of Cdc20 to the APC/C. We propose that, while processing of cyclin A by the APC/C requires stoichiometric cyclin A-Cdc20 complexes, Nek2A degradation is directed by a catalytic effect of Cdc20 on the APC/C that immediately springs into action at the prophase-to-prometaphase transition.

Nek2A is recruited to the APC/C in interphase as well as in mitosis

Previous *in vitro* work has shown that Nek2A can bind directly to the APC/C even in the absence of Cdc20²⁶⁴. To explain the sudden disappearance of Nek2A when cells enter mitosis, we hypothesized that Nek2A recruitment to the APC/C might be regulated in the cell cycle. We compared binding of Nek2A to the APC/C in extracts from cells synchronized in G2 phase or in mitosis. To stabilize Nek2A, we arrested cells in nocodazole and added the proteasome inhibitor MG132. Surprisingly, Nek2A bound strongly to the APC/C in G2 phase, as well as in mitosis (**Fig. 4A, Fig. 4B, APC4 IPs; Supplemental Fig. 3C** shows validation of the specificity of the detected

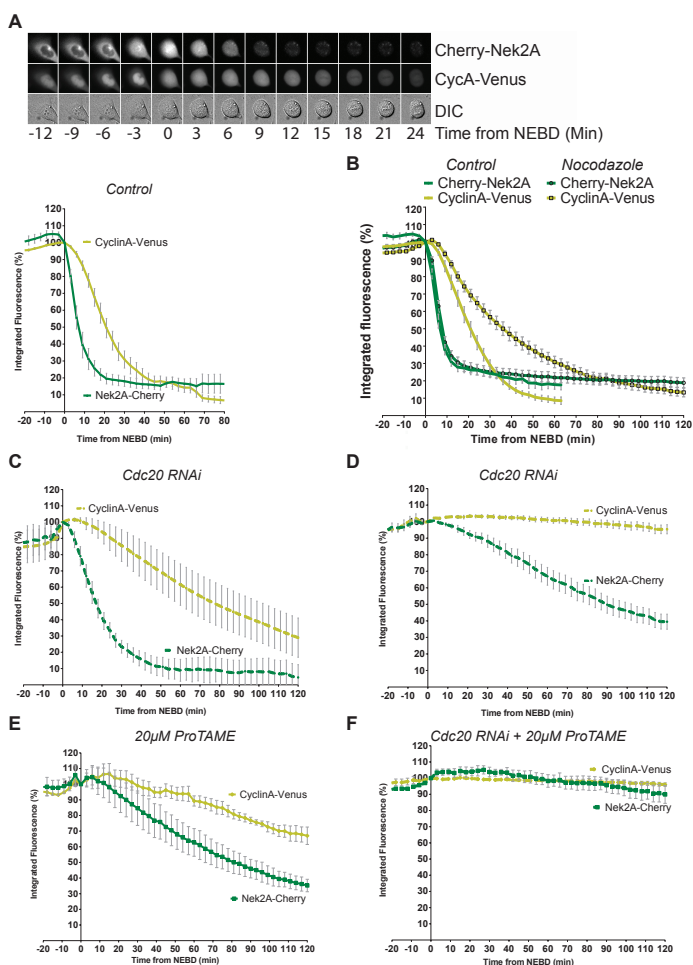


Figure 3. Compared to the spindle checkpoint-independent APC/C^{Cdc20} substrate cyclin A, Nek2A is not effectively stabilized by depletion of Cdc20.

(A) Montage of U2OS cells with TET inducible Cyclin A2-Venus, also stably expressing Cherry-Nek2A. Cells were imaged during normal mitotic progression. Integrated fluorescence for both fusion-constructs was measured and plotted as in Figure 1B (solid lines, n=10). (B) U2OS cells were synchronized with thymidine and release after which tetracycline was added to induce cyclinA-Venus expression. Nocodazole was added 6h after release and cells were imaged at 3 minute intervals. Symbol free lines are control cells (n=15 3 separate experiments) while dark symbols indicate nocodazole treated cells (n=15 3 separate experiments) plotted is mean \pm s.e.m. (C) U2OS cells were treated with Cdc20 RNAi (dotted line, n=8), synchronized with thymidine and treated with tetracycline after thymidine release to induce cyclinA-Venus expression. See also **Supplemental Fig2A**. (D) U2OS cells were treated with Cdc20 RNAi (dotted line n=11) Cells were synchronized with thymidine after transfection, and released in the presence of tetracycline to induce Cyclin A-Venus expression. Efficiency of the knockdown is revealed in a single cell manner by the stability of Cyclin A-Venus during the first 120 minutes of the mitotic delay and greatly increased time from NEBD-Anaphase, see also **Supplemental Fig.2B**. (E) Similar to **B**, but cells were treated with ProTAME for 6h after thymidine release. (F) U2OS cells were transfected with Cdc20 RNAi as in **D**, but ProTAME was added 6h after thymidine release and imaged by fluorescence and DIC microscopy at 3 min intervals.

Nek2A and Nek2B bands). Low levels of Nek2A protein were also detected in Cdc20 immunoprecipitations, together with the APC/C (**Fig. 4B**, Cdc20 IPs). Whereas Mad2 bound predominantly to mitotic APC/C^{Cdc20}, Nek2A similarly bound G2-phase or mitotic APC/C^{Cdc20} (**Fig. 4B**). Apparently, and in contrast to cyclin A, Nek2A is recruited to the APC/C in interphase, before it gets degraded in mitosis. Furthermore, APC/C-binding of Nek2A occurred independently of Cdc20 or Cdh1 (**Fig. 4C**,^{35,264}). Cdc20 or Cdh1 depletion did not affect binding of Nek2A to the G2-phase APC/C, indicating there is no competition between co-activators and Nek2A for APC/C binding, nor is there a clear stimulatory effect of the co-activators on recruitment of Nek2A to the APC/C (**Fig. 4C**). This shows that degradation of Nek2A is not initiated by its increased binding to APC/C^{Cdc20} and implies that the start of Nek2A degradation, which we show is entirely APC/C^{Cdc20}-dependent, reflects the exact moment when Cdc20 activates the APC/C.

For its timely degradation, cyclin A needs to compete Mad2 and/or BubR1 away from Cdc20^{86,251,265}. However, in nocodazole-arrested cells treated with MG132 after mitotic shake-off, we found that Nek2A is in complex with Cdc20 as well as Mad2 (**Fig. 4D**). Furthermore, in BubR1 IPs of mitotic cells treated with nocodazole and, treated with MG132 after mitotic shake-off, we detected APC/C, Cdc20 and Nek2A (**Fig. 4E,F**). This is in agreement with earlier *in vitro* experiments that showed Nek2A does not interfere with BubR1-Cdc20 complex formation⁸². While both Nek2A and checkpoint proteins bind the APC/C, only a small amount of Nek2A re-accumulates on the MCC-bound APC/C during the course of MG132 treatment. Nek2A will probably also bind apo-APC/C (**compare Fig. 4E**, APC4 IP versus BubR1 IP).

We conclude that the mechanisms by which cyclin A and Nek2A escape stabilization by the spindle checkpoint are most likely different, for the following reasons: i) Nek2A starts to be degraded exactly at the prophase-to-prometaphase transition, which in most experiments, is detectable several minutes before cyclin A starts to decline; this difference may be explained by the special dependence of cyclin A destruction on competition between spindle checkpoint proteins and cyclin A for Cdc20 binding; ii) in contrast to that of cyclin A, Nek2A destruction is completely insensitive to increased MCC formation, induced by nocodazole treatment; iii) Nek2A destruction, but not cyclin A destruction, proceeds effectively under conditions of approximately 95% Cdc20 depletion, or after 20 mM proTAME treatment; iv) while cyclin A degradation was found to depend on a competition mechanism between cyclin A and BubR1, required to liberate Cdc20²⁵¹, Nek2A, even at high concentrations, does not compete for BubR1 binding to Cdc20 *in vitro*⁸²; indeed, here we show that Nek2A can form complexes with BubR1-inhibited APC/C, and v) Nek2A binds to the APC/C in G2 phase, prior to its

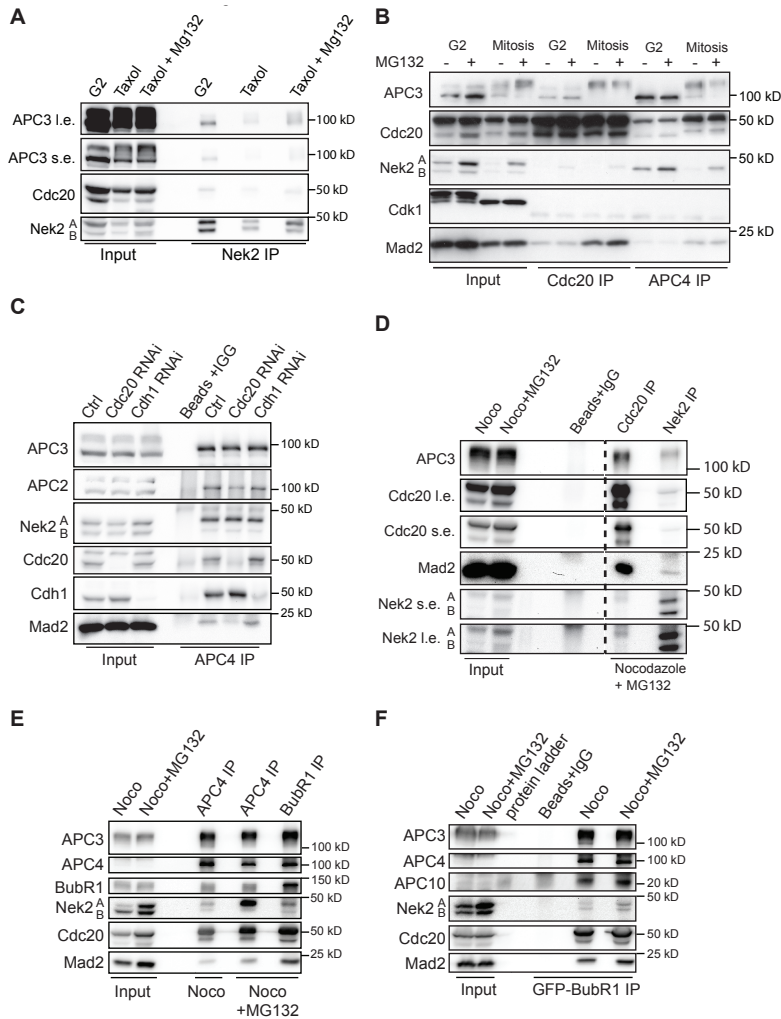


Figure 4. Nek2A is recruited to the APC/C in G2-phase as well as in mitosis, independently of Cdc20.

(A) To compare binding of Nek2A to the APC/C in G2-phase versus mitosis, we compared 8h thymidine released U2OS cells to cells released from 24h thymidine block into taxol for 16h and after 2 hours addition of MG132. Nek2 antibodies were used for precipitation, followed by Western blot analysis. (B) Immunoprecipitations were performed on 8h thymidine-released cells in G2-phase, and cells synchronized by thymidine and released into nocodazole collected by mitotic shake off. Proteasome inhibitor MG132 was added where indicated, to reveal unstable protein. Lysates were equally divided for precipitations with antibodies as indicated. (C) U2OS cells were transfected with indicated RNAi and synchronized in G2-phase by thymidine treatment followed by 8h release. APC4 antibodies were used to immunoprecipitate the APC/C. (D) Cells were synchronized by thymidine and release into nocodazole, and treated for the final 2h with proteasome inhibitor. Lysate was divided and Cdc20 and Nek2 were precipitated with antibodies. Take note that the Nek2 antibody recognizes and precipitates both the Nek2A and Nek2B isoform. (E) U2OS cells were synchronized as in D and lysate from mitotic cells treated for 2h with proteasome inhibitor were divided to precipitate either APC4 or BubR1. (F) HeLa cells expressing LAP-BubR1 were synchronized as in D, and GFP antibodies were used to precipitate the ectopically expressed BubR1.

destruction in mitosis, whereas cyclin A, in complex with Cdc20, is only recruited to the APC/C from prometaphase onwards, when it is also degraded⁸⁶.

Interestingly, in *in vitro* APC/C ubiquitination assays, Cdc20 that is part of the MCC has a small positive effect on APC/C activity, too^{11,216,266}. Also, autoubiquitination of Cdc20 occurs while the checkpoint is actively inhibiting the APC/C, showing that the APC/C, in principle, can target its substrates regardless of being bound to the MCC^{96,103,191,267,268}. Taken all observations together, we therefore propose that, in cells, binding of spindle checkpoint proteins does not completely prevent the ability of Cdc20 to activate the APC/C, to the minimal level that is required to efficiently process Nek2A. APC/C^{MCC} (or APC/C^{MCC-CDC20}, see Izawa and Pines 2014) probably has a catalytic activity that is slightly higher than that of late prophase APC/C, when Emi1 is degraded but Cdc20 is not yet bound. This activity forms right at nuclear envelope breakdown, by the binding of MCC to phosphorylated APC/C. Formation of APC/C^{MCC} alone does not lead to cyclin A turn-over, but may just be sufficient to catalyze the Cdc20-dependent degradation of Nek2A, immediately at the prophase-to-prometaphase transition. Nevertheless, we cannot fully rule out that, in cells, a small amount of Cdc20 will never be incorporated into the MCC, but still binds to the APC/C at the start of mitosis and is responsible for Nek2A destruction.

Degradation of a Nek2A mutant that is not pre-recruited to the APC/C, Nek2A Δ MR, requires spindle checkpoint release

Mutation of the TPR-binding MR tail of Nek2A prevents its binding to the APC/C, also in G2 phase (**Fig. 5A**) and delays, but does not prevent, Nek2A degradation in mitosis^{82,264}. Because we found that Nek2A destruction is entirely Cdc20-dependent, we reasoned that in the absence of APC/C binding by its MR tail, Nek2A should turn into a spindle checkpoint-controlled substrate. To test this, we generated cell lines stably expressing a mutant of Venus-Nek2A lacking the MR tail (Venus-Nek2A Δ MR) together with the spindle checkpoint-target geminin-Cherry²⁴⁵. When comparing these two substrates in single cells, we found a complete overlap of their destruction curves (**Fig. 5B**, note that here the graphs are synchronized around anaphase onset; **Supplemental Fig. 1A**). Importantly, degradation of Nek2A Δ MR became highly sensitive to Cdc20 depletion, similar to that of geminin (**Fig. 5C**). We also compared the timing of Nek2A Δ MR destruction to that of Aurora-eCFP, a known APC/C^{Cdh1} substrate^{70,269}, and found that Venus-Nek2A Δ MR was degraded well before Aurora A (**Supplemental Fig. 4A**) and independently of Cdh1 (**Supplemental Fig. 4B**). Nek2A Δ MR remained largely stable during a taxol-induced mitotic delay (**Supplemental Fig. 4C**), similar to cyclin B1^{247,270,271}. When the spindle checkpoint was silenced by the Mps1 inhibitor reversine, destruction of Geminin-Venus and Cherry-Nek2A Δ MR began at nuclear envelope breakdown (**Fig. 5D**). We conclude that abolishing the binding of Nek2A to

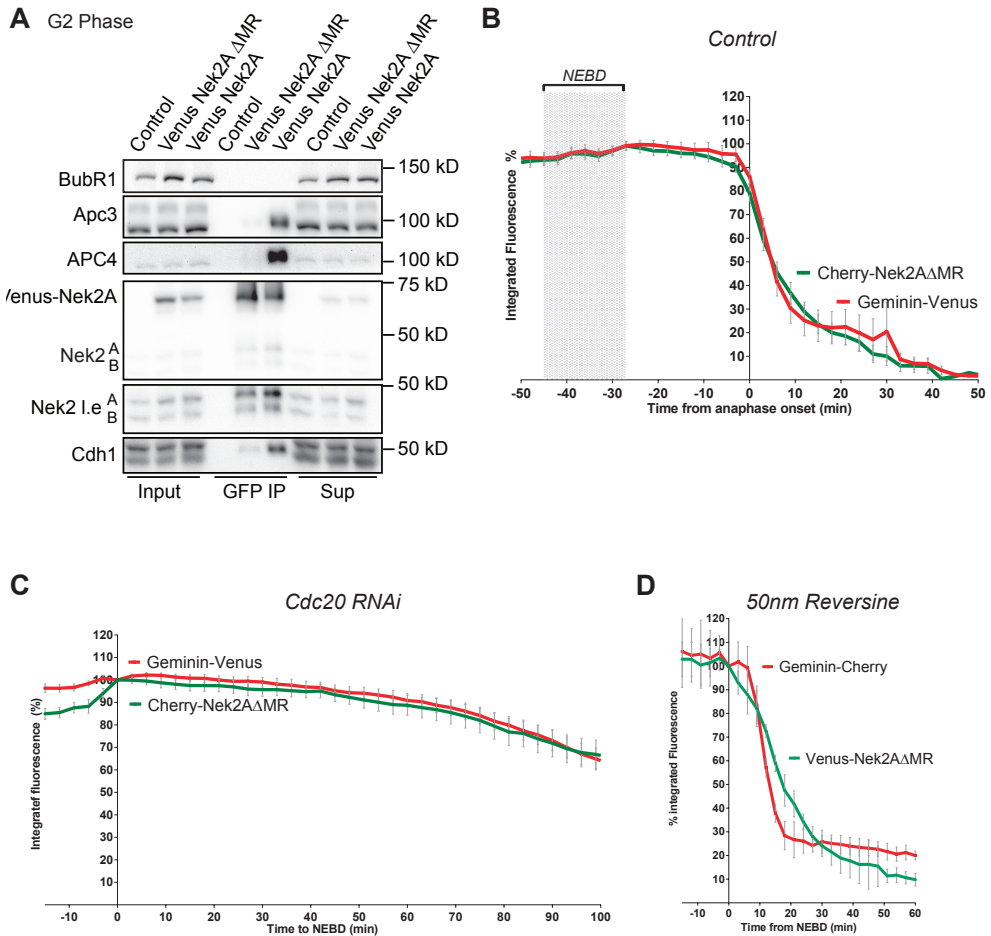


Figure 5. Degradation of a Nek2A mutant that is not recruited to the APC/C, Nek2A Δ MR, is delayed until spindle checkpoint release.

(A) U2OS cells stably expressing with Venus-Nek2A or Venus-Nek2A Δ MR were synchronized in G2 by an 8h release from thymidine block. Nek2A fusion protein was precipitated with anti-GFP nano-trap beads after lysis. The supernatant shows protein not bound to antibody-coupled beads. (B) U2OS cells stably transduced with Venus-Nek2A Δ MR and Geminin-Cherry constructs were imaged by fluorescence and DIC microscopy at 3 minute intervals. In this case, the degradation curves were synchronized by the onset of sister chromatid separation at the start of anaphase, as judged by DIC. N=10 mean \pm s.e.m. (C) U2OS cells stably transduced with Venus-Nek2A Δ MR and Geminin-Cherry constructs were treated with *Cdc20* siRNAi and cells with mitotic delay were quantified for fluorescent levels (mean time from NEBD-Ana 113.5 min), combined n=17 from 3 independent experiments. Plotted is the mean \pm s.e.m. (D) U2OS cells stably transduced with Venus-Nek2A Δ MR and Geminin-Cherry were imaged by fluorescence and DIC microscopy at 3 minute intervals, in the presence of 50nm reversine. Levels were normalized to the frame of NEBD. n=5 Mean \pm s.d. Scale bar = 10 μ M.

the APC/C makes Nek2A destruction strictly dependent on an activity of Cdc20 that can only be released by passing the spindle checkpoint.

A Nek2A mutant that lacks the APC/C recruitment tail and the KEN destruction motif is stable in mitosis

The model emerging from our study is that spindle checkpoint-restricted APC/C^{Cdc20} has sufficient catalytic activity to initiate destruction of Nek2A, provided that Nek2A is constitutively recruited towards the APC/C. Spindle checkpoint proteins typically prevent the binding of Cdc20 to a destruction motif such as the D-box or the KEN box. The Nek2 gene is spliced into 3 different isoforms of which Nek2A is the longest²⁷². This is the only isoform to contain an evolutionary conserved KEN box. In line with the spindle-checkpoint independence of Nek2A destruction, mutating the KEN box did not stabilize Nek2A (Cherry-Nek2A-AEN, **Fig. 6A**; **Supplemental Fig. 1A**; also see⁸²). Then, we investigated whether the KEN box could contribute to the spindle checkpoint-dependent destruction of Nek2A Δ MR. Interestingly, a double Nek2A mutant, lacking both the APC/C-binding tail and the KEN destruction motif, remained fully stable throughout mitosis (**Fig. 6B**; **Supplemental Fig. 1A**). First, this result confirms that Nek2A degradation is indeed entirely dependent on the APC/C. Secondly, it shows that the spindle checkpoint very effectively blocks the recognition of the Nek2A KEN box by APC/C^{Cdc20}. Normally, this does not occur in mitosis because Nek2A has largely disappeared when cells reach anaphase. The Nek2A KEN box did not play a role in binding Nek2A to the APC/C in G2 phase (**Fig. 6C**). These results imply that preventing binding of destruction motifs, like the KEN box, to Cdc20 is the main mechanism by which the spindle checkpoint stabilizes APC/C substrates in prometaphase. Indeed, the MCC complex inhibits APC/C-Cdc20 by binding to the KEN box and D-box receptor²⁶⁶. Nek2A destruction normally does not depend on a destruction motif, so it can start in the presence of an active spindle checkpoint as soon as Cdc20 activates the APC/C. Only after satisfaction of the spindle checkpoint, APC/C^{Cdc20} starts to recognize APC/C destruction motifs such as the cyclin B1 D-box, or the Nek2A KEN box.

Removal of the spindle checkpoint accelerates Nek2A degradation

Although the spindle checkpoint inhibits the binding of Cdc20 to destruction motifs²⁴⁶, it is possible that the checkpoint also impairs, at least to some extent, the ability of Cdc20 to promote the catalytic activity of the APC/C⁴⁸. Indeed, *in vitro* APC/C^{MCC}, although not completely inactive, was less active than checkpoint-free APC/C^{Cdc20}^{11,225,273}. This is in line with several other studies showing that the checkpoint inhibits APC/C catalytic activity^{163,189,274}.

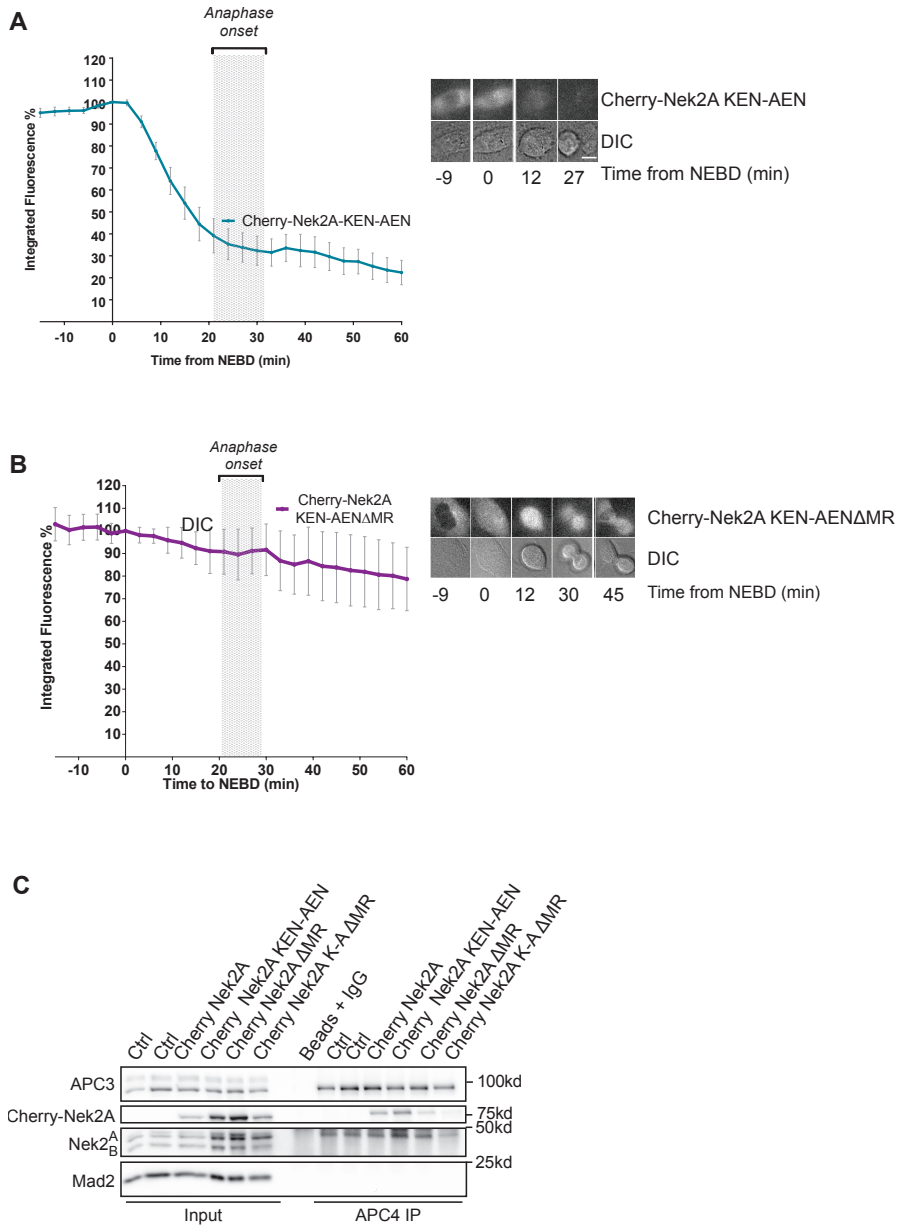


Figure 6. A Nek2A double mutant lacking its APC/C pre-recruitment tail as well as its spindle checkpoint controlled Cdc20-binding box (KEN) is fully stable in mitosis.

(A) U2OS cells stably transduced with Cherry-Nek2A KEN-AEN were imaged by fluorescence and DIC microscopy. Integrated fluorescence was measured and normalized to 100% at the start of NEBD as described in the Legend to Figure 1 Scale bar = 10 μ M. (B) U2OS cells stably transduced with Cherry-Nek2A AEN Δ MR were imaged by fluorescence and time lapse microscopy. (C) U2OS- cells stably expressing Cherry-Nek2A or its mutant versions were synchronized in G2 by 8h release after 24h thymidine treatment. After lysis the APC/C was immuno-precipitated using APC4 antibodies and analysed by Western blot.

Next, we tested whether inability to activate the spindle checkpoint at the prophase-to-prometaphase transition would further increase APC/C^{Cdc20} activity towards Nek2A, as also shown for cyclin A¹⁴⁸. Therefore, we abolished the spindle checkpoint by treating G2 phase cells with the Mps1 inhibitor reversine,^{275,276} or with Mad2 RNAi, and measured the degradation of geminin-Cherry and Venus-Nek2A as cells entered mitosis (**Fig. 7A**, upper panel and lower panel, respectively). The average time of NEBD to anaphase in control cells was 25.4 minutes (± 4.8 s.d.) (**Fig. 7B,C**) while bypass of the checkpoint reduced the duration of mitosis to 14.3 (± 2.5 s.d.; reversine) and 12.6 (± 1.9 s.d. min; Mad2-RNAi) min (**Fig. 7B,C**). Geminin-Cherry levels reached 50% of their maximal fluorescence within 31.3 minutes in controls (± 8.1 s.d.), which was accelerated approximately two-fold by either means of checkpoint inhibition, to 15.8 minutes ± 2.1 s.d. in reversine-treated cells and 15.4 minutes ± 3.0 s.d. for Mad2 RNAi cells (**Fig. 7B,C**). Remarkably, Nek2A was also degraded approximately two fold faster after silencing the spindle checkpoint: we found a decrease in half-life from 14.36 minutes in controls to 8.0 minutes (± 1.5 s.d.) for reversine-treated cells and 8.7 minutes (± 1.8 s.d.) for Mad2-depleted cells (**Fig. 7A,B,C**). Under both experimental conditions the order of substrate degradation was unaltered, in line with the idea that direct Nek2A binding to the APC/C makes it a uniquely effective substrate. We then investigated whether the KEN box played a critical role in accelerating degradation of Nek2A in the absence of the spindle checkpoint. While a single point mutant in the KEN box was enough to prevent binding in the absence of the MR tail (**Fig. 6C**), we now mutated the complete KEN box. Importantly, the destruction of a complete alanine-substitution mutant of the Nek2A KEN box, Venus-Nek2A-KEN-AAA, also occurred faster upon reversine treatment (**Fig. 7D**). Altogether, these results therefore indicate that removal of the spindle checkpoint, independently from facilitating the recognition of a KEN box by Cdc20, slightly increases APC/C^{Cdc20} activity from the start of prometaphase onwards. In conclusion, the spindle checkpoint predominantly blocks binding of Cdc20 to destruction motifs of APC/C substrates, but also slightly attenuates the catalytic activity of APC/C^{Cdc20} in prometaphase. The latter inhibitory effect of the spindle checkpoint is insufficient to prevent Nek2A destruction and is also not enforced by spindle poisons.

DISCUSSION

Different pathways direct the spindle checkpoint-independent destruction of Nek2A and cyclin A

The stability of every APC/C substrate may be governed in a unique way to ensure its degradation occurs at a specific point in the cell cycle (e.g.²⁷⁷) Cyclin A and cyclin B1 are both APC/C substrates that similarly depend on Cdc20 for their destruction, but they are degraded at different times in mitosis²⁵⁰. Whereas cyclin A gets degraded in prometaphase, cyclin B1 is stabilized by the spindle checkpoint until metaphase.

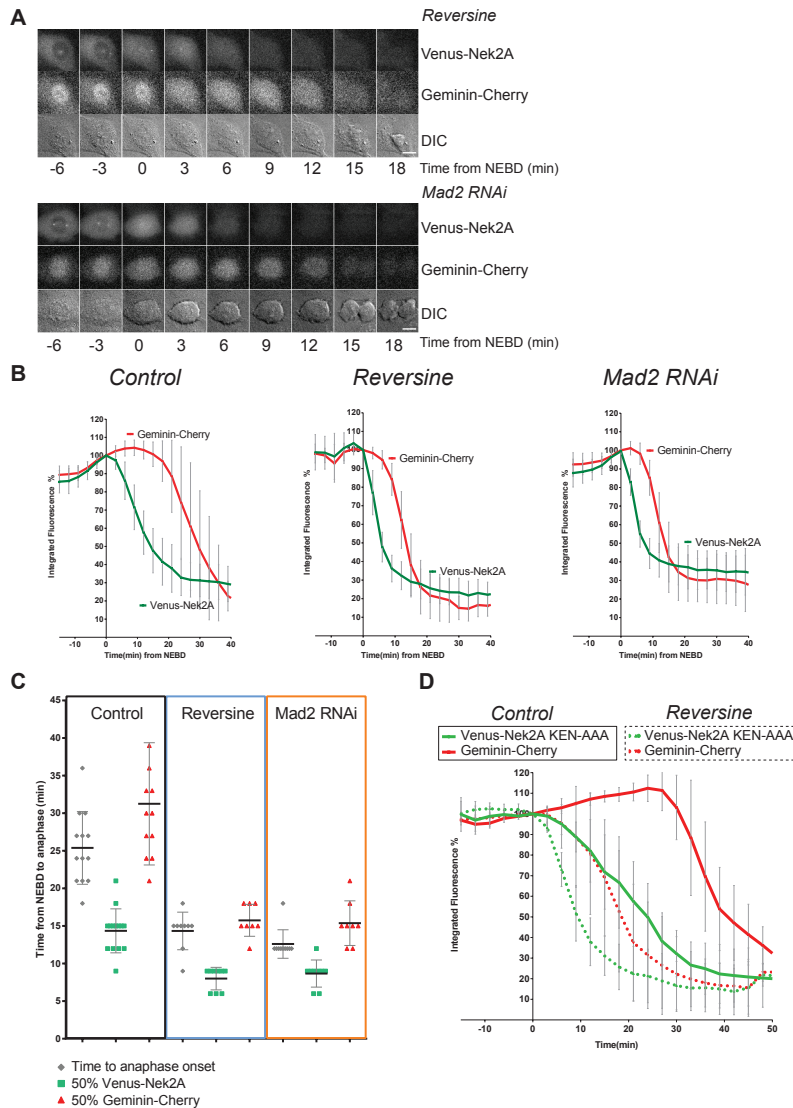


Figure 7. Checkpoint silencing accelerates Nek2A destruction independently of the Nek2A KEN box, but does not alter the order of substrate processing.

(A) Panels of U2OS cells stably transduced with Geminin-Cherry and Venus-Nek2A were imaged by fluorescent and DIC microscopy. The spindle checkpoint was abrogated by treatment with 50 nm reversine, upper panel or by depletion of Mad2 by RNAi, lower panel Scale bar = 10 μ M. (B) Graphs represent mean \pm s.d., normalized to 100% fluorescence at frame of NEBD as indicated in the legend of Figure 1. Control cells n=10, reversine n= 10, Mad2 RNAi n=10. (C) From the time lapse experiments shown in B, the time from NEBD to anaphase as judged by fluorescent and DIC channel as well as the time to 50% fluorescence is plotted for Venus-Nek2A and Geminin-Cherry in normal mitosis, or reversine-treated and Mad2-depleted mitotic cells. (D) Cells expressing stably expressing Venus-Nek2A-KEN-AAA were imaged at 3 minute intervals as described in the Legend to Figure 1, in either control situation (solid line) or in the presence of 50nm reversine (dotted line).

Previously, we and others showed that the N-terminus of cyclin A binds to Cdc20 in such a way that it competitively inhibits the ability of checkpoint proteins to bind Cdc20. These ‘checkpoint-free’ cyclin A-Cdc20 complexes are then recruited to the phosphorylated APC/C in mitosis (**Fig. 8**). Here, we show that another mitotic regulator that disappears rapidly in prometaphase, Nek2A, requires only very limited amounts of Cdc20 to be degraded effectively. Nek2A destruction also does not detectably depend on binding to Cdc20, or on a canonical KEN box or D-box destruction motif. Inhibiting the ability of APC/C^{Cdc20} to bind to destruction boxes, by treatment with the recently discovered APC/C inhibitor APCin, did not stabilize Nek2A (¹⁹⁹ and unpublished data). Nevertheless, Nek2A relies exclusively on APC/C^{Cdc20} to be degraded in mitosis: simultaneously reducing Cdc20 levels by RNAi, combined with inhibiting Cdc20 binding to the APC/C by proTAME, completely blocks Nek2A destruction. Reducing the levels of APC/C subunits by RNAi had surprisingly little effect on Nek2A degradation, especially when compared to spindle checkpoint-dependent APC/C^{Cdc20} substrates. This most likely reflects the fact that Nek2A is a very effective APC/C substrate: Nek2A is constantly targeted to the APC/C, possibly to the TPR motif containing APC8 (although a role for other subunits has not been excluded, see also⁸²), and this renders Nek2A highly sensitive for efficient Cdc20-dependent degradation.

By treating mitotic cells with nocodazole, more checkpoint signal is generated, as Mad2 is bound threefold as effectively to Cdc20¹⁴⁸. This slows down cyclin A degradation, but not Nek2A degradation. An attenuating effect of increasing spindle checkpoint strength on cyclin A disappearance fits with the unique requirement for competition between cyclin A and spindle checkpoint proteins for Cdc20 binding.

The time when Nek2A destruction begins in mitosis is not set by increased Nek2A recruitment to Cdc20 or the APC/C, but marks the point when Cdc20 starts to catalytically activate the APC/C (**Fig. 8**). In contrast, cyclin A destruction requires the prior formation of stable complexes between cyclin A and Cdc20, their timely recruitment to the prometaphase APC/C, and finally a function of Cdc20 that is sensitive to the spindle checkpoint, possibly the positioning of the cyclin A N-terminus towards the active site of the APC/C (**Fig. 8**).

Nek2A disappearance marks the point when Cdc20, regardless of the spindle checkpoint, activates the APC/C

While we recently discovered that Nek2A is very slowly degraded by an APC/C-dependent mechanism during S- and G2-phases (²⁷⁸, and unpublished data), Nek2A disappears only in mitosis. This not due to decreased translation of Nek2A at mitotic entry, because Nek2A is still rapidly synthesized in mitosis (e.g. see Fig. 4B). We think that the simplest model explaining our data is that rapid Nek2A disappearance marks

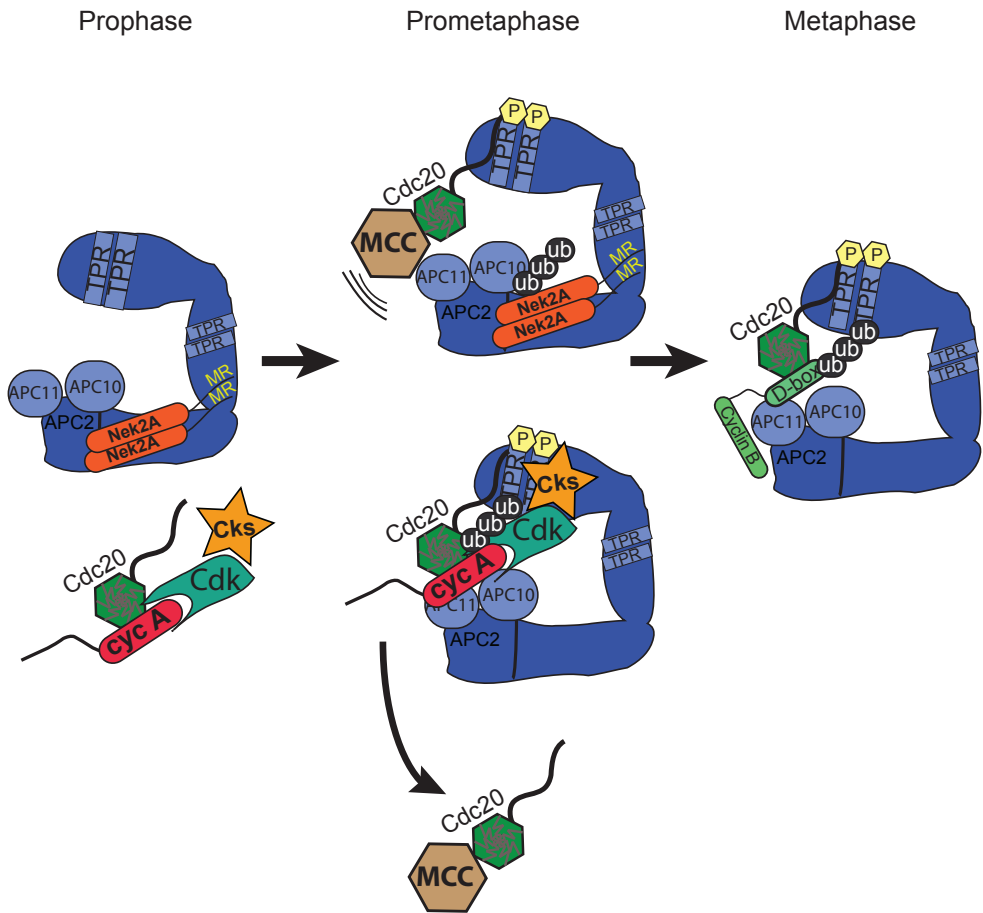


Figure 8. Cdc20-independent binding of Nek2A in G2, and activation of the APC/C by Cdc20, direct the destruction of Nek2A in the spindle checkpoint.

In prophase, the APC/C inhibitor Emi1 is degraded, and Cdh1 is removed from the APC/C, e.g. by increasing Cdk1-dependent phosphorylation. Therefore, at this time in the cell cycle, the APC/C is mostly present as a complex without co-activator bound. At mitotic entry, Cdc20 starts to bind the APC/C and the spindle checkpoint is activated. Nek2A binding to the APC/C is not regulated by mitotic entry or the presence of a co-activator. Upon transition to mitosis, Cdc20 activates the APC/C, whether or not it is restricted by the mitotic checkpoint (MCC) and this allows for immediate degradation of pre-recruited Nek2A, in a manner independent of a known Cdc20-binding destruction motif or of significant amounts of Cdc20. We observe no competition between Cdc20 and Nek2A for APC/C binding, nor an increase in Nek2A binding to the APC/C when cells enter mitosis. We propose that this reflects the catalytic activation of the APC/C by induced binding of Cdc20. Geminin and cyclin B1 bind the APC/C in a D-box and Cdc20-dependent manner and is processed in metaphase.

the point when Cdc20, regardless of its incorporation into or inhibition by the MCC, activates the APC/C at the prophase-to-prometaphase transition.

At mitotic entry, Cdc20 binds the APC/C by means of its C-terminal tail⁴⁴, the KILR motif²⁴⁸ and by its N-terminal C-box³⁵. The binding of Cdc20 to the APC/C is enforced by mitotic phosphorylation of the APC/C, but also by the spindle checkpoint: the Cdc20 C-box may be involved in stabilizing complexes between the APC/C and spindle checkpoint proteins⁴⁹. So, Cdc20, when incorporated in the MCC, effectively complexes with the APC/C at the start of prometaphase. Recent *in vitro* data showed that Nek2A ubiquitination may be refractory to increasing levels of checkpoint proteins²¹⁶. Moreover, activation of the E2 enzyme Ube2S does not seem to be hindered by the checkpoint proteins in its ability to elongate Nek2A mono-ubiquitin chains *in vitro*²¹⁶. Intriguingly, the MCC has been shown to bind two Cdc20 molecules²⁶⁶, as also hypothesized before²¹. BubR1 blocks the substrate recognition domain of the Cdc20 molecule bound to the APC/C^{41,146}. We also find that the spindle checkpoint predominantly acts to prevent Cdc20 from binding to destruction motifs (Fig. 5 and Fig. 6). Nek2A destruction is only dependent on an APC/C activating step that coincides with the association of Cdc20 to the APC/C in mitosis. However, a mutant of Nek2A, Nek2ADMR, critically needs a KEN box for its destruction and is easily stabilized by Cdc20 depletion, as well as strictly controlled by the spindle checkpoint. This fits with the concept that the spindle checkpoint particularly blocks stoichiometric complex formation between Cdc20 and APC/C substrate destruction motifs.

Virtually no BubR1-free APC/C^{Cdc20} was detected in spindle poison-arrested cells, unless these cells were treated with proteasome inhibitor¹¹. This indicates that any Cdc20 free of checkpoint proteins is rapidly degraded in nocodazole-arrested cells (e.g. see Fig 4E). This, combined with the observation that enforcing the spindle checkpoint does not delay Nek2A degradation, supports our hypothesis that even spindle checkpoint-inhibited Cdc20 is able to partially activate the APC/C at prometaphase (Fig. 8). Alternatively, however, a very small fraction of APC/C^{Cdc20} remains completely uninhibited during prometaphase and is sufficient for Nek2A destruction to proceed entirely regardless of the spindle checkpoint.

Role for spindle checkpoint silencing in further activating the APC/C after metaphase?

Our results reveal a paradoxical role of the spindle checkpoint in Nek2A degradation. Drug-induced enforcement of the spindle checkpoint cannot delay the time when Nek2A degradation starts but ablating the spindle checkpoint, by treating cells with Mps1 inhibitor or depleting Mad2, increases the rate by which Nek2A disappears. This can be explained by assuming that whereas the spindle checkpoint blocks recognition

of destruction motifs very effectively, it only moderately impairs the catalytic activity of the APC/C^{Cdc20} during prometaphase.

Interestingly, this would also imply that, in cells that pass through mitosis normally, APC/C^{Cdc20} gains further activity after spindle checkpoint release during metaphase and anaphase⁶⁹. The nature of the increased APC/C^{Cdc20} activity could be two-fold: either the C-box of Cdc20 becomes unrestricted by checkpoint release and triggers a catalytic activation of the APC/C complex to which it is already bound, or the total number of APC/C^{Cdc20} complexes in cells increases at metaphase, because the spindle checkpoint prevents accumulation of Cdc20 onto the APC/C in prometaphase^{103,189,191}. While we were preparing this manuscript, the Barford lab published that binding of the N-terminal part of Cdh1, containing the C box, identical to the C box in Cdc20, interacts with APC1¹², and allows for conformational change of the APC/C catalytic module, APC2-APC11. Their work also implies that release of the spindle checkpoint enhances binding of ubiquitin-bound UbcH10, boosting the activity of the APC/C. Likely, checkpoint silencing will not only permit increased UbcH10 binding, but also increased Ube2S binding and thus higher APC/C catalytic activity³⁷. Recently, we and others proposed that enhanced APC/C^{Cdc20} activity upon spindle checkpoint release might help to avoid the ‘anaphase problem’: the risk that separating sister chromatids when losing tension could re-impose the spindle checkpoint in case cyclin B1 is not completely degraded when cells reach anaphase^{279–282}. The implications of these findings require further analysis of the way changes in APC/C^{Cdc20} influence mitotic exit.

MATERIALS AND METHODS

Tissue Culture and cell cycle synchronization

Human Osteosarcoma cells were grown in DMEM (Gibco) containing FCS (Sigma), penicillin, streptomycin and cultured at 37°C in 5% CO₂. 24 or 48 hours before synchronization or transfection, cells were plated on 9 cm Falcon dishes or, for time-lapse fluorescence microscopy on 3,5 mm glass-bottom dishes (Wilco Wells) or 4-well glass bottom dishes (Labtek II). For enrichment of cells in G2 phase, cells were treated for 24 hours with thymidine (Sigma, 2,5 mM final concentration) and incubated for 8 hours after release.

Other drugs, used as indicated: Mps1 inhibitor reversine (#10004412, 50 nM final concentration; Cayman Chemicals); proteasome inhibitor MG132 (#13697, 5 μM final concentration; Cayman Chemicals); translation inhibitor cycloheximide (#C6255, 5 or 10 μM final concentration; Sigma-Aldrich), RO-3306 (#217699, 3 μM final concentration [Calbiochem]), ProTAME (I-440, 12μM final concentration or as noted; R&D systems).

Plasmids

Nek2A was cloned from cDNA into Clontech C1 vector, encoding either a Cherry or Venus fluophore, and subsequently cloned into Clontech pLib vectors. To create stable cell lines Phoenix-ecotropic cellines were transfected in 6 well plates with 4µg of pLIB-vector containing the insert of choice, using standard calcium phosphate transfection. Viral supernatant was collected three times, 40, 48 and 64h after transfection. The supernatant was cleared through a 0.45-µm filter (EMD Millipore). U2OS cells expressing the ecotropic receptor (from Johan Kuiken, NKI, Amsterdam, Netherlands) were infected twice in the presence of polybrene.

Transfections and retroviral infection

Cells were transfected with 40 nM siRNA oligo pools (ON-TARGET-plus oligos, Dharmacon) using lipofectamine 2000 (Invitrogen) according to manufacturer's protocol. The siRNAs to target Nek2 (targeting both Nek2A and Nek2B)

(5'-GGAUCUGGCUAGUGUAAUU-3' 5'- GCAGACAGAUCUGGGCAU
-3' 5'- GGCAAUACUUAGAUGAAGA -3' 5'- GCUAGAAUUAUAAACCAUG
-3') Cdc20 (CDC20)(5'- CGGAAGACCUGCCGUUACA-3'

5'-GGGCCGAACUCCUGGCAAA-3' 5'-GAUCAAAAGAGGGCAACUAC-3'
5'-CAGAACAGACUGAAAGUAC-3'), Mad2 (MAD2L1)

(5'-UUACUCGAGUGCAGAAAUA-3' 5'-CUACUGAUCUUGAGCUCAU-3'
5'-GGUUGUAGUUAUCUCAAUU-3' 5'-GAAAUCCGUUCAGUGAUCA-3'),
Cdh1 (FZR) (5'-CCACAGGAUUAACGAGAAU-3'

5'-GGAACACGCUGACAGGACA-3' 5'-GCAACGAUGUGUCUCCCUA-3'
5'-GAAGAAGGGUCUGUUCACG-3'), APC2 (ANAPC2)

(5'-GAGAUGAUCCAGCGUCUGU-3' 5'-GACAUCAUCACCCUCUAUA-3'
5'-GAUCGUAUCUACAACAUGC-3' 5'-GAGAAGAAGUCCACACUAU-3'),

Apc10 (ANAPC10) (5'-GAGCUCCAUUGGUAAAUUU-3'

5'-GAAAUUGGGUCACAAGCUG-3' 5'-GCAAUCAGAUGGUUCCAG-3'
5'-CAUGAUGUAUCGUUCAUA-3', APC3 (Cdc27)

(5'-GGAAAUAGCCGAGAGGUAA-3' 5'-CAAAGAGCCUUAGUUUAA-3'
5'- AAUGAUAGCCUGGAAAUUA-3' 5'-GCAUAUAGACUCUUGAAAG-3'),

Ube2S (UBE2S) (5'-ACAAGGAGGUGACGACACU-3'

5'-GGAGGUCUGUCCGCAUGA-3' 5'-GCAUCAAGGUCUUUCCCAA-3'
5'-CCAAGAAGCAUGCUGGCGA-3', UbcH10 (Ube2C)

5'-GAACCCAACAUUGAUAGUC-3', 5'-UAAAUAAGCCUCGGUUGA-3',

5'-GUAUAGGACUCUUUAUCUU-3' and 5'-GCAAGAAACCUACUCAAG-3'

were purchased from Thermo Fisher Scientific as ON-TARGET plus SMART pools.

Antibodies

goat anti-actin (Santa Cruz SC-1616), rabbit anti-APC2 (provided by J.Pines), mouse anti-APC3 (BD Transduction), goat anti-APC4 (Santa Cruz, SC21414), goat anti-Cdc16/APC6 (SC-6395 1:1000), rabbit anti-APC10 (Biolegend 611501/2), mouse anti-BubR1 (Chemicon MAB3612 (1:500)), rabbit anti-BubR1 (Bethyl A300-386a), mouse anti-Cdc20/p55 (Santa Cruz sc-13162), mouse anti-Nek2 (BD 610593 (1:500)), mouse anti-Cdk1 (Cell Signaling), mouse anti-Mad2 (MBL K0167-3), mouse anti-Cdh1 (Neomarkers MS1116-p1), goat anti-Cdk4 (Santa Cruz sc-260), rabbit anti-cyclin A2 (Santa Cruz, H-432), rabbit anti-TopoII α (Bethyl A300-054A-1), rabbit anti-PTTG-1/Securin (Zymed 34-1500 (1:500)), custom rabbit anti-GFP '2C'

Western blotting and Immunoprecipitations

Immunoprecipitations and western blots. Cells were lysed in ELB+ (150 mM NaCl, 50 mM HEPES (pH 7.5), 5 mM EDTA, 0.3% NP-40, 10 mM β -glycerophosphate, 6% glycerol, 5 mM NaF, 1 mM Na₃VO₄ and Roche protease inhibitor cocktail). Lysates were cleared by centrifugation (13,000x g, 12 min at 4°C). Protein levels were equalized by using Bradford analysis. For immunoprecipitations, 2 μ g antibodies were precoupled for 4–12 hours to 20 μ l of protein G Sepharose (Amersham Biosciences) and washed with ELB+. Precoupled beads and lysates were incubated overnight at 4°C and washed three times with 1.0 ml of ice-cold ELB+. All remaining buffer was removed and beads were resuspended in 60 μ l sample buffer; 25 μ l was separated on SDS-PAGE and blotted on nitrocellulose (0.4 μ m pore). Immunoprecipitations of GFP were performed with GFP-Trap_A beads (Chromotek), according to the manufacturer's protocol. Membranes were blocked with 4% ELK in PBS containing 0.1% Tween. Development of blots was either performed with silver film and scanned or using the Chemidoc Imaging System (Bio-Rad Laboratories) and quantification was done with the Image Lab (Bio-Rad Laboratories) software.

Time-lapse fluorescence microscopy

U2OS or RPE1-TERT cells transfected with siRNA and indicated plasmids were followed by fluorescence time-lapse microscopy. Acquisition of DIC and fluorescence images started 24 or 48 h after transfection on a microscope (Axio Observer Z1; Carl Zeiss) in a heated culture chamber (5% CO₂ at 37°C) using DMEM with 8% FCS and antibiotics. The microscope was equipped with an LD 0.55 condenser and 40 \times NA 1.40 Plan Apochromat oil DIC objective and CFP/YFP and GFP/HcRed filter blocks (Carl Zeiss) to select specific fluorescence. Images were taken using AxioVision Rel. 4.8.1 software (Carl Zeiss) with a charge-coupled device camera (ORCA R2 Black and White CCD [Hamamatsu Photonics] or Roper HQ [Roper Scientific]) at 100-ms exposure times. Alternatively imaging was performed on a Deltavision Elite system, using L15

Leibovits medium (Gibco), in a 37°C culture chamber, without the need of supplying CO₂.

For quantitative analysis of degradation, MetaMorph software (Universal Imaging), ImageJ (National Institute of Health) and Excel (Microsoft) were used. Captured images were processed using Photoshop and Illustrator software (Adobe).

ACKNOWLEDGEMENTS

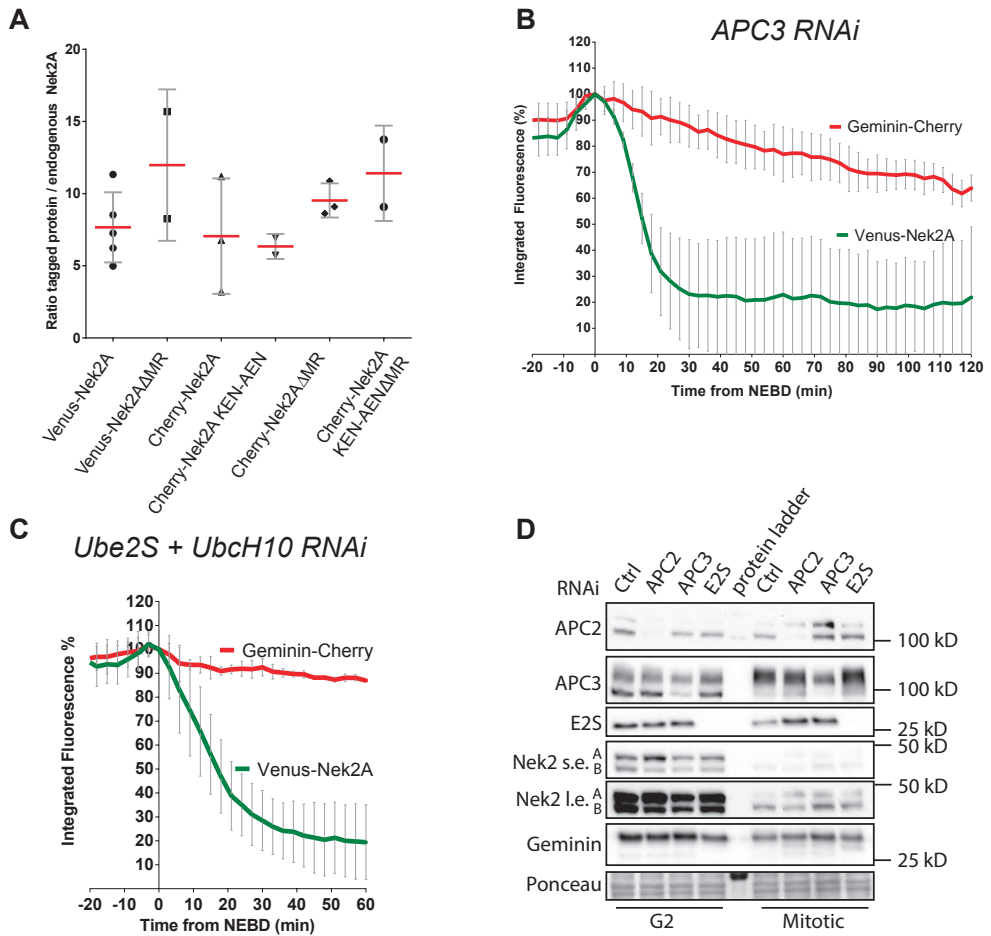
We thank Daisuke Izawa and Jon Pines for providing the APC2 antibody, Arne Lindqvist for sharing the U2OS Tet inducible Cyclin A2-Venus cell line, the Hyman lab for the LAP-BubR1 HeLA celline and Katarzyna Kedziora for assistance with Image J macro writing. We thank Erik Voets and other division members for fruitful discussion and critically reading the manuscript. This project was supported by Human Frontiers Science Program grant RGP0053/2010 (M.B., R.M.F.W.).

Author contributions

R.M.F.W devised the project and designed experiments, MB designed and performed all experiments. M.B. wrote initial draft of the paper which was supervised and edited by R.M.F.W.

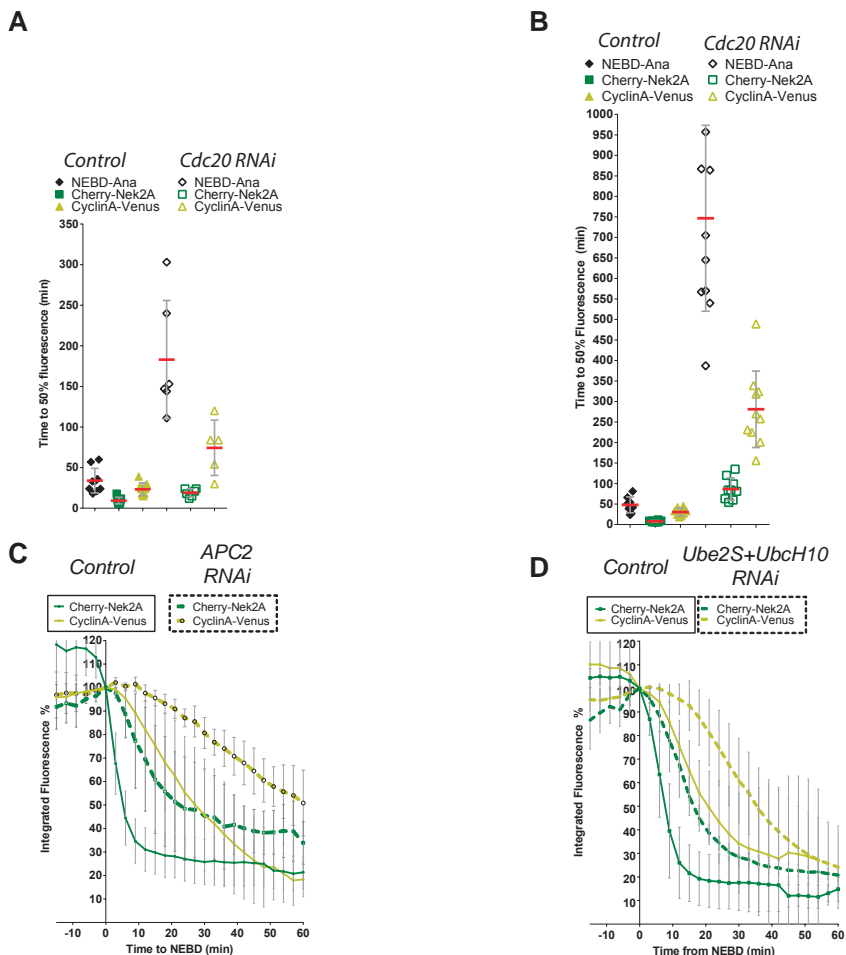
Conflict of Interest

The authors declare that they have no conflict of interest.



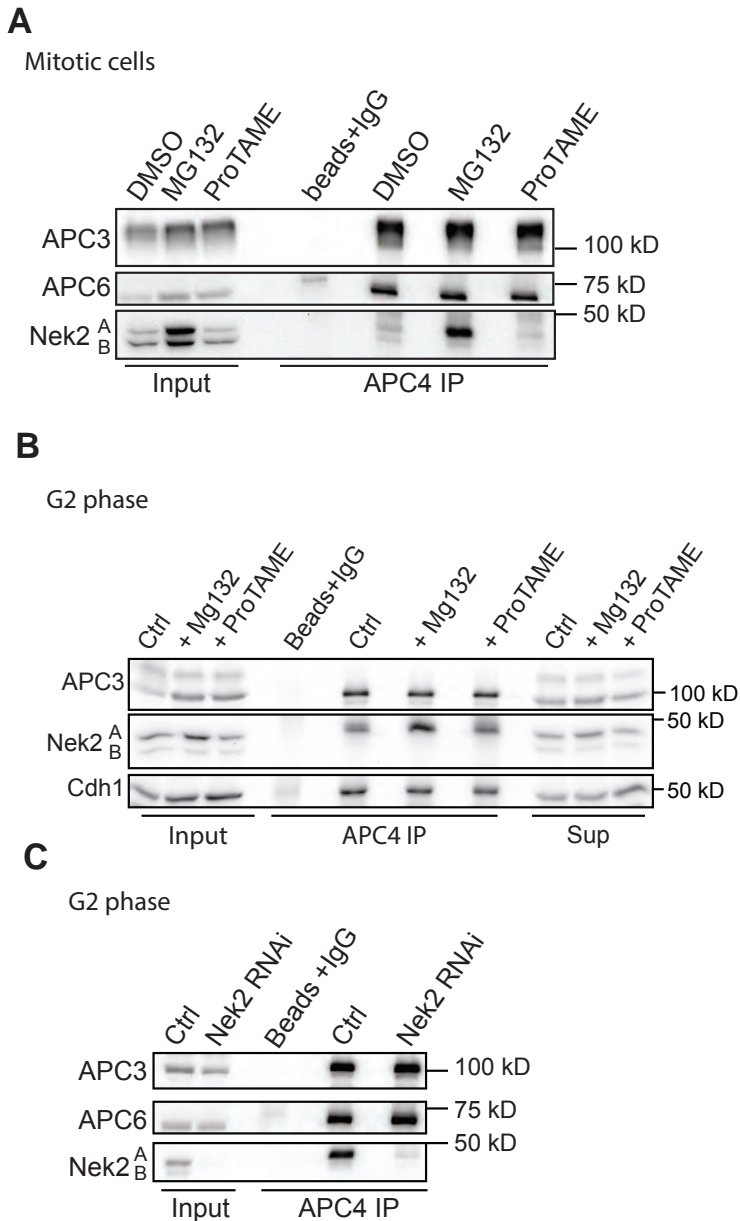
Supplemental Figure 1. Nek2A is not stabilized efficiently by depletion of APC3 RNAi or APC/C E2s.

(A) Lysates of U2OS cells stably expressing indicated fusion protein were analyzed by western blot and ratio of tagged versus endogenous Nek2A are plotted red bar indicates mean \pm s.d.; (B) U2OS cells expressing Venus-Nek2A and geminin-Cherry were transfected siRNA directed against APC3 and analysed by fluorescent and DIC time lapse microscopy as described in the Legend to Figure1. Graphs depicted show mean \pm s.d.; (C) U2OS cells stably expressing Venus-Nek2A and geminin-Cherry were consecutively transfected with UbcH10 and Ube2S RNAi, imaged by time lapse microscopy and quantified as in (B) (D) U2OS cells were transfected by RNAi as indicated, blocked by thymidine for 24h and released for 8h to obtain G2 samples, or released into nocodazole for 16h and, collected by mitotic shake off, and analysed by Western blot.



Supplemental Figure 2. Partial APC/C inhibition does not stabilize Nek2A.

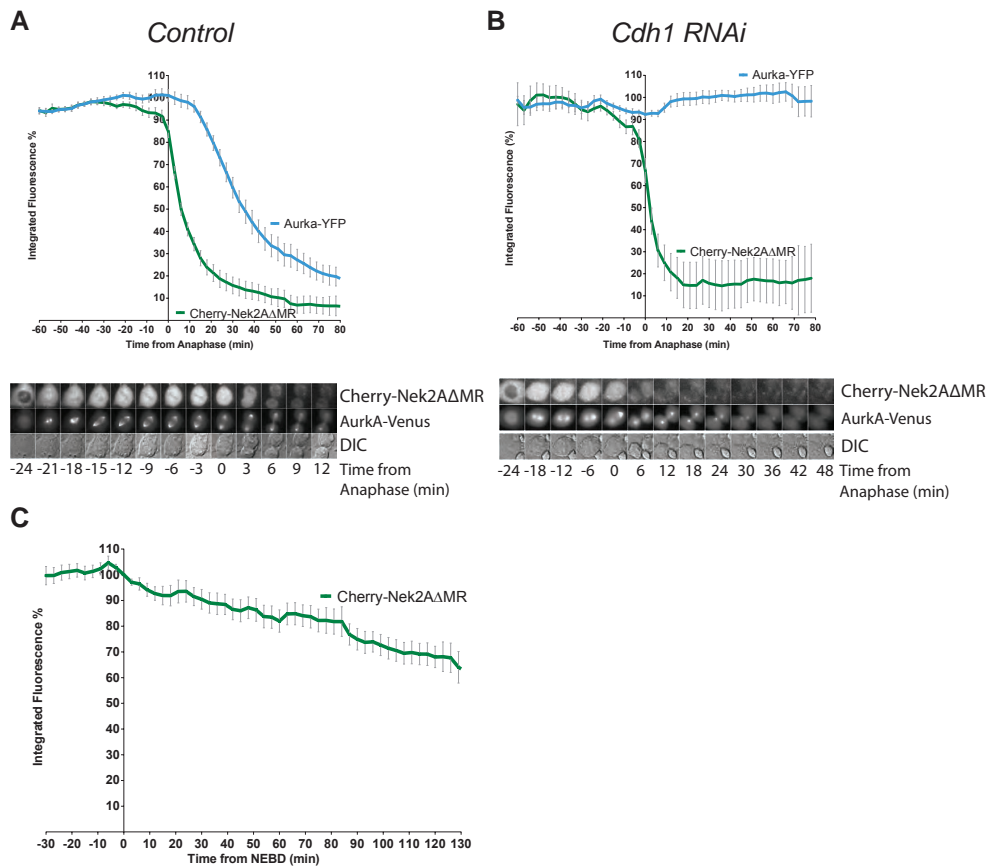
(A) Quantification of fluorescent protein half-life of Cherry-Nek2A and cyclin A-Venus, and time from NEBD to anaphase measured in minutes. Left half of graph shows control situation (closed symbols), right half of graph shows quantification of *Cdc20* RNAi shown in **Fig.3C** (open symbols). (B) Quantification of fluorescent protein half-life of Cherry-Nek2A and cyclin A-Venus, and time from NEBD to anaphase measured in minutes from the experiment shown in **Fig.3D**. Left half of graph shows control situation (closed symbols), right half of graph shows quantification of *Cdc20* RNAi shown in C (open symbols). Please note, that CyclinA in this experiment is more stable than in Fig. 3C and that this is also reflected in a longer time from NEBD-ANA as compared to **Supplemental Fig 2A**. (C) U2OS cells with Tet inducible CyclinA were transfected with APC2 siRNA and analysed by fluorescent and DIC time-lapse microscopy. Levels of fluorescence were normalized to 100% at NEBD as indicated in the Legend to Figure 1. Control shown in solid line, APC2 RNAi with dashed line. Graphs depicted show mean \pm s.d. (D) U2OS cells stably expressing Cherry-Nek2A and with Tet inducible Cyclin A-Venus were transfected with siRNA targeting Ube2S and UbcH10, arrested with thymidine for 16h, released and treated with tetracycline. Cells were analysed by fluorescent and DIC microscopy, levels of fluorescence were normalized to the frame of NEBD as in Legend to Figure1. Control cells shown with solid line, RNAi cells with dashed line, graph shows mean \pm s.d.



Supplemental Figure 3. Binding of Nek2A to the APC/C is not inhibited by ProTAME

(A) U2OS cells were synchronized with thymidine and released into mitosis and subsequently treated with either DMSO, proteasome inhibitor MG132 or 20 μ M proTAME for the final 2h before lysis and precipitation of APC complexes by APC4 antibodies. (B) U2OS cells were synchronized by thymidine treatment, released for 5h and treated with 2h of indicated drug before lysis and APC/C precipitation by APC4 antibodies.

(C) U2OS Cells were transfected with Nek2A RNAi or mock transfected, synchronized by thymidine block and released for 7h, lysed and APC complexes were precipitated using APC4 antibodies.



Supplemental Figure 4. Degradation of Cherry-Nek2AΔMR upon spindle checkpoint release is not dependent on Cdh1.

(A) U2OS cells stably expressing Cherry-Nek2AΔMR were transiently transfected with the known APC/C^{Cdh1} substrate Aurora A-eCFP and analyzed by time lapse microscopy as in Legend to Figure 1. n=10
 (B) Similar to A, but alongside Aurora A-eCFP, siRNA directed towards Cdh1 were transfected. Cells were imaged by fluorescent and DIC time lapse at 3 minute intervals. Cdh1 RNAi n = 7 Graphs depict mean ± s.e.m. (C) U2OS stably expressing Cherry-Nek2AΔMR were treated with taxol and imaged with a 3 minute interval. Slow loss of the fluorescent protein indicates slippage as previously shown by others for other APC/C spindle checkpoint proteins.

Chapter 3

Dynamic Instability of Nek2A in G2 Phase Requires APC/C^{Cdh1}

Michiel Boekhout¹ & Rob Wolthuis^{1,2}

Affiliations:

1: Division of Cell Biology I (B5) and Division of Molecular Carcinogenesis (B7), The Netherlands Cancer Institute (NKI-AvL), 1066 CX Amsterdam;

2: Department of Clinical Genetics (Division of Oncogenetics), VUmc and VUmc Cancer Center Amsterdam, CCA/V-ICI Research Program Oncogenesis, VUmc Medical Faculty, The Netherlands.

Under Review

ABSTRACT*Background*

Prior to mitosis, in normal G2 phase, the APC/C ubiquitin ligase is thought to be completely inactive as a result of: i) its inability to bind Cdc20, and ii) its binding to Emi1, a powerful APC/C inhibitor which blocks Cdh1 and APC2 functions. At the G2-to-mitosis transition, Emi1 is degraded, but phosphorylation of Cdh1 by cyclin B1-Cdk1 prohibits APC/C^{Cdh1} complex formation. Phosphorylation of the APC/C by mitotic kinases induces Cdc20 recruitment and boosts APC/C^{Cdc20} activity. This catalyzes the rapid degradation of Nek2A and cyclin A during prometaphase.

Approach

We studied the mechanisms of Nek2A degradation by the APC/C. We found that Nek2A, in contrast to cyclin A, is already bound to the APC/C in G2 phase, prior to the rapid Cdc20-dependent disappearance of Nek2A in mitosis. Here, we investigated whether Nek2A turn-over is affected by APC/C^{Cdh1} activity in G2 phase.

Results and Conclusion

We found that inhibition of Nek2A protein synthesis leads to loss of Nek2A during G2 phase. Nek2A degradation in G2 phase is slow compared to its degradation in mitosis, requires APC/C^{Cdh1} and is critically dependent on binding of Nek2A to the APC/C. Inhibiting Cdk1 at the end of G2 phase destabilizes Nek2A, which indicates that cyclin B1-Cdk1 protects the stability of APC/C substrates at the end of G2 phase, when Emi1 disappears. Interestingly, Nek2A is synthesized during mitosis, so shut-down of Nek2A translation at prometaphase is not the mechanism by which Nek2A disappears in the spindle checkpoint. We conclude that Nek2A is continuously synthesized and degraded during G2 phase. The APC/C is not fully inhibited prior to mitosis and supports the dynamic instability of Nek2A. Any block in the synthesis of Nek2A during G2 phase could thus lead to “interphase slippage” of Nek2A.

INTRODUCTION

The Anaphase-promoting Complex or Cyclosome (APC/C) is the E3 ubiquitin ligase that induces the timely destruction of securin and cyclin B1 in metaphase. Destruction of securin and cyclin B1 is required for sister chromatid separation and mitotic exit, respectively, after the mitotic checkpoint has been satisfied^{21,106}. The APC/C is an immense protein complex (approximately 1.2 mDa), but for its activation it critically depends on either one of two activators, Cdc20 or Cdh1³³, to target its many different substrates for degradation. Cdc20 is the direct target of the mitotic checkpoint^{138–140,266} consisting of Mad2, BubR1 and Bub3 bound to Cdc20, which keep Cdc20 inhibited until all kinetochores are correctly attached to the mitotic spindle^{106,135}. However, while it is clear that the mitotic checkpoint is essential for formation of two genetically identical daughter cells, its ability to block APC/C^{Cdc20} is not absolute. This explains the process of “mitotic slippage”, which refers to the eventual escape from cells arrested by the mitotic checkpoint, due to slow loss of cyclin B1. Mitotic slippage occurs even in the presence of Nocodazole, a spindle poison that hyper-activates the mitotic checkpoint^{148,270,271}. Furthermore, we recently found evidence that mitotic checkpoint restricted APC/C^{Cdc20} can catalyze the rapid destruction of Nek2A at the start of prometaphase, right after nuclear envelope breakdown (NEBD)⁸³. So, while the mitotic checkpoint blocks Cdc20 efficiently, some APC/C^{Cdc20} substrates are completely or partially degraded in an APC/C^{Cdc20} dependent manner, while the checkpoint is still active.

At the end of mitosis, Cdh1 is dephosphorylated and starts to bind to, and activate, the APC/C. Throughout interphase the APC/C remains bound to Cdh1, but this complex starts to be inhibited at the end of G1. This allows accumulation of cyclins and entry into S-phase²⁸³. The inhibition of APC/C^{Cdh1} at the end of G1 phase is mediated by the *de novo* synthesis of the E2F target Emi1¹⁰⁷. The ability of Emi1 to block APC/C^{Cdh1} depends on the synergistic action of multiple motifs in Emi1, which contribute to APC/C and Cdh1 binding^{112,121}. At the end of G2 phase, rising Plk1 activity ensures phosphorylation of Emi1^{127,128}, which leads to recognition and degradation of Emi1 via SCF^{β-TRCP}^{116,284}. Shortly after the onset of Emi1 degradation, cells enter mitosis¹³⁰. It is believed that rising mitotic cyclin B1-Cdk1 activity can replace the Cdh1-inactivating function of Emi1, by inhibitory phosphorylation of Cdh1 that block Cdh1 binding to the APC/C in mitosis, preventing the precocious activation of APC/C^{Cdh1}^{115,129}. Right after metaphase, when cyclin B1 is degraded, Cdh1 is de-repressed and so APC/C^{Cdh1} becomes active^{41,80}.

Also cells that encounter DNA damage in G2 phase may activate the APC/C, at least for a period of time, which is accomplished by removal of Emi1, either through inactivation or degradation, to allow a temporary cell cycle halt^{75,76}, and Cdk1 inhibition. Unscheduled disappearance of Emi1 leads to re-replication through the loss of geminin and cyclin

A, which in turn leads to re-licensing and re-firing of origins of replication^{115,285}. This process is rescued by co-depleting Cdh1²⁸⁵, which show that Emi1 and Cdh1 critically control inhibition and activation of the APC/C in interphase.

We showed that Nek2A degradation is a very sensitive marker of APC/C activity⁸³. Here, we describe how Nek2A, which is recruited to the APC/C regardless of the cell cycle phase^{83,243}, is continuously degraded by the APC/C in interphase. We show this relies on the C-terminal MR tail of Nek2A, previously shown to be required for direct APC/C binding and Nek2A processing by the APC/C^{82,243}. We conclude that the APC/C is not fully inhibited in G2 phase and controls that dynamic instability of Nek2A. Right before mitosis, inhibition of APC/C^{Cdh1} becomes increasingly dependent on the activity of the mitotic kinase Cdk1.

RESULTS

Inhibition of translation, or of degradation, reveals the dynamic instability of Nek2 before mitosis

Nek2A protein levels drop rapidly upon entry into mitosis, as a consequence of APC/C^{Cdc20} ubiquitination^{82,83,243,286}. We were investigating the mechanism of Nek2A degradation in mitosis, and tested whether translation inhibition, which typically occurs in mitosis, could play a role in the sudden loss of Nek2A upon NEBD. However, when we treated G2 phase cells with translation inhibitors, they failed to enter mitosis. Then we noticed that Nek2A was already unstable during interphase (**Fig. 1A**), as shown by loss of Nek2A protein after treatment of cells with cycloheximide (Chx). Conversely, when we inhibited proteasomal degradation of Nek2A with Mg132 (Mg), we found that Nek2A levels increased (**Fig. 1B**), while inhibiting both translation and degradation kept levels at a steady state level. These results show that Nek2A levels are dynamically unstable in G2 phase: they depend on simultaneous synthesis and degradation. We validated these findings for shorter incubation times specifically during G2, which reproducibly showed active Nek2A translation as well as degradation (**Fig. 1C**). We observed a half-life of 30-60 minutes, which is shorter than the previously estimated 4 hours measured during S-phase²⁸⁷. We next investigated Nek2A degradation in G2 phase by time-lapse fluorescence imaging. We imaged cells stably expressing both Venus-Nek2A and Geminin-Cherry⁸³ in the presence of cycloheximide, synchronized in G2 phase by thymidine release. Addition of Cycloheximide led to a gradual drop of total levels of Nek2A over the course of 2 hours imaging. We could not confidently determine differences in rate of protein loss on a subcellular level, but we observed that both the centrosomes and cytoplasm decreased in a similar fashion. Venus-Nek2A dropped to almost 50% over 90 minutes, which indicate it might be degraded slightly more slowly

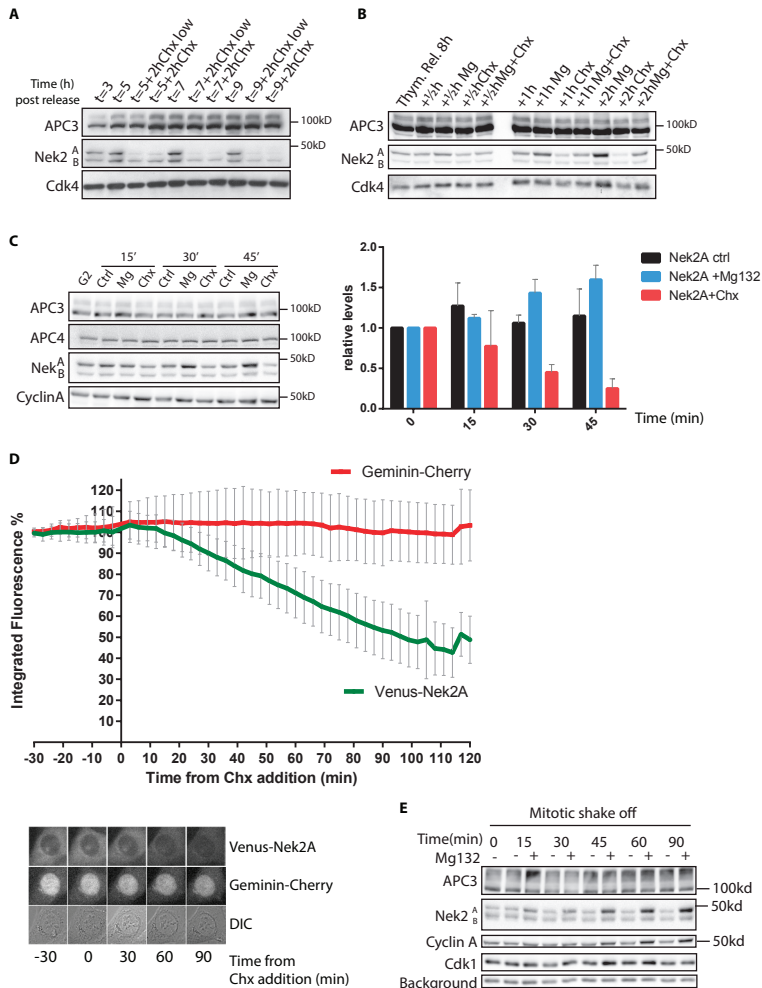


Figure 1. Inhibition of translation, or inhibition of protein degradation, reveal instability of APC/C substrate Nek2A during interphase.

A) U2OS cells were treated for 24h with thymidine to synchronize them at the G1-S border, after which they were released and treated with 10 $\mu\text{g/ml}$ Cycloheximide (Chx) or with half this concentration (Chx low) for 2 hours at several time points after thymidine release, after which they were analyzed by western blot. **B)** U2OS cells released for 8h from a 24h thymidine block, were treated with either MG132(MG), Chx, or both for the time in hours as indicated, lysed and analyzed by western blot. **C)** Similar to **B**, although now treatment time is indicated in minutes, after which cells were lysed and analyzed by western blot. The right graph shows the mean and s.d. of 3 independent experiments (normalized for loading by APC4) **D)** U2OS cells stably expressing Geminin-Cherry (red line) and Venus-Nek2A (green line) released from an 16h thymidine block for 7h and then imaged by time lapse fluorescence and DIC microscopy at 3 minute intervals. Integrated fluorescent levels were measured, and normalized to 100% at 30 minutes before Chx addition, to which the x-axis set to $t=0$. Plotted are mean \pm s.d. $n=16$ from 3 independent experiments. Lower panel shows representative montage. **E)** U2OS cells were synchronized with thymidine, released into medium containing nocodazole and collected by mitotic shake off 16 hours later. Mitotic cells were replated in presence of Mg132 or DMSO and collected after incubation time as indicated.

compared to endogenous Nek2A (**Fig. 1C**). Geminin-Cherry levels measured in the same cells remained constant throughout the experiment.

Interphase Nek2A degradation is dependent on the APC/C catalytic core

Specifically at centrosomes, Nek2A was previously found to be degraded and replaced by newly synthesized Nek2A during G2 phase^{278,287}. Nevertheless, when protein translation and degradation are unperturbed, the total protein levels of Nek2A do not change during G2 phase, while Nek2A disappears rapidly at mitotic entry. Here, we wondered whether Nek2A turn-over in G2 phase, which becomes apparent after inhibition of protein synthesis, could be dependent on the APC/C. Nek2A binds directly to the APC/C via the C-terminal MR tail already^{83,243,287}, but degradation normally begins only at mitotic entry^{82,83,243}. We showed that mitotic disappearance of Nek2A depends on Cdc20 recruitment to the APC/C, which triggers APC/C^{Cdc20} activation⁸³.

When we depleted APC2, a core subunit of the APC/C, we found that Nek2A levels increased drastically before cells entered mitosis (**Fig. 2A**). Also after treatment with APC11 RNAi, we detected higher levels of Nek2A (**Fig. 2A** and **Supplemental Fig. 1A**), but depletion of the E2 enzymes, UbcH10 and Ube2S, which are known to cooperate with the APC/C, did not lead to Nek2A accumulation or clearly prevent Nek2A loss in the presence of Cycloheximide (**Supplemental Fig. 1A**). We suspected that degradation of Nek2A in the presence of cycloheximide, if APC/C dependent, required Cdc20 or Cdh1^{83,286}. However, when depleting either one, or both activators, Nek2A was not stabilized to the same level as upon depleting APC2 or APC11 (**Fig. 2B**). Interestingly, we observed that when depleting APC11 or APC2, Cdh1 levels also increased (**Fig. 2B**, **Supplemental Fig. 1C**), which may result from the inhibition of APC/C-dependent Cdh1 degradation during interphase. These long-term effects of APC/C subunit depletion may thus obscure the role of Cdh1 in Nek2A degradation as detected by western blots of synchronized cells. To more directly measure the involvement of APC/C^{Cdh1} in the instability of Nek2A after Chx (**Fig. 1D**, **Fig. 2C**), we then imaged Nek2A degradation during G2 phase, after treatment with Cdh1 RNAi. This partially stabilized Nek2A (**Fig. 2C**). Previously, we showed that Nek2A degradation via APC/C^{Cdc20} is strictly dependent on Cdc20, but very low levels of Cdc20 are sufficient for rapid Nek2A degradation in mitosis. Therefore, it is possible that even after treatment with Cdh1 RNAi, sufficient Cdh1 remained to support slow Nek2A degradation. We conclude therefore that Nek2A is degraded in interphase in a manner that is at least partially, but perhaps completely, dependent on APC/C^{Cdh1}. To further verify that Nek2A degradation in G2 phase was strictly mediated by the APC/C, we imaged the degradation of a Nek2A C-terminal truncation mutant, that does not bind to the APC/C. Indeed, Venus-Nek2AΔMR remains almost completely stable during G2 phase after cycloheximide treatment (**Fig. 2D**). On western blot, Venus-Nek2A protein produced a smear shifted

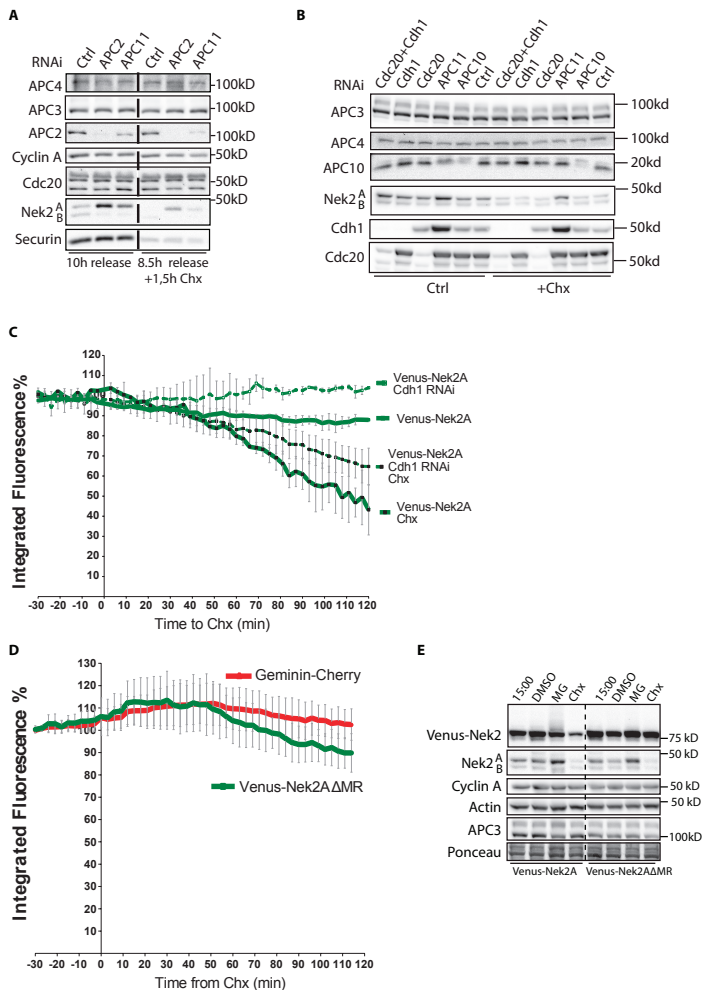


Figure 2. Interphase Nek2A degradation is APC/C dependent

A) RPE1-TERT cells treated with siRNA oligos directed against the APC/C catalytic core units, APC2 or APC11, were thymidine blocked for 24h, released and treated with Chx for 1.5h as indicated, before lysis and analysis by western blot. **B)** U2OS cells were treated with siRNA oligonucleotides as indicated (RNAi), blocked with thymidine for 16h, released and lysed after 8h with either addition of 1h Chx or in a control situation. **C)** U2OS cells stably expressing Venus-Nek2A were treated with siRNA oligos directed against Cdh1 or control oligos, thymidine blocked and released for 7h, and imaged at 3 minute intervals with fluorescence and DIC microscopy. Levels are normalized to 100% at the start of imaging at 33 minutes before addition of Chx. Time of Chx addition is set to 0 on the x-axis. Punctate lines indicate cells treated with Cdh1 oligos, dark symbols indicate Chx treatment. Integrated fluorescence was measured, plotted are mean \pm s.d. n=3 per condition. **D)** U2OS Cells stably expressing Geminin-Cherry and Venus-Nek2A Δ MR were synchronized 16h with thymidine, released and imaged with fluorescence and DIC microscopy at 3 minute intervals. Levels were normalized at 30 minutes before addition of Chx, which is set as t=0 on the x-axis. Plotted is mean integrated fluorescence \pm s.d. n=5 **E)** U2OS cells stably expressing Venus-Nek2A or Venus-Nek2A Δ MR were thymidine blocked for 24h, released, lysed 7h after release (15:00) or treated with 1h DMSO, MG132 or Chx before lysis and analysis by western blot.

upwards in the gel after proteasome inhibition, indicating ubiquitination (**Fig. 2E**), which is not observed for the APC/C binding mutant, further supporting that Nek2A is a substrate of the APC/C in G2 phase. Contrarily, we found the full-length Venus-Nek2A levels dropped after Chx treatment, while the Δ MR mutant was refractory to inhibition of translation (**Fig. 2E**). We conclude therefore that the APC/C is already partially active prior to mitosis and contributes to Nek2A turn-over in G2 phase.

Stabilization of Nek2A leads to its nuclear accumulation, dependent on the APC/C MR binding tail.

Next, we investigated the accumulation of Nek2A after preventing its degradation in further detail. We confirmed that Nek2A levels increased on the centrosome²⁷⁸ after inhibition of the proteasome. At later time points, we also observed strong accumulation of Nek2A in the nucleus (**Fig. 3A top panels**). Surprisingly, nuclear accumulation of Nek2A was not observed when we analyzed the APC/C-binding mutant of Nek2A, Nek2A Δ MR (**Fig. 3A lower panels**)^{83,243,286,287}. Interestingly, a previous study showed that a C-terminally truncated mutant of Nek2A had a higher residence time on the centrosome²⁷⁸. This suggested that the APC/C targeting of Nek2A plays a role in its turnover at the centrosome. Our results indicate that Nek2A is fluxed over the centrosomes and moves to the nucleus, where it accumulates under conditions when Nek2A binds the APC/C but is not degraded by the proteasome. This might mean that, normally in G2 phase, low amounts of Nek2A are imported into the nucleus in a manner that is directed by its binding to the APC/C. When we treated cells with ProTAME, a specific APC/C inhibitor^{197,263}, Nek2A also partially accumulated into the nucleus (**Fig. 3B**).

We then asked whether the accumulation of Nek2A in the nucleus after its artificial stabilization, indicated that G2-phase, APC/C-dependent Nek2A degradation would normally occur in the nucleus. The APC/C is reported to be present in nucleus in interphase, as is also the case for Emi1, E2S and Cdh1, but the localization of active APC/C is not precisely known, or thought to be focused at centrosomes and kinetochores in mitosis^{288,289}. While Nek2A is normally present on centrosomes with low residence time²⁷⁸, we hypothesized that it constantly entered the nucleus and is degraded there, and therefore not observed unless stabilized. To test this hypothesis, we inhibited the proteasome while imaging Venus-Nek2A and Geminin-Cherry expressing U2OS cells, followed by removal of the inhibitor, which indeed led to respective accumulation and subsequent disappearance of nuclear Nek2A (**Fig. 3C, quantified in Fig. 3D**). In conclusion, we propose that Nek2A needs to be turned over via the APC/C during G2 phase for control of both protein levels and nuclear localization.

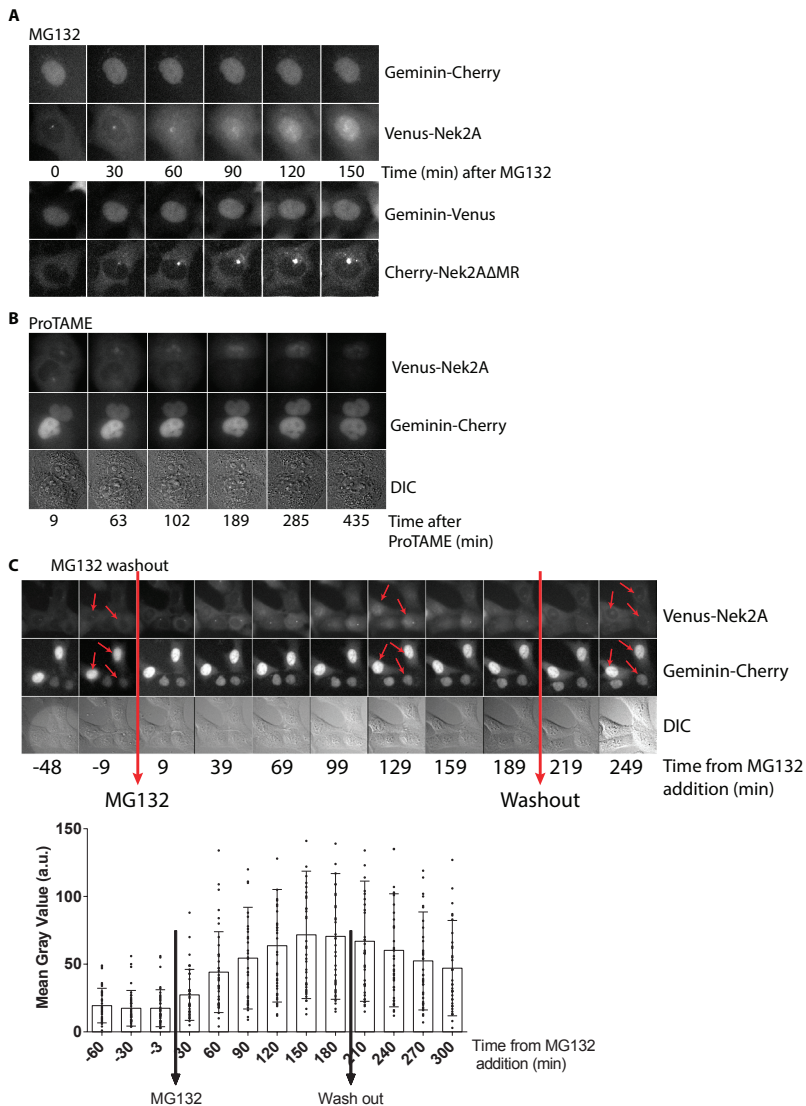


Figure 3. Inhibition proteasomal degradation leads nuclear accumulation of Nek2A dependent on the APC/C MR binding tail.

A) U2OS cells stably expressing Geminin-Cherry and Venus-Nek2A (Top panel) or U2OS cells expressing Geminin-Venus and Cherry-Nek2AΔMR (Bottom panel) were imaged by fluorescence and DIC microscopy at 3 minute intervals in the presence of MG132. Time indicated in minutes from MG132 addition). **B)** Cells were treated with 20 μM ProTAME and imaged by fluorescence and time-lapse microscopy at 3 minute intervals. **C)** U2OS cells stably expressing Venus-Nek2A and Geminin-Cherry were imaged with fluorescence and DIC microscopy at 3 minute intervals. Red arrows indicate nuclei that accumulate Nek2A after MG132 addition, subsequently degrade the protein after washout. As indicated MG132 was added during filming, and washed out by washing 4 times with warm PBS. Lower graph shows plotted mean gray values in the nucleus for a set region. This region was measured at each time point and plotted over time. Cells were followed over all indicated time points, plotted are mean ± s.d. n=38

APC/C activation leads to Cdh1 mediated Nek2A degradation in G2

Because Nek2A degradation in G2 phase was dependent on the APC/C, we wondered whether increasing APC/C activity in G2 phase could also lead to premature loss of Nek2A. Previous reports indicated that APC/C activity in G2 requires Cdh1⁷⁶, and that during G2 phase Cdh1 is kept in check by Cdk1 phosphorylations^{27,75}. We hypothesized that partially inhibiting Cdk1 right before mitosis could lead to premature APC/C^{Cdh1} activation⁷⁵.

To this end, we treated cells with RO-3306, a specific Cdk1 inhibitor, at a low concentration, which still allowed for mitotic entry^{290–292} (Voets, under review). We clearly observed a delay in mitosis after RO-3306 treatment at this concentration, as previously described²⁹² (Voets, under review), and Geminin-Cherry remained stable until right before the onset of anaphase (**Fig. 4A**). However, Venus-Nek2A declined before NEBD (note that levels were put at 100% at mitotic entry, absolute fluorescence signals of Venus-Nek2A are lower than those of geminin-Cherry). We can attribute the RO-3306 induced degradation of Venus-Nek2A in late G2 phase to the APC/C: in the same setting Venus-Nek2A Δ MR was stable up to the point of checkpoint satisfaction, overlapping with the behavior of Geminin-Cherry (**Fig. 4B**), and in line with our proposed mechanism for Nek2A degradation in mitosis⁸³.

To further verify that degradation of Nek2A, induced by Cdk1 inhibition, was APC/C^{Cdh1} dependent, we investigated the effect of Cdh1 depletion by RNAi (**Fig. 4C, 4D**). We found that depleting Cdh1 at least partially stabilized Nek2A in the presence of RO-3306, until cells entered mitosis. We showed before that in mitosis, Nek2A is degraded in a Cdh1-independent, Cdc20-dependent manner. In conclusion, we propose that Nek2A is an unstable protein in G2 phase, due to its constant targeting to the APC/C^{Cdh1}. Right before mitosis, Nek2A becomes more dependent on Cdk1 activity, to remain protected from APC/C^{Cdh1} mediated degradation. This might relate to ability of cyclin B1-Cdk1 to inactivate Cdh1 by phosphorylation.

DISCUSSION

Here, we show that Nek2A, which is an APC/C^{Cdc20} substrate in prometaphase, is already targeted for degradation during G2 phase in an APC/C^{Cdh1} dependent manner. This was surprising, as Emi1 should at this point fully block APC/C activity. Indeed, Emi1 is likely responsible for stabilizing the other APC/C substrates that we investigated, which are also not lost after cycloheximide treatment. The turnover of Nek2A is critically dependent on its APC/C-binding motif. Interestingly, Nek2A degradation in G2 phase seems to take place on centrosomes as well as in the nucleus. When Nek2A is unable to

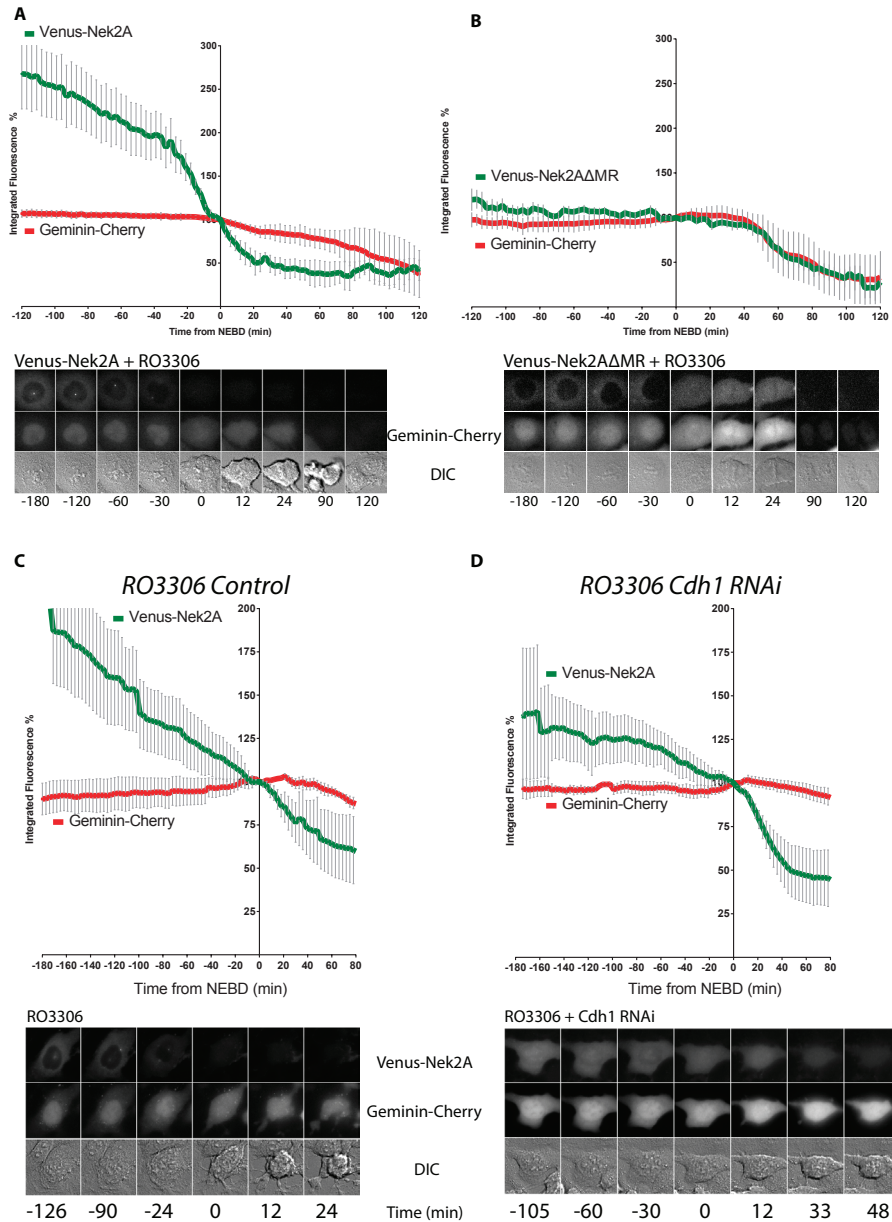


Figure 4. APC/C activation leads to Cdh1 mediated Nek2A loss in G2

A) U2OS cells stably expressing Venus-Nek2A and Geminin-Cherry were synchronized for 16h in thymidine released for 4h after which 3 μ M RO3306 was added and images were acquired with fluorescence and DIC microscopy at 3 minute intervals. Integrated mean fluorescence was measured, normalized to 100% at the moment of NEBD, plotted is the mean \pm s.e.m. n=11 from 2 independent experiments. **B)** As in **A**, except cells U2OS cells stably expressing Venus-Nek2A Δ MR and Geminin-Cherry. Plotted are mean \pm s.e.m. **C)** As in **A**, U2OS cells expressing Venus-Nek2A and Geminin-Cherry treated with 3 μ M RO3306 with transfection of control siRNA oligos. **D)** As in **C**, but with siRNA oligos directed against Cdh1.

bind to the APC/C, levels strongly increase on centrosomes, instead of in the nucleus, indicating that Nek2A needs to be destroyed by the APC/C in the nucleus to prevent excessive centrosomal accumulation.

“Interphase slippage”

Residual APC/C activity, escaping the effects of a potent inhibitory pathway, is also observed during a prolonged mitotic arrest. This phenomenon has been coined ‘mitotic slippage’^{247,270,271}, where slow cyclin B1 APC/C mediated destruction leads to exit aberrant mitotic exit. We propose that we identified a similar form of APC/C activity in interphase.

One unaddressed issue is the absolute amount of different APC/C compositions during different cell cycle phases. Not all APC/C complexes are bound to activator, and the bare complex is identified from cryo-EM studies, called ‘apo-APC/C’¹¹. In either interphase or mitosis the amount of activator is the rate-limiting factor for APC/C activity, which is exemplified by experiments in which the activator is overexpressed. Overexpression of Cdh1 leads to loss of APC/C targets during interphase, while overexpression of Cdc20 may overcome the mitotic checkpoint. As Nek2A is not hindered by the absence of activator, it will bind all different APC/C configurations. This leads to the possibility that there may be a window in which Nek2A bound to apo-APC/C may encounter Cdh1 in the absence of Emi1. As Nek2A is currently the only known substrate to directly bind the APC/C during G2 phase, this might explain its exclusive sensitivity for APC/C activation. However, while Emi1 can bind APC/C independently of Cdh1, Emi1 has a not fully understood preference for APC/C^{Cdh1} over apo-APC/C. This conclusion is based on the finding that upon depleting Emi1 from HeLa nuclear extracts, all Cdh1 is co-depleted, while 20% of the total APC/C remains as apo-APC/C¹². This suggests Emi1 efficiently inhibits all Cdh1, while leaving a minor amount of apo-APC/C uninhibited. This makes it unlikely there is a functional window APC/C^{Cdh1}, which is free of Emi1 inhibition. However, even if APC/C^{Cdh1} transiently is uninhibited by Emi1, any bound Nek2A would likely be immediately targeted for degradation (**Fig. 5**).

The alternative possibility may be that Nek2A is slowly degraded by Emi1-inhibited APC/C^{Cdh1}. This agrees with our unpublished result that ND-Emi1 (this thesis, Chapter 5) which arrests cells in mitosis, only minimally slows Nek2A degradation. However, we found that in this setting the mitotic checkpoint is still recruited, which we have shown is already sufficient for Nek2A destruction. This suggests that, for Nek2A, APC/C inhibitors do not prevent ubiquitination. As Nek2A protein is present and stable in G2, either the recruitment of Nek2A is regulated, or the degradation via APC/C^{Cdh1-Emi1} is inefficient to such an extent, it allows for sufficient residual Nek2A protein throughout the cell. Although we do not have a clear structural explanation of how Nek2A might

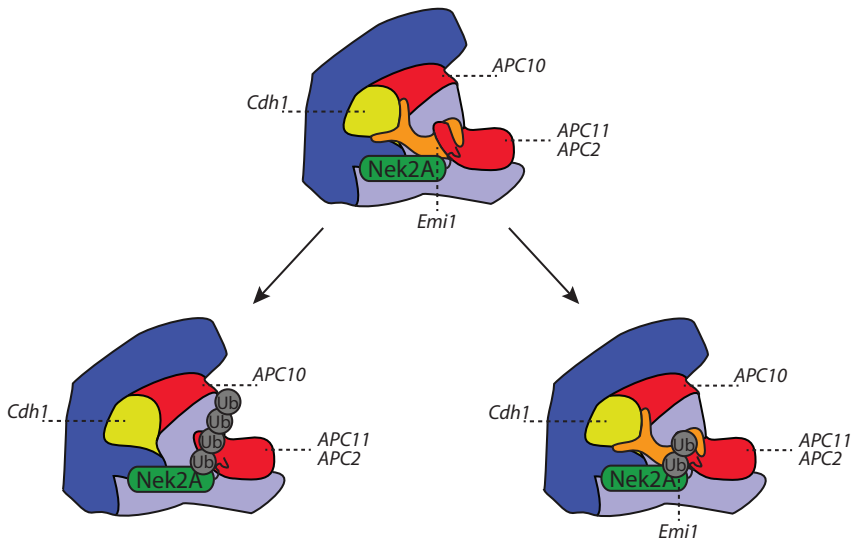


Figure 5. Two models for Nek2A turnover during G2 by APC/C^{Cdh1}

Depicted is the APC/C with the catalytic core in red, simultaneously bound to Emi1, Cdh1 and Nek2A. We propose two pathways for Nek2A degradation. Ubiquitination of Nek2A could either take place via small windows in which Emi1 is transiently not bound to the APC/C^{Cdh1}, or ubiquitination of Nek2A could take place regardless of the presence of Emi1. However, this is likely less efficient than free Cdh1, which explains both why levels of Nek2A are normally stable in G2.

circumvent Emi1 mediated inhibition, our results indicate that the APC/C catalytic core mediates Nek2A interphase turnover.

APC/C Localization and substrate recruitment during interphase

Before NEBD, the APC/C can already be detected in the nucleus⁸⁹, while also Ube2S, Cdh1 and Emi1 are all thought to also reside within the nucleus. However, the presence of Emi1 and activation of Cdk1 restrain APC/C^{Cdh1} activity during this cell cycle phase. Interestingly, Cdh1 is not only inhibited by Cdk activity, but JNK stress kinases also phosphorylate Cdh1²⁹³. Phosphorylation by JNK on Cdh1 hampers its ability to activate the APC/C *in vitro*, and *in vivo* also leads to cytoplasmic translocation of Cdh1. During normal cell cycle progression, when cyclin B1 levels start to rise, the protein is retained in the cytoplasm until the onset of prophase²⁹⁴. However, after DNA damage, cyclin B1 is retained by p21 in the nucleus where it is degraded by APC/C^{Cdh1}^{75,77}. An alternative manner of APC/C^{Cdh1} activation is Emi1 depletion, leading to loss of all substrates^{111,115}. The order in which APC/C^{Cdh1} degrades substrates after activation during interphase has not been characterized to the same extent as the mitotic substrates of APC/C^{Cde20}. Speculatively, there might be a preference for degrading nuclear substrates such as cyclin A and geminin over for instance centrosomal substrates such as Plk1, cyclinB1

and Aurora A. However, we propose that efficiency of recruitment to the APC/C can outweigh localization, which we also find for Nek2A, which resides on the centrosome but is probably the most efficient APC/C substrate. Nek2A is rapidly turned over, but does not have a nuclear localization, while geminin is localized in the nucleus but remains stable. We propose this is due to the fact that APC/C^{Cdh1} constantly degrades Nek2A in the nucleus. Interestingly, Nek2A is reported to have a weak NLS motif, which would be in line with nuclear translocation of the protein²⁹⁵. While Nek2A is detected in the cytoplasm and on the centrosome, of this latter location 70% of the protein is highly mobile with a residence half time of only 3 seconds²⁷⁸. Combined with our findings that Nek2A is both synthesized rapidly and also degraded by APC/C^{Cdh1}, this creates the possibility highly dynamic control of protein levels. However, the role of its rapid turnover, as well as a possible functional role in the nucleus, remain to be determined.

Acknowledgements

We thank Daisuke Izawa and Jon Pines for providing the APC2 antibody, we thank the members of our lab and our division for fruitful discussion.

MATERIALS AND METHODS

Tissue Culture and cell cycle synchronization

We followed the same procedures as previously described; (Boekhout and Wolthuis 2015), but briefly; U2OS cells were grown in DMEM (Gibco) containing FCS (Sigma), penicillin, streptomycin and cultured at 37°C in 5% CO₂. 24 before synchronization or transfection, cells were plated on 9 cm Falcon dishes or, for time-lapse fluorescence microscopy on 3,5 mm glass-bottom dishes (Wilco Wells) or 4-well glass bottom dishes (Labtek II). For enrichment of cells in G2 phase, cells were treated for 24 hours with thymidine (Sigma, 2,5 mM final concentration) and incubated for 8 hours after release, or as indicated.

Other drugs, used as indicated: proteasome inhibitor MG132 (#13697, 5 µM final concentration; Cayman Chemicals); translation inhibitor cycloheximide (#C6255, 5 or 10 µM final concentration; Sigma-Aldrich), RO-3306 (#217699, 3 µM final concentration [Calbiochem]), ProTAME (I-440, 12µM final concentration R&D systems). Stable cellines were created and used as previously described (Boekhout and Wolthuis 2014)

Transfections

Cells were transfected with 40 nM siRNA oligo pools (ON-TARGET-plus oligos, Dharmacon) using lipofectamine 2000 (Invitrogen) according to manufacturer's protocol. The siRNAs to target

APC2 (ANAPC2) APC11 (ANAPC11), Cdh1 (FZR), APC3 (Cdc27), APC6 (ANAPC6), Ube2S (UBE2S), UbcH10 (UBE2C) were purchased from Thermo Fisher Scientific as ON-TARGET plus SMART pools.

Antibodies

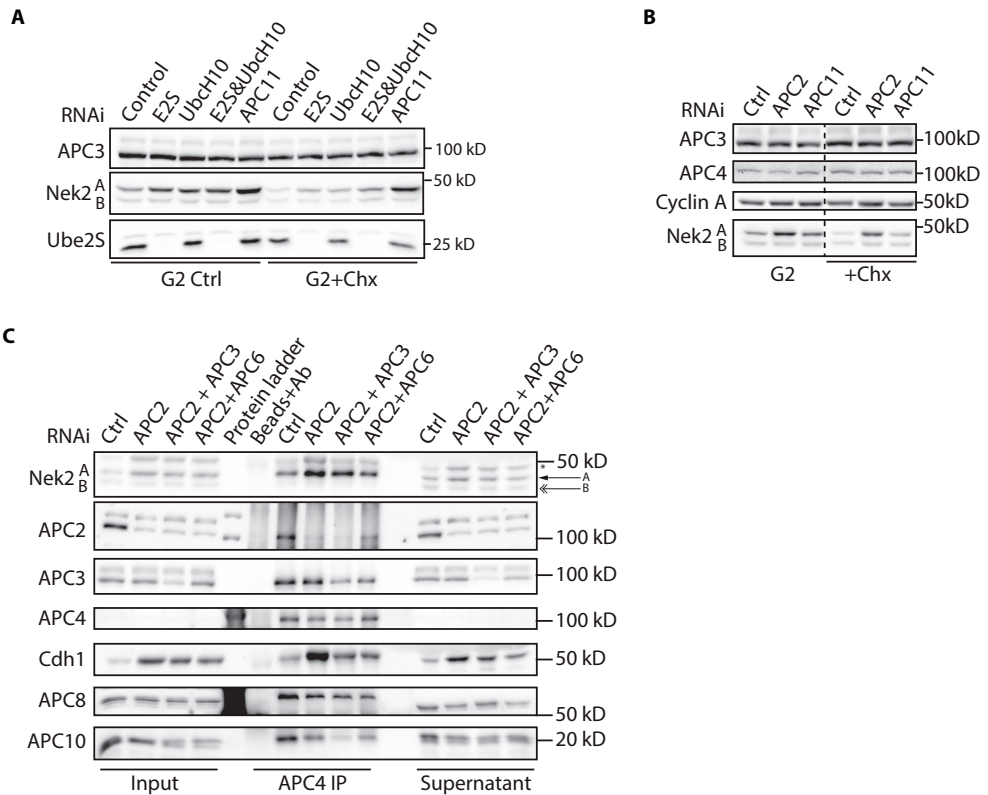
Antibodies used were: goat anti-actin (Santa Cruz Biotechnology SC-1616), rabbit anti-APC2 (provided by Jon Pines, Zoology Dept, Gurdon Institute, UK, London), mouse anti-APC3 (BD Transduction), goat anti-APC4 (Santa Cruz Biotechnology, SC21414), goat anti-Cdc16/APC6 (SC-6395 1:1000), rabbit anti-APC10 (Biolegend 611501/2), mouse anti-Cdc20/p55 (Santa Cruz Biotechnology sc-13162), mouse anti-Nek2 (BD 610593 (1:500)), mouse anti-Cdh1 (Neomarkers MS1116-p1), goat anti-Cdk4 (Santa Cruz sc-260), rabbit anti-cyclin A2 (Santa Cruz Biotechnology, H-432), rabbit anti-PTTG-1/Securin (Zymed 34-1500 (1:500)).

Western blotting and Immunoprecipitation

Cells were lysed in ELB+ (150 mM NaCl, 50 mM HEPES (pH 7.5), 5 mM EDTA, 0.3% NP-40, 10 mM β -glycerophosphate, 6% glycerol, 5 mM NaF, 1 mM Na₃VO₄ and Roche protease inhibitor cocktail). Lysates were cleared by centrifugation (13,000x g, 12 min at 4°C). Protein levels were equalized by using Bradford analysis. For immunoprecipitations, 2 μ g antibodies were precoupled for 4–12 hours to 20 μ l of protein G Sepharose (Amersham Biosciences) and washed with ELB+. Precoupled beads and lysates were incubated overnight at 4°C and washed three times with 1.0 ml of ice-cold ELB+. All remaining buffer was removed and beads were resuspended in 60 μ l sample buffer; 25 μ l was separated on SDS-PAGE and blotted on nitrocellulose (0.4 μ m pore). Membranes were blocked with 4% ELK in PBS containing 0.1% Tween. Development of blots was performed using the Chemidoc Imaging System (Bio-Rad Laboratories) and quantification was done with the Image Lab (Bio-Rad Laboratories) software.

Time-lapse fluorescence microscopy

U2OS cells stably expressing indicated fluorescently tagged proteins transfected with siRNA oligos or treated with inhibitors and followed by fluorescence time-lapse microscopy. Acquisition of DIC and fluorescence images started 24 or 48 h after transfection on a microscope (Axio Observer Z1; Carl Zeiss) in a heated culture chamber (5% CO₂ at 37°C) using DMEM with 8% FCS and antibiotics. The microscope was equipped with an LD 0.55 condenser and 40 \times NA 1.40 Plan Apochromat oil DIC objective and CFP/YFP and GFP/HcRed filter blocks (Carl Zeiss) to select specific fluorescence. Images were taken using AxioVision Rel. 4.8.1 software (Carl Zeiss) with a charge-coupled device camera (ORCA R2 Black and White CCD [Hamamatsu Photonics] or Roper HQ [Roper Scientific]) at 100-ms exposure times. Alternatively imaging was performed on a Deltavision Elite system, using L15 Leibovits medium (Gibco), in a 37°C culture chamber, without the need of supplying CO₂. For quantitative analysis of degradation, MetaMorph software (Universal Imaging), ImageJ (National Institute of Health) and Excel (Microsoft) were used. Captured images were processed using Photoshop and Illustrator software (Adobe).



Supplemental Figure 1. Nek2A degradation is mediated by the APC/C catalytic core

A) U2OS cells were treated with siRNA oligos as indicated, blocked with thymidine, released and treated with either control or Chx for 1h. 8h after thymidine release cells were lysed and analyzed by western blotting **B)** As in **A**, U2OS cells were treated with siRNA oligos directed against the APC/C catalytic core, synchronized by thymidine, released and either treated with cycloheximide or control treated before lysis and western blot analysis. **C)** Cells were treated with either ctrl RNAi, APC2 RNAi or a combination of APC2 RNAi with APC3 or APC6. After RNAi treatment, cells were synchronized with thymidine released and lysed in G2, 8h after release. On cleared protein lysates APC4 antibodies precoupled to beads were used to immune precipitate the APC/C complex (APC4 IP). Non-bound protein lysate was also analyzed by western blot (Supernatant).

Chapter 4

Feedback regulation between atypical E2Fs and APC/C^{Cdh1} controls the G1/S phase transition.

Bart Westendorp^{1,*a}, Michiel Boekhout^{2*}, Annelotte P. Wondergem¹,
Hendrika A Segeren¹, Elsbeth A. van Liere¹, Nesibu Awol Ababelgu¹, Imke Jansen¹,
Rob Wolthuis^{2,3}, Alain de Bruin^{1,4,a}.

* Equal contribution.

^a Corresponding author.

1 Department of Pathobiology, Faculty of Veterinary Medicine, Utrecht University. Yalelaan 1, 3584 CL
Utrecht, The Netherlands

2 Division of Cell Biology I (B5), The Netherlands Cancer Institute (NKI-AvL), Plesmanlaan 121 1066
CX Amsterdam, The Netherlands.

3 Department of Clinical Genetics (Division of Oncogenetics), VUmc and VUmc Cancer Center
Amsterdam, CCA/V-ICI Research Program Oncogenesis, VUmc Medical Faculty, 1081 HV Amsterdam,
The Netherlands.

4 Department of Pediatrics, Division of Molecular Genetics, University Medical Center Groningen,
University of Groningen, Groningen, 9713 AV, the Netherlands

Adapted version under Review

ABSTRACT

The family of E2F transcription factors is responsible for the regulation of multiple genes required for G1-S-phase transition. Rb phosphorylation during G1 phase removes inhibition on transcription factors E2F1-3, which allows for transcription of target genes. However, two atypical E2Fs, E2F7 and E2F8, are transcriptional repressors and not regulated by Rb or other pocket proteins, and counteract E2F mediated activation of transcription. E2F7/8 are also direct E2F targets themselves, but regulation of E2F7/8 beyond their transcription has not been well characterized. Here, we show that E2F7 and E2F8 are degraded by the Anaphase Promoting Cyclosome/Complex, APC/C^{Cdh1}, during mitotic exit and during G1. We show that removal of activator CDH1 or mutating APC/C recognition motifs leads to stabilization of E2F7/8. The consequence of failure to degrade E2F7/8 is reduced S-phase entry, and eventually this results in cell cycle arrest and cell death. In addition, we show E2F7/8 also directly negatively regulate the levels of the APC/C^{Cdh1} inhibitor Emi1. Hereby we have uncovered a direct feedback loop between the destruction of atypical E2Fs and inhibition of APC/C^{Cdh1} activity at the G1-S transition, required for normal cell cycle progression.

INTRODUCTION

Eukaryotic cell division is tightly controlled by transcriptional and post-translational regulation of genes that drive progression through the different phases of the cell cycle. The decision to enter S phase is of critical importance, because unscheduled entry leads to replication stress, which may result in DNA mutations through errors during replication, and eventually could lead to genetic instability and cancer^{296,297}. The activity of E2F transcription factors plays a central role in the decision to enter S phase. Vertebrate species have no less than eight different E2F family members (E2F1-8), three dimerization partners (DP1-3) and 3 pocket proteins (Rb, P107, P130), whose concerted action determines transcription of hundreds of target genes in mammalian cells.

Dissecting the specific and unique functions of the E2F family members in various cellular processes, including S phase entry, has proven a difficult task²⁹⁸. For instance, activator E2Fs 1-3 switch from activators to repressors during differentiation of intestinal progenitor cells, depending on pocket protein binding²⁹⁹. However, the actions of the atypical E2F family members, E2F7 and -8, seem almost exclusively repressive, as they lack transactivation domains and are not regulated by pocket proteins. With the notable exception of *VEGFA*, we and others previously showed that E2F7 and -8 repress gene transcription³⁰⁰⁻³⁰⁴. After the start of S phase, E2F7 represses many genes that drive G1/S transcription, via occupation of E2F promoter sites³⁰³. Based on their high extent of homology and redundant functions *in vivo*, E2F8 is expected to have a similar function³⁰⁵. In addition, E2F7/8 drive the switch from mitotic cell cycles to endocycles in placenta and liver, and can suppress apoptosis during embryonic development³⁰⁵⁻³⁰⁷, confirming the central role of E2F7 and -8 in cell cycle regulation.

Expression of atypical E2Fs is comparatively high in tissues with high rates of cell division^{300,301}. Thus, given that E2F7 and -8 are potent cell cycle regulators, their activities must be tightly controlled. During late G1, a feed forward loop is triggered through activation of E2F1-3 resulting in a rise of cyclin-dependent kinase (Cdk) activity and rapid transcriptional activation of E2F target genes, including Cyclins and activator E2Fs themselves³⁰⁸. However, E2F7 and -8 are also E2F target genes, and we predicted the existence of another mechanism to inhibit their preliminary activation in late G1^{303,304}.

Another important mechanism that coordinates progression from G1 to S phase is the inactivation of the anaphase-promoting complex/cyclosome APC/C^{Cdh1}. This permits accumulation of proteins that are required to progress through a single round of S phase properly, such as Cyclin A, Geminin and CDC6^{245,239}. Inactivation of APC/C^{Cdh1} also relies on rising Cdk activity, leading to inactivation of CDH1, as well as E2F-

mediated transcription of *Emi1*, a direct APC/C^{Cdh1} inhibitor^{107,112,309,59}. APC/C^{Cdh1} activity maintains a necessary time window in G1 to prepare the cell for replication³¹⁰, illustrated by the fact that loss of CDH1 can lead to premature S phase entry, induces replication stress and the accumulation of DNA damage^{71,311}.

Here, we show that E2F7 and -8 are targeted for ubiquitin-mediated proteasomal degradation by APC/C^{Cdh1} during the late stages of mitosis and G1 phase. Paradoxically, E2F7 and -8 in turn can activate the APC/C^{Cdh1} via repression of *Emi1* and Cyclin A and E, which are all known to inhibit APC/C activity. Thus, E2F7 and -8 mediate their own degradation, via this auto inhibitory feedback. Collectively these data show that atypical E2Fs and APC/C^{Cdh1} are engaged in a feedback loop that tightly regulates S-phase entry. Importantly, we show that blocking the APC/C^{Cdh1} mediated destruction of E2F7/8 prevents cells from entry and progression of S phase, and results in cell death. The combination of high expression of atypical E2Fs and inactivation of APC/C^{Cdh1} may thus be an efficient strategy to induce a cell cycle arrest and prevent unscheduled cell proliferation.

RESULTS

E2F7 and -8 are targeted for proteasomal degradation during G1.

We first explored whether atypical E2Fs are subjected to post-translational regulation. First, we treated RPE1-TERT (RPE1) cells with the protein translation inhibitor cycloheximide (CHX), and found a robust decrease in E2F7/8 protein levels within 1 hour of treatment (**Fig. 1A**). The disappearance of E2F7 and -8 was prevented by co-treatment with the proteasome inhibitor MG132. Then, we arrested RPE1 cells in G1 with the selective CDK4/6 inhibitor PD0332991 (PD). Protein expression of E2F7 and E2F8 was markedly reduced after 16 hours of treatment (**Fig. 1B**). U2OS cells, osteosarcoma cells with intact Rb function³¹², also showed a reduction in E2F7/8 protein levels after 16 hours of PD treatment. Arresting these cells in G2 phase with the CDK2 inhibitor NU6140 did not decrease E2F7/8 expression, suggesting that this effect is cell cycle phase-specific (**Fig. 1B**). We found that the disappearance E2F7/8 by PD0332991 treatment could be rescued by adding the proteasome inhibitor MG132 two hours prior to harvesting (**Fig. 1C**). Together, these results strongly point towards a high turnover of E2F7 and -8 via proteasomal degradation, particularly during the G1 phase of the cell cycle.

One likely candidate responsible for proteasomal degradation early in G1 phase is APC/C^{Cdh1} E3 ubiquitin ligase. Using the ELM protein sequence analysis resource (<http://elm.eu.org>), we found that atypical E2Fs contain evolutionary conserved KEN domains, which are the canonical substrate recognition motifs for APC/C^{Cdh1} (**Fig. 1D**)⁹⁴.

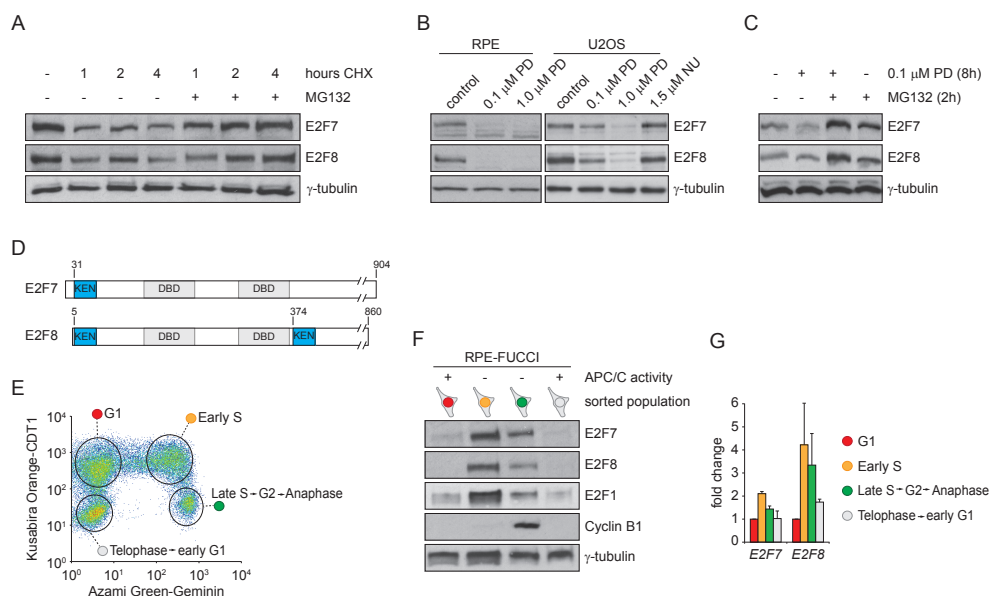


Figure 1. High turnover of E2F7 and E2F8 via proteasomal degradation during G1 phase.

(A) Protein expression E2F7 and E2F8 in RPE cells treated with 100 mg/mL cycloheximide (CHX) and MG132 (10 mM). MG132 was added simultaneously with CHX. (B) Protein levels of E2F7 and E2F8 in RPE and U2OS cells after 16 hours of treatment with the CDK4/6 inhibitor PD0332991, or the CDK2 inhibitor NU6140, respectively. (C) Protein expression of E2F7 and E2F8 after 8 hours of PD0332991 treatment, in presence or absence of the proteasome inhibitor MG132 (10 mM) for two hours prior to harvesting. (D) Schematic overview of conserved KEN motifs in human/mouse E2F7 and E2F8 proteins. (E) FACS profile showing expression of cell cycle markers in RPE-FUCCI cells. Encircled areas indicate the gates used to sort cell cycle-specific populations. (F) Immunoblots of FACS-sorted RPE cells with stable expression of the FUCCI system. Cells were sorted based on expression of truncated versions of Azami Green-tagged Geminin (aa1-130) and Kusabira Orange-tagged CDT1 (aa30-120), respectively. Blots are representative examples of four independent replicates derived from two different stable RPE-FUCCI clones. (G) Transcript levels of atypical E2Fs in sorted RPE-FUCCI cells measured by qPCR. Bars represent average \pm s.e.m. of fold change, relative to expression in G1 ($n=3$).

Furthermore, observations in a cell free system suggested that atypical E2Fs may be substrates of the APC/C³¹³. We then took advantage of the Fluorescent Ubiquitination-based Cell Cycle Indicator (FUCCI) system, which is based on the activities of APC/C^{Cdh1} and SCF^{Skp2}³¹⁴. Using FACS-sorting, we isolated cell populations in different phases of the cell cycle as indicated to determine protein and mRNA levels of atypical E2Fs (Fig. 1E). From the onset of anaphase until the next S phase the APC/C is active, and Azami Green-Geminin¹⁻¹¹⁰ is absent. Notably, E2F7 and E2F8 proteins were nearly undetectable in these G1 cells (Fig. 1F). The protein levels of E2F1 and cyclin B1, which are also APC/C substrates^{247,315,316}, showed expression patterns consistent with APC/C activity (Fig. 1F). Transcript levels of *E2F7* and *E2F8* in sorted cells showed a similar trend, although they were only mildly regulated in the cell cycle, while protein

levels changed drastically, confirming the important contribution of post-translational regulation mechanisms (**Fig. 1G**). Collectively, these data show that E2F7 and E2F8 are unstable proteins during G1-phase and that their degradation coincides with high APC/C activity.

E2F7 and -8 are APC/C^{Cdh1} substrates.

We went on to test whether E2F7 and -8 are *bona fide* APC/C^{Cdh1} substrates in human cells. We first transfected 293T cells with flag-tagged CDH1, and observed a robust reduction of endogenous E2F7/8 proteins after overexpression of CDH1 similar to the known APC/C^{Cdh1} substrates CDC6 and Aurora kinase A (**Fig. 2A**). Contrary to CDH1, we did not find a noticeable reduction in E2F7 and -8 protein levels after CDC20 transfection. To rule out an indirect transcriptional effect of CDH1 overexpression on *E2F7/8*, we then expressed EGFP-tagged E2F7 or E2F8 (transcriptionally controlled by a CMV promoter) in combination with CDH1 or CDC20. We observed a dramatic reduction in exogenous E2F7/8 by CDH1 –but not by CDC20– overexpression (**Fig. 2B**). We performed an inverse experiment by depleting CDH1 in cells with stable doxycycline-inducible expression of E2F7 or E2F8 using RNAi. CDH1 knockdown stabilized exogenous E2F7 and E2F8 proteins (**Fig. 2C**). We then performed co-immunoprecipitation experiments, and found that E2F7/8 and CDH1 physically interacted with each other (**Fig. 2D**).

Next, we followed the levels of E2F7 and E2F8 when cells progressed through mitosis and G1-phase. We used time-lapse microscopy experiments in HeLa cell lines with stable inducible overexpression of E2F7 and E2F8. These experiments revealed that both proteins are degraded during telophase and the subsequent G1 phase, coinciding with APC/C^{Cdh1} activation (**Fig. 2E, F**). Importantly, we could prevent the degradation of E2F7/8 by treating cells with siRNA oligos targeted against CDH1. We then tested whether manipulation of APC/C activity directly affects endogenous E2F7/8 levels. Although depletion of CDH1 with siRNA did not lead to a noticeable increase in E2F7/8 or the known APC/C substrate CDC6 in HeLa cells (**Fig. S1**), we found that treatment with the APC/C inhibitor proTAME caused a partial, but consistent prevention of E2F7/8 degradation in cycloheximide-treated RPE cells (data not shown). Collectively, our data clearly demonstrate that the atypical E2Fs are targeted for degradation by the APC/C^{Cdh1} complex.

APC/C^{Cdh1}-mediated destruction of E2F7 and -8 in G1 is crucial for S-phase entry and progression.

To study the importance of regulated destruction of E2F7/8 for cell cycle progression, we expressed non-degradable versions of E2F7 and E2F8 and monitored cells as they progress from mitosis to S-phase. E2F8 has two conserved KEN motifs, located at

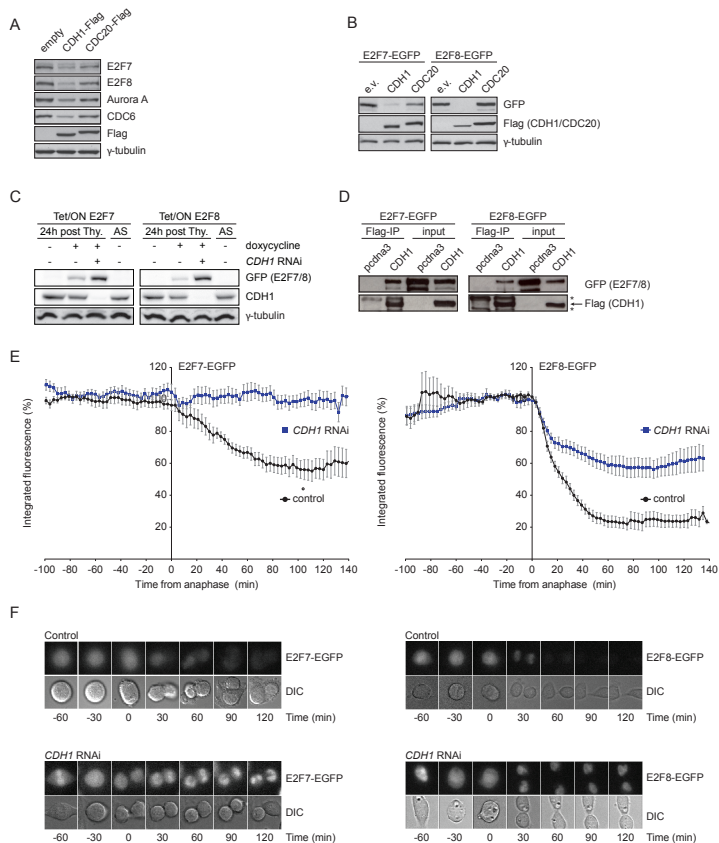


Figure 2. Atypical E2Fs are targeted for degradation by APC/C^{Cdh1}.

(A) Protein levels of E2F7/8 and two known APC/C^{Cdh1} substrates in 293T cells 48 hours after transfection with CDH1-Flag or CDC20-Flag. Immunoblots are representative examples of two independent replicates. (B) Expression of EGFP-tagged E2F7/8 in 293T cells 48 hours after transfection of flag-tagged CDH1, flag-tagged CDC20 or empty vector. Immunoblots are representative examples of two independent experiments. (C) Effect of CDH1 depletion on protein levels of E2F7/8 in HeLa cells with stable expression of inducible E2F7/8-EGFP. Overexpression of E2F7 was induced using tetracycline at the onset of release from a thymidine block. (D) Co-immunoprecipitation of EGFP-tagged E2F7/8 with CDH1-Flag after 48 hours of co-expression in 293T cells. Cells were treated with 10 mM MG132 for 5 hours prior to harvesting to limit immediate proteasomal degradation of E2F7/8 after binding to CDH1. Immunoblots are representative examples of three independent experiments. Asterisks indicate IgG bands, arrow indicates the CDH1-Flag band (E) HeLa cells with stable inducible E2F7/8-EGFP were imaged by fluorescence and differential contrast (DIC) microscopy at 3 minute intervals. Cells were treated with CDH1 siRNA for 10 hours, synchronized at the G1-S border by 16h thymidine treatment, followed by thymidine release and induction of E2F7/8-EGFP by doxycycline. Mean integrated fluorescence of the cells was measured and normalized to the intensity in the frame of nuclear envelope breakdown (NEBD) (set at 100%), as determined by cytoplasmic dispersal of the fluorescent signal. The x-axis is set to 0 at the onset of anaphase, as observed in the DIC channel. Graphs shown are mean±s.e.m. Left graph: control n=15, Cdh1 RNAi n=14 both from 3 independent experiments. Right graph: control n=13, Cdh1 RNAi n=13 both from 2 independent experiments (F) Montages of representative cells from experiments shown in (E) Time (min) indicates time from onset of anaphase.

amino acids 5-7 and 374-376, respectively; we therefore created single (E2F8^{KEN5mut}, E2F8^{KEN374mut}) as well as double mutant (E2F8^{K/Kmut}) plasmids in which the KEN motifs were replaced with three consecutive alanine residues (**Fig. S2A**). To investigate whether KEN mutants are less sensitive to CDH1-dependent proteasomal degradation, we first co-transfected 293T cells with equal amounts of these constructs in combination with CDH1-Flag or empty vector. Notably, KEN mutant versions of E2F7 and -8 were clearly protected against APC/C^{Cdh1} mediated degradation (**Fig. 3A**). Because both KEN mutations in E2F8 had a similar effect, we concluded that both domains are functional and decided to perform all subsequent experiments with the double mutant (E2F8^{K/Kmut}). We then performed stable transfection of these constructs in HeLa cells expressing the Tet repressor. We confirmed that the KEN mutants are not misfolded or otherwise dysfunctional, by showing repression of the known E2F target genes CDC6 and Cyclin A2 after 16 hours of doxycycline treatment (**Fig. 3B**). In fact, cell lines expressing KEN mutants showed stronger repression, notwithstanding comparable overall expression levels. Using FACS analysis to plot levels of E2F7/8 (EGFP) against DNA content (propidium iodide) we noted that stable cell lines expressing the wild-type versions of E2F7/8 have only few EGFP-positive cells with 2C DNA content (G1 phase, **Fig. 3C**). However, during E2F7/8^{KENmut} expression, a much higher percentage of EGFP-positive cells with 2C DNA content was found, indicating that degradation of E2F7/8 by APC/C^{Cdh1} is required for cells to enter S-phase (**Fig. 3C**). Importantly, CDH1 RNAi prior to doxycycline induction caused a massive increase in the number of strongly EGFP-positive E2F7^{WT} or E2F8^{WT} expressing cells with 2C DNA content, comparable to the effect of KEN mutation, confirming CDH1-dependent degradation of overexpressed E2F7/8 during G1 (**Fig. 3C**).

Using time-lapse microscopy we found that E2F7^{KENmut} and E2F8^{K/Kmut} degradation after anaphase is blocked, in sharp contrast to their wild-type counterparts (**Fig. 3D, E**). We found that E2F8^{K/Kmut} degradation was not completely prevented, unlike E2F7^{KENmut}. This residual degradation may be explained by the presence of alternative binding domains for CDH1, or by APC/C binding via CDC20. Indeed, we found 3 putative D-boxes in E2F8 (**Fig. S2B**). Notably, both wild-type and KEN mutant E2F8 co-immunoprecipitated with CDC20-Flag (**Fig. S2C**). Summarizing, these data show that E2F7 and -8 have functional KEN domains, and mutation of these domains results in stabilization of E2F7 and -8 during anaphase and G1.

Prolonged E2F7/8 stability inhibits cell proliferation by reduced S-phase entry and increased cell death

We previously showed that inducible E2F7^{WT} overexpression inhibits proliferation by delaying S-phase progression, while not affecting S phase entry³⁰³. This could indicate that during unperturbed cell cycles, cells efficiently degrade E2F7/8 for normal

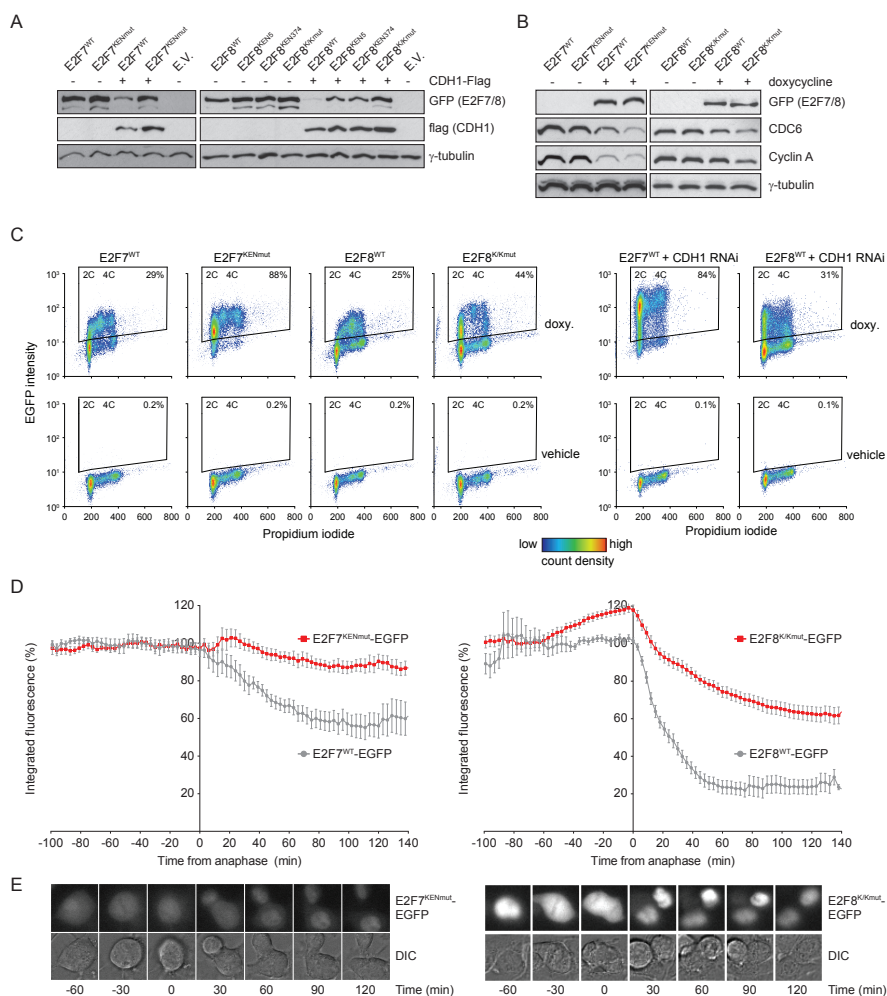


Figure 3. Mutation of KEN domains results in marked stabilization of E2F7 and E2F8.

(A) Protein expression of wild type and KEN-mutant E2F7 and E2F8 in 293T cells in presence or absence of CDH1-flag 48 hours after transfection. For E2F8, KEN motifs starting at amino acid 5 (KEN5) or 374 (KEN374) were mutated separately into 3 consecutive alanines or in combination (K/Kmut). Blots are representative of two independent experiments. (B) Immunoblots showing repression of the E2F target genes CDC6 and Cyclin A in HeLa cells with stable doxycycline-inducible expression of wild type and KEN double-mutant E2F7/8 after 16 hours of doxycycline treatment. (C) FACS plots showing DNA content on the x-axis (propidium iodide) of HeLa cells with stable expression of wild type or KEN-mutant E2F7, after 24 hours of doxycycline. Thresholds for EGFP positivity were set by applying the same gate to vehicle- and doxycycline treated cells. (D) HeLa cells expressing inducible E2F7-eGFP (left destruction graph) or E2F8-eGFP (right destruction graph) were blocked with thymidine for 16h, then released in fresh medium with doxycycline. Imaging was performed at 3-min intervals, as in Figure 2E. The x-axis is set to 0 at the frame of anaphase onset. Graphs show mean \pm s.e.m. wildtype (wt) shown from Figure 2E in gray. E2F7-EGFP-KENmut n=13 from 2 independent experiments, E2F8-eGFP K/Kmut n=26 from 3 independent experiments. (E) Montages of representative cells from experiments shown in (D). Time (min) indicates time from onset of anaphase.

progression through G1 phase. Stabilization of E2F7 or E2F8 in G1 by preventing its APC/C^{dh1}-mediated degradation would then prevent cells from starting S phase. To test this, we quantified incorporation of the thymidine-analog BrdU in cells with stable inducible expression of mutant and wild-type E2F7/8. Both E2F7^{WT} and E2F8^{WT} expressing cells continued to incorporate BrdU at high levels after 24 and even 48 hours of doxycycline treatment (**Fig. 4A, S3**). Nevertheless, proliferation was severely inhibited by induced overexpression of the wild-type versions of E2F7 and -8 (**Fig. 4B**). However, induction of E2F7^{KENmut} reduced BrdU incorporation, indicating that APC/C-mediated degradation of E2F7 in G1 is critical for S-phase entry (**Fig. 4A**). The overexpression of E2F8^{K/Kmut} also demonstrated a significant reduction in BrdU incorporation, although the effect was less pronounced than that of E2F7^{KENmut}.

To trace cell cycle fates on the individual cell level, we quantified S-phase entry using PCNA-mCherry as marker, and followed its subcellular distribution with time-lapse imaging (**Fig. 4C**). The onset of S-phase is characterized by formation of PCNA dots, known as replication factories³¹⁷. Whereas the bulk of cells without expression of KEN mutant E2F7 and -8 (EGFP negative) entered S-phase during the 40 hours of imaging, only very few cells expressing E2F7^{KENmut} did so (**Fig. 4D, S4A**). E2F8^{K/Kmut} expressing cells also showed a reduced percentage of cells entering S-phase, but again the effect was less pronounced. Instead of entering S-phase, many of the E2F7^{KENmut} expressing cells died, as detected by cell blebbing, and leakage of PCNA into the cytoplasm (**Fig. 4E, S4A**).

The KEN domain mutations in E2F8 caused a less severe S-phase entry defect than in E2F7, and while many E2F7^{KENmut} cells died during imaging, E2F8^{K/Kmut} were mostly still alive at the end of analysis. We therefore asked whether a subset of E2F8^{K/Kmut} expressing cells is able to progress through S-phase normally. To this end, we released E2F8 expressing cells from a HU arrest and monitored cell cycle progression (**Fig. 4F**). We observed a marked delay in S-phase progression of cells expressing E2F8^{K/Kmut} compared to E2F8^{WT} expressing cells, suggesting that unscheduled expression of E2F8 in G1 causes problems in DNA replication (**Fig. 4G**).

Next, we tested whether depletion of CDH1 would also impair S phase entry in E2F7/8^{WT} expressing cells, using BrdU incorporation and live PCNA imaging. Treatment with *CDH1* RNAi slightly reduced the percentage of BrdU-positive E2F7/8^{WT} expressing cells (**Fig. 4H**). However, time-lapse microscopy using PCNA showed that *CDH1* RNAi completely prevented normal S phase entry as seen by PCNA dot formation in the E2F7^{WT}- or E2F8^{WT}-EGFP expressing cells, whereas the majority of cells expressing E2F7^{WT}-EGFP in presence of normal CDH1 levels entered S phase (**Fig. 4I**). Instead, almost all cells with combined CDH1 depletion and overexpression

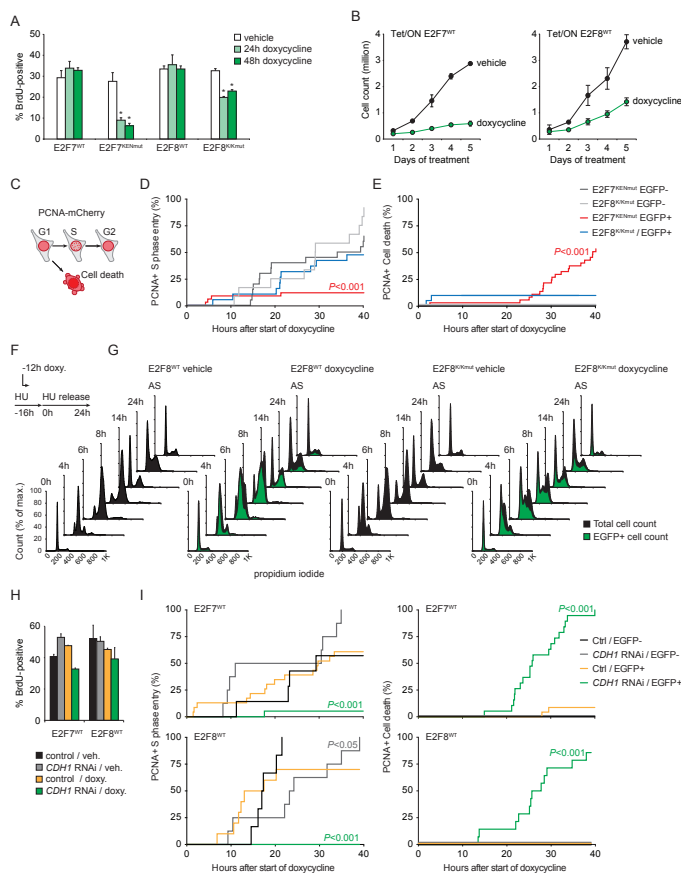


Figure 4. Stabilization of E2F7 and E2F8 during G1 markedly impairs S-phase entry and progression.

(A) Quantification of percentages of BrdU-positive cells after induction of wild type and KEN mutant E2F7/8 expression measured by flow cytometry. Bars represent mean \pm sem (n=3). * $P < 0.05$ versus vehicle. (B) Cell proliferation curves of cell lines with stable inducible wild type E2F7-EGFP and E2F8-EGFP expression after doxycycline treatment. Dots represent average \pm sem of two replicates. (C) Schematic overview of live microscopy using mCherry-tagged PCNA to monitor cell cycle progression. At the onset of S phase, nuclear dots are formed, which disappear when S phase is completed. PCNA leaks into the cytosol when cells become apoptotic. (D) Cumulative progression into S phase of HeLa cells expressing KEN mutant E2F7/8-EGFP, monitored by nuclear PCNA dot formation. P value indicates significant change of EGFP-positive versus negative cells from the same cell line. (E) Cumulative cell death of HeLa cells expressing KEN mutant E2F7/8-EGFP, monitored by cell blebbing and cytosolic PCNA-mCherry. (F) Schematic overview of synchronization experiment. Cells were arrested at the onset of S phase with 2 mM hydroxyurea (HU), and induction of E2F8^{WT} or E2F8^{K/mut} was started 12 hours prior to release from HU. (G) DNA content of synchronized cells described under (F) measured by flow cytometry. Green overlays indicate the fraction of E2F8-EGFP positive cells within each doxycycline-treated cell line. (H) Effect of CHD1 RNAi on percentages of BrdU-positive cells after induction of E2F7/8 expression, measured by flow cytometry. Bars represent mean \pm s.e.m. (n=3). (I) Effect of CHD1 RNAi on cumulative S phase entry of cells with inducible expression of E2F7/8^{WT}, measured by coexpressed PCNA-mCherry. P value indicates significant change of CHD1 RNAi versus control. (J) Effect of CHD1 RNAi on cumulative death of cells with inducible expression of E2F7/8^{WT}. P values indicate significant change of CHD1 RNAi versus control.

of E2F7/8 underwent cell death, as seen by leakage of PCNA-mCherry into the cytosol and cell blebbing (Fig. 4J). Notably, *CDH1* RNAi did not cause a discernible effect on S phase entry or cell death in EGFP-negative control cells, except for a minor delay in S-phase entry of EGFP-negative cells in the E2F8^{WT} cell line. These data demonstrate that APC/C^{Cdh1} dependent degradation of E2F7 or E2F8 during G1 is required for the initiation and progression of DNA replication.

Balanced activity of E2F7/8 and APC/C^{Cdh1} is critical for proper regulation of proteins involved in G1/S progression.

During late G1 phase, APC/C^{Cdh1} is inhibited by two mechanisms. First, phosphorylation of CDH1 by Cyclin A/CDK2 or Cyclin E/CDK2 prevents its interaction with APC/C, and second, the endogenous APC/C inhibitor Emi1 starts to be expressed^{16,318}. Both mechanisms are at least in part dependent on E2F activity, although the role of E2F7/8 has not been explored yet^{107,319}. Indeed, we found that doxycycline-induced expression of E2F7 and E2F8 caused a severe reduction in Emi1 protein levels (**Fig. 5A**). To show that this is a direct effect, we then performed quantitative PCR in FACS-sorted, HU-synchronized cells (Fig. S4B,C). Quantitative PCR showed that 8 hours of doxycycline treatment was sufficient to cause a marked repression of *FBXO5*, the gene encoding Emi1 (**Fig. 5B**). Conversely, RNAi directed against *E2F7* and *E2F8* in synchronized HeLa cells caused a significant increase in *FBXO5* transcripts (**Fig. 5C**). The CDK2 activating cyclins E1 and A2 were also repressed by E2F7/8 (**Fig. 5B, C**). Collectively, these results demonstrate a direct feedback loop between E2F7/8 and APC/C^{Cdh1} (**Fig. 5D**).

DISCUSSION

Using a combination of time-lapse fluorescence imaging experiments, in which we followed cells as they progress through the cell cycle, we found that E2F7 and -8 are degraded during late mitosis via APC/C^{Cdh1}. Furthermore, we demonstrate that APC/C^{Cdh1} plays an important role in keeping E2F7/8 levels low throughout G1, because mutations in the KEN box or depletion of Cdh1 stabilized atypical E2Fs during this phase of the cell cycle. Interestingly, CDH1 depletion resulted in severely impaired S-phase entry when E2F7 or -8 were overexpressed, in line with the cell cycle inhibitory functions of E2F7 and -8. Nevertheless, this is a surprising observation, because knock-down, or deletion, of CDH1 has been linked to the faster accumulation of Cyclin A and other E2F1 targets that promote the G1/S transition, leading to G1 shortening, replication stress and DNA damage^{311,72,78}. In the presence of ectopic E2F7/8, loss of Cdh1 shows the opposite effect, decreasing the ability of cells to enter S-phase. This could imply that E2F7/8 can function as tumor suppressors upon loss of CDH1. Although in vivo studies will have to confirm this, compelling experimental data

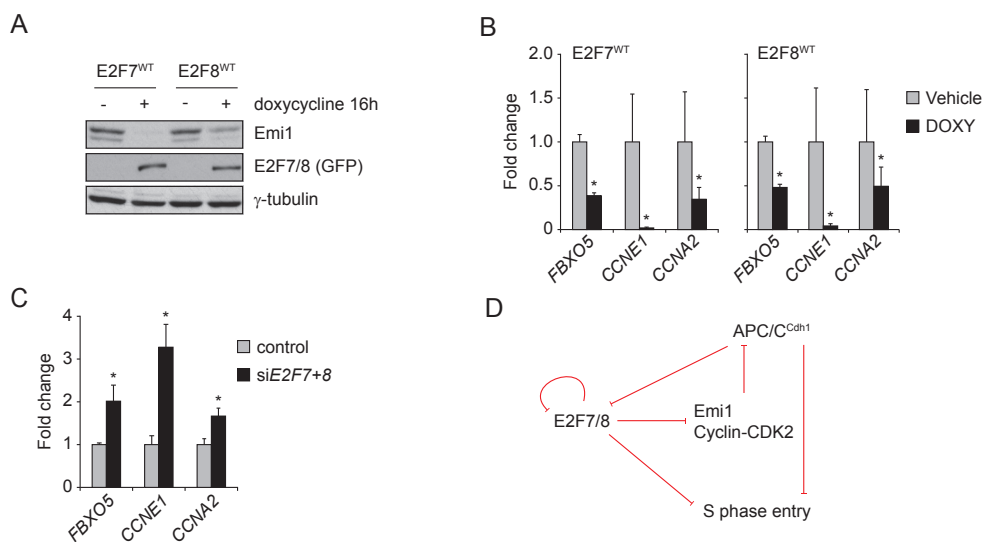


Figure 5. Atypical E2Fs can activate APC/C by repressing transcription of Emi1 and CDK2-associated cyclins.

(A) Immunoblots showing Emi1 protein levels in cell lines with stable inducible expression of E2F7 or E2F8 after 16 hours of doxycycline treatment. (B) Quantitative PCR of *FBXO5* transcripts in FACS-sorted cells with moderate or high levels of E2F7/8 expression, after 8 hours of doxycycline treatment. To avoid bias from cell cycle defects, cells were released from HU arrest at the onset of doxycycline treatment, resulting in a strong enrichment of cells in late S or G2 of both vehicle and doxycycline-treated cells (see Fig. S4C). (C) Quantitative PCR of *FBXO5* transcripts in HeLa cells treated with siRNA against E2F7 or E2F8. Cells were harvested 6 hours after release from HU block to enrich for cells in mid- to late S phase. Bars in (B) and (C) indicate mean \pm sem (n=3); asterisks indicate $P < 0.05$ versus vehicle and scrambled siRNA, respectively. (D) Working model of interaction between atypical E2Fs and APC/C based on the work described in this paper.

support this possibility. E2F7/8 restrain cell cycle progression after DNA damage, by repressing E2F1 targets³²⁰. Furthermore, E2F7 is transcriptionally activated by p53 after DNA damage or during senescence, and cooperates with Rb to keep cells arrested by repressing E2F1 targets^{321,322}. Even more so, E2F7 is suggested to be able to compensate for Rb loss, preventing unscheduled proliferation, further underlining the potential of atypical E2Fs as tumor suppressors.

In many cellular contexts, the activator E2Fs and atypical E2Fs counterbalance each other^{305–307,323}. Thus it seems counterintuitive that both classes of E2Fs would be regulated in the same manner. Nevertheless, activator E2Fs were found to be targeted for destruction by the APC/C under specific conditions. E2F3 degradation via APC/C^{Cdh1} was linked to cell cycle exit and differentiation³²⁴. E2F1 is degraded via APC/C^{Cdc20} in prometaphase, but also by APC/C^{Cdh1}^{315,316}. It is likely however, that a preference in E2F

degradation order by the APC/C exists. For instance, interaction with DP protects E2F1 from destruction via the APC/C³¹⁵. In addition, we could detect substantial expression of E2F1 in cells with active APC/C (**Fig. 1C**), suggesting that a significant pool of E2F1 is insensitive to degradation in G1 cells. In contrast, E2F7/8 do not interact with DP^{300,301,304,325}, and thus cannot be protected against degradation in this manner. Thus, the APC/C appears to play an important role in balancing the effects of activator and atypical E2Fs.

The currently described feedback loop between atypical E2Fs and APC/C^{Cdh1} could impact the transition between mitotic cell cycles and endocycles. Both atypical E2Fs and CDH1 are associated with endocycles, and there is evidence that oscillating activity of these proteins may depend on their cross-talk. First, deletion of the CDH1 encoding gene *Fzr1*, or *E2f7/8* loss, both cause defects in trophoblast giant cell polyploidization and an embryonic lethal phenotype^{307,71}. Secondly, the plant E2F7/8 homolog E2Fe/DEL1 inhibits endoreplication, via repression of *CCS52A2*, the plant homolog of CDH1³²⁶. Notably, atypical E2Fs promote polyploidization in mammalian cells, which is opposite to their function in plants^{306,307}. It is noteworthy that the effect of E2F7/8 on APC/C^{Cdh1} activity is also opposite in mammalian cells. Our data now show that E2F7/8 can activate the APC/C^{Cdh1} complex by repressing its inhibitors *Emi1* and *Cyclin A/E-CDK2*.

Strikingly, CDKs as well as *Emi1* are critical players in endocycle regulation. Loss of the APC/C inhibitor *Emi1* in *Drosophila* causes endoreplication via APC/C^{Cdh1} activation, presumably by causing enhanced degradation of Geminin and *Cyclin A*^{115,111}. Interestingly, expressing a non-degradable variant of *Cyclin A* rescued rereplication in the absence of *Emi1*¹¹⁵, while additional removal of *Cyclin A* in the absence of E2F7/8 restores polyploidy in trophoblasts cells and hepatocytes^{307,115}. These data indicate that to induce endocycles, CDK activity needs to be inhibited beneath a certain threshold to allow for assembly of pre-replication complexes, and subsequent rereplication. It should be noted that APC/C^{Cdh1}, which lowers CDK activity by removal of cyclin proteins, does not target *Cyclin E-CDK2*, while E2F7/8 represses synthesis of both *Cyclin E* and *Cyclin A*. This may be an essential difference, as *Cyclin E* has been shown responsible for inhibiting APC/C^{Cdh1} during endocycles in *Drosophila*³²⁷, and its overexpression also lead to polyploidization and aneuploidy by excessive inactivation of APC/C^{Cdh1}⁵⁹. Thus, E2F7/8 could play an important role in controlling endocycles by inhibiting overall S phase CDK activity. Whereas previously activating APC/C^{Cdh1} or expression of E2F7/8 have been reported as two separate mechanisms to induce endocycles, we now provide evidence that these are firmly intertwined.

Concluding, we show that a novel and important role for the atypical E2Fs in determining the balance between synthesis and repression of E2F target genes, and balancing APC/C activity. The expression levels of E2F7 and -8 may determine whether APC/C^{Cdh1} has a positive or negative effect on the G1/S transition.

METHODS

Generation of cell lines and cell culture

Mouse E2F8 cDNA (Reference sequence: NM_001013368.5) was amplified with primers that introduced a NotI site at the 5' and a XhoI site at the 3' end, using *Pfu* polymerase (New England Biolabs). The cDNA was then cloned into the pEGFP-N3 plasmid (Invitrogen) using a double digestion with these two enzymes, followed by ligation with T4 ligase (New England Biolabs), in such a way that a C-terminal E2F8-EGFP fusion protein is transcribed. Subsequently, *E2F8-EGFP* was digested from the pEGFP plasmid by an enzymatic digestion with NotI, and subsequently ligated into the pcDNA4/TO plasmid (Invitrogen) using T4 ligase. Correct orientation of *E2F8-EGFP* in the plasmid was verified by running XhoI-digested plasmids in an agarose gel. Plasmids containing E2F7 were generated as described before³⁰³.

Site-directed mutagenesis against sequences encoding KEN domains was performed by PCR amplification with *Pfu* polymerase of the E2F7/8 plasmids with primers encoding the required mutations. To ensure complete inhibition of these motifs, the KEN sequences were replaced by three consecutive alanines. Successful cloning and mutagenesis were confirmed with Sanger sequencing (Macrogen).

Tet repressor-expressing HeLa cells (T-REx HeLa, Invitrogen) were transfected with these constructs, and stable clones were established by Zeocin selection (Invitrogen, 300 mg/mL). The cells were cultured in DMEM containing 10% Tet System Approved fetal bovine serum (Clontech). Overexpression was induced by adding 0.2 mg/mL doxycycline (Sigma) to the cell culture medium. Cells were synchronized by adding 2mM hydroxyurea (Sigma Aldrich) to the medium for 16 hours, or 2.5 mM thymidine to arrest cells at the onset of S phase. Cells were released from the block by washing three times with PBS and adding fresh medium containing 10% FBS.

Flow cytometry and FACS sorting

For measurement of DNA contents, cells were trypsinized, washed with PBS, fixed with 70% ethanol and stored at 4 °C up to 1 week. Cells were washed twice with TBS, and then reconstituted in PBS containing 20 mg/mL propidium iodide, 250 mg/mL RNase A, and 0.1% bovine serum albumin (BSA).

DNA synthesis was measured by adding 100 mM 5-bromo-2'-deoxyuridine (BrdU, Sigma) to the culture medium for two hours prior to harvesting. Ethanol-fixed samples were washed once with PBS, cells were incubated with 0.1N HCl/0.5 mg/mL pepsin for 20 minutes. After washing with TBS/0.5% Tween/0.1%BSA, 2N HCl was added for 12 minutes, followed by pH neutralization with sodium-tetraborate buffer (pH 8.5). After washing twice with TBS-0.1% Tween, cells were incubated for 1h with a FITC-conjugated antibody against BrdU (Becton Dickinson 347583). Cells were washed with TBS, and labeled with propidium iodide as indicated above. All samples were measured on a BD FACS Canto II (BD Biosciences) and further analyzed using FlowJo software.

Two-way FACS sorting based on FUCCI markers was performed on a BD-Influx system by a senior operator. Cells were collected in cold PBS, briefly centrifugated at 800 G, and lysis buffers were added. For RNA isolation, 50.000 cells were collected, and for protein 300.000 cells.

Transfections

HEK 293T cells were seeded at a density of 3 million in 10 cm petri dishes. The next morning cells were transfected with 10 mg of E2F7/8 plasmid and/or 2 mg of CDH1-flag using the calcium phosphate method. After 48 hours, transfected cells were harvested. For coimmunoprecipitation experiments, 10 mM of MG132 (Cayman chemicals) was added to the culture medium 5 hours prior to harvesting.

For siRNA experiments, RPE or HeLa cells were plated in 6-well dishes and transfected with 40 nM of CDH1, Emi1, or scrambled siRNA (SmartPool, Dharmacon) using RNAiMAX or Lipofectamine according to the manufacturer's instructions, with the modification that transfection complexes were added to the cells for 6 hours in basic medium containing no serum or antibiotics. Afterwards, cells were washed and fresh medium containing 10% FBS and pen/strep was added.

To create inducible E2F7/8-EGFP cellines coexpressing Cherry-PCNA, cells were created via infection of the viral plasmid pLIB-Cherry-PCNA as described before²⁴⁵. Virus carrying Cherry-PCNA was created by calcium phosphate transfection of HEK293T cells, and double infection of target cells in the presence of polybrene.

Time-lapse fluorescence microscopy

Acquisition of differential interference contrast (DIC) and fluorescence images started 24h after transfection on a microscope (Axio Observer Z1; Carl Zeiss) in a heated culture chamber (5% CO₂ at 37°C) using DMEM with 8% FCS and antibiotics. The microscope was equipped with an LD 0.55 condenser and 40× NA 1.40 Plan Apochromat oil DIC objective and CFP/YFP and GFP/HcRed filter blocks (Carl Zeiss)

to select specific fluorescence. Images were taken using ZEN 2012 acquisition software (Carl Zeiss) with a charge-coupled device camera [ORCA R2 Black and White CCD (Hamamatsu Photonics) at 50-ms exposure time for eGFP excitation and 200-300-ms exposure time for mCherry excitation at 30% LED intensity.

For quantitative analysis of degradation ImageJ (National Institute of Health) and Excel (Microsoft) were used. Captured images were processed using Photoshop and Illustrator software (Adobe). Plots were created by Graphpad Prism version 6.0f, for Mac OS X, (Graphpad Software). Individual curves for S-phase entry and cell death were compared as pairs by Log-rank (Mantel-Cox) test

Quantitative PCR

Isolation of RNA, cDNA synthesis, and qPCR were performed as previously described³⁰³. Gene expression was calculated using a DDCT method adapted for multiple-reference gene correction³²⁸. All samples were corrected for two reference genes: β -Actin and GAPDH. Primer sequences are provided in Table S1.

Co-IP and immunoblotting

Cells were harvested by washing twice with PBS, and scraped in a lysis buffer containing 50 mM Tris-HCl, 1 mM EDTA, 150 mM NaCl, 0.25% deoxycholic acid, 1% Nonidet-P40, 1 mM NaF, 1 mM NaV₃O₄, and protease inhibitor cocktail (Roche). Cells were lysed on ice for 20 minutes, and centrifuged for 10 minutes at 12000 g. The supernatants were then immunoblotted with standard SDS-PAGE techniques. Antibodies used throughout this paper are listed in Table S2. Visualization was done by ECL (GE Healthcare RPN2106) and exposure to a film (GE Healthcare). All blot photos are representative examples of 3 independent experiments, unless stated otherwise.

Co-immunoprecipitations were performed as following; one near confluent 10 cm dish of cells were harvested in 1 mL of protein lysis buffer as described above. Then, BSA-blocked prot G beads (Fastflow, Millipore) were added and incubated for 30 minutes at 4°C to preclear the lysates. One 1% of the total input was kept separately, and immunoprecipitation was done by rotating samples at 4°C for 1 hour in presence of 2 mg of anti-Flag and BSA-blocked prot G beads. After washing the beads with lysis buffer, protein was eluted using Laemmli loading buffer and immunoblots were performed as described above.

Acknowledgements

We thank Dr. Daniele Guardavaccaro for kindly providing CDH1 and CDC20 constructs and helpful discussion. The stable RPE-FUCCI cell lines were provided by Prof. René Medema. Ger Arkesteijn provided expert assistance with FACS sorting

experiments. This work was financially supported by a KWF project grant (UU2013-5777) to BW and AdB and a HFSP project grant to MB and RMFW (RGP0053/2010).

Author contributions

BW, MB, APW, HAS, EAvL, NAA, and IJ performed experiments. BW, MB, RW, and AdB designed experiments, analyzed and interpreted the data, and wrote the manuscript.

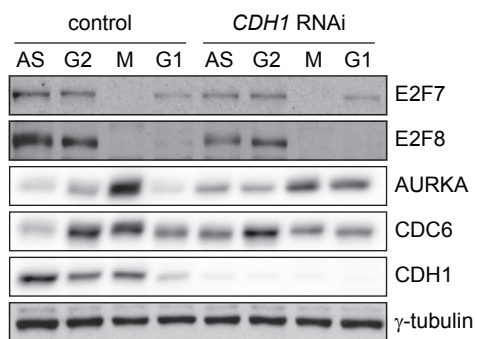
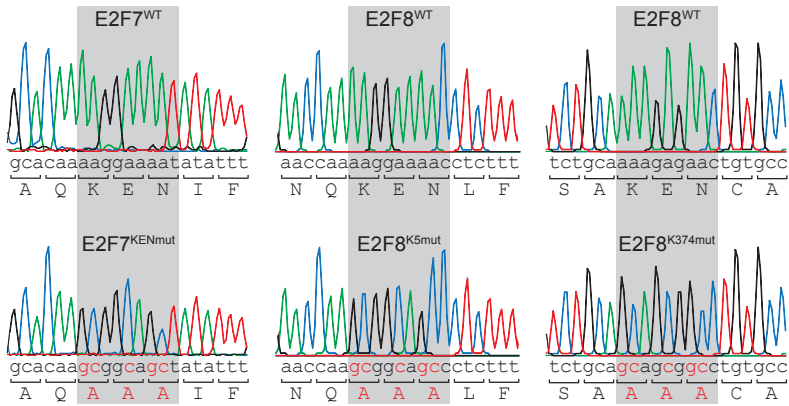


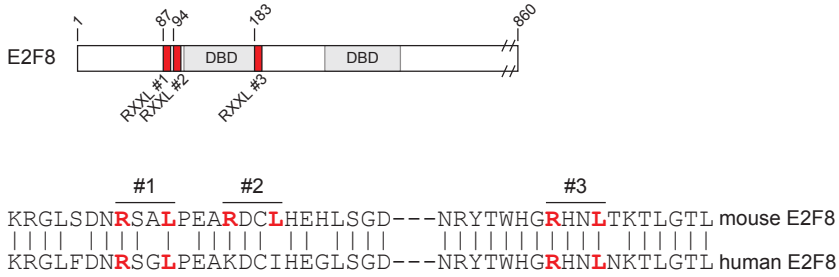
Figure S1. No consistent accumulation of APC/C substrates after CDH1 knockdown.

Protein expression of E2F7/8 and two known APC/C^{CDH1} substrates in asynchronously growing HeLa cells (AS; asynchronous, G2; 8 hours after thymidine release, M; nocodazole arrested 24 hours after thymidine release, G1, 24 hours after thymidine release).

A



B



C

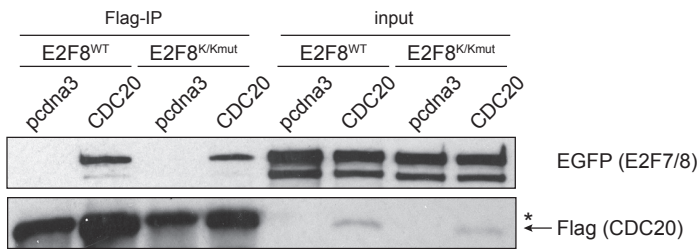


Figure S2. Generation of KEN-mutant E2F7 and E2F8.

(A) Sanger sequencing result after site-directed mutagenesis of the nucleotides encoding the KEN domains in E2F7 and E2F8. The middle panel shows the N-terminal KEN sequence starting at amino acid 5, the right panel shows the KEN domain starting at amino acid 374 in E2F8. (B) Schematic overview of putative D-boxes (RXYL) in mouse E2F8, and alignment of human and mouse E2F8 sequences. (C) Co-immunoprecipitation of EGFP-tagged E2F8^{WT} or E2F8^{K/Kmut} with CDC20-Flag after 48 hours of co-expression in 293T cells. Cells were treated with 10 mM MG132 for 5 hours prior to harvesting to prevent immediate proteasomal degradation of E2F7/8 after binding to CDH1.

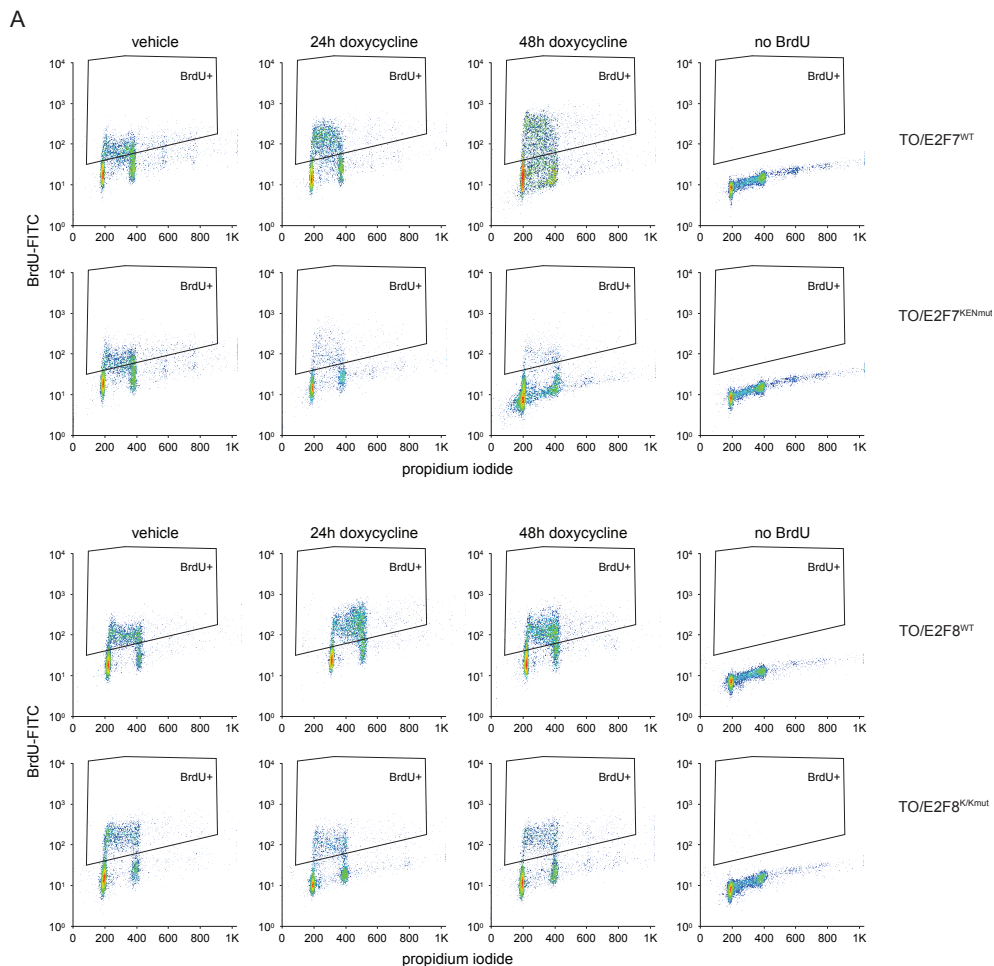


Figure S3. Stabilization of KEN-mutant E2F7/8 inhibits DNA replication.

FACS data showing scatterplots of DNA synthesis (anti-BrdU-FITC) versus DNA content (propidium iodide) in cells with stable expression of indicated inducible constructs. Gates were used to calculate the percentage of BrdU-positive cells shown in Fig. 4A of the main paper.

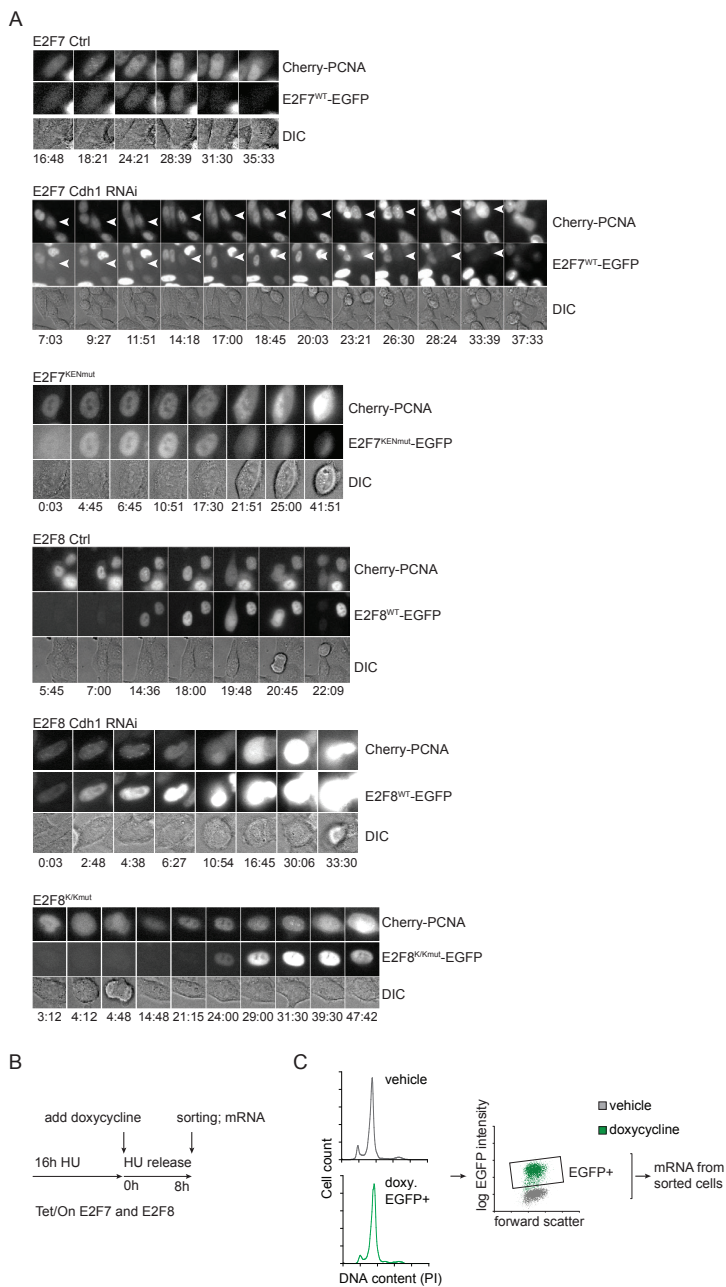


Figure S4. Live imaging of S phase, and FACS-sorting of E2F7/8-expressing cells.

(A) Montages of PCNA dot formation and cell death in cells with inducible expression of indicated constructs, and effect of CDH1 RNAi. Arrowheads indicate a cell that enters S phase, but undergoes cell death. Time is indicated in hh:mm from the onset of imaging and doxycycline induction. (B) Experimental scheme of FACS sorting in synchronized cells with stable expression of E2F7/8 in presence or absence of doxycycline induction. (C) Example of gating strategy to sort cells with detectable E2F7/8-EGFP.

Chapter 5

**Cyclostop, a non-degradable APC/C-binding Emi1 fragment
that blocks cells in metaphase independently of the mitotic
checkpoint**

Michiel Boekhout and Rob Wolthuis

ABSTRACT*Background*

Emi1 is a protein that binds and inhibits the APC/C in interphase, but is degraded at the end of G2 phase and in prophase. Subsequently, in prometaphase, the APC/C is phosphorylated, binds Cdc20 and becomes highly active. Nevertheless, current models, based on micro-injection experiments of a stable version of Emi1, propose that Emi1 degradation is not the step that liberates APC/C^{Cdc20} when cells enter mitosis. This suggests that Emi1 is either inactivated in mitosis by a mechanism independent of degradation, such as phosphorylation by mitotic kinases, or that Emi1 is incapable of inhibiting APC/C^{Cdc20}.

Results

Unexpectedly, here we show that, when stably expressed, non-degradable Emi1 (ND-Emi1) is not inactivated in mitosis but causes a very profound mitotic block. This block is on par with the mitotic arrest induced by clinically relevant spindle poisons. Mitotic block as a result of ND-Emi1 expression requires its C-terminal APC/C binding motif, the LRRL tail, which Emi1 shares with another APC/C binding protein, Ube2S. This indicates that ND-Emi induces a direct APC/C blockade. Next, we generated an APC/C inhibitory protein fragment of Emi1, named Cyclostop, consisting of different proposed APC/C interacting motifs. When expressed under the control of an inducible promoter, Cyclostop blocks cells in metaphase, after cyclin A and Nek2A are degraded. This block is therefore similar to the effect of spindle poisons, but occurs in a manner at least partially independent of a functional mitotic checkpoint. Mechanistically, Cyclostop might prevent efficient APC/C^{Cdc20} formation by locking the APC/C into an inactive APC/C APC/C^{Cdh1-MCC} complex

Conclusion

Emi, when stabilized and overexpressed in mitosis, prevents mitotic exit. This mitotic arrest is different from direct APC/C^{Cdc20} inhibition by cell-permeable APC/C inhibitory molecules such as proTAME or apcin, or from indirect inhibition of the Cdc20 by activation of the spindle checkpoint. Our observations re-open the discussion of how the APC/C is activated when cells enter mitosis, indicating a role for Emi1 degradation next to regulated binding of Cdc20 to the APC/C. Furthermore, our results provide evidence that developing cell-permeable APC/C inhibitors with a mode of action different from Cdc20 displacement (proTAME) or Cdc20 D-box competition (apcin) might be a feasible strategy. When expressed as an inducible construct, Cyclostop provides a new tool to induce a profound drug-independent metaphase arrest that does not target the mitotic spindle.

INTRODUCTION

The Anaphase-Promoting Complex/Cyclosome (APC/C) is the E3 ubiquitin ligase responsible for degrading securin and cyclin B in mitosis, allowing sister chromatid separation and mitotic exit, respectively. Maximal APC/C activation normally occurs only after the mitotic checkpoint has been satisfied, when the chromosomes are bi-orientated and correctly attached to the mitotic spindle.

The inhibition exerted by the mitotic checkpoint acts on the APC/C-activator Cdc20 and is crucial for maintenance of genomic stability. However, outside of mitosis, APC/C inhibition is also essential. During interphase, Cdc20 is either absent or not bound to the APC/C, but the APC/C can now use its other activator, Cdh1. In G1 phase, or after severe DNA damage in S- or G2-phase, APC/C^{Cdh1} is highly active. At the end of G1 phase, APC/C^{Cdh1} becomes inhibited by the synthesis of Emi1, an APC/C^{Cdh1} binding protein that inhibits the function of this complex^{112,121}. Emi1 transcription is driven by E2F transcription factors¹⁰⁷ and is necessary for S-phase entry, by stabilizing newly synthesized cyclin A as well as the DNA replication inhibitor geminin.

Emi1 depletion by RNAi causes massive activation of APC/C^{Cdh1}, and a cell cycle delay that ultimately leads to DNA re-replication cycles in the absence of mitosis, as a result of accumulating cyclin E-Cdk2 activity and concomitant disappearance of geminin and the mitotic cyclins^{111,115}. This effect of Emi1 depletion can be completely rescued by co-depletion of Cdh1, showing that Emi1 has no other function in late G1 apart from inhibiting APC/C^{Cdh1}. At the end of G2 and during prophase, in a manner dependent on Plk1 phosphorylation^{127,128}, Emi1 is recognized and degraded by the ubiquitin ligase SCF^{-TRCP}^{116,284}.

Emi1 was proposed to inhibit the APC/C as a 'pseudosubstrate'¹¹², utilizing a D-box motif that is normally found in many APC/C substrates, to block the APC/C activator. However, recently the separate contributions of singular domains have been identified on a biochemical and structural level^{121,126}. These showed that, besides the D-box, a linker region, the Zinc-binding region (ZBR) and C-terminal tail (together dubbed 'DLZT') play a role in inhibiting the APC/C¹²¹. Summarized, the D-box binds the co-activator to compete with substrates, the linker binds to the central cavity of the APC/C, while the ZBR collaborates with the C-terminal tail to inhibit the catalytic core, the APC2 and APC11 subunits. The ZBR is thought to suppress chain elongation mediated by UbcH10, while the C-terminal tail competes with Ube2S¹²⁶. Direct binding though the conserved LRRL tail to the APC/C during meiosis has been shown for Emi2 previously¹²⁴, as has competition for Ube2S¹²³.

The meaning of the latter observation is unknown, because cells can divide normally with very low levels of Ube2S, and so competition between Ube2S and Emi1 for APC/C binding does not seem to be the major mechanism by which Emi1 works. Nevertheless, it is possible that the LRRL tail is one of the most important motifs by which Emi1 binds the APC/C (see below).

While the inhibitory potential of Emi1 on APC/C^{Cdh1} is undisputed^{111,112}, the potency of Emi1 as an inhibitor of APC/C^{Cdc20} still remains controversial. In *Xenopus*, significant APC/C^{Cdc20} inhibition was shown¹⁰⁸, while in *Drosophila* exclusively APC/C^{Cdh1} was inhibited^{109,110}. Emi1 independently binds directly to the APC/C¹¹², but can also directly bind to the co-activator^{107,108,114}, in a D-box dependent manner.

Besides through degradation, direct Cdk1 phosphorylation of Emi1 may also inhibit Emi1 function in mitosis¹²⁹. However, rather than a modest delay in mitosis^{108,111}, we unexpectedly found that expressing a non-degradable (ND) mutant of Emi1 from interphase onwards was sufficient to cause a severe mitotic block, on par with the effects of spindle poisons. Even more so, this arrest was largely independent of the mitotic checkpoint. By expressing the APC/C inhibitory domains of ND-Emi1 in a construct that is controlled by a doxycycline inducible promoter, we created a useful tool for blocking cells in mitosis with an intact spindle. So, this construct, Cyclostop, stops the cell cycle in mitosis by preventing APC/C^{Cdc20} activation, in a manner that is mostly independent of functional mitotic checkpoint activity.

RESULTS

Expression of ND-Emi1 leads to a checkpoint independent mitotic arrest.

We generated a non-degradable version of Emi1 (ND-Emi1) by mutating two Serines in the phospho-degron, Ser145 and Ser149¹¹¹. When testing the effect of ectopically expressed Cherry-tagged ND-Emi1, we found that Cherry positive cells entered mitosis. Once in mitosis, these cells progressed through prometaphase, reached metaphase, as detected by the stable expression of dynein-Venus, a marker of the mitotic spindle, and transient co-transfected H2B-CFP. Subsequently these cells stayed arrested in metaphase (**Fig. 1A**). Fluorescent cells spent up to 20 hours in the mitotic arrest (**Fig. 1B**). When transiently transfecting Cherry-ND-Emi1 in U2OS cells, concomitantly with the APC/C^{Cdc20} substrate Geminin-Venus we found that that cells displaying a mitotic arrest also retained high levels of Geminin throughout the delay (**Fig. 1C**).

As Emi1 directly interacts with the APC/C through the LRRL C-terminal tail^{121,124}, we wondered whether this domain was crucial for the observed phenotype. Interestingly, this LRRL tail is identical to the C-terminus of the E2 enzyme which extends the poly-ubiquitin chains on APC/C substrates, Ube2S (**Supplemental Fig. 1A**). In vitro these two proteins may also compete for direct binding on the APC2 subunit¹²⁶. However, upon transient transfection we could not detect significant or reproducible competition between Ube2S and ND-Emi1, using mitotic delay as a read out, either by FACS or fluorescent time lapse imaging (**Supplemental Fig. 1B, 1C**), even though GFP-Ube2S expression was over a 100 fold of the levels of GFP-ND-Emi1.

Viral mediated expression of ND-Emi1 leads to an efficient mitotic delay.

As transfection was inefficient and resulted in large cell to cell variation of expression levels, we set out to use a viral system to achieve higher efficiency, combined with lower expression of the fusion protein per cell. We were able to reproducibly infect RPE1-eco cells, so that 48h after the initial infection we could clearly detect a tail dependent mitotic arrest (**Fig. 1A, top panel**). We verified that this was not cell type specific effect, by reproducing this effect in both U2OS-eco (**Fig. 2A, lower panel**) and HeLa cells (data not shown). The arrest of the non-degradable mutant was dependent on the ND-Emi1 LRRL tail, and not dependent on high levels of expression of the LRRL mutant compared to the wild type GFP-Emi1 protein (**Fig. 2B**). To quantify mitotic duration in a single cell manner, we used fluorescence microscopy. This also permitted the identification of GFP positive cells, although the signal to noise ratio was insufficient for accurate segmentation. However, also by only using phase contrast to detect all mitotic events, we could determine that GFP-ND-Emi1 in a subset of cells led to a mitotic delay that lasted over 500 minutes, which was not observed for the non-APC/C binding GFP-ND-Emi tail mutant (**Fig. 2C**). Interestingly, we could clearly observe both

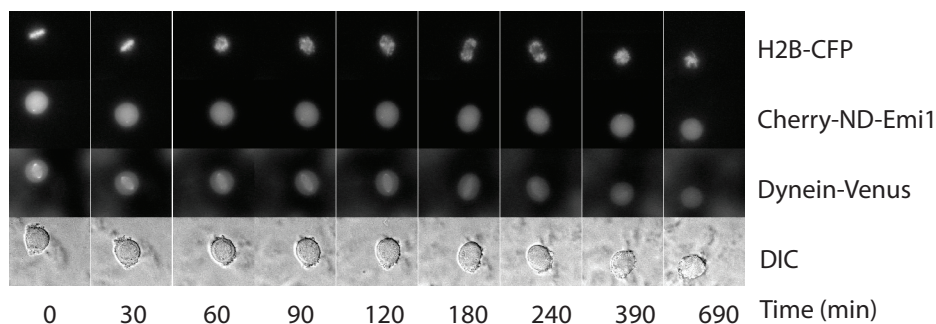
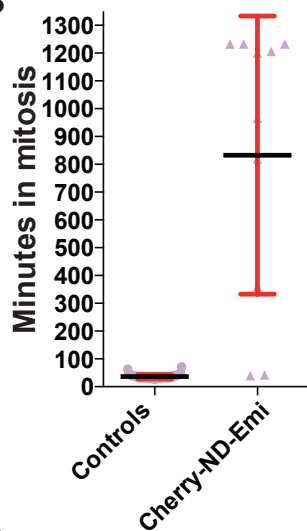
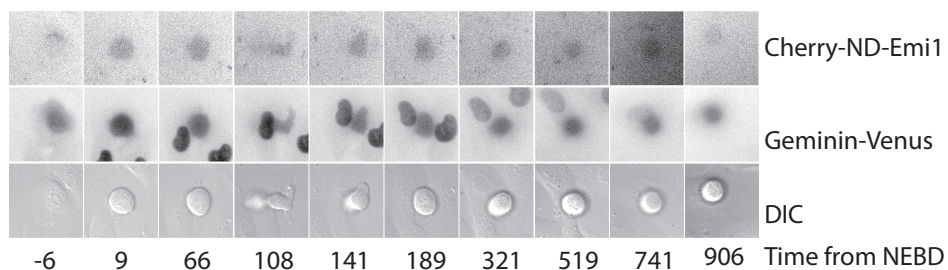
A**B****C**

Figure 1 Expression of non-degradable Emi1 expression leads to a mitotic arrest

A) U2OS cells stably expressing Dynein-Venus were transfected with H2B-CFP and Cherry-ND-Emi1 and imaged at 3 minute intervals by fluorescence and DIC microscopy B) From the cells in A, the time in mitosis, measured from NEBD, is plotted of transfected cells vs non transfected cells. Plotted are mean \pm s.d. C) U2OS cells were transfected with both Cherry-ND-Emi1 and Geminin-Venus and imaged with 3 minute intervals by fluorescence and DIC microscopy.

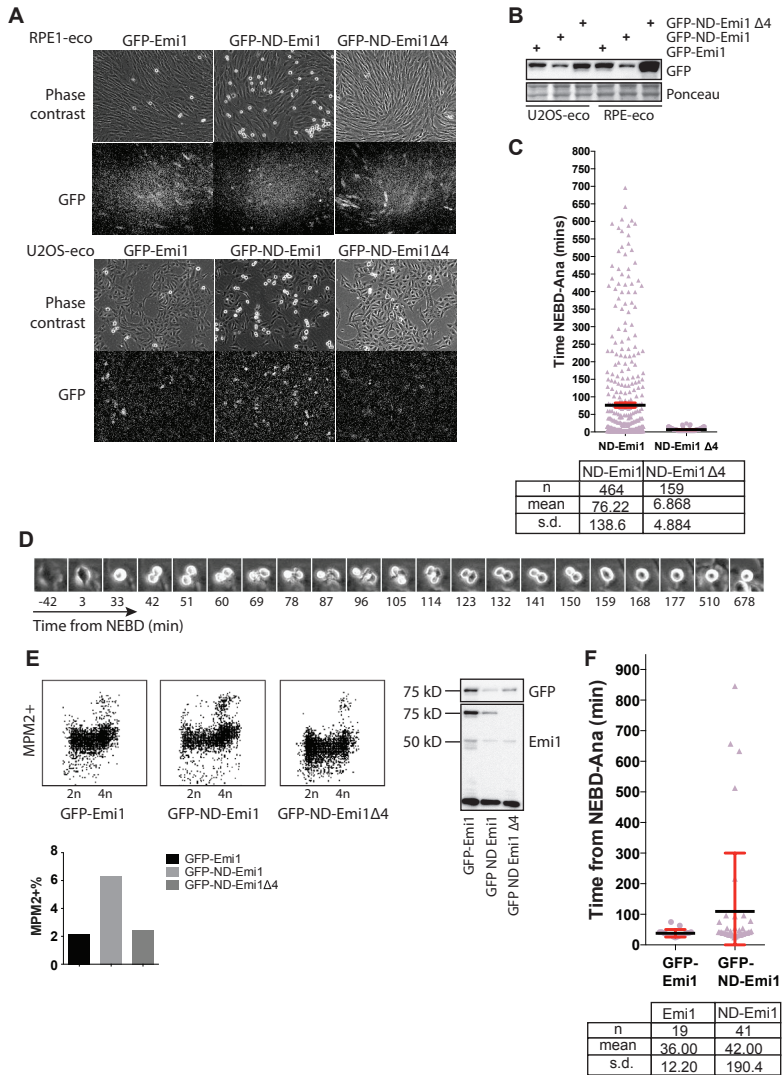


Figure 2 Integrating ND-Emi1 retrovirally efficiently induces mitotic arrest

A) Ecotropic RPE1 cells (top panel) and ecotropic U2OS cells (lower panel) were infected with retrovirus leading to expression GFP-Emi1, GFP-ND-Emi1 or GFP-ND-Emi1Δ4 as observed by phase contrast and fluorescence microscopy. **B)** Cells treated as in **A**, lysed 48 hours after initial infection and analyzed by Western blot. **C)** RPE1-eco cells infected with GFP-ND-Emi1 or GFP-ND-Emi1Δ4 were imaged using a Macro designed for recognizing all mitotic events, based on phase contrast images. GFP-ND-Emi1 n=464, GFP-ND-Emi1 n=159 **D)** Montage of U2OS cell infected with GFP-ND-Emi1 attempting anaphase to form two daughter cells, but collapsing back to into singular mitotic cell. **E)** Similar to **A**, U2OS cells analyzed by FACS analysis after infection. Plots show cells by DNA content (x-axis) and MPM2 intensity (y-axis), 4N MPM2+ cells are quantified in the lower bar graph. Right image shows western blot of infected cells. **F)** U2OS cells were virally infected with either GFP-Emi1 or GFP-ND-Emi1Δ4 and all mitotic events were scored by measuring the time from NEBD-anaphase by time-lapse phase contrast microscopy. GFP-Emi1 n=19, GFP-ND-Emi1 n=41.

distinct metaphase plates in some arrested cells, as well as a very small fraction of cells attempting anaphase and cytokinesis, but subsequently reverting to undivided, rounded mitotic cells (**Fig. 2D**). The observed 2N MPM2+ population might represent these cells, which are attempting cytokinesis, in the FACS profile of GFP-ND-Emi1 infected cells, by a 2N MPM2+ population (**Fig. 2E**) We only observed this MPM2+ 2N cell population in the ND-Emi1 infected cells. Unfortunately, because the fraction of these cells was 1% or less of the total population, we were unable to firmly identify their cell cycle status. However, FACS analysis did confirm that increase in mitotic population is dependent on the ND-Emi1 C-terminal tail (**Fig. 2E**). Analysis of protein levels by western blot indicated GFP-Emi1 was expressed 5 fold compared to endogenous Emi1 (**Fig. 2E** right image.). After correction for protein levels we found that GFP-ND-Emi1 and GFP-ND-Emi1 Δ 4 were present 2-fold and 3-fold in comparison to the endogenous level of Emi1. Similar as for RPE-1 cells, by measuring all mitotic events by phase contrast we also identified a sub group of U2OS cells that arrested over 500 minutes after GFP-ND-Emi1 infection. These were not observed upon ectopic expression of the degradable GFP -Emi1 wild type protein (**Fig. 2F**).

Emi1 binds both activators and a minimal amount of APC/C

As we now had determined that viral expression was highly efficient in ecotropic RPE1 cells, we continued with this cell line to biochemically assay Emi1 function. To be able to use GFP-ND-Emi1 Δ 4 as a negative control, we added nocodazole to arrest these cells in mitosis. As we were uncertain whether inhibiting spindle formation would perturb Emi1 function, we isolated cells arrested by the expression of ND-Emi1, treated with or without nocodazole and immunoprecipitated the fusion protein (**Fig. 3A**, M or M+N). We found that the Emi1 fusion protein bound to Cdc20 as well as Cdh1, although the latter more prominently in the non-mitotic, adherent cells which most likely represent G2 phase cells predominantly (**Fig. 3A**, I). Detection of the interaction with either activator was dependent on the LRRL tail. Binding to the APC/C subunits was also detected, but appeared to be weaker. Also for the full length ND-Emi1, the most efficient APC/C binding was detected in non-mitotic cells. Nevertheless, the binding that was detected in mitosis was completely dependent on the C-terminal APC/C interaction motif. Interaction of Emi1 with the APC/C has been attributed to electrostatic interactions¹²⁶, but immunoprecipitations under conditions of lower salt concentrations also showed no increased complex formation between APC/C and Emi1, in our hands (data not shown). To investigate how the interaction between Emi1 and the APC/C changes when cells enter mitosis, we synchronized cells in G2, or collected cells that were arrested in mitosis by expression of our fusion construct. We confirmed activator binding in both G2 and mitosis when using GFP-ND-Emi1 as bait (**Fig. 3B**). Surprisingly, we found no binding of the Emi1 fusion-protein co-immunoprecipitating in extracts from either G2 or mitotic cells, in Cdc20 IPs (data not shown). This could still relate to interference

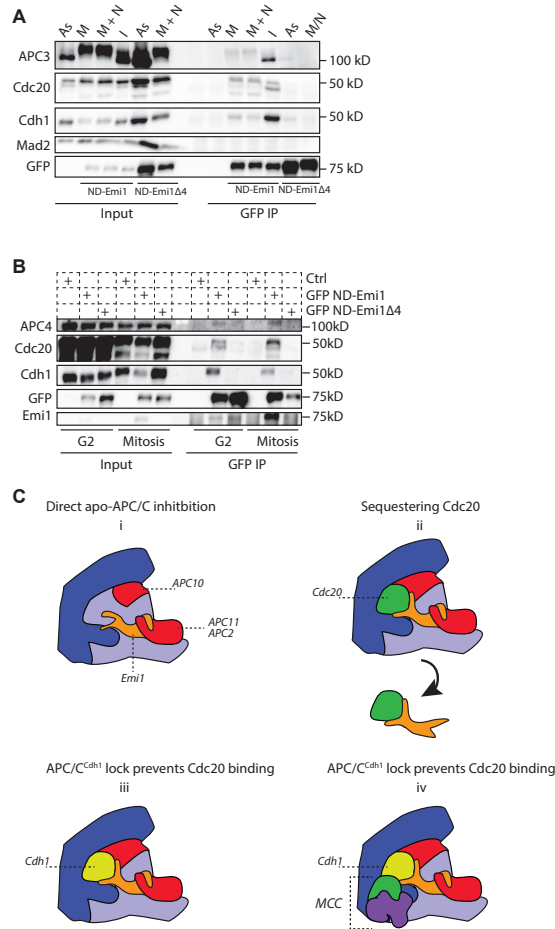


Figure 3: Interaction of Emi1 with the APC/C and activators is dependent on the C-terminal tail

A) Ecotropic RPE cells were infected with virus carrying constructs for expression of either ND-Emi1 or ND-Emi1Δ4 as indicated. Cells were synchronized for 24h with thymidine and released to arrest on either GFP-ND-Emi1 or nocodazole. Mitotic cells were collected by mitotic shake off (M), upon GFP-ND-Emi1 expression or by the addition of nocodazole (M+N). The remaining non mitotic interphase (I) and an asynchronously growing dish (As) were also lysed and immunoprecipiations using antibodies directed against GFP were performed. B) Ecotropic U2OS cells were infected with either GFP-ND-Emi1 or GFP-ND-Emi1Δ4. Cells were synchronized for 24h with thymidine and released for 8h to synchronize cells in G2 or released to arrest in mitosis on expression of ND-Emi1 or for GFP-ND-Emi1Δ4 released into nocodazole. Mitotic cells were collected by mitotic shake off and lysed, followed by immunoprecipitation of GFP. C) Proposed models of interaction between the APC/C, Emi1 and the activators. APC/C TPR lobe in dark blue, APC/C platform in light blue, catalytic core in red, Emi1 in orange. Model i shows direct inhibition of the APC/C catalytic core, regardless of the presence of an activator. Model ii suggests binding and inhibiting Cdc20 when bound to the APC/C, but Emi1 also remains bound to Cdc20 when free of the APC/C. Model iii shows Emi1 binding to inactivated Cdh1, locking it onto the APC/C, sterically hindering Cdc20 mediated activation. Model iv incorporates recent data that the MCC is able to inhibit APC/C^{Cdc20} (Izawa & Pines 2014) although we propose that instead of Cdc20, Cdh1 can also remain bound, based on our immunoprecipitation results.

of the antibodies with protein complex stability. Furthermore, we only detected a weak interaction of Emi1 with the APC/C subunits, but this was completely dependent on the C-terminal APC/C binding motif, indicating it was specific (**Fig. 3B**, GFP IP APC4 blot).

We hypothesized four possibilities to explain the mitotically arrested phenotype i) Emi1 may directly inhibit the APC/C regardless of the activator; ii) Emi1 scavenges all Cdc20 (or APC/C^{Cdc20}), preventing mitotic activation of the APC/C; iii) Emi1 binds to APC/C^{Cdh1} and keeps Cdh1 locked in an inactive state, and thus blocks Cdc20 from activating the APC/C upon mitotic entry. A final possibility, derived from the observation that MCC may inhibit APC/C^{Cdc20} ²⁶⁶, could be that iv) ND-Emi1 keeps Cdh1 bound, while the checkpoint can also still bind the APC/C (**Fig. 3C**). Our results indicate that it is indeed possible that Cdc20 can be sequestered by Emi1, but only a fraction of the total cellular pool of Cdc20 is detected in our GFP-Emi1 IPs. It seems unlikely therefore, that all Cdc20 is inactivated by direct Emi1 binding. Furthermore, Emi1 is expected to bind APC/C-activator complexes based on the structural analysis of the APC/C^{Cdh1-Emi1} complex. From this, we infer that APC/C binding by Emi1 is still a crucial step in the inhibitory mechanism. It seems possible, therefore, that Emi1 blocks both apo-APC/C as well as APC/C^{Cdh1}, the latter in a form that is either in complex with the mitotic checkpoint proteins or not (iv).

Cyclostop, an Emi1 derived inducible APC/C inhibitor

Next, we aimed to generate a derivative of Emi1 that could be used to block cells in mitosis, in a way that is different from activation of the mitotic checkpoint, such as occurs upon inducing mitotic spindle damage. Furthermore, we aimed to study protein complex formation with the APC/C in more detail. Therefore, we cloned the ‘DLZT’ region¹²¹ of Emi1, preceded by a triple Flag-tag and an Auxin inducible degron³²⁹, expressed by a Doxycycline inducible promoter (**Fig. 4A**). We dubbed this construct ‘Cyclostop’. Upon doxycycline addition, we found that expression of Cyclostop, induces arrest of cells in mitosis. (**Supplemental Fig. 2A**). Next, we wished to biochemically characterize these mitotically arrested cells. To this end, we synchronized cells and arrested them in mitosis by induced Cyclostop expression. From these mitotic cells we pulled down the APC/C, Cdc20 and the Flag-tagged Cyclostop protein (**Fig. 4B**). We found that, in mitosis, Cyclostop binds to the APC/C and both activators, but more notably to Cdc20. We found low levels of checkpoint proteins, which we suspect are bound via Cdc20, or APC/C^{MCC}, rather than direct binding of checkpoint proteins to Cyclostop. We considered that if inhibition of Cyclostop on the APC/C was direct, it might be independent of checkpoint function. To test this, we used U2OS and RPE1 cells that had been stably infected with inducible Cyclostop, and transfected these cells with siRNA oligos directed against the checkpoint component Mad2 (**Fig. 4C**). While

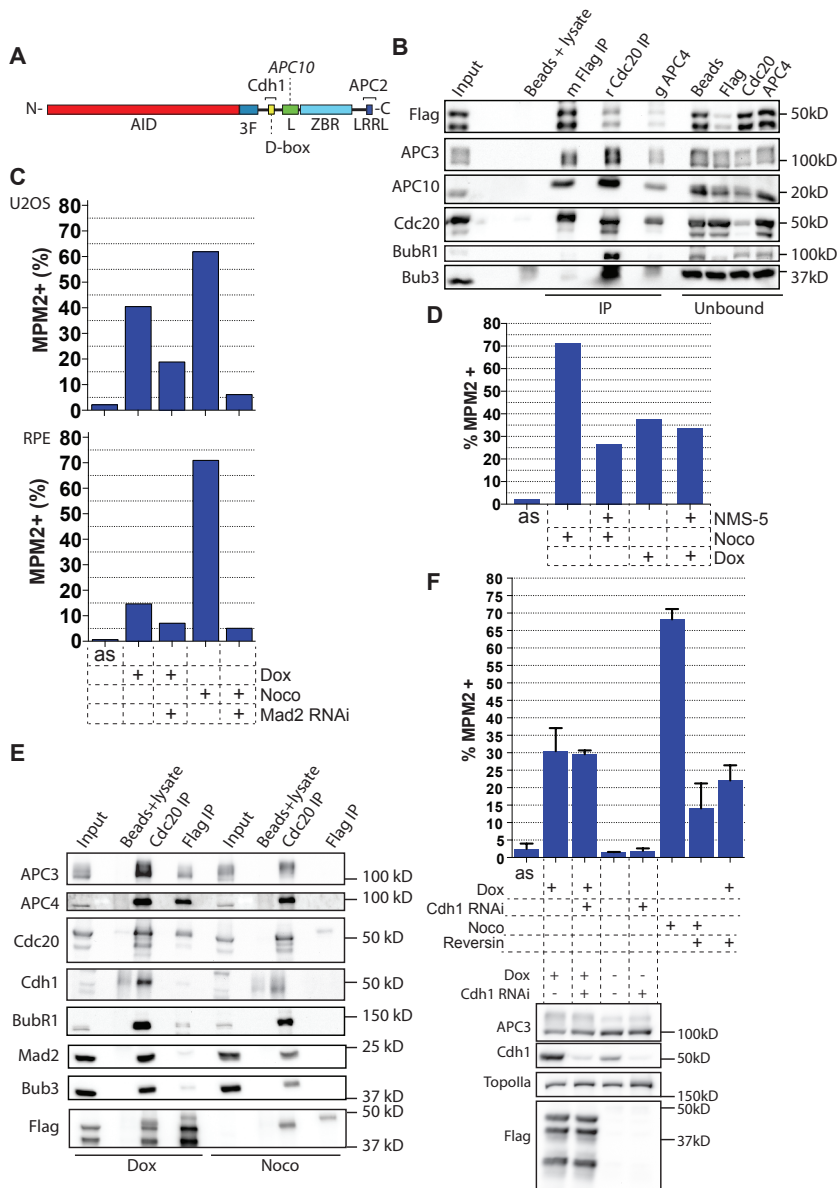


Figure 4: Creation of an inducible DLZT domain creates a potent APC/C inhibitor largely independent of the mitotic checkpoint

A) Protein overview of 'cyclostop' from N to C terminus. AID= Auxin Inducible Degron, 3F= 3 FLAG constructs, L=Linker region, ZBR= Zinc-binding Region, LRRL = LRRL tail. See also Frye *et al.* 2013. B) Cells were synchronized for 24h with thymidine, followed by release into medium containing doxycycline. Mitotically arrested cells were collected by mitotic shake off, lysed and divided in three equal parts to allow for precipitation via antibodies directed against Flag, Cdc20 or APC4 as indicated. The unbound proteins were collected after incubating with antibody but before washing of the precipitate and also analyzed by Western blot C) Stable inducible polyclonal Cyclostop cells of either U2OS (upper graph), RPE (lower graph).

graph) lineage were treated with Mad2 RNAi or control transfected, before thymidine synchronization and release into medium containing either nocodazole or doxycycline. Cells were fixed and stained by MPM2 antibody to assess the amount of mitotic cells by FACS analysis. **D)** U2OS cells stably expressing inducible cyclostop were synchronized with thymidine, released and treated with nocodazole, doxycycline and NMS-5 as indicated. Cells were fixed, stained for with MPM2 antibody and analyzed by FACS. **E)** U2OS cells stably expressing inducible cyclostop were synchronized by thymidine for 24h, released in medium containing either doxycycline or nocodazole for 16h and collected by mitotic shake off. Lysates were split into two and probed with antibodies directed against either Cdc20 or Flag and analyzed by Western blot. **F)** Polyclonal U2OS cyclostop cells were treated with siRNA oligonucleotides targeting Cdh1 or control transfected, synchronized by thymidine and released in fresh medium, or fresh medium containing doxycycline. Control cells were synchronized and treated with nocodazole or doxycycline, and subsequently treated with Reversin for 1.5h before fixation, MPM2 staining and FACS analysis. Bar graph shows mean of 2 independent experiments \pm s.d. Before fixation, half of the cells were separated and analyzed by western blotting, lower image.

removal of the checkpoint diminished the mitotic population of mitotic cells when treated with nocodazole, we found only a partial override of mitosis in Cyclostop-arrested cells. To test checkpoint independence of the Cyclostop arrest, we wished to verify our results further, by investigating the effect of chemically removing the mitotic checkpoint. Nocodazole treatment lead to a larger mitotic population, likely due to the fact that Cyclostop expression was not penetrant in all cells. This fraction disappeared specifically upon treatment with NMS-5. However, the while cells arrested by expression of Cyclostop were refractory to checkpoint inhibition (**Fig. 4D**) By immunofluorescence experiments, we indeed determined that Cyclostop was not expressed in all cells of our polyclonal cell line (**Supplemental Fig. 2B**). Also of note is that Cyclostop does not seem to be located on the DNA or kinetochores, suggesting it acts diffusely throughout the cell. It should be noted that Cyclostop in this respect differs from full length Emi1, which at least during prometaphase and metaphase is present on the mitotic spindle and the spindle poles^{127,330}. This is very likely due to the fact that the N-terminal portion of Emi1 interacts with NuMa and Plk1 which respectively directly and indirectly mediate Emi1 localization to the spindle³³⁰.

We hypothesized that Cyclostop arrested cells might be used to further investigate our models (**Fig. 3C**). To this end we arrested polyclonal U2OS Cyclostop cells on either nocodazole or Cyclostop and from both conditions pulled down Cdc20 and the Cyclostop construct (**Fig. 4E**). We could determine that Cdc20 still binds the other checkpoint components Mad2, Bub3 and BubR1 at the same or even higher levels in cells arrested by Cyclostop compared to nocodazole arrested cells. This shows that Cyclostop does not prevent Cdc20 from binding the APC/C, disfavoring model i) and iii). However, the most notable difference is the unexpected presence of Cdh1 when pulling down Cdc20 when cells are arrested on Cyclostop supporting model iv). As we find a slight increase of APC/C binding and Cdc20 in Cyclostop arrested cells, it seems

unlikely that Cyclostop actively dissociates Cdc20 from the APC/C, but we cannot rule out, that it still exerts an inhibitory effect on free Cdc20, or on APC/C^{Cdc20-MCC}. We wondered whether the Cdh1 that we detected in Cdc20 IPs, and to a lesser extent Flag IPs, upon Cyclostop expression, also played a functional role in inhibiting the APC/C. Even if Cdh1 would not prevent Cdc20 binding to the APC/C, it might still sterically hinder Cdc20 function. To test this we depleted cells of Cdh1 RNAi, followed by Cyclostop induced mitotic arrest (**Fig. 4F**). However, loss of Cdh1 did not result in a difference in the amount of cells arresting in mitosis. This suggests that, although Cdh1 might still be bound to the APC/C in mitosis in the presence of Cyclostop, its binding is not not causal for the arrest. Similar to GFP-ND-Emi, we were unable to detect competition with Ube2S by FACS analysis (**Supplemental Fig. 2C, 2D**).

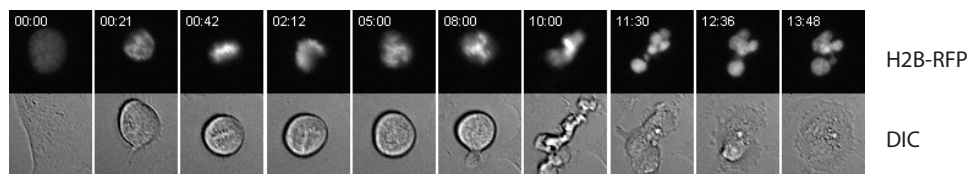
Cytokinesis defects after checkpoint override in Cyclostop

We attempted to determine the fate of cells arrested upon Cyclostop by time-lapse imaging. We transiently transfected H2B-RFP to more closely analyze progression through mitosis. We observed that cells did eventually exit mitosis, but did not undergo a regular anaphase (**Fig. 5A**). We also wanted to confirm in a single cell manner if Cyclostop arrests cells checkpoint independently in mitosis in a way that is independent of the mitotic checkpoint. Therefore, we measured the timing from NEBD to anaphase in the presence of checkpoint inhibitor and categorized the mitotic exit in either: “abnormal”, if two daughter cells were generated but no clear anaphase was observed or “slipped”, if rather than two daughter cells a single 4N G1 daughter cell was formed (**Fig. 5B**). In this experiment, we also clearly found that a fraction of cells progressed through mitosis in a manner that was identical to the situation in control cells, indicating not all cells expressed Cyclostop, which we had also detected by immunofluorescence of the polyclonal cell line (**Supplemental Fig. 2B**) However, similarly as we had detected for cells infected with ND-Emi1, a large fraction of Cyclostop-arrested cells remained unaffected, while the addition of NMS-5 clearly prevented cells from arresting in mitosis in the presence of nocodazole. Nevertheless, on average there was still a decrease in the time required from NEBD-Ana, in the presence of NMS-5 compared to cells treated only with doxycycline. Nevertheless, we previously found a minor decrease by FACS analysis by inhibiting the checkpoint (**Fig. 4D, 4F**), which could indicate that there was a small, but reproducible contribution of the checkpoint to the Cyclostop-mediated arrest.

Cyclostop leads to a metaphase arrest but does not fully inactivate the APC/C

From sparsely plated cells we picked single colonies and tested these for efficacy to arrest in mitosis following treatment with doxycycline from asynchronously growing populations by FACS analysis (data not shown). We picked the most responsive clones for both U2OS and RPE cells for follow up experiments. We again tested the effect of

A



B

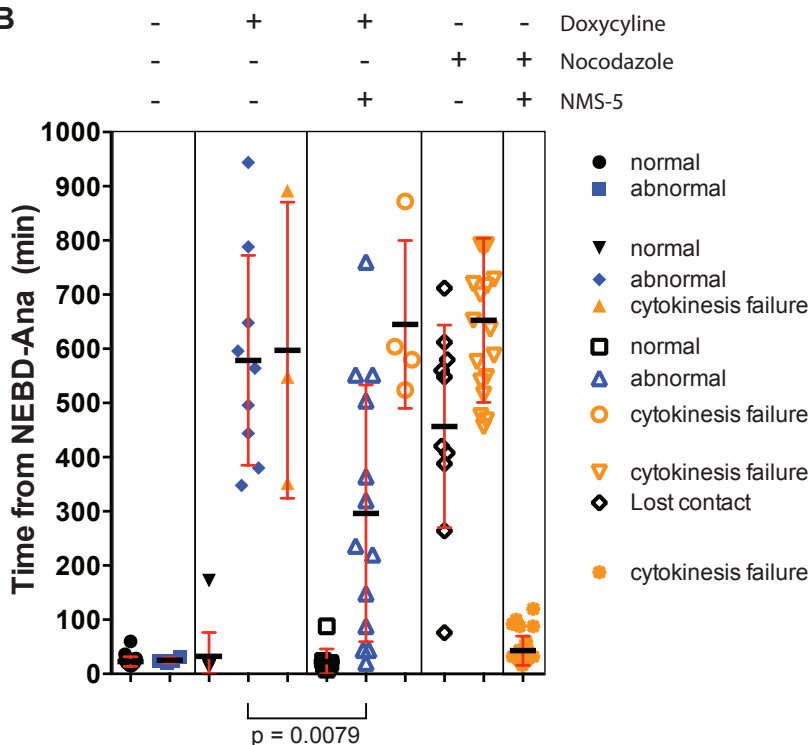


Figure 5: Cyclostop does not prevent formation of the checkpoint, or of MCC binding to the APC/C

A) U2OS cells stably expressing inducible cyclostop were transfected with H2B-RFP and imaged at 3 minute intervals with fluorescence and light microscopy. B) U2OS cells stably expressing inducible cyclostop were treated as indicated and imaged at 3 minute intervals by time-lapse microscopy. Mitosis was measured from NEBD to anaphase, which was categorized as 'normal' if two daughter cells formed, as 'abnormal' if cells showed problems in forming two daughter cells or as 'cytokinesis failure' if a mitotic cell flattened out into a single daughter cell. Comparison of abnormal exit in cyclostop arrested cells after addition of NMS-5 vs ctrl performed by two tailed Student t test.

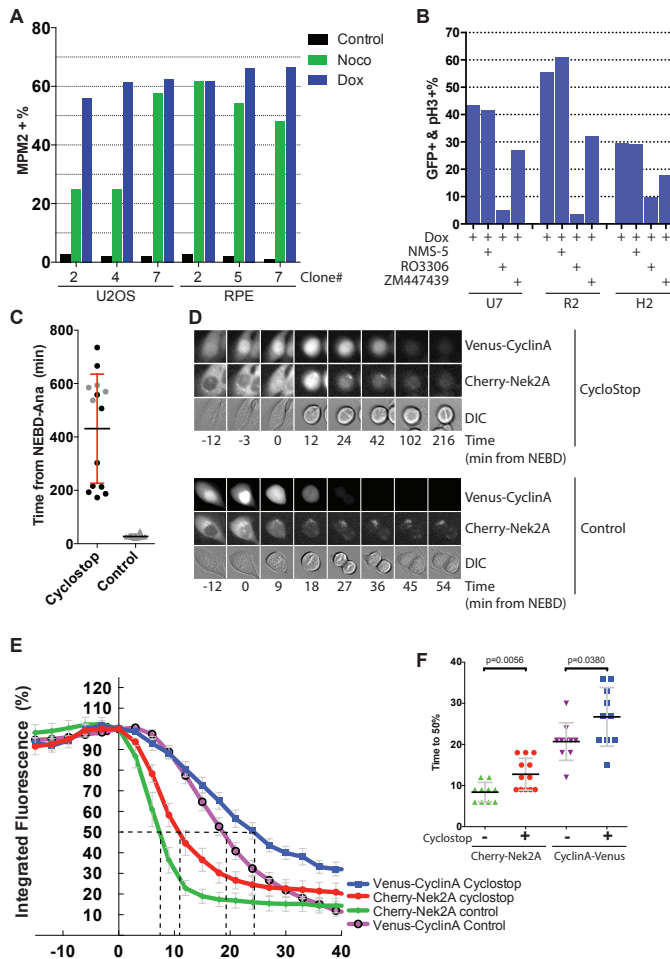


Figure 6: Cyclostop recapitulates an inducible ND-Emi1 mitotic arrest.

A) Single colonies were picked from sparsely plated polyclonal cyclostop expressing U2OS and RPE cells, and treated for 16h with either nocodazole or doxycycline before fixation, staining for MPM2 and analysis by FACS. **B**) Cells derived from the same clonal lineage of U2OS#7 (U7), RPE#2 (R2) and HeLa#2 (H2) stably expressing inducible cyclostop were synchronized with thymidine, released into doxycycline for 16h and subsequently treated as indicated with either NMS-5, RO3306 or 2 μ M ZM44739 for 1.5 h, before fixation and analysis by FACS. **C**) Polyclonal U2OS cells stably expressing Cherry-Nek2A, Tet inducible Cyclin A-Venus and Dox inducible Cyclostop were thymidine arrested for 16h, released and either imaged at a 3 minute interval in the presence of Tet (Control cells), or of Tet + Dox (Cyclostop). Time from NEBD-Ana plotted, as determined by DIC and fluorescent channels, black symbols indicate end of time-lapse imaging before mitotic exit was observed. **D**) Montage of the cells measured in **C**. Upper panel shows Cyclostop arrested cells, lower panel shows control cells. **E**) From cells measured in **C** and shown in **D**, Integrated fluorescence was measured per cell at each time frame and normalized to the level of fluorescence on NEBD. Time of NEBD is set to 0 on the x-axis. Dashed lines indicated the time and amount of 50% remaining fluorescence. Lines depict mean \pm s.e.m. n=2 separate experiments each line consists of at least 10 individually measured cells. **F**) From the data depicted in **E**, time measured to 50% fluorescence, per construct per condition. P values were determined using a two tailed unpaired student t test.

doxycycline treatment on cells that were released from a thymidine arrest, and also made a direct comparison to nocodazole. In this experiment, we found that the amount of cells arresting on Cyclostop had increased to similar levels as observed after nocodazole treatment (**Fig. 6A**). We continued to use the most efficiently inducible clones to reassess the requirement of the checkpoint by FACS analysis (**Fig. 6B**). After synchronization and arresting monoclonal cell lines on Cyclostop, we added chemical inhibitors in the three different cell types. Interestingly, we now found no effect for inhibiting the checkpoint by MPS1 inhibitor. Additionally, we tested the Cdk1 inhibitor RO3306 and Aurora B inhibitor ZM 447439, and clearly found that inhibiting Cdk1 activity pushed cells out of mitosis, (due to inactivation of the mitotic kinas cyclin B1-Cdk1), while inhibiting Aurora B, showed a partial effect. This is similar to the observations made for ProTAME, discussed below in more detail¹⁹⁸.

To evaluate the extent of APC/C inhibition mediated by Cyclostop, we also introduced the Cyclostop construct to U2OS cells that stably expressed Cherry-Nek2A and Tet inducible cyclin A-Venus⁸³. After thymidine synchronization and release in the presence of both doxycycline and tetracyclin, these cells arrested in mitosis due to Cyclostop expression. In this experiment, we only saw cells escaping from mitosis 9 hours after entry (**Fig. 6C**). By single cell time-lapse fluorescence microscopy we determined the rate of destruction of both fluorescent proteins in control cells and in Cyclostop-arrested cells during mitosis (**Fig. 6D, 6E**). In control cells, we confirmed our previous finding that Cherry-Nek2A is a more efficient substrate than CyclinA upon entry into mitosis, and that both APC/C^{Cdc20} substrates are rapidly degraded from the start of prometaphase onwards. We discovered a small delay in both Nek2A and CyclinA degradation, which was more apparent if we measured the time required to reach 50% fluorescence (**Fig. 6F**). Nevertheless, this minor delay in degradation of cyclin A and Nek2A did not reflect the substantial delay in mitosis, as a result of Cyclostop expression (**Fig. 6C**). Both cyclin A Nek2A require the Cdc20 activator for APC/C mediated degradation. Nek2A can even be degraded by Cdc20 bound to checkpoint proteins, and most likely only requires binding of the C-box to activate the APC/C^{83,331}. However, Cyclin A binds Cdc20 before onset of mitosis, ahead of the Cdc20 inhibition by mitotic checkpoint proteins. We observed that, even though Cyclostop stop does not rely on the mitotic checkpoint to arrest cells in mitosis, it does not block formation or recruitment of the MCC to the APC/C (**Fig. 4E**). We hypothesize that Cyclostop to directly inhibits the catalytic core of the APC/C, or locks the APC/C in an inactive APC/C^{MCC-Emi1} complex (**Fig. 3C**, model iv) as shown for Emi1¹²¹, but this is not sufficient to completely inactivate Cdc20.

DISCUSSION

Here, we have further delved into the controversy of APC/C^{Cdc20} inhibition by Emi1. During normal cell cycle, almost all endogenous Emi1 will be degraded upon mitotic entry, although a small remaining pool has previously been identified at the spindle poles. This fraction is required for limit spindle-associated cyclin B destruction^{127,330}. However, Emi1 remaining during mitosis had also been shown to have little, if any, effect on APC/C activity^{89,111} by either mutations, or chemical inhibition of Plk1, at least when measuring cyclin A destruction as a read out^{130,332}. This suggested that at least some other mechanism may normally be in place to prevent Emi1 from inhibiting the APC/C. Alternatively, in the published experiments, Emi1 was not incorporated into inhibitory APC/C^{Cdh1} complexes due to its short expression time prior to mitotic entry. Nevertheless, cellular extracts revealed that besides degradation, direct Cdk1 phosphorylation of Emi1 may also be sufficient to block Emi1 function in mitosis¹²⁹. Similar mechanisms have been described for Emi2 during meiosis in *Xenopus*^{333,334}. Interestingly, ubiquitination of XErp1 by the APC/C itself leads to dissociation of the inhibitor, as a direct negative feedback loop³³⁵.

We were intrigued to find a long-lasting mitotic delay with a seemingly intact spindle and clear metaphase alignment by expressing ND-Emi1. Interestingly, this arrest was largely independent of the checkpoint. This prompted us to attempt and create a fully controllable APC/C inhibitor, in which we were partially successful, which we named Cyclostop. Single cell clones that were synchronized and in which Cyclostop was induced, created the opportunity to arrest sufficient cells in mitosis for both time-lapse imaging as well as biochemical assays. Unfortunately, several truncated forms of the Cyclostop construct were also translated, which lack the AID domain, and thus were also not degraded in Tir1 cells upon the addition of Auxin (data not shown,³²⁹). Potentially, further developing this construct by removing any alternative start sites could create a protein based APC/C inhibitor, which can be switched off by induced protein destruction, so that release of APC/C inhibition is possible. This direct controlled release of inhibition would also allow use of Cyclostop as a tool for studying mitotic exit.

Cyclostop compared to chemical APC/C inhibitors

Recently, the combination of two chemical inhibitors was shown to greatly inhibit the APC/C by ejecting Cdc20 and at the same time blocking the D-box recognition site on Cdc20, called ProTAME and apcin respectively¹⁹⁹. While ProTAME resembles the IR tail found in both Cdc20 and Cdh1, required for binding APC3, apcin binds directly to Cdc20, stabilizing specifically substrates that are dependent on their D-box for destruction. ProTAME by itself already leads to prolonged metaphase¹⁹⁷, and indeed, in many cases shows identical phenotypes as we observe upon expression of ND-Emi1. ProTAME arrests cells in mitosis, with an intact spindle, but both depleting either Mad2

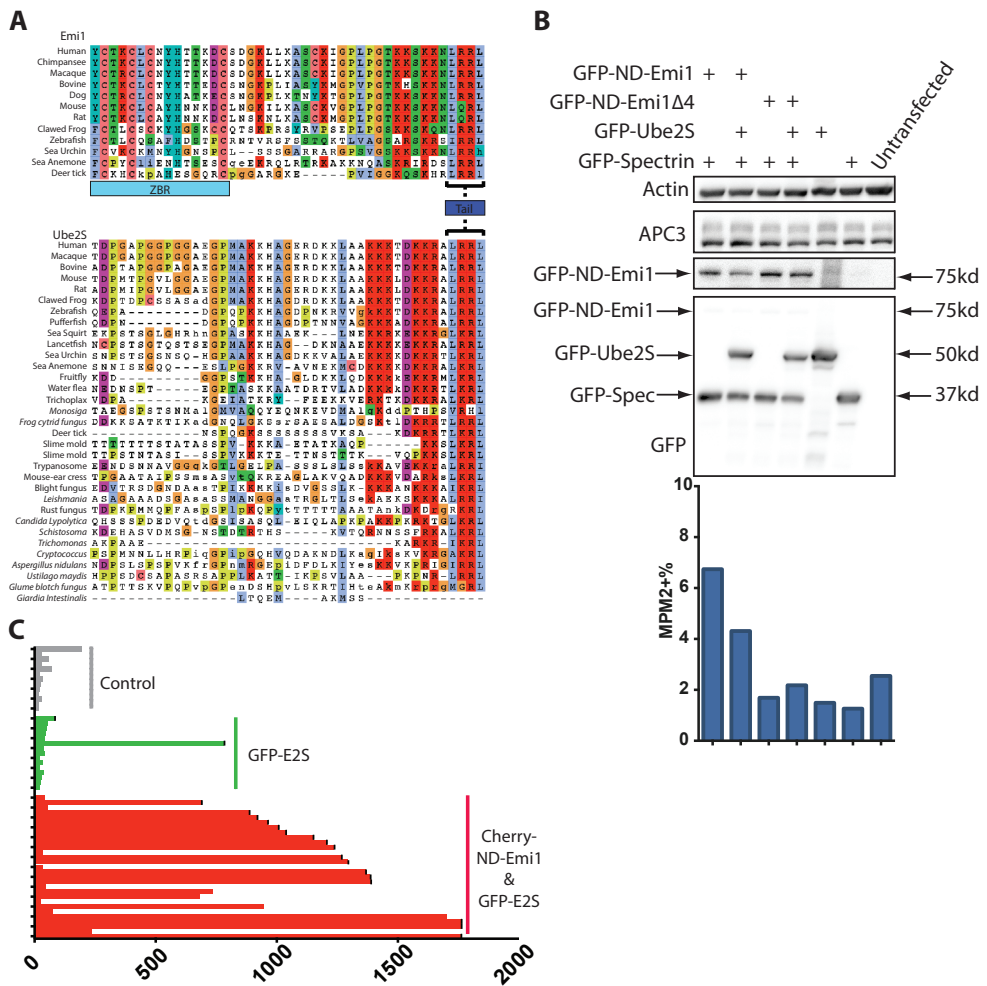
or inhibiting Aurora B greatly shortens the arrest, although not to control levels¹⁹⁸. ProTAME also leads to dissociation of Cdc20 from the APC/C, resulting in premature termination of cyclin B ubiquitination¹⁹⁷. Interestingly, while ProTAME induces a mitotic checkpoint-dependent arrest, this was later shown to be due to checkpoint re-activation after cohesion fatigue, discussed in more detail below¹⁹⁸. Intriguingly, the same study shows that removal of the MCC from the APC/C is also dependent on APC/C activity. Indeed, the fact that we may find increased binding of checkpoint proteins in the presence of Cyclostop, could lead to the same conclusion (**Fig. 4E**). However, since Cyclostop also binds to the activator, this suggests it may at least partially function differently from proTAME. Possibly, it partially obscures MCC-free Cdc20 from binding to the APC/C, while also binding to Cdc20 that does bind the APC/C, similar to apcin. In mitosis, Cyclostop may bind to APC/C^{MCC} as well (model iv). Previously, we have shown that ProTAME causes a minor delay in Nek2A degradation⁸³, and that only in combination with Cdc20 RNAi, Nek2A is fully stabilized. The use of apcin at high very high concentrations does lead to a delay from NEBD to anaphase (**Supplemental Fig. 4A**) but does not delay either Nek2A or CyclinA degradation, even at 200 μ M concentration (**Supplemental Fig. 4B**). This is in line with the results that, *in vitro*, apcin alone does not stabilize Nek2A¹⁹⁹. Considering that we find some Nek2A and CyclinA stabilization indicates that Cyclostop might act as the combination of proTAME and apcin rather than mimicking apcin alone. It should be noted that mitotic arrest induced by proTAME could be rescued by overexpression of Ube2S, leading to full poly-ubiquitination of substrates¹⁹⁷. Mitotic arrest by ND-Emi1 or Cyclostop was not rescued by Ube2S expression (**Supplemental Fig. 1, 2**). It should be noted that the direct competition between ProTAME and Cdc20 for APC/C binding via the IR tail is unlikely the mechanism of action for Cyclostop. Even though Ube2S can rescue full-length formation of ubiquitin chains, its LRRL does not compete for binding, as it does not bind APC3, but rather close to the catalytic core^{52,216}. The same seems to hold true for Emi1 and thus Cyclostop¹²¹. While the interaction of the LRRL tail with the APC/C on its own is likely weak, we did find that fusing either the last 10 amino acids of Emi1 or Ube2S did increase degradation of a model substrate upon entry into mitosis (**Supplemental Fig. 3A, 4B**). This suggests that during normal mitosis, the LRRL tail does provide an APC/C recruitment signal, independently of the other inhibitory Emi1 domains.

Cohesion Fatigue

As we find similarities between the effects of Cyclostop and the effects of ProTAME, and still a partial dependence on the mitotic checkpoint, this could indicate that the checkpoint dependent component is induced by a process called cohesion fatigue, as shown for ProTAME¹⁹⁸. An extended metaphase in the presence of an intact mitotic spindle leads to chromatid cohesion loss, due to the tension exerted by microtubule

pulling forces^{336,337}. Several other situations are known to cause cohesion fatigue such as expression of ND-CyclinB and efficient depletion of Cdc20^{336,338}. As Cyclostop does not fully block APC/C activity, as observed by cyclinA and Nek2A degradation (**Fig. 6C**), this probably also still allows for release of MCC from the APC/C via ubiquitination, regardless of degradation¹⁹⁸. Also, both inhibition of Aurora B (**Fig. 6B**) or depletion of Mad2 (**Fig. 4C**), show that some Cyclostop arrested cells exit mitosis upon abrogation of the mitotic checkpoint. Although we did not yet perform the necessary biochemical experiments to verify this, it seems likely that MCC turnover and checkpoint reactivation are at least in part responsible for the amount of checkpoint dependence that we observe (**Fig. 4D, 4F, 5B**). It would be interesting to determine cyclin B degradation kinetics in the presence of Cyclostop or test whether cells arrest more efficiently after depletion of Wapl, which would both be informative about the occurrence of cohesion fatigue.

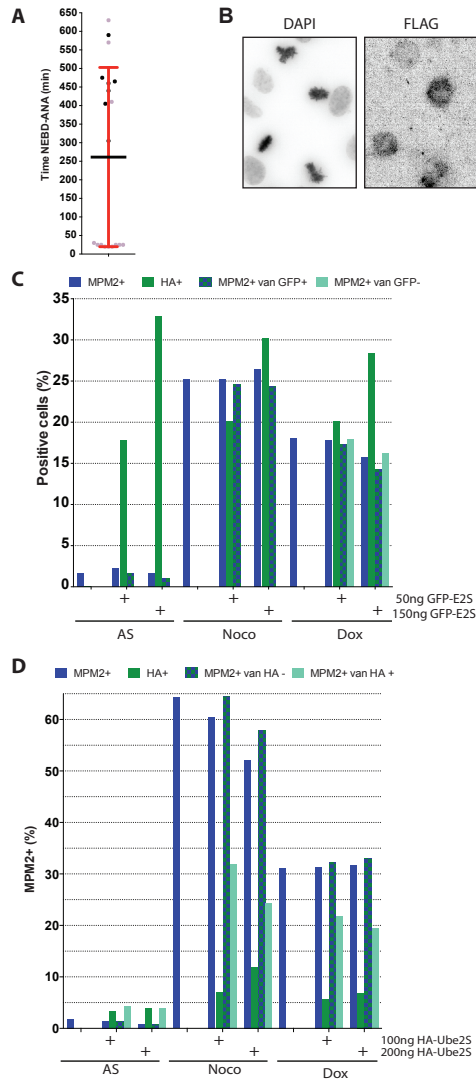
In conclusion, we propose that a combination of model i and ii are plausible, and also not mutually exclusive. We suspect Cyclostop indiscriminately binds both apo-APC/C, as well as activator bound APC/C. While bound to the APC/C, Cyclostop does not prevent binding of the MCC, and also allows for MCC release. Even in our IP conditions we find that ND-Emi1 is still bound to the activator while interaction with the APC/C is lost. This might indicate that indeed, Cyclostop directly inhibits the APC/C and catalytic core, but also retains Cdc20 binding, leading to a robust mitotic inhibition of the APC/C.



Supplemental 1: The LRRL tail is conserved between Emi1 and Ube2S, but is an evolutionary more widespread trait for Ube2S.

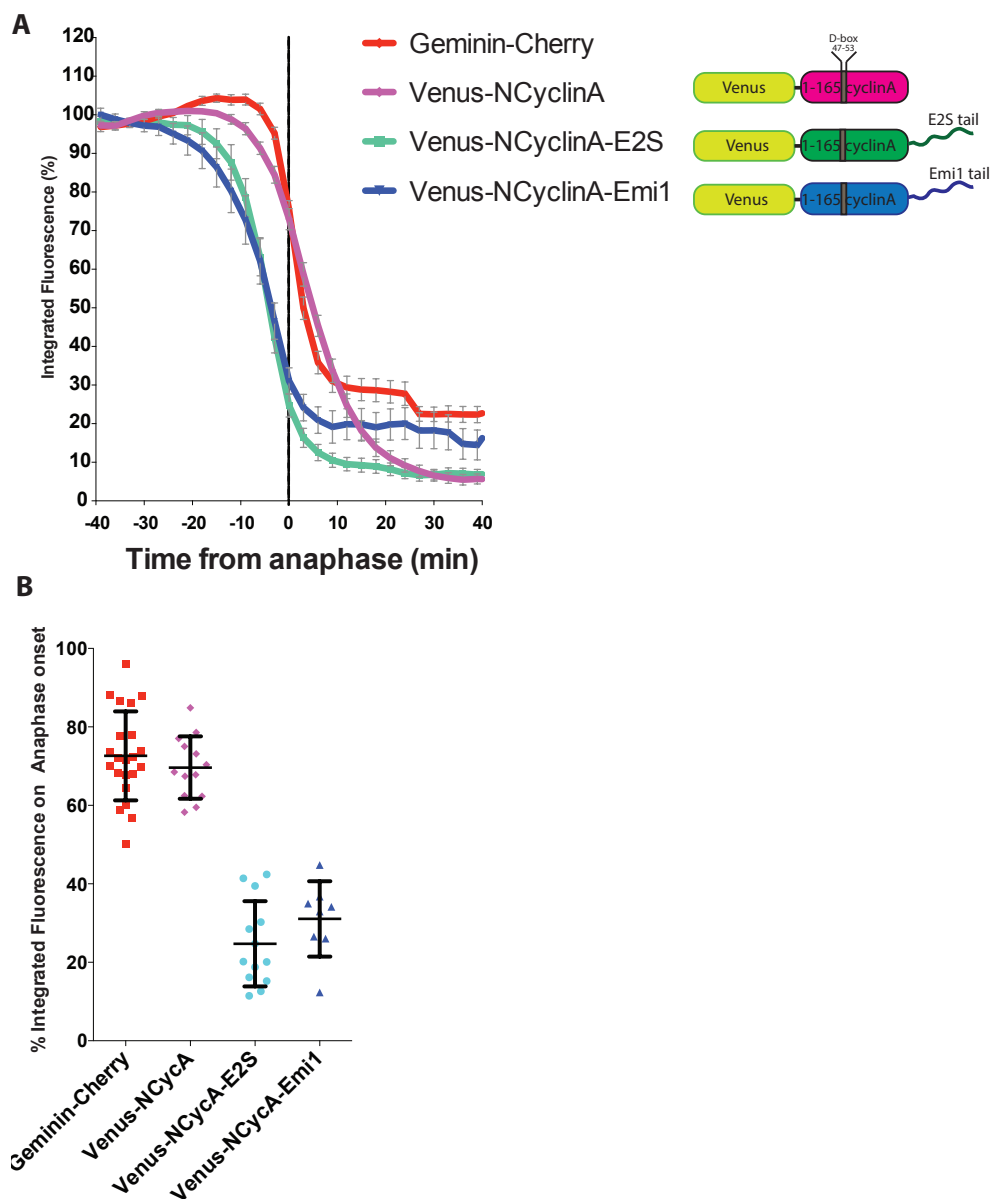
A) Standard settings of the GOPHER server (<http://bioware.ucd.ie/>) were used to align orthologous proteins of the C-terminal tail of both the FBXO5 (Emi1) protein and for Ube2S. Identical settings for including species into the alignment were used. Likely conserved amino acids are colour coded following ClustalX, based on amino acid characteristics. ZBR: Zinc-binding region. **B)** U2OS cells were transfected with constructs as indicated, split and subsequently lysed and analyzed by Western blot (upper panel) or fixed to be analyzed by FACS (lower graph)

C) U2OS cells were transfected with GFP-Ube2S and Cherry-ND-Emi1 and imaged at a 3 minute interval. A single bar represents a single cell. Plotted is time (min) in mitosis from NEBD to anaphase for non-fluorescent cells (gray) cells expressing only GFP-Ube2S (green), or cells expressing both GFP-Ube2S and Cherry-ND-Emi1 (red). No cells expressing only Cherry-ND-Emi1 were observed. Bars ending in a black vertical line indicate imaging ended before exit of mitosis was observed.



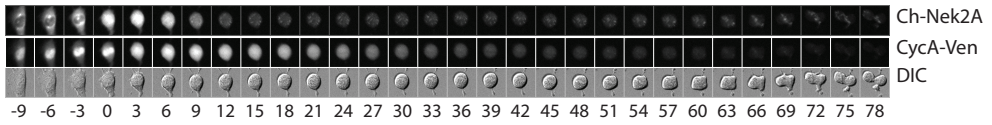
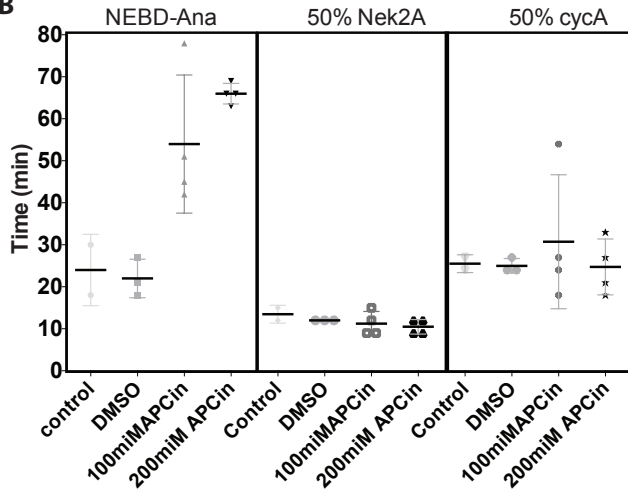
Supplemental 2: ND-Emi1 binding to the APC/C causes a mitotic arrest in multiple cell lines

A) Polyclonal U2OS stably expressing the cyclostop construct were synchronized with thymidine and released in the presence of doxycyclin, and subsequently imaged by phase contrast microscopy with a 5 min time interval. All mitotic events were manually analyzed and time from NEBD to onset of anaphase is plotted on the y-axis. Cells still arrested in mitosis at the end of imaging are represented with a black circle. **B)** Polyclonal U2OS cyclostop cells were synchronized with thymidine, released in the presence of doxycyclin and fixed after 16h for immunofluorescence. **C)** U2OS cells stably expressing inducible cyclostop were transfected with 2 different concentrations of GFP-Ube2S, and either arrested on nocodazole or induction of cyclostop via addition of doxycyclin. Subsequently cells were fixed, stained for mitotic cells by MPM2 antibody and analyzed by FACS. **D)** Polyclonal U2OS inducible cyclostop cells were transfected with the amount of HA-Ube2S indicated and either left growing asynchronously or treated with thymidine and subsequently released in either doxycyclin or nocodazole containing medium. After 16 hours of incubation cells were fixed, stained and analyzed by FACS.



Supplemental Figure 3: APC/C targeting tails are transferable

A) U2OS cells were transiently transfected with both Geminin-Cherry and Venus-tagged N-terminal fragment of the first 165 amino acids of cyclin A, with varying C-terminal tails as indicated. 48 hours after transfection cells were imaged by fluorescence and DIC time-lapse microscopy at 3 minute intervals. Integrated fluorescence levels were measured for entire single cells at each time point and normalized to 100% for the frame of NEBD. Destruction curves are in silico synchronized at the first frame of anaphase and plotted over time. Mean \pm s.e.m. At least 8 cells per construct. B) Derived from the same data as A, the amount of fluorescence at the moment of anaphase onset plotted per measured construct.

A**B**

Supplemental Figure 4: Apcin does not prevent Cherry-Nek2A and Cyclin A-Venus degradation.

A) U2OS cell stably expressing Cherry-Nek2A and Tetracycline inducible Cyclin A-Venus were synchronized with thymidine for 24h and released in the presence of with tetracycline. Cells were imaged by time-lapse light and fluorescence microscopy at a 3 minute interval. Integrated fluorescence was measured and normalized to the levels of NEBD as observed by loss of nuclear integrity by distribution of Cherry-Nek2A and CyclinA-Venus. B) Lower graph depicts time from NEBD-Ana in minutes, and time to 50% fluorescence for control cells or cells treated with different concentrations of apcin for Cherry-Nek2A and Cyclin A-Venus.

Chapter 6

Summary & General Discussion

SUMMARY

Correct transition through the different phases of the cell cycle is clearly not only driven by the force of expressed regulatory cell cycle genes and proteins. Cell cycle progression is also particularly dependent on destroying such proteins at the right time. The APC/C is one of the major E3 ubiquitin ligases responsible for destruction of a still growing number of cell cycle regulatory substrates. *Chapter 2* shows Nek2A is a remarkably sensitive substrate, which is even degraded when Cdc20 is repressed by the spindle checkpoint and incorporated into the MCC (*Chapter 2*). Indeed, as Nek2A directly binds to the APC/C before mitosis, without the requirement of an activator, we even find it to be unstable in interphase cells (*Chapter 3*). Because destruction of Nek2A is so sensitively regulated, one might expect that stabilizing the protein might lead to severe cellular dysfunction. Nek2A overexpression is a poor prognostic marker for several types of cancers, but surprisingly, we did not yet find a striking phenotype upon stabilization Nek2A. In many other examples, generally the removal of APC/C substrates at the right time during the cell cycle is imperative for normal transition between the relevant cell cycle phases, or for maintenance of genome stability and cellular fitness. Whereas cyclin B and securin are stereotypical APC/C^{Cdc20} substrates, whose destruction is required to allow for exit of mitosis, here we show that E2F7 and E2F8 are APC/C^{Cdh1} substrates, and that failure to degrade these transcription factors can prevent normal S-phase entry (*Chapter 4*). Finally, we show that Emi1 needs to be degraded for APC/C activation in mitosis. We demonstrate that we can artificially keep the APC/C inhibited by a peptide derived from non-degradable Emi1, named Cyclostop, which when expressed in interphase, halts cells in mitosis. Cyclostop does not prevent formation of the checkpoint or its recruitment to the APC/C (*Chapter 5*). This creates an interesting new tool to study both the mitotic APC/C as well as the fate of cells that are arrested in mitosis, independently of the mitotic checkpoint. Together with cell permeable APC/C inhibitory compounds, Cyclostop adds to an increasing toolbox of APC/C inhibitors¹⁹⁹.

GENERAL DISCUSSION

It's possible to shift gears, but the APC/C always wants to drive

We have discussed inhibition of the APC/C by both Emi1 and the MCC, but here we argue the APC/C truly is a 'machine built to destroy'¹³. It is already long known that APC2 and APC11, combined with E1 and E2 proteins, are in vitro already sufficient to ubiquitinate substrates^{24,25}. We advocate that the APC/C is prone to be active, therefore capable brakes are required to counterbalance this driving force. The mitotic checkpoint is a dynamic inhibitor, and responsive up and until the last kinetochore is attached to the mitotic spindle. Nevertheless, even full activation of the mitotic checkpoint by destabilizing all kinetochores by spindle poisons does not lead to a full blockade of the APC/C. The eagerness of the APC/C in this aspect is related to a phenomenon called 'mitotic slippage'²⁷⁰, the process of cells that remain in mitosis with a fully activated mitotic checkpoint still gradually lose cyclin B, due to residual APC/C activity, as well as other APC/C substrates. Eventually this leads to loss of the mitotic state, and the formation of polyploidy G1 cells. Even more exemplary in this regard are the prometaphase substrates cyclin A and Nek2A. Cyclin A is degraded in prometaphase because it competes with the mitotic checkpoint proteins for Cdc20 binding. Nek2A is also degraded in prometaphase, by using Cdc20 that is still bound to the checkpoint proteins. Furthermore, Nek2A is also targeted and degraded during interphase, regardless of the presence of Emi1, albeit at a slower rate, which is counterbalanced by protein synthesis. While Nek2A is fatally attracted to the APC/C by its C-terminal tail, many other substrates are dependent on modifications or cues before they gain an increased binding affinity for the APC/C. Interestingly, in the face of Emi1 loss by RNAi, all APC/C substrates seem to be equally nullified, regardless of their modifications or localization. So, in the absence of Emi1, and in interphase, the APC/C is maximally active. Similar effects are seen upon Cdh1 overexpression, that can overcome Emi1 inhibition and thereby has an identical effect as Emi1 depletion³³⁹. The levels of Cdc20 are tightly regulated¹⁰², and overexpression of Cdc20 may overpower the mitotic checkpoint under certain conditions. Clearly, with such a hungry engine, the brakes have to be formidable to drive safely: mistakes in inhibition of the APC/C can lead to premature S-phase entry, DNA replication stress, re-replication, G2 arrest, and loss or gain of chromosomes. Reversely, mistakes in releasing the break in the right way and at the right time can lead to lethal mitotic arrest and, through mitotic slippage, also to aneuploidy and chromosomal breaks.

In yeast, APC/C inhibitors are particularly important after cell cycle perturbations. This is also apparent from the mitotic checkpoint proteins, which only become essential after cells are challenged by spindle poisons^{132,133}, although this is not the case for mice, see below. Yeast does not have a clear orthologue of Emi1, but expresses another specific APC/C^{Cdh1} inhibitor called Acm1^{144,340}, deletion of which becomes

lethal after mild overexpression of Cdh1, or upon loss of the Cdk1 inhibitor Sic1³⁴¹. In metazoans Emi1 plays a crucial role, as in mice loss of Emi1 is embryonic lethal¹¹⁵, and only trophoblast giant cells survive³⁴². Depletion in cells leads to substantial DNA re-replication, dependent on the presence of Cdh1¹¹¹. Mice lacking Mad2 or BubR1 suffer from chromosome missegregations, which lead to aneuploid daughter cells^{136,137}. BubR1 knockout mice die at day 8 in utero¹³⁶, and mice with low levels of BubR1 lead to progeroid disease type³⁴³. In humans, mutations in BubR1 are associated with mosaic variegated aneuploidy syndrome^{344,345}, as are low levels³⁴⁶. Indeed, loss of integrity of the mitotic checkpoint has been suggested to be either causal, or permissive for, aneuploidy and tumorigenesis³⁴⁷, but aneuploidy may also become too severe, and may function as a tumor suppressor for certain other tumor types³⁴⁸.

It should be noted that the overexpression, or loss, of various components of the mitotic checkpoint can be contributing to tumorigenicity, and thus simply adding more restraint to the APC/C does not simply create a safe cell cycle (Reviewed in Holland & Cleveland 2009). Likewise, Emi1 has recently been dubbed an ‘emerging oncogene’³⁴⁹, although this concept is largely based on tumor expression data. Because Emi1 is an E2F target, the reported effects might be a byproduct of E2F transcription, rather than a direct cause for tumor development. Nevertheless, it is remarkable that there is a substantial overlap between E2F targets and APC/C substrates.

Releasing the brakes

In case the APC/C possesses the intrinsic property of being active, an important step in controlling APC/C activity lies in the mechanisms that activate and release the brakes. The two main APC/C brakes in the human cell cycle are Emi1, in interphase, and the mitotic checkpoint. Furthermore, while the mitotic checkpoint blocks Cdc20, in mitosis Cdh1 is inactivated by mitosis-specific phosphorylation. Recently, structural insight has been gained on how the MCC and Emi1 bind and inhibit the APC/C^{121,230}. The mitotic checkpoint is clearly linked through individual unattached kinetochores, and this intrinsically feeds back in silencing the formation of inhibitory signal: the more kinetochores become properly attached, the less MCC is generated^{148,149}. At least several signals are responsible for removing the MCC from the APC/C again, including autoubiquitination of Cdc20^{98,103} and other MCC components³⁵⁰, indicating that APC/C activity supports its own activation to drive mitotic exit. Furthermore, the APC15 subunit is implicated in dissociation of the MCC from the APC/C itself^{96,189}, while p31^{comet} is thought to dissociate Mad2 from cytosolic MCC, generating BubR1-Bub3-Cdc20 complexes¹⁹².

To enter mitosis, Emi1 inhibition needs to be removed. Both degradation as well as inhibitory phosphorylation of Emi1 may play a role at the end of G2, when the APC/C

switches from one brake to the next. While it is clear that the levels of Emi1 have to be tightly regulated, it is currently unclear whether Emi1 has a preference for APC/C^{Cdh1} over apo-APC/C, that is, APC/C complexes devoid of activator. We show that by overexpressing either ND-Emi1, or a truncated form of Emi containing the inhibitory domains, we are able to efficiently arrest cells in mitosis, although this also does not fully prevent the degradation of the most efficient APC/C^{Cdc20} substrates Cyclin A and Nek2A (Chapter 5). This is in line with our findings that ProTAME mediated APC/C inhibition alone also does not fully stabilize Cyclin A or Nek2A (Chapter 2). It should be noted that treating cells with ProTAME alone already stabilizes Nek2A to a further extent than Cyclostop. Although solid evidence is currently lacking, this could be explained by a model in which Cyclostop does not inhibit formation or binding of the mitotic checkpoint, which we find is sufficient for Nek2A destruction. In line with the model that APC/C^{Cdc20} can be inhibited by the MCC, it is possible that APC/C^{Cyclostop}, also still engages the MCC.

Alternatively, prolonged mitotic arrest leads to re-activation of the spindle checkpoint. Possibly, enforced mitotic checkpoint activity could compete with Cyclostop for Cdc20 binding and so prolonged MCC activation also leads to partial disruption of the APC/C-Cyclostop interaction. In such a model, checkpoint-re-engagement, and subsequent checkpoint override with Mps1 inhibitors, can lead to partial APC/C activation in the presence of Cyclostop. This also shows that Cyclostop needs a certain time to start inhibiting the APC/C, which would explain why micro-injection of non-degradable Emi1 in late G2 phase does not lead to a mitotic arrest, whereas viral transduction of ND-Emi1 can block cells in mitosis substantially.

After DNA damage, the APC/C may also need to be activated, to halt cell cycle progression by targeting Cdh1^{73,75-77}, which is performed via dephosphorylation of 4 Cdk sites on Cdh1, by Cdc14B⁷⁵. Whether Cdh1 is released and binds apo-APC/C, or whether Emi1 needs to be actively removed from APC/C-Cdh1, to activate the APC/C in response to DNA damage is unclear. One study reports Emi1 binding regardless of DNA damage⁷⁵, while others have shown loss of Emi1 protein as the mechanism for APC/C activation³⁵¹. Possibly the control of Emi1 is similar that of to Emi2, the paralogue of Emi1 and the inhibitor of the APC/C during meiosis. Emi2 inhibition of the APC/C is directly controlled by Cdk1 phosphorylations and PP2A activity control, which respectively inactivate or positively regulate Emi2³³³. However, Emi1 is controlled differently, because it is not inactivated in mitosis (Chapter 5).

Does inhibiting the APC/C provide a therapeutic opportunity?

As cell division is the deadly hallmark of tumors, targeting the cell cycle can be an effective strategy. More specifically, targeting mitosis might be an especially sensible

approach, especially for CIN tumors^{352,353}. As the APC/C is even named for its role in promoting mitotic progression, it might be worth considering as a direct therapeutic target. However, it has become clear that the APC/C also performs many non-mitotic functions, as reviewed¹⁷, including inducing differentiation^{354,355} and maintaining quiescence³⁵⁶. As a consequence, only APC/C inhibition directed towards the Cdc20 activator provides an immediate rationale as a cancer therapeutic strategy, while blocking Cdh1 might under some conditions be tumor promoting. Similarly, paclitaxel, a microtubule hyperstabilizer, leads to inhibition of APC/C^{Cdc20} by activating the mitotic checkpoint. Paclitaxel has already been successfully used in the clinic for decades. For several types of cancer, such as ovarian, breast and lung cancer, ~50% of the patients benefit from paclitaxel treatment³⁵⁷. While in tissue culture treatment with paclitaxel leads to a mitotic arrest lasting for several hours, the efficacy found in patients is probably more subtle and caused by chromosome missegregations through the induction of multipolar spindles^{358,359}. However, paclitaxel resistance is a prevalent problem^{360,361}, and although widely screened for, this has not led to the identification of a single predictive biomarker^{360,362,363}.

Following the rationale of targeting mitosis to battle cancer, several other and possibly more specific mitotic targets are in (pre)clinical trials, although none so far have been able to replace paclitaxel^{352,353} (and references therein). Rather than activating the mitotic checkpoint, focusing on the prevention of mitotic exit has been suggested to offer a better therapeutic window, specifically by targeting Cdc20^{87,364}.

Depending on the activator, the APC/C is driving in a different direction.

Interestingly, Cdc20 is exclusive in providing APC/C activity in the relatively short time of the cell cycle, from NEBD, to right after the satisfaction of the mitotic checkpoint, while in all other instances Cdh1 is responsible for activating the APC/C. This also supports the conclusion that APC/C^{Cdc20} activity leads to cell cycle progression, while APC/C^{Cdh1} leads to cell cycle delay. APC/C^{Cdh1} mediated Aurora A and B destruction at the end of mitosis do not strictly fit this distinction⁷⁰, although disappearance of Aurora A and Aurora B clearly is not required for mitotic exit or G1 entry.

Considering Cdh1 and its similarity to Cdc20, this raises two questions in relation to the strategy of therapeutic targeting: 1) is specific inhibition of APC/C^{Cdc20} possible? 2) how harmful is undesired inhibition of APC/C^{Cdh1}? Cells depleted of Cdh1, or Cdh1 knock-out cells, become hypersensitive towards DNA damage, which results in genomic instability, both in yeast⁶⁶ as well as in human cells³¹¹. Sensitization to DNA damage could provide a window for other treatments, such as radiation to specifically target tumor cells. From single cell analysis after low dose of ionizing radiation, it seems that while APC/C^{Cdh1} is responsible for the destruction of Cyclin B, both p53 and p21 are

the actual determinants of cell fate⁷⁷. Nevertheless, Cdh1 may act as a tumor suppressor, also in the absence of induced DNA damage, as its loss leads to accumulation of DNA damage, at least partially via replicative stress^{71,72,78}. Short term Cdh1 inhibition may in normal cells cause DNA damage, and possibly result in cell cycle halt, while tumor cells might enter mitosis, leaving them vulnerable for targeting by mitotic specific drugs. Interestingly, we show that the outcome of Cdh1 inhibition could also be dictated by the presence of E2F7 and E2F8, which reduce S-phase entry if they are stabilized by Cdh1 RNAi or by mutation of their APC/C recognition motifs (Chapter 4).

Yet, indiscriminate APC/C inhibitors that would equally target Cdh1 and Cdc20, may have a limited therapeutic window, as the induced replication stress in healthy cells could be far more detrimental than the benefit of tumor cells specifically arrested in mitosis leading to mitotic catastrophe. While we make a clear discrimination between Cdc20 and Cdh1 roles, especially at the transition from Cdh1 to Cdc20, regulation might be more complex. Speculatively, there may be a role for the MCC to inhibit APC/C^{Cdh1} at the end of G2, when the MCC is already generated from nucleopores, and Emi1 is already slowly being degraded. Indeed, at least one report suggests that there is a role for the checkpoint generation by Mad1 at the nuclear pore, which plays a role in stabilizing cyclin B before entry into mitosis¹⁸⁵.

Current structures of the APC/C have been resolved in the presence or absence of the activator¹⁰, associated with Cdh1^{6,12,56}. Structures of the PAC/C bound to the inhibitory region of Emi1¹²¹ or bound by the MCC¹¹ have become available, too. The biochemical data suggest that the MCC inhibits a Cdc20 that is already bound to the APC/C, but so far no structure provides an obvious solution of fitting two activators on the APC/C physically. However, this might have important consequences for chemical inhibitor function, and possible future design of inhibitors.

While, in theory, inhibition by ProTAME can inhibit both Cdh1 and Cdc20²⁶³, as it competes with the C-terminal tail of the activator for binding to APC3, it only has a modest effect on the cell cycle during interphase. This may relate to the ability of proTAME to stabilize cyclin B1-Cdc20 complexes¹⁹⁷. Indeed, there is a preference for ejecting Cdc20 from the APC/C, which is still auto-ubiquitinated in the presence of TAME. This does not occur in the case of Cdh1¹⁹⁷.

The second inhibitor, apcin, specifically binds the Cdc20 D-box binding pocket¹⁹⁹. Apcin strongly synergizes with TAME, both in vitro as well as in vivo. In *Xenopus* extracts it is less efficient in inhibiting Cdh1 than Cdc20, offering some Cdc20 selectivity. Indeed, while proTAME induces a mitotic arrest dependent on the SAC²⁶³ through cohesion fatigue¹⁹⁸, the combination of proTAME and apcin prevents mitotic arrest in a mitotic

checkpoint-independent manner, as shown previously for full Cdc20 depletion^{87,250}. As several different types of cancer show upregulation of Cdc20³⁶⁵ and this is also correlated with poor prognosis³⁶⁶ (and references therein), Cdc20 inhibition might especially be useful in such a subset of malignancies. In conclusion, as both APC/C-inhibitory drugs seem to target APC/C^{Cdc20} more effectively than APC/C^{Cdh1}, the combination of the two drugs holds some promise for specifically targeting cells in mitosis, while leaving non-mitotic cells unperturbed.

The potential benefit of targeting mitotic exit via Cdc20, rather than blocking mitosis by mitotic checkpoint activation, also relates to the observation that tumor cells arrested in the mitotic checkpoint can survive by mitotic slippage^{87,270}, thus producing polyploid G1 cells. Possibly, the fate of cells that are arrested in mitosis, is best described by the 'competing networks' model²⁷¹. In this model, slow cyclin B degradation competes with the accumulation of pro-apoptotic signals, and whichever signal reaches its threshold first, determines the biological outcome^{367,368} (**Fig. 1**)

There is some evidence that the accumulation of pro-apoptotic signals are produced by the gradual loss of MCL-1 during a mitotic arrest, via an APC/C^{Cdc20} pathway³⁶⁹, or by the dephosphorylation of caspase-9 during mitosis³⁷⁰. Similarly, activation of caspase 7, 9 and cleavage of ICAD during a prolonged mitosis were also shown to lead to DNA damage in cells, inducing a cell cycle arrest after exiting mitosis³⁷¹. In this regard, enhancing specific mitotic pro-apoptotic signals might be especially beneficial as an anti-mitotic cancer therapy³⁷². Combined with findings in animal models and the clinic, that tumor cells are not always rapidly dividing, or mitotically-arrested after treatment, this has led to some skepticism about targeting mitosis as a cancer therapy^{373,374}. Alternative theories exist on the factors that determine taxol efficacy³⁷⁵. Clearly, it will be important to test the effects of directly inhibiting the APC/C by cell permeable inhibitors, by Cdc20 knockout, or by Cyclostop induction, in tumor models. Possibly, identifying mitotic specific pro-apoptotic pathways might reveal which tumor types or oncogenetic backgrounds are sensitive for inhibition of mitotic exit. Hypothetically, using drugs enhancing death signaling in mitosis could even further enlarge the therapeutic window.

Measuring the APC/C driving speed

There are several different ways of assaying APC/C activity; we here briefly discuss their merits and drawbacks, which are summarized in **Table 1**.

In vitro assays are a powerful method of looking at the ubiquitinating potential and comparing different substrates in an identical experimental setting. However, they require purification of the proper, complete APC/C complex, addition of E1, E2 en

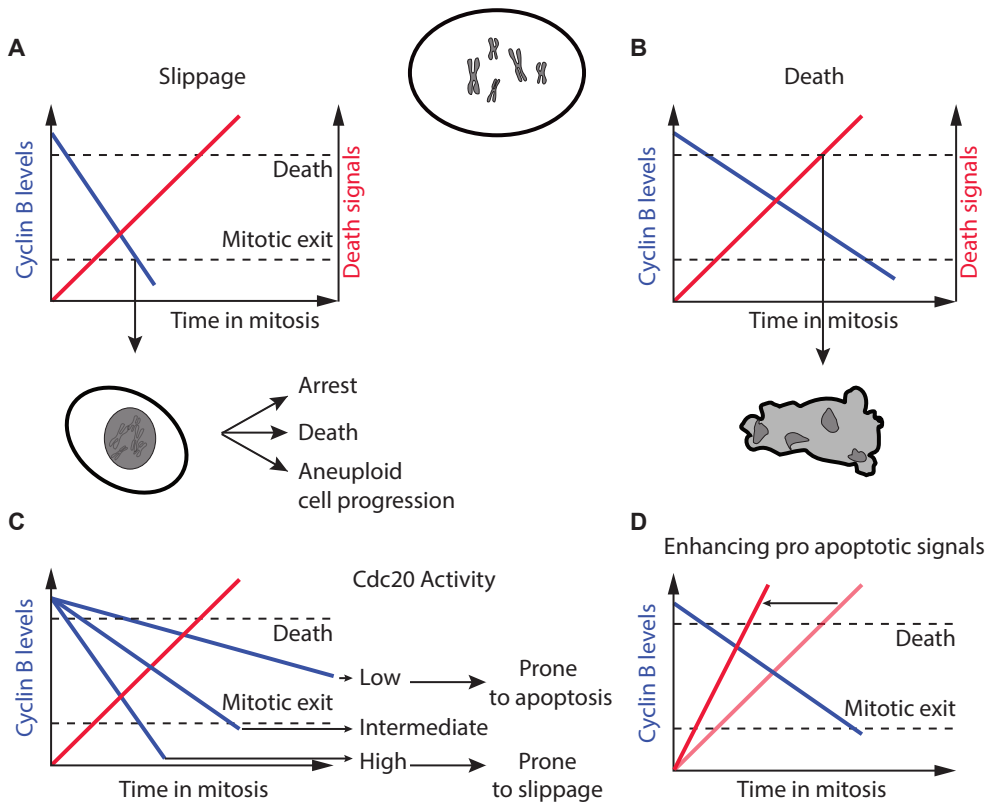


Figure 1 Competing networks model

During a mitotic delay two networks may determine the outcome in either death or mitotic exit. **A)** If the levels of cyclin B drop below the threshold required to maintain the mitotic state cells slip into G1, followed by cell cycle arrest, post slippage death or cell cycle progression. **B)** If the levels promoting apoptosis accumulate faster than cyclin B reaches the threshold to exit the result will be mitotic cell death. **C)** Influencing the amount of Cdc20 activity could influence the rate of cyclin B slippage, in such a way that the lower levels of Cdc20 lead to more stable cyclin B, and thus enhance the chance of mitotic death over slippage. **D)** By stimulating the pro apoptotic response cells arrested in mitosis might also be pushed towards death rather than slipping into G1. (Based on Gascoigne and Taylor 2008) See also ; Rieder Medema, Holland Cleveland and Nilsson.

activator proteins at the right stoichiometry, and also the right substrate concentrations and compositions to be truly reflective of the APC/C activity in cells.

The use of different ubiquitin mutants *in vitro* can resolve the length of the formed ubiquitin chains, and has led to the discovery of the priming ubiquitin by Ubch10 and the elongation role of Ube2S. More recently, largely based on *in vitro* assays, it was shown that APC/C^{Cdc20} tracks the most distal ubiquitin²¹⁶. As ubiquitin itself possesses 7 lysines, these are all potential sites for addition for a consecutive ubiquitin. The different forms

Table 1

| Method | Advantage | Drawback |
|---------------------|--|---|
| in vitro assays | <ul style="list-style-type: none"> - No unknown factors perturbing measurement - Easy mutational analysis of motifs - Allows for investigation of ubiquitin chain topology | <ul style="list-style-type: none"> - No cellular context - Non physiological concentrations |
| Western Blot | <ul style="list-style-type: none"> - By synchronization possible to analyze in specific cell cycle phases - RNAi and knockout allow for analysis individual protein contributions - Measuring multiple substrates on endogenous level simultaneously | <ul style="list-style-type: none"> - Heterogeneous cell populations - Inefficient RNAi may hinder results - Knockouts may not be viable - Single cell differences not detectable |
| FACS | <ul style="list-style-type: none"> - Cell cycle specific markers provide single cell resolution - Measurement up to 3-4 markers simultaneously | <ul style="list-style-type: none"> - No single cell temporal resolution - No subcellular localization |
| Immuno Fluorescence | <ul style="list-style-type: none"> - Subcellular localization of endogenous protein - Fixed material allows for analysis of high number of cells - Inference of time and kinetics possible - Up to 4-5 different markers simultaneously in a single cell | <ul style="list-style-type: none"> - No single cell kinetics - Not capable of measuring single cell progression or cell fate |
| Time-lapse Imaging | <ul style="list-style-type: none"> - Subcellular localization - High single cell temporal resolution - possible to derive degradation kinetics - Up to 3 different markers simultaneously - allows for manipulation while experimenting | <ul style="list-style-type: none"> - Exposure to excitation light - Fluorescent tags may perturb protein function - Sensitive to single cell variation when n is low - single cell fate analysis - analysis can be demanding |

Different experimental methods to determine APC/C activity based either on ubiquitination or (model) substrate protein levels.

of polyubiquitin chains are denoted by K (for the lysine amino acid) and the location within ubiquitin e.g. K11, K48 etc. The chain conformation and preference for K11 linked polyubiquitin chains formed by the APC/C in metazoans have also largely been discovered by in vitro ubiquitination assays^{64,211,376}. In vitro ubiquitination assays are also convenient for measuring the contribution of different motifs by comparing wildtype versus mutant protein, although this does require purified proteins, and the insurance that the mutant is not artificially stabilized due to misfolding^{64,377}. Very recently, by using substrates fixed to glass slides, with the addition of purified components, but also with concentrated cellular extracts, the Kirschner lab was able to determine both the speed and length of chain formation by using fluorescent ubiquitin and TIRF microscopy²²⁶.

However, even with an estimation of cellular concentration, the context of the cell, including possible modifiers or localization of either the APC/C or the substrates are not in place. Therefore classical **western blotting** of synchronized cells, combined with siRNA depletion can confirm roles of mediators or activators for several substrates concurrently. The risk however, is that measured effects could also be off target or

indirect, so proper rescue experiments may be required. Most importantly, any form of synchronization might elicit undesired DNA damage or stress responses, confounding results. Furthermore, even with synchronization methods, cells do not progress through the cycle at the exact same speed, and a heterogeneous population might be causal in missing differences in protein degradation.

Single cell resolution can be obtained by **FACS analysis**, which also allows for rapid quantification of a high number of cells. Through antibody staining of fixed cells, it allows for identification of sub populations on a single cell level. One example is Cdh1 mediated Aurora A degradation, still present in mitotic cells, but which is lost as cells enter G1³⁷⁸. With the introduction of the FUCCI system³¹⁴, directly based on APC/C activity, it is possible to sort out single cells depending on substrate prevalence (Chapter 4). In this manner even live cell sorting can be performed to allow for synchronization of chemically unperturbed cell populations. However, while high numbers of single cells can be analyzed, sub cellular resolution is lost.

Analysis by **immunofluorescence** allows single cell analysis and subcellular precision, as well as looking at the level of APC/C substrate on an endogenous level. One particularly powerful aspect of immunofluorescence is the possibility to look at posttranslational modifications through specific antibodies. This can give clues to how certain modifications possibly lead to translocation or degradation. Also, as immunofluorescence is widely used, many different antibodies have been characterized. These can often also be used to gain temporal insight of the cell cycle state. The major disadvantage of immunofluorescence is its requirement for fixation, a possible source of artifacts. Another major caveat for is the loss of direct high temporal resolution. Fast cell cycle transitions, which could be highly variable between cells, might be detected by immunofluorescence, but determining protein level differences over time can obviously not be inferred from a frozen frame. However, a recent study showed that the combination of micropatterning of cells, and controlling for background subtraction in an antibody specific manner, allows for inferring kinetics and timing of cell cycle events, provided that variation in the measured feature is not too large and large amount of images are analyzed³⁷⁹.

With **time-lapse fluorescence single cell imaging**, both high temporal and spatial resolution is possible, but the assay is invariably dependent on the ectopic expression of fluorescently tagged proteins. These potentially may not recapitulate the endogenous protein in every regard, or the approach might suffer from over expression artifacts such as aggregation. This can of course be probed by testing if validated interactions and other functionalities are not perturbed. One of the greatest benefits of time-lapse imaging is directly determining the order of events, which for the APC/C entails protein

destruction²⁷⁷. Indeed, only by time-lapse microscopy could it be determined that cyclin A and Nek2A are such efficient substrates, in which Nek2A even surpasses cyclin A in degradation rates^{83,248–250,380}. Time-lapse imaging was also instrumental to support the model that the mitotic checkpoint behaves as a rheostat, rather than an all or nothing response, as different amount of checkpoint activation lead to only subtle differences in Cyclin A degradation¹⁴⁸. Support for this model also came from another feature exclusive to time-lapse imaging: experimental perturbation while performing an experiment¹⁴⁹. By laser ablation, after checkpoint satisfaction, it is possible by measuring single cell substrate degradation rates, to determine how APC/C activity responds to unattached kinetochores. Cyclin A was already identified as an APC/C target over 10 years ago, as was the observation that stabilization of cyclin A led to a prolonged mitosis²⁴⁹. However, its direct influence on stabilizing kinetochore-microtubule dynamics was discovered by time-lapse imaging only recently. This became apparent by imaging Cherry tagged-cyclin A with high temporal resolution and simultaneously measuring kinetochore-microtubule attachment in single cells through photoactivatable GFP-tubulin²⁵³.

Similarly, addition of chemical inhibitors while the measurement of protein degradation is ongoing, allows determination of single cell responses, and importantly, the time frame required for the response²⁴⁷. Time-lapse imaging with the appropriate markers allows for cell cycle events to be directly coupled or correlated to cellular reaction. Especially the use of FRET probes allows for measuring protein activity, such as Cyclin B-Cdk1 kinase activity, rather than solely measuring protein abundance²⁹⁴. Several other FRET sensors for APC/C substrates have been developed, such as for Aurora B and Plk1, revealing location and timing in a single cell manner³⁸¹.

Another merit of time-lapse imaging is the ability to distinguish between the requirement of Cdc20 and Cdh1. As especially during mitosis degradation of APC/C substrates occurs rapidly, the high temporal resolution of time-lapse imaging can be instrumental in discriminating the contribution of Cdc20 and Cdh1 in a substrate specific manner^{245,382}. This has for instance revealed that while cell death is dependent on the concentration of paclitaxel, the duration of the mitotic arrest does not correlate with cell fate²⁷¹. More strikingly, the same study also showed that there is a huge cell-to-cell variation in paclitaxel response, even in the same genetic background. This argues that teasing apart the response to explain the biological variation will also have to be performed in a single cell manner. This also highlights another pitfall of time-lapse imaging, as drawing conclusions on a small number of analyzed cells might be misleading.

Discovery of novel APC/C substrates: known unknowns and unknown unknowns

Decades after discovery of the APC/C, it is reasonable to suspect that the most crucial APC/C substrates, such as cyclin B, securin, and geminin, have already been identified.

However, the list of APC/C substrates is still expanding, and has recently been expanded by, for instance, CtIP³¹¹, casein kinase delta³⁸³ and E2F7 -8³¹³ (this thesis, Chapter 4). These recent substrates were validated in more specific biological conditions, such as upon the induction of DNA damage, or are relevant for specific cell types. Likely, more substrates are yet to be discovered, similarly dependent on more specific context. In this respect, the number of potential targets is limited, as essentially all validated APC/C substrates are dependent on either a D-box or KEN-box.

Naively analyzing the human proteome, following the short linear motif (SLIM) as currently provided by ELM, reveals that there are 14.947 D-boxes and 2.680 KEN-boxes, in respectively 8.953 and 2.208 proteins (elm.eu.org). Interestingly, when taking into account amino acid prevalence, the amount of KEN boxes is 30% more than expected by random distribution (E.Tromer unpublished results). However, more in depth and informative analysis can be performed to narrow the amount of potential true APC/C substrates, filtering for local protein structure, cross-species conservation of the motif, GO-annotation and taking cell cycle regulation of the protein itself into account. This bio-informatic approach has previously been performed for KEN-boxes specifically³⁸⁴, and for both KEN and D-boxes, resulting in algorithms to help predict the validity of either motif³⁸⁵. Our lab has performed a similar analysis for both KEN and D-boxes, but as this latter motif is more degenerate, the amount of false positives is expected to be higher than for the KEN-box. When aforementioned masks are applied, analysis for ~30 highest ranking proteins with a KEN-box, include 14 validated substrates, 2 known APC/C regulators, while the residual proteins could be allow for a smaller set to be tested (**Table 2**, E.Tromer unpublished results). When the same filters are applied for the D-box, this results in 23 top ranking proteins of which 9 are validated APC/C substrates, 1 is an APC/C regulator and also leaving for a manageable amount of proteins to be tested as APC/C substrate (**Table 2**). Indeed, both Eg5 and Claspin have been validated by other groups^{386,387}. Also HURP and NuSAP have been identified as spindle associated APC/C substrates after this analysis was performed³⁸⁸.

A finding that could quite radically increase the amount of potential APC/C substrates is that the Cdh1 receptor for the KEN-box is also able to recognize a NEN motif (He 2013). In the same line of reasoning the authors show that the O-box in Spo-13 and the GxEN-box in xKid are likely a degenerate D-box and KEN-box respectively^{389,390}. In the case of ACM1 it should be noted that it utilizes at least one additional motif, the 'ABBA-motif', to interact with Cdh1⁴². This motif is possibly required for enhancing the recognition of the weaker degenerate NEN-box.

One additional layer of regulation that might help identify *bona fide* KEN and D-box motifs might prevail from increased understanding from the surrounding sequences.

Table 2 Potential APC/C substrates containing a D-box or KEN box

| D-Box | | | KEN-Box | | |
|-----------|------------|----------|-----------|------------|----------|
| Validated | Regulators | Controls | Validated | Regulators | Controls |
| AurkA | Bub1B | Astrin | Cdc20 | Bub1 | Caf1B |
| AurkB | Putative | Anln | Sororin | Bub1B | ESCO2 |
| CyclinA2 | | Caf1B | CKAP2 | Putative | Separin |
| CyclinB1 | Cdc25B | CyclinB2 | DTL | | NASP |
| Geminin | Cdc25C | DCC1 | E2F8 | CENPE | TPX2 |
| PLK1 | CENPE | FAM83D | FoxM1 | CENPF | |
| Securin | CENPF | Kif14 | Geminin | HURP | |
| SKP2 | HURP | PSRC1 | Cdc25A | GTSE1 | |
| TOME-1 | | | Cdc25C | KI67 | |
| | | | Nek2 | KIF11 | |
| | | | PRC1 | Cdc25B | |
| | | | Securin | NUSAP | |
| | | | RIR2 | TACC3 | |
| | | | SGOL2 | | |
| | | | STK6 | | |
| | | | TOME-1 | | |

Top ranking candidate APC/C substrates based on presence of structurally accessible and conserved D-box or KEN box. Subsequently filtered by cell cycle regulation (Whitfield database) of the protein, Cdc20 coexpression (7 Oncomine derived microarray sets and an in house NKI breast cancer dataset) and GO-annotation. Names in orange indicate expression levels fluctuate over 4 fold during cell cycle. Protein names follow Uniprot nomenclature.

While not as well defined as the motif itself, analysis of known motifs has made clear that true KEN motifs are likely enriched for flanking serines in the surrounding 20 amino acids, especially at the -1 position³⁹¹. For the D-box an increased number of lysines in the vicinity of 60 amino acids of the motif could be an indication of a valid motif²²⁶. As unstructured regions are normally relatively poorly conserved, giving extra weight to relative local conservation may aid identification of authentic APC/C motifs³⁹². Another approach that might help the identification of genuine APC/C degrons from more degenerate motifs, is taking into account protein localization, as there seems the possibility of enrichment ‘hotspots’ for identified APC/C substrates, such as the spindle, the kinetochore, the midbody and the centrosome³⁸⁵.

Discovery of novel APC/C substrates: The devil might be in the deTail

Another APC/C binding motif that has been only partly resolved is the C-terminal targeting tail (**Fig. 2**). As previously discussed, the IR tails of both activators APC10 directly interact with APC3, while the MR tail of Nek2A less conclusively binds at least APC8, and probably several other TPR containing APC/C subunits, too⁸². Interestingly, the same study identified Kif18A as an APC/C substrate, which is also dependent on APC/C binding via a C-terminal LR tail. The recurring C-terminal presence of these

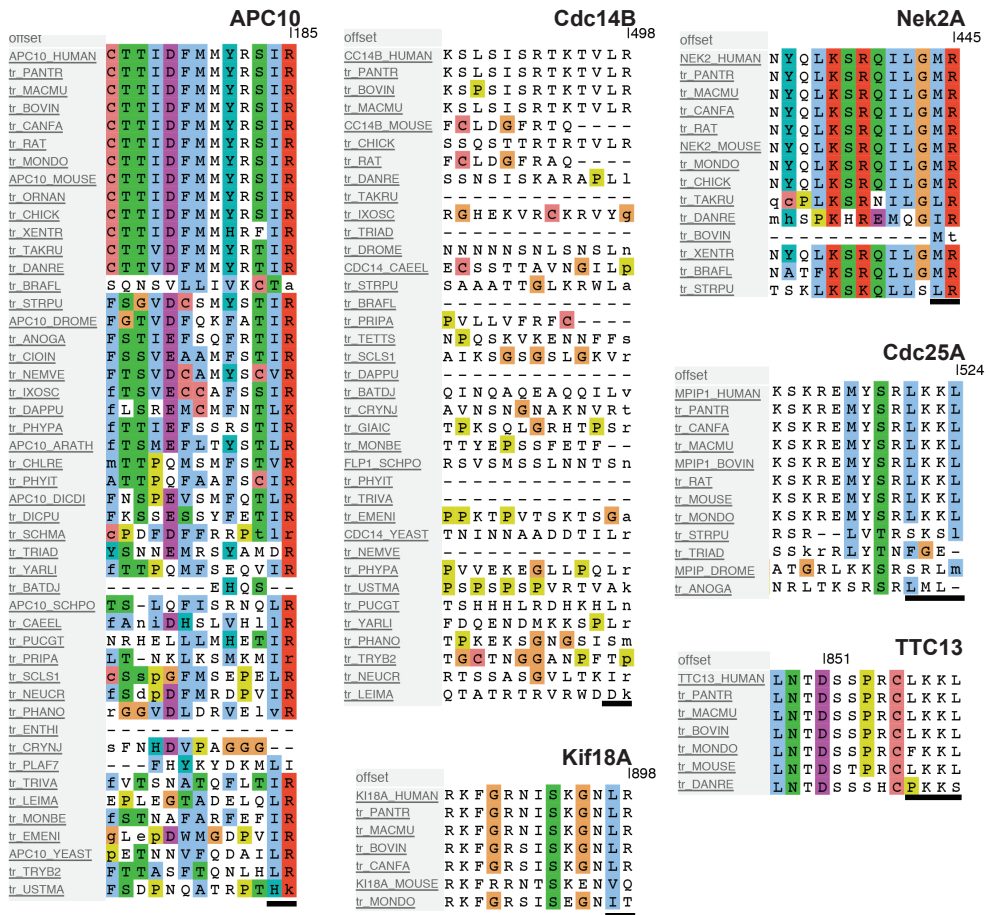


Figure 2 Cross species alignment of known and potential APC/C interacting tails

Alignments acquired by SlimSearch (<http://bioware.ucd.ie/>) for [ILM]R\$ and [ILM][RK][RK][ILM]\$.This results in other putative APC/C targeting tails here aligned with GOPHER. APC10, Kif18A and Nek2A are confirmed APC/C interacting tails. Amino acids depicted following the ClustalX colour code.

motifs suggest somehow that the acceptor site on the APC/C is so narrow that only a single string of amino acids is able to access it, without the possibility for the protein to continue. Furthermore, it is unclear how the tail helps to position the substrate towards the catalytic site of the APC/C.

A second class of C-terminal APC/C targeting tails is represented by the Emi1/E2S tails, with the amino acid sequence LRRL (Fig. 2). This tail has also not been completely unambiguously linked to a single APC/C subunit, although APC2 is a likely

candidate^{52,216}. The constraints of degeneration for either of these tails have not been fully explored, and could potentially also identify new APC/C regulators and substrates.

The [ILM]R\$, indicating the possibility of Isoleucine, Lysine or Methionine [ILM] followed by an obligatory Arginine (R), at the C-terminal end of the protein (\$), motif already shows some flexibility between species. For instance, Nek2A alternatively ends in an IR tail in zebrafish, but an LR tail in both fugu and sea urchin. The LR tail also replaces an IR tail in APC10 in both fission and budding yeast, as well as in *C.elegans*, indicating amino acid flexibility, although these proteins have not been experimentally confirmed to bind the APC/C. C-terminal targeting is also present in plants: the *Arabidopsis* specific APC/C inhibitor OSD1/GIG1 also depends on both a D-box and MR tail to bind the APC/C. More interesting could be the fact that Cdc14B also possesses an LR tail, although only conserved in vertebrates and notably not conserved in budding yeast, in which it is a clear activator of Cdh1 and thus facilitates mitotic exit. Nevertheless, Cdc14 plays a role in dephosphorylating Cdh1 after DNA damage in human cells⁷⁵, and this LR tail might potentially assist in APC/C binding. Unfortunately, either direct or indirect APC/C recruitment of Cdc14B has not yet been tested.

Cross species inspection of the LRRL tail also offers interesting insights as Emi1 in rodents ends in LQRL, while the C-terminal tail of Ube2S alternatively is often characterized by LKRL [Chapter 5, Supplemental Fig. 1A]. Surprisingly, querying the human proteome only results in two potential new targets: olfactory receptor 56A, a transmembrane G-protein coupled receptor, and DUSP22, a dual specificity phosphatase. The first has no canonical KEN or D-box motif, thus is very likely not an APC/C substrate, while the latter only contains a D-box motif in the structured phosphatase domain, which makes it an unlikely candidate. However, when following the degeneration observed for the [ILM]R tail, allowing for similar substitutions, additional proteins with Emi1/Ube2S-like tails can be identified, including the poorly characterized tetratricopeptide repeat protein 13 (TTC13), as well as Cdc25A. Multiple labs showed that Cdc25A is degraded after DNA damage^{332,393}, similar to other APC/C substrates. Indeed, one study reports that Cdc25A might be degraded by APC/C^{Cdh1} in a KEN box dependent manner, but all tested mutants included the LKKL tail, so a possible direct APC/C targeting role of the tail has not been investigated³⁹⁴. As Cdc25A is directly involved in cell cycle progression by dephosphorylating Cdk1 and stimulating its activation, enforcing entry from G2 into mitosis²⁹¹, this offers a potentially interesting targeting tail to be further analyzed.

Appendix

References

Nederlandse Samenvatting

English Summary

Dankwoord

Curriculum Vitae

List of Publications

REFERENCES

1. Schulman, B. a & Harper, J. W. Ubiquitin-like protein activation by E1 enzymes: the apex for downstream signalling pathways. *Nat. Rev. Mol. Cell Biol.* **10**, 319–331 (2009).
2. Li, W. *et al.* Genome-wide and functional annotation of human E3 ubiquitin ligases identifies MULAN, a mitochondrial E3 that regulates the organelle's dynamics and signaling. *PLoS One* **3**, (2008).
3. Chang, L. & Barford, D. Insights into the anaphase-promoting complex: a molecular machine that regulates mitosis. *Curr. Opin. Struct. Biol.* **29C**, 1–9 (2014).
4. King, R. W. *et al.* A 20S complex containing CDC27 and CDC16 catalyzes the mitosis-specific conjugation of ubiquitin to cyclin B. *Cell* **81**, 279–288 (1995).
5. Sudakin, V. *et al.* The cyclosome, a large complex containing cyclin-selective ubiquitin ligase activity, targets cyclins for destruction at the end of mitosis. *Mol. Biol. Cell* **6**, 185–197 (1995).
6. Dube, P. *et al.* Localization of the coactivator Cdh1 and the cullin subunit Apc2 in a cryo-electron microscopy model of vertebrate APC/C. *Mol. Cell* **20**, 867–79 (2005).
7. Thornton, B. R. *et al.* An architectural map of the anaphase-promoting complex. *Genes Dev.* **20**, 449–60 (2006).
8. Zhang, Z. *et al.* Recombinant expression, reconstitution and structure of human anaphase-promoting complex (APC/C). *Biochem. J.* **449**, 365–71 (2013).
9. Da Fonseca, P. C. a *et al.* Structures of APC/C(Cdh1) with substrates identify Cdh1 and Apc10 as the D-box co-receptor. *Nature* (2010). doi:10.1038/nature09625
10. Schreiber, A. *et al.* Structural basis for the subunit assembly of the anaphase-promoting complex. *Nature* **470**, 227–232 (2011).
11. Herzog, F. *et al.* Structure of the Anaphase-Promoting Complex/cyclosome Interacting with a mitotic Checkpoint Complex. *Science (80-.)*. **1985**, 1477–1481 (2009).
12. Chang, L., Zhang, Z., Yang, J., McLaughlin, S. H. & Barford, D. Molecular architecture and mechanism of the anaphase-promoting complex. *Nature* **17**, 13–17 (2014).
13. Peters, J. M. The anaphase promoting complex/cyclosome: a machine designed to destroy. *Nat. Rev. Mol. Cell Biol.* **7**, 644–656 (2006).
14. Acquaviva, C. & Pines, J. The anaphase-promoting complex/cyclosome: APC/C. *J. Cell Sci.* **119**, 2401–4 (2006).
15. Thornton, B. & Toczyski, D. Precise destruction: an emerging picture of the APC. *Genes Dev.* 3069–3078 (2006). doi:10.1101/gad.1478306.also
16. Van Leuken, R., Clijsters, L. & Wolthuis, R. To cell cycle, swing the APC/C. *Biochim. Biophys. Acta - Rev. Cancer* **1786**, 49–59 (2008).
17. Eguren, M., Manchado, E. & Malumbres, M. Non-mitotic functions of the Anaphase-Promoting Complex. *Semin. Cell Dev. Biol.* (2011).
18. Kim, S. & Yu, H. Mutual regulation between the spindle checkpoint and APC/C. *Semin. Cell Dev. Biol.* **22**, 551–8 (2011).
19. Pines, J. The APC/C: a smörgåsbord for proteolysis. *Mol. Cell* **34**, 135–6 (2009).
20. Pines, J. Cubism and the cell cycle: the many faces of the APC/C. *Nat. Rev. Mol. Cell Biol.* **1**, (2011).

21. Primorac, I. & Musacchio, A. Panta rhei: the APC/C at steady state. *J. Cell Biol.* **201**, 177–89 (2013).
22. Sivakumar, S. & Gorbsky, G. J. Spatiotemporal regulation of the anaphase-promoting complex in mitosis. *Nat. Rev. Mol. Cell Biol.* 7–9 (2015). doi:10.1038/nrm3934
23. Barford, D. Structural insights into anaphase-promoting complex function and mechanism. *Philos. Trans. R. Soc. Lond. B. Biol. Sci.* **366**, 3605–24 (2011).
24. Tang, Z. *et al.* APC2 Cullin protein and APC11 RING protein comprise the minimal ubiquitin ligase module of the anaphase-promoting complex. *Mol. Biol. Cell* **12**, 3839–51 (2001).
25. Gmachl, M., Gieffers, C., Podtelejnikov, a V, Mann, M. & Peters, J. M. The RING-H2 finger protein APC11 and the E2 enzyme UBC4 are sufficient to ubiquitinate substrates of the anaphase-promoting complex. *Proc. Natl. Acad. Sci. U. S. A.* **97**, 8973–8978 (2000).
26. Leverson, J. D. *et al.* The APC11 RING-H2 finger mediates E2-dependent ubiquitination. *Mol. Biol. Cell* **11**, 2315–2325 (2000).
27. Kramer, E. R., Scheuringer, N., Podtelejnikov, a V, Mann, M. & Peters, J. M. Mitotic regulation of the APC activator proteins CDC20 and CDH1. *Mol. Biol. Cell* **11**, 1555–69 (2000).
28. Lahav-Baratz, S., Sudakin, V., Ruderman, J. V & Hershko, a. Reversible phosphorylation controls the activity of cyclosome-associated cyclin-ubiquitin ligase. *Proc. Natl. Acad. Sci. U. S. A.* **92**, 9303–9307 (1995).
29. Fang, G., Yu, H. & Kirschner, M. W. The checkpoint protein MAD2 and the mitotic regulator CDC20 form a ternary complex with the anaphase-promoting complex to control anaphase initiation. *Genes Dev.* **12**, 1871–1883 (1998).
30. Kotani, S. *et al.* PKA and MPF-activated polo-like kinase regulate anaphase-promoting complex activity and mitosis progression. *Mol. Cell* **1**, 371–380 (1998).
31. Van Zon, W. *et al.* The APC/C recruits cyclin B1-Cdk1-Cks in prometaphase before D box recognition to control mitotic exit. *J. Cell Biol.* **190**, 587–602 (2010).
32. Voets, E. & Wolthuis, R. MASTL promotes cyclin B1 destruction by enforcing Cdc20-independent binding of cyclin B1 to the APC/C. *Biol. Open* 1–12 (2015). doi:10.1242/bio.201410793
33. Visintin, R., Prinz, S. & Amon, a. CDC20 and CDH1: a family of substrate-specific activators of APC-dependent proteolysis. *Science* **278**, 460–463 (1997).
34. Schwab, M., Lutum, A. S. & Seufert, W. Yeast Hct1 is a regulator of Cib2 cyclin proteolysis. *Cell* **90**, 683–693 (1997).
35. Kimata, Y., Baxter, J. E., Fry, A. M. & Yamano, H. A role for the Fizzy/Cdc20 family of proteins in activation of the APC/C distinct from substrate recruitment. *Mol. Cell* **32**, 576–83 (2008).
36. Matsusaka, T., Enquist-Newman, M., Morgan, D. O. & Pines, J. Co-activator independent differences in how the metaphase and anaphase APC/C recognise the same substrate. *Biol. Open* **1**, 1–9 (2014).
37. Van Voorhis, V. a & Morgan, D. O. Activation of the APC/C Ubiquitin Ligase by Enhanced E2 Efficiency. *Curr. Biol.* **24**, 1556–62 (2014).
38. Schwab, M., Neutzner, M., Möcker, D. & Seufert, W. Yeast Hct1 recognizes the mitotic cyclin Clb2 and other substrates of the ubiquitin ligase APC. *EMBO J.* **20**, 5165–75 (2001).
39. Smith, T. F., Gaitatzes, C., Saxena, K. & Neer, E. J. The WD repeat: A common architecture for diverse functions. *Trends Biochem. Sci.* **24**, 181–185 (1999).

40. Tian, W. *et al.* Structural analysis of human Cdc20 supports multisite degron recognition by APC/C. *Proc. Natl. Acad. Sci. U. S. A.* **109**, 18419–24 (2012).
41. Kraft, C., Vodermaier, H. C., Maurer-Stroh, S., Eisenhaber, F. & Peters, J.-M. The WD40 Propeller Domain of Cdh1 Functions as a Destruction Box Receptor for APC/C Substrates. *Mol. Cell* **18**, 543–553 (2005).
42. He, J. *et al.* Insights into Degron Recognition by APC/C Coactivators from the Structure of an Acm1-Cdh1 Complex. *Mol. Cell* 1–12 (2013). doi:10.1016/j.molcel.2013.04.024
43. Passmore, L. a. *et al.* Doc1 mediates the activity of the anaphase-promoting complex by contributing to substrate recognition. *EMBO J.* **22**, 786–796 (2003).
44. Vodermaier, H. C., Gieffers, C., Maurer-stroh, S., Eisenhaber, F. & Peters, J. TPR Subunits of the Anaphase-Promoting Complex Mediate Binding to the Activator Protein CDH1. **13**, 1459–1468 (2003).
45. Matyskiela, M. E. & Morgan, D. O. Analysis of activator-binding sites on the APC/C supports a cooperative substrate-binding mechanism. *Mol. Cell* **34**, 68–80 (2009).
46. Matyskiela, M. E. & Morgan, D. O. Analysis of activator-binding sites on the APC/C supports a cooperative substrate-binding mechanism. *Mol. Cell* **34**, 68–80 (2009).
47. Izawa, D. & Pines, J. How APC/C-Cdc20 changes its substrate specificity in mitosis. *Nat. Cell Biol.* **13**, 223–33 (2011).
48. Izawa, D. & Pines, J. Mad2 and the APC/C compete for the same site on Cdc20 to ensure proper chromosome segregation. *J. Cell Biol.* **199**, 27–37 (2012).
49. Hein, J. B. & Nilsson, J. Stable MCC binding to the APC/C is required for a functional spindle assembly checkpoint. *EMBO Rep.* **15**, 264–72 (2014).
50. Tian, W. *et al.* Structural analysis of human Cdc20 supports multisite degron recognition by APC/C. *Proc. Natl. Acad. Sci.* **109**, (2012).
51. Labit, H. *et al.* Dephosphorylation of Cdc20 is required for its C-box-dependent activation of the APC/C. *EMBO J.* **31**, 3351–3362 (2012).
52. Brown, N. G. *et al.* Mechanism of Polyubiquitination by Human Anaphase-Promoting Complex: RING Repurposing for Ubiquitin Chain Assembly. *Mol. Cell* **56**, 246–260 (2014).
53. Pashkova, N. *et al.* WD40 Repeat Propellers Define a Ubiquitin-Binding Domain that Regulates Turnover of F Box Proteins. *Mol. Cell* **40**, 433–443 (2010).
54. Carroll, C. W. The APC subunit Doc1 promotes recognition of the substrate destruction box. *Curr. Biol.* **15**, 11–18 (2005).
55. Eytan, E., Moshe, Y., Braunstein, I. & Hershko, A. Roles of the anaphase-promoting complex/cyclosome and of its activator Cdc20 in functional substrate binding. *Proc. Natl. Acad. Sci. U. S. A.* **103**, 2081–6 (2006).
56. Da Fonseca, P. C. A. *et al.* Structures of APC/CCdh1 with substrates identify Cdh1 and Apc10 as the D-box co-receptor. *Nature* **470**, 274–278 (2011).
57. Buschhorn, B. a *et al.* Substrate binding on the APC/C occurs between the coactivator Cdh1 and the processivity factor Doc1. *Nat. Struct. Mol. Biol.* **18**, 6–13 (2011).
58. Chao, W. C. H., Kulkarni, K., Zhang, Z., Kong, E. H. & Barford, D. Structure of the mitotic checkpoint complex. *Nature* **484**, 208–13 (2012).
59. Keck, J. M. *et al.* Cyclin E overexpression impairs progression through mitosis by inhibiting APCCdh1. *J. Cell Biol.* **178**, 371–385 (2007).

60. Zachariae, W. Control of Cyclin Ubiquitination by CDK-Regulated Binding of Hct1 to the Anaphase Promoting Complex. *Science (80-.)*. **282**, 1721–1724 (1998).
61. Yudkovsky, Y., Shteinberg, M., Listovsky, T., Brandeis, M. & Hershko, A. Phosphorylation of Cdc20/Fizzy Negatively Regulates the Mammalian Cyclosome/APC in the Mitotic Checkpoint. *Biochem. Biophys. Res. Commun.* **271**, 299–304 (2000).
62. Chung, E. & Chen, R.-H. Phosphorylation of Cdc20 is required for its inhibition by the spindle checkpoint. *Nat. Cell Biol.* **5**, 748–753 (2003).
63. D'Angiolella, V. & Mari, C. The spindle checkpoint requires cyclin-dependent kinase activity. *Genes Dev.* 2520–2525 (2003). doi:10.1101/gad.267603.2520
64. Jin, L., Williamson, A., Banerjee, S., Philipp, I. & Rape, M. Mechanism of ubiquitin-chain formation by the human anaphase-promoting complex. *Cell* **133**, 653–65 (2008).
65. Blanco, M. a, Sa, A., Prada, Â. M. De & Moreno, S. in G 1 and is inhibited by cdc2 phosphorylation. *EMBO J.* **19**, 3945–3955 (2000).
66. Ayuda-Durán, P. *et al.* The CDK regulators Cdh1 and Sic1 promote efficient usage of DNA replication origins to prevent chromosomal instability at a chromosome arm. *Nucleic Acids Res.* **42**, 7057–68 (2014).
67. Taguchi, S. I. *et al.* Degradation of human Aurora-A protein kinase is mediated by hCdh1. *FEBS Lett.* **519**, 59–65 (2002).
68. Littlepage, L. E. & Ruderman, J. V. Identification of a new APC/C recognition domain, the A box, which is required for the Cdh1-dependent destruction of the kinase Aurora-A during mitotic exit. *Genes Dev.* **16**, 2274–2285 (2002).
69. Lindon, C. & Pines, J. Ordered proteolysis in anaphase inactivates Plk1 to contribute to proper mitotic exit in human cells. *J. Cell Biol.* **164**, 233–41 (2004).
70. Floyd, S., Pines, J. & Lindon, C. APC/CCdh1 Targets Aurora Kinase to Control Reorganization of the Mitotic Spindle at Anaphase. *Curr. Biol.* **18**, 1649–1658 (2008).
71. García-Higuera, I. *et al.* Genomic stability and tumour suppression by the APC/C cofactor Cdh1. *Nat. Cell Biol.* **10**, 802–811 (2008).
72. Sigl, R. *et al.* Loss of the mammalian APC/C activator FZR1 shortens G1 and lengthens S phase but has little effect on exit from mitosis. *J. Cell Sci.* **122**, 4208–17 (2009).
73. Sudo, T. *et al.* Activation of Cdh1-dependent APC is required for G 1 cell cycle arrest and DNA damage-induced G 2 checkpoint in vertebrate cells. *EMBO J.* **20**, 6499–6508 (2001).
74. Engelbert, D., Schnerch, D., Baumgarten, a & Wäsch, R. The ubiquitin ligase APC(Cdh1) is required to maintain genome integrity in primary human cells. *Oncogene* **27**, 907–917 (2008).
75. Bassermann, F., Frescas, D. & Guardavaccaro, D. The Cdc14B-Cdh1-Plk1 axis controls the G2 DNA-damage-response checkpoint. *Cell* **134**, 256–267 (2008).
76. Wiebusch, L. & Hagemeyer, C. p53- and p21-dependent premature APC/C-Cdh1 activation in G2 is part of the long-term response to genotoxic stress. *Oncogene* **29**, 3477–89 (2010).
77. Krenning, L., Feringa, F. M., Shaltiel, I. a., vandenBerg, J. & Medema, R. H. Transient activation of p53 in G2 phase is sufficient to induce senescence. *Mol. Cell* **55**, 59–72 (2014).
78. Eguren, M. *et al.* The APC/C cofactor Cdh1 prevents replicative stress and p53-dependent cell death in neural progenitors. *Nat. Commun.* **4**, 2880 (2013).
79. Listovsky, T. & Sale, J. E. Sequestration of cdh1 by mad2l2 prevents premature apc/c activation prior to anaphase onset. *J. Cell Biol.* **203**, 87–100 (2013).

80. Hagting, A. *et al.* Human securin proteolysis is controlled by the spindle checkpoint and reveals when the APC/C switches from activation by Cdc20 to Cdh1. *J. cell ...* **157**, 1125–1137 (2002).
81. Yu, H. Cdc20: a WD40 activator for a cell cycle degradation machine. *Mol. Cell* **27**, 3–16 (2007).
82. Sedgwick, G. G. *et al.* Mechanisms controlling the temporal degradation of Nek2A and Kif18A by the APC/C-Cdc20 complex. *EMBO J.* **32**, 303–14 (2013).
83. Boekhout, M. & Wolthuis, R. M. F. Nek2A destruction marks APC/C activation at the prophase-to- prometaphase transition by spindle-checkpoint restricted Cdc20. *J. Cell Sci.* (2015).
84. Dawson, I., Roth, S. & Artavanis-Tsakonas, S. The Drosophila Cell Cycle Gene fizzy Is Required for Normal Degradation. *Cell* **129**, (1995).
85. Li, M., York, J. P. & Zhang, P. Loss of Cdc20 causes a securin-dependent metaphase arrest in two-cell mouse embryos. *Mol. Cell. Biol.* **27**, 3481–3488 (2007).
86. Wolthuis, R. *et al.* Cdc20 and Cks direct the spindle checkpoint-independent destruction of cyclin A. *Mol. Cell* **30**, 290–302 (2008).
87. Huang, H. C., Shi, J., Orth, J. D. & Mitchison, T. J. Evidence that Mitotic Exit Is a Better Cancer Therapeutic Target Than Spindle Assembly. *Cancer Cell* **16**, 347–358 (2009).
88. Rudner, A. D. & Murray, A. W. Phosphorylation by Cdc28 activates the Cdc20-dependent activity of the anaphase-promoting complex. *J. Cell Biol* **149**, 1377–1390 (2000).
89. Kraft, C. *et al.* Mitotic regulation of the human anaphase-promoting complex by phosphorylation. *EMBO J.* **22**, 6598–6609 (2003).
90. Steen, J. a J. *et al.* Different phosphorylation states of the anaphase promoting complex in response to antimitotic drugs: a quantitative proteomic analysis. *Proc. Natl. Acad. Sci. U. S. A.* **105**, 6069–6074 (2008).
91. Hegemann, B. *et al.* Systematic Phosphorylation Analysis of Human Mitotic Protein Complexes. *Sci. Signal.* **4**, rs12–rs12 (2011).
92. Tang, Z., Shu, H., Oncel, D., Chen, S. & Yu, H. Phosphorylation of Cdc20 by Bub1 provides a catalytic mechanism for APC/C inhibition by the spindle checkpoint. *Mol. Cell* **16**, 387–97 (2004).
93. Kang, J. *et al.* Structure and Substrate Recruitment of the Human Spindle Checkpoint Kinase Bub1. *Mol. Cell* **32**, 394–405 (2008).
94. Pflieger, C. & Kirschner, M. W. The KEN box: an APC recognition signal distinct from the D box targeted by Cdh1. *Genes & Dev.* 655–665 (2000). doi:10.1101/gad.14.6.655
95. Reis, A., Levasseur, M., Chang, H.-Y., Elliott, D. J. & Jones, K. T. The CRY box: a second APCcdh1-dependent degron in mammalian cdc20. *EMBO Rep.* **7**, 1040–1045 (2006).
96. Foster, S. & Morgan, D. The APC/C subunit Mnd2/Apc15 promotes Cdc20 autoubiquitination and spindle assembly checkpoint inactivation. *Mol. Cell* **47**, 921–932 (2012).
97. King, E. M. J., van der Sar, S. J. a & Hardwick, K. G. Mad3 KEN boxes mediate both Cdc20 and Mad3 turnover, and are critical for the spindle checkpoint. *PLoS One* **2**, (2007).
98. Pan, J. & Chen, R.-H. Spindle checkpoint regulates Cdc20p stability in *Saccharomyces cerevisiae*. *Genes Dev.* **18**, 1439–51 (2004).
99. Reddy, S. K., Rape, M., Margansky, W. a & Kirschner, M. W. Ubiquitination by the anaphase-promoting complex drives spindle checkpoint inactivation. *Nature* **446**, 921–5 (2007).

100. Stegmeier, F. *et al.* Anaphase initiation is regulated by antagonistic ubiquitination and deubiquitination activities. *Nature* **446**, 876–881 (2007).
101. Foe, I. T. *et al.* Ubiquitination of Cdc20 by the APC occurs through an intramolecular mechanism. *Curr. Biol.* **21**, 1870–1877 (2011).
102. Heinrich, S. *et al.* Determinants of robustness in spindle assembly checkpoint signalling. *Nat. Cell Biol.* **15**, 1328–39 (2013).
103. Nilsson, J., Yekezare, M., Minshull, J. & Pines, J. The APC/C maintains the spindle assembly checkpoint by targeting Cdc20 for destruction. *Nat. Cell Biol.* **10**, 1411–20 (2008).
104. Nilsson, J. Insights & Perspectives Cdc20 control of cell fate during prolonged mitotic arrest. *BioEssays* 1–7 (2011). doi:10.1002/bies.201100094
105. Fry, A. M. & Yamano, H. Under arrest in mitosis: Cdc20 dies twice. *Nat. Cell Biol.* **10**, 1385–7 (2008).
106. Lara-Gonzalez, P., Westhorpe, F. G. & Taylor, S. S. The Spindle Assembly Checkpoint. *Curr. Biol.* **22**, R966–R980 (2012).
107. Hsu, J. Y., Reimann, J. D. R., Sørensen, C. S., Lukas, J. & Jackson, P. K. E2F-dependent accumulation of hEmi1 regulates S phase entry by inhibiting APC(Cdh1). *Nat. Cell Biol.* **4**, 358–366 (2002).
108. Reimann, J. D. *et al.* Emi1 is a mitotic regulator that interacts with Cdc20 and inhibits the anaphase promoting complex. *Cell* **105**, 645–55 (2001).
109. Dong, X. *et al.* Control of G1 in the developing Drosophila eye: rcal regulates Cychn A. *Genes Dev.* **6**, 94–105 (1997).
110. Grosskortenhaus, R. & Sprenger, F. Rca1 inhibits APC-Cdh1(Fzr) and is required to prevent cyclin degradation in G2. *Dev. Cell* **2**, 29–40 (2002).
111. Di Fiore, B. & Pines, J. Emi1 is needed to couple DNA replication with mitosis but does not regulate activation of the mitotic APC/C. *J. Cell Biol.* **177**, 425–437 (2007).
112. Miller, J. J. *et al.* Emi1 stably binds and inhibits the anaphase-promoting complex/cyclosome as a pseudosubstrate inhibitor. *Genes Dev.* **20**, 2410–20 (2006).
113. Yamano, H., Gannon, J., Mahbubani, H. & Hunt, T. Cell cycle-regulated recognition of the destruction box of cyclin B by the APC/C in Xenopus egg extracts. *Mol. Cell* **13**, 137–47 (2004).
114. Reimann, J. D. R., Gardner, B. E., Margottin-Goguët, F. & Jackson, P. K. Emi1 regulates the anaphase-promoting complex by a different mechanism than Mad2 proteins. *Genes Dev.* **15**, 3278–3285 (2001).
115. Machida, Y. J. & Dutta, A. The APC/C inhibitor, Emi1, is essential for prevention of rereplication. *Genes Dev.* **21**, 184–194 (2007).
116. Guardavaccaro, D. *et al.* Control of meiotic and mitotic progression by the F box protein beta-Trcp1 in vivo. *Dev. Cell* **4**, 799–812 (2003).
117. Margottin-Goguët, F., Hsu, J. & Loktev, A. destruction of Emi1 by the SCF β TrCP/Slimb ubiquitin ligase activates the anaphase promoting complex to allow progression beyond prometaphase. *Dev. Cell* **4**, 813–826 (2003).
118. Ban, K. H. *et al.* Supplemental Data The END Network Couples Spindle Pole Assembly to Inhibition of the Anaphase-Promoting Complex / Cyclosome in Early Mitosis. 1–11
119. Riley, B. B. *et al.* Characterization of harpy/Rca1/emi1 mutants: patterning in the absence of cell division. *Dev. Dyn.* **239**, 828–43 (2010).

120. Robu, M. E., Zhang, Y. & Rhodes, J. Rereplication in *emi1*-deficient zebrafish embryos occurs through a *Cdh1*-mediated pathway. *PLoS One* **7**, e47658 (2012).
121. Frye, J. J. *et al.* Electron microscopy structure of human APC/C(CDH1)-EMI1 reveals multimodal mechanism of E3 ligase shutdown. *Nat. Struct. Mol. Biol.* 1–11 (2013). doi:10.1038/nsmb.2593
122. Tung, J. J. *et al.* A role for the anaphase-promoting complex inhibitor *Emi2/XErp1*, a homolog of early mitotic inhibitor 1, in cyostatic factor arrest of *Xenopus* eggs. *Proc. Natl. Acad. Sci. U. S. A.* **102**, 4318–4323 (2005).
123. Sako, K. *et al.* *Emi2* mediates meiotic MII arrest by competitively inhibiting the binding of *Ube2S* to the APC/C. *Nat. Commun.* **5**, 3667 (2014).
124. Ohe, M. *et al.* *Emi2* Inhibition of the Anaphase-promoting Complex / Cyclosome Absolutely Requires *Emi2* Binding via the C-Terminal RL Tail. *Mol. Biol. Cell* **21**, 905–913 (2010).
125. Tang, W. *et al.* *Emi2*-mediated Inhibition of E2-substrate Ubiquitin Transfer by the Anaphase-promoting Complex/Cyclosome through a D-Box-independent Mechanism. *Mol. Biol. Cell* **21**, 4042–4056 (2010).
126. Wang, W. & Kirschner, M. W. *Emi1* preferentially inhibits ubiquitin chain elongation by the anaphase-promoting complex. *Nat. Cell Biol.* **15**, 1–11 (2013).
127. Hansen, D., Loktev, A., Ban, K. H. & Jackson, P. K. *Plk1* Regulates Activation of the Anaphase Promoting Complex by Phosphorylating and Triggering SCFTrCP- dependent Destruction of the APC Inhibitor *Emi1*. *Mol. Biol. Cell* **16**, 1–13 (2004).
128. Moshe, Y., Boulaire, J., Pagano, M. & Hershko, A. Role of Polo-like kinase in the degradation of early mitotic inhibitor 1, a regulator of the anaphase promoting complex/cyclosome. *Proc. Natl. Acad. Sci. U. S. A.* **101**, 7937–7942 (2004).
129. Moshe, Y., Bar-On, O., Ganoth, D. & Hershko, a. Regulation of the action of early mitotic inhibitor 1 on the Anaphase-Promoting Complex/Cyclosome by Cyclin-Dependent Kinases. *J. Biol. Chem.* (2011). doi:10.1074/jbc.M111.223339
130. Lénárt, P. *et al.* The Small-Molecule Inhibitor BI 2536 Reveals Novel Insights into Mitotic Roles of Polo-like Kinase 1. *Curr. Biol.* **17**, 304–315 (2007).
131. Cromer, L. *et al.* OSD1 Promotes Meiotic Progression via APC/C Inhibition and Forms a Regulatory Network with TDM and CYCA1;2/TAM. *PLoS Genet.* **8**, e1002865 (2012).
132. Li, R. & Murray, A. W. Feedback control of mitosis in budding yeast. *Cell* **66**, 519–531 (1991).
133. Hoyt, M. A., Totis, L. & Roberts, B. T. *S. cerevisiae* genes required for cell cycle arrest in response to loss of microtubule function. *Cell* **66**, 507–517 (1991).
134. Foley, E. a & Kapoor, T. M. Microtubule attachment and spindle assembly checkpoint signalling at the kinetochore. *Nat. Rev. Mol. Cell Biol.* **14**, 25–37 (2013).
135. Musacchio, a. Spindle assembly checkpoint: the third decade. *Philos. Trans. R. Soc. B Biol. Sci.* **366**, 3595–3604 (2011).
136. Wang, Q. *et al.* BUBR1 deficiency results in abnormal megakaryopoiesis. *Blood* **103**, 1278–85 (2004).
137. Dobles, M., Liberal, V., Scott, M. L., Benezra, R. & Sorger, P. K. Chromosome missegregation and apoptosis in mice lacking the mitotic checkpoint protein *Mad2*. *Cell* **101**, 635–645 (2000).

138. Hardwick, K. G., Johnston, R. C., Smith, D. L. & Murray, A. W. MAD3 Encodes a Novel Component of the Spindle Checkpoint which Interacts with Bub3p, Cdc20p, and Mad2p. **148**, 871–882 (2000).
139. Fracchini, R. *et al.* Bub3 interaction with Mad2, Mad3 and Cdc20 is mediated by WD40 repeats and does not require intact kinetochores. *EMBO J.* **20**, 6648–6659 (2001).
140. Sudakin, V., Chan, G. K. T. & Yen, T. J. Checkpoint inhibition of the APC/C in HeLa cells is mediated by a complex of BUBR1, BUB3, CDC20, and MAD2. *J. Cell Biol.* **154**, 925–936 (2001).
141. Hwang, L. H. *et al.* Budding Yeast Cdc20 : A Target of the Spindle Checkpoint. **279**, (1998).
142. Luo, X., Tang, Z., Rizo, J. & Yu, H. The Mad2 spindle checkpoint protein undergoes similar major conformational changes upon binding to either Mad1 or Cdc20. *Mol. Cell* **9**, 59–71 (2002).
143. Sironi, L. *et al.* The Mad1-Mad2 complex: implications of a ‘safety belt’ binding mechanism for the spindle checkpoint. *Acta Crystallogr. Sect. A Found. Crystallogr.* **58**, c223–c223 (2002).
144. Burton, J. L., Xiong, Y. & Solomon, M. J. Mechanisms of pseudosubstrate inhibition of the anaphase promoting complex by Acm1. *EMBO J.* **30**, 1818–1829 (2011).
145. Elowe, S. *et al.* Uncoupling of the spindle-checkpoint and chromosome-congression functions of BubR1. *J. Cell Sci.* **123**, 84–94 (2009).
146. Lara-Gonzalez, P., Scott, M. I. F., Diez, M., Sen, O. & Taylor, S. S. BubR1 blocks substrate recruitment to the APC/C in a KEN-box-dependent manner. *J. Cell Sci.* (2011). doi:10.1242/jcs.094763
147. Rieder, C. L., Cole, R. W., Khodjakov, A. & Sluder, G. The checkpoint delaying anaphase in response to chromosome monoorientation is mediated by an inhibitory signal produced by unattached kinetochores. *J. Cell Biol.* **130**, 941–948 (1995).
148. Collin, P., Nashchekina, O., Walker, R. & Pines, J. The spindle assembly checkpoint works like a rheostat rather than a toggle switch. *Nat. Cell Biol.* **15**, 1378–85 (2013).
149. Dick, A. E. & Gerlich, D. W. Kinetic framework of spindle assembly checkpoint signalling. *Nat. Cell Biol.* **15**, 1370–7 (2013).
150. Allshire, R. C. & Karpen, G. H. Epigenetic regulation of centromeric chromatin: old dogs, new tricks? *Nat. Rev. Genet.* **9**, 923–937 (2008).
151. Santaguida, S. & Musacchio, A. The life and miracles of kinetochores. *EMBO J.* **28**, 2511–2531 (2009).
152. Cheeseman, I. M. & Desai, A. Molecular architecture of the kinetochore-microtubule interface. *Nat. Rev. Mol. Cell Biol.* **9**, 33–46 (2008).
153. McAinsh, A. D. & Meraldi, P. The CCAN complex: Linking centromere specification to control of kinetochore–microtubule dynamics. *Semin. Cell Dev. Biol.* **22**, 946–952 (2011).
154. Cheeseman, I. M., Chappie, J. S., Wilson-Kubalek, E. M. & Desai, A. The Conserved KMN Network Constitutes the Core Microtubule-Binding Site of the Kinetochore. *Cell* **127**, 983–997 (2006).
155. Joglekar, A. P. *et al.* Molecular architecture of the kinetochore-microtubule attachment site is conserved between point and regional centromeres. *J. Cell Biol.* **181**, 587–594 (2008).
156. Karess, R. Rod-Zw10–Zwilch: a key player in the spindle checkpoint. *Trends Cell Biol.* **15**, 386–392 (2005).

157. Weiss, E. & Winey, M. The *Saccharomyces cerevisiae* spindle pole body duplication gene MPS1 is part of a mitotic checkpoint. *J. Cell Biol.* **132**, 111–123 (1996).
158. Primorac, I. *et al.* Bub3 reads phosphorylated MELT repeats to promote spindle assembly checkpoint signaling. *Elife* **2013**, 1–20 (2013).
159. Overlack, K. *et al.* A molecular basis for the differential roles of Bub1 and BubR1 in the spindle assembly checkpoint. *Elife* **4**, (2015).
160. Sacristan, C. & Kops, G. J. P. L. Joined at the hip: kinetochores, microtubules, and spindle assembly checkpoint signaling. *Trends Cell Biol.* **25**, 21–28 (2014).
161. Vleugel, M. *et al.* Sequential Multisite Phospho-Regulation of KNL1-BUB3 Interfaces at Mitotic Kinetochores. *Mol. Cell* **57**, 824–835 (2015).
162. Santaguida, S., Tighe, A., D'Alise, A. M., Taylor, S. S. & Musacchio, A. Dissecting the role of MPS1 in chromosome biorientation and the spindle checkpoint through the small molecule inhibitor reversine. *J. Cell Biol.* **190**, 73–87 (2010).
163. Maciejowski, J. *et al.* Mps1 directs the assembly of Cdc20 inhibitory complexes during interphase and mitosis to control M phase timing and spindle checkpoint signaling. *J. Cell Biol.* **190**, 89–100 (2010).
164. Heinrich, S., Windecker, H., Hustedt, N. & Hauf, S. Mph1 kinetochore localization is crucial and upstream in the hierarchy of spindle assembly checkpoint protein recruitment to kinetochores. *J. Cell Sci.* 4720–4727 (2012). doi:10.1242/jcs.110387
165. Santaguida, S., Vernieri, C., Villa, F., Ciliberto, A. & Musacchio, A. Evidence that Aurora B is implicated in spindle checkpoint signalling independently of error correction. *EMBO J.* **30**, 1508–1519 (2011).
166. Lampson, M. a. & Cheeseman, I. M. Sensing centromere tension: Aurora B and the regulation of kinetochore function. *Trends Cell Biol.* **21**, 133–140 (2011).
167. Hewitt, L. *et al.* Sustained Mps1 activity is required in mitosis to recruit O-Mad2 to the Mad1-C-Mad2 core complex. *J. Cell Biol.* **190**, 25–34 (2010).
168. Jelluma, N., Dansen, T. B., Sliedrecht, T., Kwiatkowski, N. P. & Kops, G. J. P. L. Release of Mps1 from kinetochores is crucial for timely anaphase onset. *J. Cell Biol.* **191**, 281–90 (2010).
169. Elowe, S. Bub1 and BubR1: at the Interface between Chromosome Attachment and the Spindle Checkpoint. *Mol. Cell Biol.* **31**, 3085–93 (2011).
170. Krenn, V., Wehenkel, A., Li, X., Santaguida, S. & Musacchio, A. Structural analysis reveals features of the spindle checkpoint kinase Bub1-kinetochore subunit Knl1 interaction. *J. Cell Biol.* **196**, 451–467 (2012).
171. Logarinho, E., Resende, T., Torres, C. & Bousba, H. The Human Spindle Assembly Checkpoint Protein Bub3 Is Required for the Establishment of Efficient Kinetochore–Microtubule Attachments. *Mol. Biol. Cell* **19**, 308–317 (2008).
172. Malureanu, L. a. *et al.* BubR1 N Terminus Acts as a Soluble Inhibitor of Cyclin B Degradation by APC/CCdc20 in Interphase. *Dev. Cell* **16**, 118–131 (2009).
173. Kulukian, A., Han, J. S. & Cleveland, D. W. Unattached kinetochores catalyze production of an anaphase inhibitor that requires a Mad2 template to prime Cdc20 for BubR1 binding. *Dev. Cell* **16**, 105–17 (2009).
174. Gillett, E. S., Espelin, C. W. & Sorger, P. K. Spindle checkpoint proteins and chromosome-microtubule attachment in budding yeast. *J. Cell Biol.* **164**, 535–546 (2004).

175. Johnson, V. L., Scott, M. I. F., Holt, S. V., Hussein, D. & Taylor, S. S. Bub1 is required for kinetochore localization of BubR1, Cenp-E, Cenp-F and Mad2, and chromosome congression. *J. Cell Sci.* **117**, 1577–1589 (2004).
176. Klebig, C., Korinth, D. & Meraldi, P. Bub1 regulates chromosome segregation in a kinetochore-independent manner. *J. Cell Biol.* **185**, 841–858 (2009).
177. Millband, D. N. & Hardwick, K. G. Fission yeast Mad3p is required for Mad2p to inhibit the anaphase-promoting complex and localizes to kinetochores in a Bub1p-, Bub3p-, and Mph1p-dependent manner. *Mol. Cell. Biol.* **22**, 2728–2742 (2002).
178. Perera, D. *et al.* Bub1 Maintains Centromeric Cohesion by Activation of the Spindle Checkpoint. *Dev. Cell* **13**, 566–579 (2007).
179. Howell, B. *et al.* Spindle Checkpoint Protein Dynamics at Kinetochores in Living Cells. *Curr. Biol.* **14**, 953–964 (2004).
180. Shah, J. *et al.* Dynamics of Centromere and Kinetochore Proteins: Implications for Checkpoint Signaling and Silencing. *Curr. Biol.* **14**, 942–952 (2004).
181. Mapelli, M., Massimiliano, L., Santaguida, S. & Musacchio, A. The Mad2 Conformational Dimer: Structure and Implications for the Spindle Assembly Checkpoint. *Cell* **131**, 730–743 (2007).
182. De Antoni, A. *et al.* The Mad1/Mad2 Complex as a Template for Mad2 Activation in the Spindle Assembly Checkpoint. *Development* **15**, 214–225 (2005).
183. Li, Y., Gorbea, C., Mahaffey, D., Rechsteiner, M. & Benezra, R. MAD2 associates with the cyclosome/anaphase-promoting complex and inhibits its activity. *Proc. Natl. Acad. Sci. U. S. A.* **94**, 12431–12436 (1997).
184. Campbell, M. S., Chan, G. K. & Yen, T. J. Mitotic checkpoint proteins HsMAD1 and HsMAD2 are associated with nuclear pore complexes in interphase. *J. Cell Sci.* **114**, 953–963 (2001).
185. Rodriguez-Bravo, V. *et al.* Nuclear pores protect genome integrity by assembling a premitotic and Mad1-dependent anaphase inhibitor. *Cell* **156**, 1017–31 (2014).
186. Morrow, C. J. *et al.* Bub1 and aurora B cooperate to maintain BubR1-mediated inhibition of APC/CCdc20. *J. Cell Sci.* **118**, 3639–3652 (2005).
187. Jia, L. *et al.* Defining pathways of spindle checkpoint silencing: functional redundancy between Cdc20 ubiquitination and p31(comet). *Mol. Biol. Cell* **22**, 4227–35 (2011).
188. Visconti, R., Palazzo, L. & Grieco, D. Requirement for proteolysis in spindle assembly checkpoint silencing. *Cell Cycle* **9**, 564–569 (2010).
189. Mansfeld, J., Collin, P., Collins, M. O., Choudhary, J. S. & Pines, J. APC15 drives the turnover of MCC-CDC20 to make the spindle assembly checkpoint responsive to kinetochore attachment. *Nat. Cell Biol.* **13**, 1–11 (2011).
190. Varetta, G., Guida, C., Santaguida, S., Chirolì, E. & Musacchio, A. Homeostatic control of mitotic arrest. *Mol. Cell* **44**, 710–20 (2011).
191. Uzunova, K. *et al.* APC15 mediates CDC20 autoubiquitylation by APC/C(MCC) and disassembly of the mitotic checkpoint complex. *Nat. Struct. Mol. Biol.* **19**, 1116–1123 (2012).
192. Westhorpe, F. G., Tighe, A., Lara-Gonzalez, P. & Taylor, S. S. p31comet-mediated extraction of Mad2 from the MCC promotes efficient mitotic exit. *J. Cell Sci.* (2011). doi:10.1242/jcs.093286

193. Teichner, A. *et al.* p31comet Promotes disassembly of the mitotic checkpoint complex in an ATP-dependent process. *Proc. Natl. Acad. Sci. U. S. A.* **108**, 3187–92 (2011).
194. Xia, G. *et al.* Conformation-specific binding of p31(comet) antagonizes the function of Mad2 in the spindle checkpoint. *EMBO J.* **23**, 3133–3143 (2004).
195. Mapelli, M. *et al.* Determinants of conformational dimerization of Mad2 and its inhibition by p31comet. *EMBO J.* **25**, 1273–1284 (2006).
196. Zeng, X. *et al.* Pharmacologic inhibition of the anaphase-promoting complex induces a spindle checkpoint-dependent mitotic arrest in the absence of spindle damage. *Cancer Cell* **18**, 382–395 (2010).
197. Zeng, X. & King, R. W. An APC/C inhibitor stabilizes cyclin B1 by prematurely terminating ubiquitination. *Nat. Chem. Biol.* 1–10 (2012). doi:10.1038/nchembio.801
198. Lara-Gonzalez, P. & Taylor, S. S. Cohesion fatigue explains why pharmacological inhibition of the APC/C induces a spindle checkpoint-dependent mitotic arrest. *PLoS One* **7**, e49041 (2012).
199. Sackton, K. L. *et al.* Synergistic blockade of mitotic exit by two chemical inhibitors of the APC/C. *Nature* (2014). doi:10.1038/nature13660
200. Petroski, M. D. & Deshaies, R. J. Context of multiubiquitin chain attachment influences the rate of Sic1 degradation. *Mol. Cell* **11**, 1435–1444 (2003).
201. Kirkpatrick, D. S. *et al.* Quantitative analysis of in vitro ubiquitinated cyclin B1 reveals complex chain topology. *Nat. Cell Biol.* **8**, 700–710 (2006).
202. Rodrigo-Brenni, M. C. & Morgan, D. O. Sequential E2s Drive Polyubiquitin Chain Assembly on APC Targets. *Cell* **130**, 127–139 (2007).
203. Dimova, N. V. *et al.* APC/C-mediated multiple monoubiquitylation provides an alternative degradation signal for cyclin B1. *Nat. Cell Biol.* **14**, 168–176 (2012).
204. Aristarkhov, a *et al.* E2-C, a cyclin-selective ubiquitin carrier protein required for the destruction of mitotic cyclins. *Proc. Natl. Acad. Sci. U. S. A.* **93**, 4294–4299 (1996).
205. Hershko, A. *et al.* Components of a system that ligates cyclin to ubiquitin and their regulation by the protein kinase cdc2. *J. Biol. Chem.* **269**, 4940–4946 (1994).
206. Mathe, E. *et al.* The E2-C Vihar Is Required for the Correct Spatiotemporal Proteolysis of Cyclin B and Itself Undergoes Cyclical Degradation. *Curr. Biol.* **14**, 1723–1733 (2004).
207. Townsley, F. M., Aristarkhov, a, Beck, S., Hershko, a & Ruderman, J. V. Dominant-negative cyclin-selective ubiquitin carrier protein E2-C/UbcH10 blocks cells in metaphase. *Proc. Natl. Acad. Sci. U. S. A.* **94**, 2362–2367 (1997).
208. Yu, H., King, R. W., Peters, J. M. & Kirschner, M. W. Identification of a novel ubiquitin-conjugating enzyme involved in mitotic cyclin degradation. *Curr. Biol.* **6**, 455–466 (1996).
209. Merkley, N. & Shaw, G. S. Solution structure of the flexible class II ubiquitin-conjugating enzyme Ubc1 provides insights for polyubiquitin chain assembly. *J. Biol. Chem.* **279**, 47139–47147 (2004).
210. Seino, H., Kishi, T., Nishitani, H. & Yamao, F. Two Ubiquitin-Conjugating Enzymes , UbcP1 / Ubc4 and UbcP4 / Ubc11 , Have Distinct Functions for Ubiquitination of Mitotic Cyclin. *Society* **23**, 3497–3505 (2003).
211. Williamson, A. *et al.* Identification of a physiological E2 module for the human anaphase-promoting complex. *Proc. Natl. Acad. Sci. U. S. A.* **106**, 18213–8 (2009).

212. Summers, M. K., Pan, B., Mukhyala, K. & Jackson, P. K. The unique N terminus of the UbcH10 E2 enzyme controls the threshold for APC activation and enhances checkpoint regulation of the APC. *Mol. Cell* **31**, 544–56 (2008).
213. Wickliffe, K. E., Lorenz, S., Wemmer, D. E., Kuriyan, J. & Rape, M. The mechanism of linkage-specific ubiquitin chain elongation by a single-subunit E2. *Cell* **144**, 769–81 (2011).
214. Wu, T. *et al.* UBE2S drives elongation of K11-linked ubiquitin chains by the anaphase-promoting complex. *Proc. Natl. Acad. Sci. U. S. A.* **107**, 1355–60 (2010).
215. Matsumoto, M. L. *et al.* K11-linked polyubiquitination in cell cycle control revealed by a K11 linkage-specific antibody. *Mol. Cell* **39**, 477–484 (2010).
216. Kelly, A., Wickliffe, K. E., Song, L., Fedrigo, I. & Rape, M. Ubiquitin Chain Elongation Requires E3-Dependent Tracking of the Emerging Conjugate. *Mol. Cell* **56**, 232–245 (2014).
217. Meyer, H.-J. & Rape, M. Enhanced protein degradation by branched ubiquitin chains. *Cell* **157**, 910–21 (2014).
218. Lu, Y., Lee, B. -h., King, R. W., Finley, D. & Kirschner, M. W. Substrate degradation by the proteasome: A single-molecule kinetic analysis. *Science (80-.)*. **348**, 1250834–1250834 (2015).
219. Garnett, M. J. *et al.* UBE2S elongates ubiquitin chains on APC/C substrates to promote mitotic exit. *Nat. Cell Biol.* **11**, 1363–9 (2009).
220. Wagner, K. W. *et al.* Overexpression, genomic amplification and therapeutic potential of inhibiting the UbcH10 ubiquitin conjugase in human carcinomas of diverse anatomic origin. *Oncogene* **23**, 6621–6629 (2004).
221. Jung, C.-R. *et al.* E2-EPF UCP targets pVHL for degradation and associates with tumor growth and metastasis. *Nat. Med.* **12**, 809–816 (2006).
222. Tedesco, D. *et al.* The ubiquitin-conjugating enzyme E2-EPF is overexpressed in primary breast cancer and modulates sensitivity to topoisomerase II inhibition. *Neoplasia* **9**, 601–613 (2007).
223. Rape, M. & Kirschner, M. W. Autonomous regulation of the anaphase-promoting complex couples mitosis to S-phase entry. *Nature* **432**, 588–595 (2004).
224. Walker, A., Acquaviva, C., Matsusaka, T., Koop, L. & Pines, J. UbcH10 has a rate-limiting role in G1 phase but might not act in the spindle checkpoint or as part of an autonomous oscillator. *J. Cell Sci.* (2008). doi:10.1242/jcs.031591
225. Tang, Z., Bharadwaj, R., Li, B. & Yu, H. Mad2-Independent Inhibition of APC Cdc20 by the Mitotic Checkpoint Protein BubR1 at Dallas. **1**, 227–237 (2001).
226. Lu, Y., Wang, W. & Kirschner, M. W. Specificity of the anaphase-promoting complex: A single-molecule study. *Science (80-.)*. **348**, 1248737–1248737 (2015).
227. Williamson, A. *et al.* Regulation of Ubiquitin Chain Initiation to Control the Timing of Substrate Degradation. *Mol. Cell* **42**, 744–757 (2011).
228. Glotzer, M., Murray, A. W. & Kirschner, M. W. Cyclin is degraded by the ubiquitin pathway. *Nature* **349**, 132–138 (1991).
229. King, R. W., Deshaies, R. J., Peters, J.-M. & Kirschner, M. W. How Proteolysis Drives the Cell Cycle. *Sci.* **274**, 1652–1659 (1996).
230. Chao, W. C. H., Kulkarni, K., Zhang, Z., Kong, E. H. & Barford, D. Structure of the mitotic checkpoint complex. *Nature* 1–7 (2012). doi:10.1038/nature10896

231. He, J. *et al.* Insights into degron recognition by APC/C coactivators from the structure of an Acm1-Cdh1 complex. *Mol. Cell* **50**, 649–660 (2013).
232. Hilioti, Z., Chung, Y. S., Mochizuki, Y., Hardy, C. F. J. & Cohen-Fix, O. The anaphase inhibitor Pds1 binds to the APC/C-associated protein Cdc20 in a destruction box-dependent manner. *Curr. Biol.* **11**, 1347–1352 (2001).
233. Burton, J. L. & Solomon, M. J. D box and KEN box motifs in budding yeast Hsl1p are required for APC-mediated degradation and direct binding to Cdc20p and Cdh1p. *Genes Dev.* **15**, 2381–2395 (2001).
234. Burton, J. L., Tsakraklides, V. & Solomon, M. J. Assembly of an APC-Cdh1-substrate complex is stimulated by engagement of a destruction box. *Mol. Cell* **18**, 533–42 (2005).
235. Di Fiore, B. *et al.* The ABBA Motif Binds APC/C Activators and Is Shared by APC/C Substrates and Regulators. *Dev. Cell* **32**, 358–72 (2015).
236. Araki, M., Yu, H. & Asano, M. A novel motif governs APC-dependent degradation of Drosophila ORC1 in vivo. *Genes Dev.* **19**, 2458–2465 (2005).
237. Haas, A. L. & Wilkinson, K. D. DeTEKting ubiquitination of APC/C substrates. *Cell* **133**, 570–2 (2008).
238. Duursma, A. & Agami, R. p53-Dependent Regulation of Cdc6 Protein Stability Controls Cellular Proliferation p53-Dependent Regulation of Cdc6 Protein Stability Controls Cellular Proliferation †. **25**, 6937–6947 (2005).
239. Mailand, N. & Diffley, J. F. X. CDKs Promote DNA Replication Origin Licensing in Human Cells by Protecting Cdc6 from APC/C-Dependent Proteolysis. *Cell* **122**, 915–926 (2005).
240. Holt, L. J., Krutchinsky, A. N. & Morgan, D. O. Positive feedback sharpens the anaphase switch. *Nature* **454**, 353–357 (2008).
241. Rodier, G., Coulombe, P., Tanguay, P.-L., Boutonnet, C. & Meloche, S. Phosphorylation of Skp2 regulated by CDK2 and Cdc14B protects it from degradation by APC(Cdh1) in G1 phase. *EMBO J.* **27**, 679–691 (2008).
242. Dinkel, H. *et al.* The eukaryotic linear motif resource ELM: 10 years and counting. *Nucleic Acids Res.* **42**, (2014).
243. Hayes, M. J. *et al.* Early mitotic degradation of Nek2A depends on Cdc20-independent interaction with the APC/C. *Nat. Cell Biol.* **8**, 607–14 (2006).
244. Izawa, D. & Pines, J. How APC/C-Cdc20 changes its substrate specificity in mitosis. *Nat. Cell Biol.* **13**, 1–10 (2011).
245. Clijsters, L., Ogink, J. & Wolthuis, R. The spindle checkpoint, APC/CCdc20, and APC/CCdh1 play distinct roles in connecting mitosis to S phase. *J. Cell Biol.* **201**, 1013–26 (2013).
246. Chao, W. C. H., Kulkarni, K., Zhang, Z., Kong, E. H. & Barford, D. Structure of the mitotic checkpoint complex. *Nature* **484**, 208–13 (2012).
247. Clute, P. & Pines, J. Temporal and spatial control of cyclin B1 destruction in metaphase. *Nat. Cell Biol.* **1**, 82–7 (1999).
248. Den Elzen, N. & Pines, J. Cyclin A is destroyed in prometaphase and can delay chromosome alignment and anaphase. *J. Cell Biol.* **153**, 121–36 (2001).
249. Geley, S. *et al.* Anaphase-promoting complex/cyclosome-dependent proteolysis of human cyclin A starts at the beginning of mitosis and is not subject to the spindle assembly checkpoint. *J. Cell Biol.* **153**, 137–148 (2001).

250. Wolthuis, R. *et al.* Cdc20 and Cks direct the spindle checkpoint-independent destruction of cyclin A. *Mol. Cell* **30**, 290–302 (2008).
251. Di Fiore, B. & Pines, J. How cyclin A destruction escapes the spindle assembly checkpoint. *J. Cell Biol.* **190**, 501–9 (2010).
252. Van Zon, W. *et al.* The APC/C recruits cyclin B1-Cdk1-Cks in prometaphase before D box recognition to control mitotic exit. *J. Cell Biol.* **190**, 587–602 (2010).
253. Kabeche, L. & Compton, D. a. Cyclin A regulates kinetochore microtubules to promote faithful chromosome segregation. *Nature* **502**, 110–3 (2013).
254. Fry, a M. *et al.* C-Nap1, a novel centrosomal coiled-coil protein and candidate substrate of the cell cycle-regulated protein kinase Nek2. *J. Cell Biol.* **141**, 1563–74 (1998).
255. Fry, a M., Meraldi, P. & Nigg, E. a. A centrosomal function for the human Nek2 protein kinase, a member of the NIMA family of cell cycle regulators. *EMBO J.* **17**, 470–81 (1998).
256. Bahe, S., Stierhof, Y.-D., Wilkinson, C. J., Leiss, F. & Nigg, E. a. Rootletin forms centriole-associated filaments and functions in centrosome cohesion. *J. Cell Biol.* **171**, 27–33 (2005).
257. Bahmanyar, S. *et al.* beta-Catenin is a Nek2 substrate involved in centrosome separation. *Genes Dev.* **22**, 91–105 (2008).
258. Mardin, B. R. *et al.* Components of the Hippo pathway cooperate with Nek2 kinase to regulate centrosome disjunction. *Nat. Cell Biol.* 1–13 (2010). doi:10.1038/ncb2120
259. Hames, R. S. *et al.* APC/C-mediated destruction of the centrosomal kinase Nek2A occurs in early mitosis and depends upon a cyclin A-type D-box. *Mol. Biol. Org. J.* **20**, 7117–7127 (2001).
260. Wendt, K. & Vodermaier, H. Crystal structure of the APC10/DOC1 subunit of the human anaphase-promoting complex. *Nat. Struct. ...* **8**, 2–6 (2001).
261. Matyskiela, M. E., Rodrigo-Brenni, M. C. & Morgan, D. O. Mechanisms of ubiquitin transfer by the anaphase-promoting complex. *J. Biol.* **8**, 92 (2009).
262. Fry, a M., Arnaud, L. & Nigg, E. a. Activity of the human centrosomal kinase, Nek2, depends on an unusual leucine zipper dimerization motif. *J. Biol. Chem.* **274**, 16304–10 (1999).
263. Zeng, X. *et al.* Pharmacologic inhibition of the anaphase-promoting complex induces a spindle checkpoint-dependent mitotic arrest in the absence of spindle damage. *Cancer Cell* **18**, 382–95 (2010).
264. Hayes, M., Kimata, Y., Wattam, S. & Lindon, C. Early mitotic degradation of Nek2A depends on Cdc20-independent interaction with the APC/C. *Nat. cell* **8**, 607–614 (2006).
265. Wouter van Zon and Rob M.F. Wolthuis1. Cyclin A and Nek2A: APC/C–Cdc20 substrates invisible to the mitotic spindle checkpoint. *Biochem. Soc. Trans* (2010).
266. Izawa, D. & Pines, J. The mitotic checkpoint complex binds a second CDC20 to inhibit active APC/C. *Nature* **517**, 631–4 (2014).
267. Visconti, R., Palazzo, L. & Grieco, D. Requirement for proteolysis in spindle assembly checkpoint silencing. *Cell Cycle* **9**, 564–569 (2014).
268. Ma, H. T. & Poon, R. Y. C. Orderly inactivation of the key checkpoint protein mitotic arrest deficient 2 (MAD2) during mitotic progression. *J. Biol. Chem.* **286**, 13052–9 (2011).
269. Honda, K. *et al.* Degradation of human Aurora2 protein kinase by the anaphase-promoting complex-ubiquitin-proteasome pathway. *Oncogene* **19**, 2812–9 (2000).
270. Brito, D. a & Rieder, C. L. Mitotic checkpoint slippage in humans occurs via cyclin B destruction in the presence of an active checkpoint. *Curr. Biol.* **16**, 1194–200 (2006).

271. Gascoigne, K. E. & Taylor, S. S. Cancer cells display profound intra- and interline variation following prolonged exposure to antimetabolic drugs. *Cancer Cell* **14**, 111–22 (2008).
272. Wu, W. *et al.* Alternative splicing controls nuclear translocation of the cell cycle-regulated Nek2 kinase. *J. Biol. Chem.* **282**, 26431–40 (2007).
273. Poirier, M. G., Eroglu, S. & Marko, J. F. The bending rigidity of mitotic chromosomes. *Mol. Biol. Cell* **13**, 2170–2179 (2002).
274. Sliedrecht, T., Zhang, C., Shokat, K. M. & Kops, G. J. P. L. Chemical genetic inhibition of Mps1 in stable human cell lines reveals novel aspects of Mps1 function in mitosis. *PLoS One* **5**, e10251 (2010).
275. Schmidt, M., Budirahardja, Y., Klompaker, R. & Medema, R. H. Ablation of the spindle assembly checkpoint by a compound targeting Mps1. *EMBO Rep.* **6**, 866–72 (2005).
276. Kwiatkowski, N. *et al.* Small-molecule kinase inhibitors provide insight into Mps1 cell cycle function. *Nat. Chem. Biol.* **6**, 359–68 (2010).
277. Lu, D. *et al.* Multiple mechanisms determine the order of APC/C substrate degradation in mitosis. *J. Cell Biol.* **207**, 23–39 (2014).
278. Hames, R. S. *et al.* Dynamic Recruitment of Nek2 Kinase to the Centrosome Involves Microtubules , PCM-1 , and Localized Proteasomal Degradation. *Mol. Biol. Cell* **16**, 1711–1724 (2005).
279. Kamenz, J. & Hauf, S. Slow checkpoint activation kinetics as a safety device in anaphase. *Curr. Biol.* **24**, 646–51 (2014).
280. Vázquez-Novelle, M. D. *et al.* Cdk1 inactivation terminates mitotic checkpoint surveillance and stabilizes kinetochore attachments in anaphase. *Curr. Biol.* **24**, 638–45 (2014).
281. Rattani, A. *et al.* Dependency of the spindle assembly checkpoint on Cdk1 renders the anaphase transition irreversible. *Curr. Biol.* **24**, 630–7 (2014).
282. Clijsters, L. *et al.* Inefficient degradation of cyclin B1 re-activates the spindle checkpoint right after sister chromatid disjunction. *Cell Cycle* **13**, 1–9 (2014).
283. Huang, X. *et al.* Deubiquitinase USP37 is activated by CDK2 to antagonize APC(CDH1) and promote S phase entry. *Mol. Cell* **42**, 511–23 (2011).
284. Margottin-Goguet, F. *et al.* Prophase Destruction of Emi1 by the SCF β TrCP/Slimb Ubiquitin Ligase Activates the Anaphase Promoting Complex to Allow Progression beyond Prometaphase. *Dev. Cell* **4**, 813–826 (2003).
285. Di Fiore, B. & Pines, J. Emi1 is needed to couple DNA replication with mitosis but does not regulate activation of the mitotic APC/C. *J. Cell Biol.* **177**, 425–37 (2007).
286. Kimata, Y. *et al.* A mutual inhibition between APC/C and its substrate Mes1 required for meiotic progression in fission yeast. *Dev. Cell* **14**, 446–54 (2008).
287. Hames, R. S., Wattam, S. L., Yamano, H., Bacchieri, R. & Fry, A. M. APC/C-mediated destruction of the centrosomal kinase Nek2A occurs in early mitosis and depends upon a cyclin A-type D-box. *EMBO J* **20**, 7117–7127 (2001).
288. Jackman, M., Lindon, C., Nigg, E. a & Pines, J. Active cyclin B1-Cdk1 first appears on centrosomes in prophase. *Nat. Cell Biol.* **5**, 143–148 (2003).
289. Acquaviva, C., Herzog, F., Kraft, C. & Pines, J. The anaphase promoting complex/cyclosome is recruited to centromeres by the spindle assembly checkpoint. *Nat. Cell Biol.* **6**, 892–898 (2004).

290. Vassilev, L. T. *et al.* Selective small-molecule inhibitor reveals critical mitotic functions of human CDK1. *Proc. Natl. Acad. Sci. U. S. A.* **103**, 10660–10665 (2006).
291. Lindqvist, A., van Zon, W., Karlsson Rosenthal, C. & Wolthuis, R. M. F. Cyclin B1-Cdk1 activation continues after centrosome separation to control mitotic progression. *PLoS Biol.* **5**, e123 (2007).
292. McCloy, R. a. *et al.* Partial inhibition of Cdk1 in G2 phase overrides the SAC and decouples mitotic events. *Cell Cycle* **13**, 1400–1412 (2014).
293. Gutierrez, G. J., Tsuji, T., Chen, M., Jiang, W. & Ronai, Z. a. Interplay between Cdh1 and JNK activity during the cell cycle. *Nat. Cell Biol.* **12**, 686–695 (2010).
294. Gavet, O. & Pines, J. Progressive activation of CyclinB1-Cdk1 coordinates entry to mitosis. *Dev. Cell* **18**, 533–43 (2010).
295. Wu, W. *et al.* Alternative splicing controls nuclear translocation of the cell cycle-regulated Nek2 kinase. *J. Biol. Chem.* **282**, 26431–40 (2007).
296. Burrell, R. a. *et al.* Replication stress links structural and numerical cancer chromosomal instability. *Nature* **494**, 492–496 (2013).
297. Lecona, E. & Fernández-Capetillo, O. Replication stress and cancer: It takes two to tango. *Exp. Cell Res.* **329**, 26–34 (2014).
298. Chen, H.-Z., Tsai, S.-Y. & Leone, G. Emerging roles of E2Fs in cancer: an exit from cell cycle control. *Nat. Rev. Cancer* **9**, 785–97 (2009).
299. Chong, J.-L. *et al.* E2f1-3 switch from activators in progenitor cells to repressors in differentiating cells. *Nature* **462**, 930–934 (2009).
300. Maiti, B. *et al.* Cloning and characterization of mouse E2F8, a novel mammalian E2F family member capable of blocking cellular proliferation. *J. Biol. Chem.* **280**, 18211–18220 (2005).
301. De Bruin, A. *et al.* Identification and Characterization of E2F7, a Novel Mammalian E2F Family Member Capable of Blocking Cellular Proliferation. *J. Biol. Chem.* **278**, 42041–42049 (2003).
302. Weijts, B. G. M. W. *et al.* E2F7 and E2F8 promote angiogenesis through transcriptional activation of VEGFA in cooperation with HIF1. *EMBO J.* **31**, 3871–3884 (2012).
303. Westendorp, B. *et al.* E2F7 represses a network of oscillating cell cycle genes to control S-phase progression. *Nucleic Acids Res.* **40**, 3511–3523 (2012).
304. Di Stefano, L., Jensen, M. R. & Helin, K. E2F7, a novel E2F featuring DP-independent repression of a subset of E2F-regulated genes. *EMBO J.* **22**, 6289–6298 (2003).
305. Li, J. *et al.* Synergistic Function of E2F7 and E2F8 Is Essential for Cell Survival and Embryonic Development. *Dev. Cell* **14**, 62–75 (2008).
306. Pandit, S. K. *et al.* E2F8 is essential for polyploidization in mammalian cells. *Nat. Cell Biol.* **14**, 1181–1191 (2012).
307. Chen, H.-Z. *et al.* Canonical and atypical E2Fs regulate the mammalian endocycle. *Nat. Cell Biol.* **14**, 1192–1202 (2012).
308. Bertoli, C., Skotheim, J. M. & de Bruin, R. a M. Control of cell cycle transcription during G1 and S phases. *Nat. Rev. Mol. Cell Biol.* **14**, 518–28 (2013).
309. Sørensen, C. S. *et al.* A Conserved Cyclin-Binding Domain Determines Functional Interplay between Anaphase-Promoting Complex – Cdh1 and Cyclin A-Cdk2 during Cell Cycle Progression A Conserved Cyclin-Binding Domain Determines Functional Interplay between Anaphase-Promoting Comple. *Mol. Cell. Biol.* (2001). doi:10.1128/MCB.21.11.3692

310. Sivaprasad, U., Machida, Y. J. & Dutta, A. APC/C--the master controller of origin licensing? *Cell Div.* **2**, 8 (2007).
311. Lafranchi, L. & Boer, H. de. APC/CCdh1 controls CtIP stability during the cell cycle and in response to DNA damage. *EMBO ...* **33**, 2860–2879 (2014).
312. Miller, C. W. *et al.* Alterations of the p53, Rb and MDM2 genes in osteosarcoma. *J. Cancer Res. Clin. Oncol.* **122**, 559–565 (1996).
313. Cohen, M. *et al.* Unbiased transcriptome signature of in vivo cell proliferation reveals pro- and antiproliferative gene networks. *Cell Cycle* **12**, 2992–3000 (2013).
314. Sakaue-Sawano, A. *et al.* Visualizing spatiotemporal dynamics of multicellular cell-cycle progression. *Cell* **132**, 487–98 (2008).
315. Peart, M. J. *et al.* APC/CCdc20 targets E2F1 for degradation in prometaphase. *Cell Cycle* **9**, 3956–3964 (2010).
316. Budhavarapu, V. N. *et al.* Regulation of E2F1 by APC/C Cdh1 via K11 linkage-specific ubiquitin chain formation. *Cell Cycle* **11**, 2030–8 (2012).
317. Kitamura, E., Blow, J. J. & Tanaka, T. U. Live-Cell Imaging Reveals Replication of Individual Replicons in Eukaryotic Replication Factories. *Cell* **125**, 1297–1308 (2006).
318. Nakayama, K. I. & Nakayama, K. Ubiquitin ligases: cell-cycle control and cancer. *Nat. Rev. Cancer* **6**, 369–381 (2006).
319. Botz, J. *et al.* Cell cycle regulation of the murine cyclin E gene depends on an E2F binding site in the promoter. *Mol. Cell. Biol.* **16**, 3401–3409 (1996).
320. Zalmas, L. P. *et al.* DNA-damage response control of E2F7 and E2F8. *EMBO Rep.* **9**, 252–9 (2008).
321. Carvajal, L. a, Hamard, P.-J., Tonnessen, C. & Manfredi, J. J. E2F7, a novel target, is up-regulated by p53 and mediates DNA damage-dependent transcriptional repression. *Genes Dev.* **26**, 1533–45 (2012).
322. Aksoy, O. *et al.* The atypical E2F family member E2F7 couples the p53 and RB pathways during cellular senescence. *Genes Dev.* **26**, 1546–57 (2012).
323. Ouseph, M. M. *et al.* Atypical E2F Repressors and Activators Coordinate Placental Development. *Dev. Cell* **22**, 849–862 (2012).
324. Ping, Z., Lim, R., Bashir, T., Pagano, M. & Guardavaccaro, D. APC/CCdh1 controls the proteasome-mediated degradation of E2F3 during cell cycle exit. *Cell Cycle* **11**, 1999–2005 (2012).
325. Christensen, J. *et al.* Characterization of E2F8, a novel E2F-like cell-cycle regulated repressor of E2F-activated transcription. *Nucleic Acids Res.* **33**, 5458–5470 (2005).
326. Lammens, T. *et al.* Atypical E2F activity restrains APC / C CCS52A2 function obligatory for endocycle onset. *PNAS* **105**, 1–6 (2008).
327. Narbonne-Reveau, K. *et al.* APC/CFzr/Cdh1 promotes cell cycle progression during the Drosophila endocycle. *Development* **135**, 1451–1461 (2008).
328. Vandesompele, J. *et al.* Accurate normalization of real-time quantitative RT-PCR data by geometric averaging of multiple internal control genes. *Genome Biol.* **3**, RESEARCH0034 (2002).
329. Holland, A. J., Fachinetti, D., Han, J. S. & Cleveland, D. W. Inducible, reversible system for the rapid and complete degradation of proteins in mammalian cells. *Proc. Natl. Acad. Sci. U. S. A.* **109**, E3350–7 (2012).

330. Ban, K. H. *et al.* The END network couples spindle pole assembly to inhibition of the anaphase-promoting complex/cyclosome in early mitosis. *Dev. Cell* **13**, 29–42 (2007).
331. Kimata, Y., Baxter, J. E., Fry, A. M. & Yamano, H. A role for the Fizzy/Cdc20 family of proteins in activation of the APC/C distinct from substrate recruitment. *Mol. Cell* **32**, 576–83 (2008).
332. Van Vugt, M. a T. M., Brás, A. & Medema, R. H. Polo-like kinase-1 controls recovery from a G2 DNA damage-induced arrest in mammalian cells. *Mol. Cell* **15**, 799–811 (2004).
333. Tischer, T., Hormanseder, E. & Mayer, T. U. The APC/C Inhibitor XErp1/Emi2 Is Essential for Xenopus Early Embryonic Divisions. *Science* **338**, 520–524 (2012).
334. Isoda, M. *et al.* Dynamic regulation of Emi2 by Emi2-bound Cdk1/Plk1/CK1 and PP2A-B56 in meiotic arrest of Xenopus eggs. *Dev. Cell* **21**, 506–19 (2011).
335. Hörmanseder, E., Tischer, T., Heubes, S., Stemmann, O. & Mayer, T. U. Non-proteolytic ubiquitylation counteracts the APC/C-inhibitory function of XErp1. *EMBO Rep.* **12**, 436–43 (2011).
336. Stevens, D., Gassmann, R., Oegema, K. & Desai, A. Uncoordinated loss of chromatid cohesion is a common outcome of extended metaphase arrest. *PLoS One* **6**, (2011).
337. Daum, J. R. *et al.* Cohesion fatigue induces chromatid separation in cells delayed at metaphase. *Curr. Biol.* **21**, 1018–1024 (2011).
338. Huang, H.-C., Shi, J., Orth, J. D. & Mitchison, T. J. Evidence that mitotic exit is a better cancer therapeutic target than spindle assembly. *Cancer Cell* **16**, 347–58 (2009).
339. Sorensen, C. S. *et al.* Nonperiodic activity of the human anaphase-promoting complex-Cdh1 ubiquitin ligase results in continuous DNA synthesis uncoupled from mitosis. *Mol. Cell. Biol.* **20**, 7613–7623 (2000).
340. Enquist-Newman, M., Sullivan, M. & Morgan, D. O. Modulation of the Mitotic Regulatory Network by APC-Dependent Destruction of the Cdh1 Inhibitor Acm1. *Mol. Cell* **30**, 437–446 (2008).
341. Martinez, J. S., Jeong, D.-E., Choi, E., Billings, B. M. & Hall, M. C. Acm1 is a negative regulator of the CDH1-dependent anaphase-promoting complex/cyclosome in budding yeast. *Mol. Cell. Biol.* **26**, 9162–9176 (2006).
342. Lee, H. *et al.* Mouse emi1 has an essential function in mitotic progression during early embryogenesis. *Mol. Cell. Biol.* **26**, 5373–5381 (2006).
343. Baker, D. J. *et al.* BubR1 insufficiency causes early onset of aging-associated phenotypes and infertility in mice. *Nat. Genet.* **36**, 744–749 (2004).
344. Hanks, S. *et al.* Constitutional aneuploidy and cancer predisposition caused by biallelic mutations in BUB1B. *Nat. Genet.* **36**, 1159–1161 (2004).
345. Matsuura, S. *et al.* Monoallelic BUB1B mutations and defective mitotic-spindle checkpoint in seven families with premature chromatid separation (PCS) syndrome. *Am. J. Med. Genet.* **140 A**, 358–367 (2006).
346. Suijkerbuijk, S. J. E. *et al.* Molecular causes for BUBR1 dysfunction in the human cancer predisposition syndrome mosaic variegated aneuploidy. *Cancer Res.* **70**, 4891–900 (2010).
347. Kops, G. J. P. L., Weaver, B. a & Cleveland, D. W. On the road to cancer: aneuploidy and the mitotic checkpoint. *Nat. Rev. Cancer* **5**, 773–785 (2005).
348. Holland, A. J. & Cleveland, D. W. Chromoanagenesis and cancer: mechanisms and consequences of localized, complex chromosomal rearrangements. *Nat. Med.* **18**, 1630–8 (2012).

349. Wang, Z., Liu, P., Inuzuka, H. & Wei, W. Roles of F-box proteins in cancer. *Nat. Rev. Cancer* **14**, 233–47 (2014).
350. Choi, E. *et al.* BubR1 acetylation at prometaphase is required for modulating APC/C activity and timing of mitosis. *EMBO J.* **28**, 2077–2089 (2009).
351. Lee, J., Kim, J. A., Barbier, V., Fotedar, A. & Fotedar, R. DNA Damage Triggers p21 WAF1-dependent Emi1 Down-Regulation That Maintains G2 Arrest. *Mol. Biol. Cell* **20**, 1891–1902 (2009).
352. Janssen, A., Kops, G. J. & Medema, R. H. Targeting the Mitotic Checkpoint to Kill Tumor Cells. *Horm. Cancer* **2**, 113–116 (2011).
353. Manchado, E., Guillamot, M. & Malumbres, M. Killing cells by targeting mitosis. *Cell Death Differ.* 369–377 (2012). doi:10.1038/cdd.2011.197
354. Konishi, Y., Stegmüller, J., Matsuda, T., Bonni, S. & Bonni, A. Cdh1-APC controls axonal growth and patterning in the mammalian brain. *Science* **303**, 1026–1030 (2004).
355. Van Roessel, P., Elliott, D. a., Robinson, I. M., Prokop, A. & Brand, A. H. Independent regulation of synaptic size and activity by the anaphase-promoting complex. *Cell* **119**, 707–718 (2004).
356. Wirth, K. G. *et al.* Loss of the anaphase-promoting complex in quiescent cells causes unscheduled hepatocyte proliferation. *Genes Dev.* **18**, 88–98 (2004).
357. Dumontet, C. & Jordan, M. A. Microtubule-binding agents: a dynamic field of cancer therapeutics. *Nat. Rev. Drug Discov.* **9**, 790–803 (2010).
358. Zasadil, L. M. *et al.* Cytotoxicity of paclitaxel in breast cancer is due to chromosome missegregation on multipolar spindles. *Sci. Transl. Med.* **6**, 229ra43 (2014).
359. Weaver, B. a. How Taxol/paclitaxel kills cancer cells. *Mol. Biol. Cell* **25**, 2677–2681 (2014).
360. Juul, N. *et al.* Assessment of an RNA interference screen-derived mitotic and ceramide pathway metagene as a predictor of response to neoadjuvant paclitaxel for primary triple-negative breast cancer: A retrospective analysis of five clinical trials. *Lancet Oncol.* **11**, 358–365 (2010).
361. McGrogan, B. T., Gilmartin, B., Carney, D. N. & McCann, A. Taxanes, microtubules and chemoresistant breast cancer. *Biochim. Biophys. Acta - Rev. Cancer* **1785**, 96–132 (2008).
362. Wertz, I. E. *et al.* Sensitivity to antitubulin chemotherapeutics is regulated by MCL1 and FBW7. *Nature* **471**, 110–114 (2011).
363. Njiaju, U. O. *et al.* Whole-genome studies identify solute carrier transporters in cellular susceptibility to paclitaxel. *Pharmacogenet. Genomics* **22**, 498–507 (2012).
364. Manchado, E. *et al.* Targeting mitotic exit leads to tumor regression in vivo: Modulation by Cdk1, Mastl, and the PP2A/B55 α , δ phosphatase. *Cancer Cell* **18**, 641–54 (2010).
365. Xie, Q. *et al.* CDC20 maintains tumor initiating cells. 1–14 (2015).
366. Wang, L. *et al.* Targeting Cdc20 as a novel cancer therapeutic strategy. *Pharmacology & therapeutics* (2015). doi:10.1016/j.pharmthera.2015.04.002
367. Rieder, C. L. & Medema, R. H. No Way Out for Tumor Cells. *Cancer Cell* **16**, 274–275 (2009).
368. Gascoigne, K. E. & Taylor, S. S. How do anti-mitotic drugs kill cancer cells? *J. Cell Sci.* **122**, 2579–2585 (2009).
369. Harley, M. E., Allan, L. a, Sanderson, H. S. & Clarke, P. R. Phosphorylation of Mcl-1 by CDK1-cyclin B1 initiates its Cdc20-dependent destruction during mitotic arrest. *EMBO J.* **29**, 2407–2420 (2010).

370. Allan, L. a. & Clarke, P. R. Phosphorylation of Caspase-9 by CDK1/Cyclin B1 Protects Mitotic Cells against Apoptosis. *Mol. Cell* **26**, 301–310 (2007).
371. Orth, J. D., Loewer, a., Lahav, G. & Mitchison, T. J. Prolonged mitotic arrest triggers partial activation of apoptosis, resulting in DNA damage and p53 induction. *Mol. Biol. Cell* **23**, 567–576 (2012).
372. Kurokawa, M. & Kornbluth, S. Stalling in mitosis and releasing the apoptotic brake. *EMBO J.* **29**, 2255–7 (2010).
373. Komlodi-Pasztor, E., Sackett, D., Wilkerson, J. & Fojo, T. Mitosis is not a key target of microtubule agents in patient tumors. *Nat. Rev. Clin. Oncol.* **8**, 244–250 (2011).
374. Komlodi-Pasztor, E., Sackett, D. L. & Fojo, T. Tales of How Great Drugs Were Brought Down by a Flawed Rationale--Response. *Clin. Cancer Res.* **19**, 1304–1304 (2013).
375. Mitchison, T. J. The proliferation rate paradox in antimitotic chemotherapy. *Mol. Biol. Cell* **23**, 1–6 (2012).
376. Bremm, A., Freund, S. M. V & Komander, D. Lys11-linked ubiquitin chains adopt compact conformations and are preferentially hydrolyzed by the deubiquitinase Cezanne. *Nat. Struct. Mol. Biol.* **17**, 939–947 (2010).
377. Song, L. & Rape, M. Substrate-specific regulation of ubiquitination by the anaphase-promoting complex. *Cell Cycle* **10**, 52–56 (2011).
378. Van Leuken, R. *et al.* Polo-like kinase-1 controls Aurora A destruction by activating APC/C-Cdh1. *PLoS One* **4**, (2009).
379. Akopyan, K. *et al.* Assessing kinetics from fixed cells reveals activation of the mitotic entry network at the S/G2 transition. *Mol. Cell* **53**, 843–853 (2014).
380. Di Fiore, B. & Pines, J. How cyclin A destruction escapes the spindle assembly checkpoint. *J. Cell Biol.* **190**, 501–9 (2010).
381. Fuller, B. G. *et al.* Midzone activation of aurora B in anaphase produces an intracellular phosphorylation gradient. *Nature* **453**, 1132–1136 (2008).
382. Gurden, M. D. J. *et al.* Cdc20 is required for the post-anaphase, KEN-dependent degradation of centromere protein F. *J. Cell Sci.* **123**, 321–30 (2010).
383. Penas, C. *et al.* Casein Kinase 1delta Is an APC/C(Cdh1) Substrate that Regulates Cerebellar Granule Cell Neurogenesis. *Cell Rep.* **11**, 249–260 (2015).
384. Michael, S., Travé, G., Ramu, C., Chica, C. & Gibson, T. J. Discovery of candidate KEN-box motifs using cell cycle keyword enrichment combined with native disorder prediction and motif conservation. *Bioinformatics* **24**, 453–7 (2008).
385. Liu, Z. *et al.* GPS-ARM: Computational analysis of the APC/C recognition motif by predicting D-boxes and KEN-boxes. *PLoS One* **7**, 1–9 (2012).
386. Eguren, M. *et al.* A synthetic lethal interaction between APC/C and topoisomerase poisons uncovered by proteomic screens. *Cell Rep.* **6**, 670–683 (2014).
387. Oakes, V. *et al.* Cyclin A/Cdk2 regulates Cdh1 and claspin during late S/G2 phase of the cell cycle. *Cell Cycle* **13**, 3302–3311 (2014).
388. Song, L. & Rape, M. Regulated degradation of spindle assembly factors by the anaphase-promoting complex. *Mol. Cell* **38**, 369–82 (2010).
389. Sullivan, M. & Morgan, D. O. A novel destruction sequence targets the meiotic regulator Spo13 for anaphase-promoting complex-dependent degradation in anaphase I. *J. Biol. Chem.* **282**, 19710–19715 (2007).

390. Castro, A., Vigneron, S., Bernis, C., Labbe, J.-C. & Lorca, T. Xkid is degraded in a D-box, KEN-box, and A-box-independent pathway. *Mol. Cell. Biol.* **23**, 4126–4138 (2003).
391. Min, M., Mayor, U. & Lindon, C. Ubiquitination site preferences in anaphase promoting complex/cyclosome (APC/C) substrates. *Open Biol.* **3**, 130097 (2013).
392. Davey, N. E. *et al.* SLiMPrints: Conservation-based discovery of functional motif fingerprints in intrinsically disordered protein regions. *Nucleic Acids Res.* **40**, 10628–10641 (2012).
393. Mailand, N. *et al.* Rapid destruction of human Cdc25A in response to DNA damage. *Science* **288**, 1425–1429 (2000).
394. Donzelli, M. *et al.* Dual mode of degradation of Cdc25 A phosphatase. *EMBO J.* **21**, 4875–4884 (2002).

NEDERLANDSE SAMENVATTING

Algemene introductie

Voor een geslaagde celdeling is het nodig dat cellen al hun interne materiaal precies verdubbelen en vervolgens exact verdelen om twee identieke en gezonde dochtercellen te vormen. Deze cel cyclus kan onderverdeeld worden in verschillende fasen. G1 fase is de fase waarin cellen met een enkele complete set van DNA zich voorbereiden om S fase in te gaan. Tijdens S fase (DNA Synthese fase) wordt al het DNA exact gedupliceerd, zodat cellen die deze fase voltooien en zich in de G2 fase bevinden, twee complete sets van het genoom in de celkern bezitten. De volgende cel cyclus fase is mitose, waarin cellen het verdubbelde erfelijk materiaal daadwerkelijk verdelen over de dochtercellen die tijdens dit proces gevormd worden. Dit begint met het condenseren van het DNA in hun typische 'x-vormige' chromosomen, gevolgd door het afbreken van de celkern. De chromosomen worden aan beide zijden in het midden gebonden aan de mitotische spoelfiguur, die nadat alle chromosomen correct verbonden zijn aan de trekdraden van de spoelfiguur, verantwoordelijk is voor het uit elkaar trekken van de chromosomen. Dit leidt er toe dat aan beide zijden van de cel zich weer een enkel compleet genoom bevindt. Vervolgens wordt er een ring gevormd in het midden van de cel die uiteindelijk de moedercel afsnoert en zo twee dochtercellen vormt. Met het ontstaan van een nieuwe celkern om het genetisch materiaal bevindt de dochtercel zich in G1 en kan de cyclus opnieuw beginnen.

Evolutie heeft ertoe geleid dat dit hele proces strak gereguleerd plaatsvindt en dat er verschillende controle punten zijn, zodat eventuele fouten gecorrigeerd kunnen worden. Deze fouten kunnen bijvoorbeeld DNA schade of DNA mutaties zijn. Verschillende van deze controle punten zijn gebaseerd op afbraak van eiwitten. Dat houdt in dat als alles in orde blijkt, bepaalde eiwitten afgebroken worden, wat noodzakelijk is om naar de volgende fase in de cel cyclus te gaan. Vrijwel alle eiwitten in de cel worden op een gereguleerde manier afgebroken doordat ze onder bepaalde condities gemarkeerd worden met een klein signaleiwit, genaamd ubiquitine. De eiwitten die ubiquitine plaatsen zijn 'enzymen', en de eiwitten die het ontvangen heten 'substraten'. Dit ubiquitine signaal leidt er uiteindelijk toe dat een substraat in kleine stukken geknipt wordt en dus niet meer werkzaam is in de cel. Het is natuurlijk belangrijk om te zorgen dat eiwitten alleen op het juiste tijdstip in de cel cyclus gemarkeerd worden met ubiquitine. Eiwitafbraak kan heel snel verlopen, in een kwestie van minuten kan een soort eiwit grotendeels verdwenen zijn, maar het weer aanmaken van die eiwitten kost meer tijd en energie. Deze eigenschappen maken eiwitafbraak geschikt proces voor regulatie van overgangen tussen verschillende cel cyclus fasen, die snel, en in één richting moet verlopen. Een belangrijk concept is dat als bepaalde eiwitten niet worden afgebroken, de volgende cel cyclus fase ook niet kan starten. Een groot eiwit complex dat een groot aantal

verschillende eiwitten, momenteel zijn dat er zo'n 80, voor afbraak markeert tijdens de cel cyclus, is de 'APC/C'.

De APC/C

De APC/C bestaat zelf uit 19 verschillende eiwitten, die als geheel verantwoordelijk zijn dat het complex als een enzym actief kan zijn. Behalve deze vereiste 19 eiwitten, kan het complex alleen activiteit vertonen als er ook een activator eiwit bindt, waarvan er in menselijke cellen 2, op elkaar lijkende, van zijn geïdentificeerd, te weten Cdc20 en Cdh1. Deze activator eiwitten binden de APC/C, maar gaan ook een interactie aan met het substraat, het af te breken eiwit. De APC/C met activator is in staat om bepaalde motieven in substraten herkennen. Om te zorgen dat de substraten van de APC/C op het juiste moment worden afgebroken kennen beide activator eiwitten ook een 'rem', zodat de APC/C niet altijd actief is. Voor Cdh1 is dit het eiwit 'Emi1', en voor Cdc20 is dit een complex van verschillende eiwitten dat tezamen bekend staat als het 'mitotic checkpoint complex' (MCC). Emi1 zorgt ervoor dat de APC/C in alle cel cyclus fasen behalve mitose geremd wordt, terwijl de MCC specifiek tijdens mitose de APC/C remt totdat alle lichten op groen staan. Interessant genoeg zijn er tenminste 2 substraten van de APC/C die toch worden afgebroken terwijl Cdc20 geremd wordt door het MCC. Deze 2 substraten zijn Nek2A en Cycline A.

In **hoofdstuk 2** beschrijven we hoe het APC/C substraat Nek2A wordt afgebroken, door APC/C gebonden aan Cdc20, dat in complex is met het MCC. We laten zien dat zelfs als er bijna geen werkzaam Cdc20 meer is, en andere APC/C substraten duidelijk niet worden afgebroken, Nek2A bijna onverminderd snel uit de cellen verdwijnt. Alleen door zowel Cdc20 weg te halen, en een kunstmatige remmer van de APC/C toe te voegen kunnen we laten zien dat Nek2A wel degelijk door de APC/C afgebroken wordt. We ontdekken dat Nek2A zelfs een beter substraat is dan cycline A, wat ook afgebroken wordt door de APC/C op het moment in de cel cyclus dat Cdc20 gebonden is gebonden is door de MCC. We laten zien dat dit komt doordat Nek2A al direct zelf aan de APC/C bindt voordat mitose begint, en anders dan andere substraten, ook geen activator nodig heeft om de APC/C te binden. Deze binding is afhankelijk van het uiteinde (het 'staartje' van het eiwit, een opvallend klein stukje, dat lijkt op een stuk dat de activatoren ook bezitten en gebruiken om aan de APC/C te binden. Behalve deze staart, bevat Nek2A ook een standaard motief voor herkenning door de APC/C, maar dit blijkt alleen een rol te spelen op het moment dat de staart niet functioneel is. Zonder staart en zonder herkennings motief wordt Nek2A helemaal niet meer afgebroken. Als we daarentegen de APC/C actiever maken bij aanvang van mitose door MCC te verstoren, vinden we dan Nek2A zelfs nog sneller door de APC/C afgebroken kan worden, waardoor het uitzonderlijk efficiënt substraat is.

We kijken in nog meer detail hoe Nek2A door de APC/C gebonden en herkend wordt in **hoofdstuk 3**. We vinden dat Nek2A niet alleen al via zijn staart bindt aan de APC/C voordat mitose begint, maar dat er op dat moment ook al afbraak van Nek2A plaatsvindt. Deze afbraak is wel een stuk langzamer dan op het moment dat cellen mitose in gaan. We kunnen aantonen dat als we de twee meest kritieke APC/C onderdelen weghalen, APC2 en APC11, verantwoordelijk voor het plaatsen van ubiquitine op substraten, we meer Nek2A in cellen meten. Als we de gehele eiwitafbraak verstoren ontdekken we dat Nek2A zich begint op te hopen in de celkern, waar het normaal gesproken niet voorkomt. Als laatste tonen we aan dat als we de APC/C iets actiever maken Nek2A verdwijnt voor cellen in mitose gaan.

Om cellen van G1 fase naar S-fase te laten gaan, moeten bepaalde genen door ‘aangezet’ worden door zogeheten transcriptie factoren. Dit gebeurt doordat transcriptiefactoren aan het DNA op bepaalde plekken binden en op die manier zorgen dat genen vertaald worden in eiwitten. Behalve transcriptie factoren die de celcyclus vooruit sturen, zijn er ook transcriptiefactoren die op exact dezelfde plek binden, maar juist zorgen dat genen uit blijven staan. Dit is ook het geval voor de familie van ‘E2F’ transcriptiefactoren. Hier blijkt dat 2 leden van deze familie, namelijk E2F7 en E2F8 cel cyclus remmen, terwijl leden E2F1,2 en 3 zorgen voor overgang van G1 naar S. In **hoofdstuk 4** laten we zien dat E2F7 en E2F8 aan het eind van mitose, dus aan vlak voor het begin van een nieuwe cel cyclus, door de APC/C en Cdh1 herkend en afgebroken worden. Als we deze afbraak verstoren in cellen waar meer E2F7 of E2F8 aanwezig kunnen deze cellen niet verder dan G1. Deze cellen blijven vast zitten in de cyclus en gaan uiteindelijk dood.

Om de activiteit van het APC/C enzym te beteugelen hebben we **hoofdstuk 5** gebruik gemaakt van een induceerbare remmer, gebaseerd op het eiwit Emi1. Normaal gesproken wordt dit eiwit afgebroken zodat het de APC/C niet meer kan remmen op het moment dat cellen in mitose gaan. Eerder onderzoek waarbij specifiek werd gekeken naar een vorm van Emi1 die niet afgebroken werd suggereerde dat Emi1 ook in dat geval de APC/C nog steeds niet kon remmen. Wij vinden daarentegen dat met dezelfde mutaties die zorgen dat Emi1 stabiel blijft, de APC/C zo sterk geremd wordt dat cellen in mitose blijven. We gebruiken vervolgens alleen het deel van Emi1 dat verantwoordelijk is voor APC/C remming, waarbij wederom de staart van het eiwit een belangrijke rol speelt, en hebben dit zodanig geprogrammeerd dat het alleen aanwezig als wij het middel doxycyline aan de cellen toevoegen. Deze constructie hebben we ‘Cyclostop’ genoemd. Cyclostop resulteert in cellen die in mitose worden tegengehouden om naar de G1 fase te gaan, onafhankelijk van het MCC, door directe APC/C inhibitie. Maar deze situatie blijft niet eeuwig bestaan. Het lijkt erop dat de cellen de krachten die de chromosomen over de dochter cellen probeert te verdelen uiteindelijk niet tegen kunnen houden. Dit concept is ook vanuit soortgelijke situaties bekend, waarbij cellen kunstmatig in

mitose gehouden worden met trekkrachten op het DNA, en staat bekend als ‘cohesion fatigue’. Doordat er aan de chromosomen getrokken wordt via de spoelfiguur, maar de APC/C niet de noodzakelijke eiwitten kan afbreken, ontstaat een situatie waarbij de chromosomen uiteindelijk niet normaal over de dochtercellen verdeeld worden. Het meest opvallende resultaat is echter dat ondanks dat we de APC/C efficiënt lijken te remmen, zowel cycline A als Nek2A nog steeds afgebroken worden.

In **hoofdstuk 6** stellen we dat de APC/C een erg gretig enzym is, dat erg efficiënt een groot aantal substraten afbreekt. Afhankelijk van welke activator gebonden is leidt dit of tot een halt in de cel cyclus, als Cdh1 gebonden is, of leidt dit eerder tot cel cyclus voortgang als Cdc20 gebonden is. We weten dat iedere vorm van kanker uiteindelijk ook gedreven wordt door celdeling, en er zijn ook verscheidene farmaceutische middelen gericht op het remmen van de mitotische cel cyclus fase. We beredeneren dat het remmen van de APC/C ook mogelijk een therapie zou kunnen zijn, mits wel specifiek Cdc20 en niet Cdh1 geremd wordt, aangezien dit waarschijnlijk veel ongewenste bijeffecten zou kunnen hebben. We vatten bovendien de voor- en nadelen van verschillende methoden in het lab samen om APC/C activiteit te meten. Vervolgens bediscussiëren we dat de motieven die door de APC/C in substraten herkend worden erg veel voorkomen in eiwitten, en dat het daardoor moeilijk te voorspellen is welke eiwitten nu ook daadwerkelijk door de APC/C afgebroken worden. Daarnaast is het zo dat de motieven die we nu kennen waarschijnlijk ook nog subtiel kunnen afwijken waardoor er potentieel nog meer substraten zijn dan we nu kennen. Hoewel er al veel substraten bekend zijn, zijn er waarschijnlijk specifieke omstandigheden, zoals DNA schade, of specifieke celtypen zoals neuronen, waarin bepaalde eiwitten APC/C substraat blijken te zijn. We kijken nog specifiek naar de eiwit staarten die zorgen dat eiwitten de APC/C binden. Aan de hand van vergelijkingen tussen eiwitten met een soortgelijke staart voorspellen voor een aantal eiwitten dat zij mogelijk ook op deze manier de APC/C binden.

ENGLISH SUMMARY

General introduction

To complete cell division successfully, cells need to duplicate all their internal material, both genetic and otherwise, and subsequently divide these to create two identical and healthy daughter cells. This is known as the cell cycle, and can be subdivided into different phases. During G1 phase cells prepare for S-phase. S-phase (DNA Synthesis phase) is characterized by duplicating all the genetic material, which means that when cells successfully perform this they have two entire copies of the genome in their cell nucleus, and they have successfully entered G2-phase. The next phase is mitosis, in which cells actually divide the duplicated genetic material over two daughter cells, which are formed during this phase. Mitosis starts by condensing the DNA into chromosomes known for their characteristic 'x-shape', after which the membrane surrounding the nucleus is broken down. The chromosomes are attached in the middle, to a structure known as the mitotic spindle, which originates at opposite poles in the cell. After attachment of all the chromosomes to the mitotic spindle, leaving the chromosomes biorientated, the spindle is responsible for separating the genetic material to either side of the cell. While the DNA is being separated, a ring forms in the middle of the cell, which will ensure that the mother cell is abscised, leading to the formation of two daughter cells, both with one entire copy of the genome. These daughter cells have safely arrived in G1, allowing for the start of yet a new cycle.

Evolution has led to tight control on these events, and has ensured several checkpoints are in place, to allow for repair or correction of mistakes. These mistakes can for instance be DNA damage or mutations. Several of these checkpoints are based on the degradation of proteins inside the cell. These means, that when all is well, certain proteins will be degraded, which is necessary to proceed to the next cell cycle phase. Almost all proteins are degraded in a regulated fashion, as they are marked for destruction under the right circumstances by a small signal protein called 'ubiquitin'. Ubiquitin is placed by proteins called 'enzymes' unto receiving proteins called 'substrates'. Proteins marked by ubiquitin will be cut up into small pieces, so that they are no longer functional. Obviously it is important to ensure that the right proteins are marked with ubiquitin at the right time during the cell cycle. Protein degradation can occur very fast, in a matter of minutes the pool of a certain protein can be largely gone, but resynthesizing the protein takes more time and energy. These properties make protein degradation very suited for regulating the transitions between cell cycle phases, which have to occur fast, and in a single direction. One important concept is that if certain proteins are not degraded, the next phase is also unable to start. A large protein complex inside the cell responsible for the marking many different proteins, currently about 80 have been identified, for destruction during the cell cycle, is the 'APC/C'.

The APC/C

The APC/C itself consists out of 19 different proteins, which as a whole are responsible for making an active complex. Besides these 19 subunits, the APC/C can only become active if a certain activator protein binds to it, of which in humans two similar proteins have been identified, known as Cdc20 and Cdh1. These activator proteins bind the APC/C, but they also interact with the substrate, the protein which is targeted for degradation by adding ubiquitin. The APC/C, combined with one of the activators is able to recognize certain motifs in the substrate. To ensure that proteins are degraded at the right time, certain ‘brakes’ are in place, to hold the APC/C in check. For the Cdh1 activator the brake is a protein called ‘Emi1’, while for Cdc20 it is a complex of multiple proteins known as the ‘mitotic checkpoint complex’ (MCC). Emi1 is responsible for stopping the APC/C in all cell cycles phases except mitosis, while the MCC plays this role exclusively in mitosis, until the cell is ready to move into G1. Interestingly, even when Cdc20 is held back by the MCC, the APC/C is still able to mark two substrates for destruction. These are the proteins Nek2A and cyclin A.

In **chapter 2** we describe how the APC/C substrate Nek2A is degraded, by APC/C bound by Cdc20, even when the MCC is present. We show that if we get rid of almost all Cdc20, and other substrates are no longer destroyed by the APC/C, Nek2A is destroyed almost as fast as in a normal situation. Only by both removing Cdc20, and adding an artificial APC/C inhibitor can we show that the APC/C is indeed responsible for degrading Nek2A. We also discover that Nek2A is a better substrate than cyclin A, which is also degraded when the APC/C is bound to Cdc20 and the MCC. We show that this is because Nek2A doesn’t need Cdc20, unlike other substrates, to bind to the APC/C, and also does this before mitosis starts. For Nek2A to bind to the APC/C it requires a very small part at one end of the protein. This ‘tail’ is a remarkably small piece, and is similar to the tails found in Cdc20 and Cdh1, which also use it to bind to the APC/C. Besides this tail Nek2A also uses a more common motif to be recognized by the APC/C, but this only plays a role if the tail is not functional. If Nek2A has neither the tail or the motif the APC/C does not recognize it, and it remains stable. If we make the APC/C more active at the start of mitosis, by disrupting the MCC, we find that Nek2A can be degraded even faster, showing it is an exceptionally efficient substrate.

We look even more detail of Nek2A recruitment to the APC/C and its recognition in **chapter 3**. We find that Nek2A not only already binds to the APC/C before mitosis, but is also already slowly degraded. This degradation is a lot slower than when cells enter mitosis. We find that if we get rid of the two most critical APC/C subunits, APC2 and APC11, responsible for actually placing the ubiquitin mark on the substrate, we measure higher levels of Nek2A in cells. If we disrupt protein degradation as a whole, we discover that Nek2A starts piling up in the nucleus, where it’s normally not present.

Finally we show that if we make the APC/C a bit more active, Nek2A is already lost before cells enter mitosis.

For cells to move from G1 phase to S-phase, certain genes have to be 'switched on' by so called transcription factors. They perform this by binding to the DNA and ensuring that certain genes are translated into proteins. Besides transcription factors driving the cell cycle forward, there are also transcription factors that bind at exactly the same location, but make sure the genes are not translated into proteins. This is also the case for the family of transcription factors known as the 'E2F' family. There are 2 members of the family, E2F7 and E2F8, which stop the cell cycle when they bind the DNA, while E2F1,2 and 3 are responsible for getting cells from G1 into S-phase. In **chapter 4** we show that E2F7 and 8 are degraded at the end of mitosis, so right before the start of a new cell cycle, by APC/C together with Cdh1. If we disrupt this degradation in cells with more E2F7 or 8 these cells are unable to get out of G1. These cells are stuck in the cycle, and eventually die.

To constrain the activity of the APC/C enzyme, we developed an inducible brake in **chapter 5**, based on the Emi1 protein. Normally this protein is not present when cells enter mitosis, so it is also not able to inhibit the APC/C at that time. Previous research also looked into a form of Emi1, which was still present in mitosis, but they could not detect APC/C inhibition. On the other hand, we find that with the same mutations that ensure that Emi1 is present during mitosis, that the APC/C is so strongly inhibited that cells are unable to exit mitosis. Subsequently we use only the part of Emi1 that is responsible for blocking the APC/C, which again also requires the tail of the protein, and program it in such a manner, that it only becomes active in cells if we add the compound doxycycline to our experiment. We have named this 'Cyclostop'. Cyclostop blocks cells in mitosis, which are unable to enter G1, not because of the MCC, but by directly inhibiting the APC/C. However, this situation doesn't last forever. It seems that cells are unable to also stop the pulling forces on the chromosomes, which would normally divide the DNA over the daughter cells. This phenomenon has been observed in different situation, in which cells are kept in mitosis, but the pulling forces on the chromosomes are still present, and is known as 'cohesion fatigue'. Because the pulling forces on the chromosomes are still present, but the APC/C is unable to degrade the necessary proteins, the DNA can not be normally divided over the daughter cells. The most striking result however, is that even though the APC/C seems to be blocked efficiently by Cyclostop, both cyclin A and Nek2A are still degraded.

In **chapter 6** we conclude that the APC/C is a very eager enzyme, efficiently degrading many proteins. Depending on the activator this leads to a halt in the cell cycle, if Cdh1 is bound, or this is more likely to progress cells forward through the cell cycle, which is the

case for Cdc20. We know that each form of cancer is finally driven through cell division, and as such several pharmaceutical drugs are focused on inhibiting the mitotic cell cycle phase. We argue that blocking the APC/C might also provide a window for treatment, as long as Cdc20 can be specifically inhibited without harming Cdh1 function, as this might lead to many undesirable side effects. We also summarize the different techniques for measuring APC/C activity with their drawbacks and virtues. We discuss that the different motifs in proteins recognized by the APC/C are so common among proteins, that it is hard to predict on a motif basis alone if a protein is an APC/C substrate. Also, it seems that small deviations of the motifs might also be allowed, which make it even more difficult to predict if a protein is an APC/C substrate by motifs alone. Even though many proteins have been identified as substrates, certain circumstances, such as DNA damage, or in certain cell types such as neurons, many other proteins could also prove to be substrates for the APC/C. We finalize by comparing several different tails of proteins which are known to interact with the APC/C, and make some predictions for proteins with a similar tail which might also interact with the APC/C in this manner.

DANKWOORD

Als de credits na afloop van een film komen zapt iedereen weg, maar hoe anders is dat bij een proefschrift. Fijn dat je aandacht overhebt na het lezen van al die hoofdstukken, en gelukkig maar, want de afgelopen 5 jaar heb ik dit proefschrift ook niet in m'n eentje voltooid, dus deel ik graag dank uit aan degenen die het verdiend hebben.

Ten eerste mijn leescommissie: Alain de Bruin, Susanne Lens, Marcel van Vugt, Marvin Tanenbaum en Hans Bos, hartelijk dank voor jullie inzet en tijd om mijn proefschrift te beoordelen.

René Bernards, bedankt dat je mijn promotor bent en met name bedankt voor de duwtjes in de rug op het juiste moment. Ik besef dat promotor zijn van een AiO uit een ander lab niet handig is als je zelf een sabbatical in Genentech volbrengt, dus ik ben je erg dankbaar dat je daar bereid toe was. Ik hoop dat je ambitie om kanker een chronische ziekte te maken snel waar te maken is, en ik weet zeker dat het niet aan jouw inzet zal liggen als het niet binnen 20 jaar lukt om remise te spelen.

Natuurlijk dank aan Robbie W. Met je creatieve kunstenaars geest en wetenschappelijke enthousiasme was je een bron van inspiratie door de jaren heen. Deadlines en keiharde afspraken zijn voor ons allebei niet ons sterkste punt, wat de rit hier en daar misschien wat lastiger maakte dan nodig. Dankjewel dat je me hebt aangenomen, en ondanks dat veel dingen anders zijn gelopen dan gepland, was het een leuke en hele leerzame tijd. Ook bedankt dat je met al je nieuwe verantwoordelijkheden ook nog op de valreep zoveel tijd in revisie van dit proefschrift heb gestoken. Ik hoop dat je nieuwe baan op de VU snel nog verder vlucht neemt!

Erik, mede AiO van het laatste uur. Één van de leukste dingen die ik het afgelopen jaar gedaan heb, is jouw promotie filmpje maken, waarin alle eigenschappen die ik in je bewonder ook naar voren kwamen; je discipline, je inzet, je nauwkeurigheid. Maar daarnaast weet ik dat je ook altijd de laatste op elk feestje bent. Ik vind het super tof dat jij naast me staat bij de verdediging en ook dat je inmiddels op Lange Lauwer woont, ik hoop dat je het er erg naar je zin krijgt!

Jeroen, Jerry, wat een heerlijke frisse wind bracht je mee uit New York naar B5. Jeugdige enthousiasme, ambitie, passie voor wetenschap en intelligentie. Gecombineerd met een dosis humor, bourgondisme en relativerings vermogen was dat voor mij absoluut de broodnodige eye opener en boost aan het eind van m'n promotie. Cool dat je naast me wilt staan, ik kijk vol verwachting uit naar jouw boekje in de toekomst!

I'm also very grateful to the other members of my PhD committee for supervising projects over the last years: Metello and Hein, thank you for your input and suggestions you have given me during the annual PhD meetings.

De Woltschnauzers: Linda, dank dat je me geïntroduceerd hebt bij het NKI. Gedreven in wetenschap en als partyanimal, met duidelijk passie voor wat je doet, en je 'geen blad voor de mond nemen' zou ik zeker wat van kunnen leren. Vet cool dat ik je in NYC weer meer ga zien! Wouter, eigenzinnig en relaxed, cool dat je een staartje van E2S/Emi1 hebt achter gelaten, anders was er ook vast geen "Cyclostop" geweest. Ik hoop dat jij en Maria elkaar lang gelukkig blijven maken. Bas, je hardcore proeven en hardcore muziek heb ik gemist sinds je vertrek. Janneke, dank voor je labzorgen, ik hoop het moederschap en je nieuwe baan nog steeds goed bevallen. Connie, even though you were pretty good at complaining, I think the 'translation in mitosis' project is really cool, so I hope you'll be able to get it online somewhere, and I'll definitely drink to it!

Als er iemand is die de stempel reddende engel van dit proefschrift verdient is het wel Bart Westendorp! Bart, enorm bedankt voor de ontzettend fijne, nuttige en ook gezellige samenwerking. Ik heb met veel plezier aan E2F7 en 8 gewerkt, en weet zeker dat we dit ergens mooi online kunnen krijgen.

Ik heb een aantal studenten mogen begeleiden, die hebben bijgedragen in de data in dit proefschrift: Eelco, dank je wel voor al je analyses, cool om te zien dat je met motieven door bent gegaan, ik heb er oprecht erg veel aan gehad, dat kan je aan de discussie wel zien! Aida, I hope you're doing well in Rotterdam, thanks for making sure I wasn't the only one who observed a mitotic arrest after transfecting ND-Emi1, I hope you're enjoying you PhD.

Met slechts een enkele verhuizing van B7 naar B5 verdubbelde meteen het aantal mensen dat je binnen het NKI leert kennen, ik zou iedereen op z'n tijd een interne verhuizing aanraden. Pablo, señor Perilla, hope you will continue to do well! I missed all the dirty comments when I switched tissue culture rooms. Arnoud, leuk je als buurman gehad te hebben, ik hoop dat je nieuwe burens je ook als sectie(xy) leader af en toe van koekjes voorzien. Elisabetta Leila, Veronika, Lisa it was very nice sharing the floor with you. Kees, Jeffrey, Marcel (master of FLIM), Maaïke, Kasia (microscopist extraordinair!), Elisa, Coert, ouwe krullenbol, I wish you all the best in the future! DaniEla Caliente, I miss having Dutch lunch, you should continue having them, hope we will Skype once in a while! Good luck with the wedding preparations!

Dan is er natuurlijk ook de hele roedel Medemaatjes die B5 onveilig maakt. De man zelf, René, ik vrees dat ik je input niet altijd ter harte nam, maar ben wel erg dankbaar

dat je naast directeur zijn ook ruimte vond om de werkbesprekingen bij te wonen en van feedback te voorzien. Wytse, vet dat we collega's op het NKI zijn geweest en nu weer gaan worden bij Sloan. Ik kijk uit naar bier drinken en je messcherpe grappen, en dat geviel van je, aan die witte pluk in je snor. Let the good times role! Aniek, inmiddels al 'long gone', maar ik denk nog vaak terug aan hoe je hier bezig was, en kan daar nog steeds inspiratie uit putten. Rita, you quickly became a bit of the lab mom, but that's because you're so very kind and sweet, except when it comes to women rights or soccer, but luckily I'm not concerned about either of those ;) And congratulations on getting the KWF, really awesome! Jonne, wat een aanwinst uit Utrecht, ik vond het super leuk om het lab en bier met je te delen, René boft ontzettend met jou in zijn groep. Miho, the amount of focus you have is only paralleled by the amount of surprise you display when disturbed. Sorry for teasing you so often, I didn't mean any of it (except about quitting smoking of course). Alba, crazy Catalonian, keep your head up and your hips moving! Indra, je eigenzinnigheid en intelligentie gaven je soms een diva status, maar dat kan ook gekomen zijn door je obsessie voor bruiloften en awkwardness, ik hoop dat het er in de toekomst toch nog van komt die macha frappuccino te eten! Anja, ik ben ontzettend blij dat je die KWF beurs hebt binnen gesleept! Ik hoop dat binnenkort iedereen met biochemische vraagstellingen naar je kikkers komt vragen, kicke hoe je dat voor elkaar gekregen hebt. Melinda, great you teamed up with Anja, wish I would have enjoyed more of your delicious cooking over the last few years. Mar, the future of B5 is yours for the taking! I'm sure you'll be publishing in no time. Femke en Lenno, ik hoop dat jullie artikel snel ergens moois geaccepteerd wordt! Alles wat Emi1 of de APC/C te maken heeft draag ik natuurlijk een warm hart (en hoge impact factor) toe ;)

De Rowlands: Benjamin dank je wel voor je input op E2F, en voor je lessen in cohesin en condensin, en gefelicteerd met de KWF beurs! Ahmed, all the best combining PhD life with fatherhood! Judith, ik vind het heel gezellig dat je ook op het NKI bent komen werken, ik kijk uit naar jouw promotie boekje, ik weet zeker dat dat helemaal goed komt. En samen met Jaap weet ik zeker dat wat je daarna ook gaat doen, het sowieso goed komt. En mochten jullie samen weer New York willen bezoeken hebben jullie weer een extra adresje ;)

B5 zou helemaal niet draaiende blijven zonder de inzet van onze liefvallige secretaresses Mariet en Marianne, ik hoop dat jullie nog lang en met veel plezier op B5 blijven werken. Maar B5 zou ook niet kunnen functioneren zonder de man met de gezelligste lach, Rob K. Dank voor alles wat je geregeld hebt voor mij als adoptie AiO, en voor je aanmoediging onderweg.

Special mention for the B5 Firemen, I thoroughly enjoyed our cycling, almost as much as our epic 'who is the man', it lists in some of the most hilarious memories of the last

years (decennia?!). Daniel, ik hoop dat je binnenkort ergens je mentor capaciteit snel ergens kan tentoon kan spreiden, ik heb er in ieder geval een hoop aan gehad. Dr. Dre, I know you pretend to be a grumpy German, but that the inner you just wants to 'shake it off', I'll have a hard (impossible?) time finding a replacement bench buddy, thanks for withstanding my rambling. Bram, ik hoop dat ik op een gegeven moment dezelfde ImageJ skills en macro skills heb, ik vind dat je inmiddels wel recht hebt op een Makro kaart namens de afdeling ;) Royminator, sorry dat ik je promotie mis, net als met fietsen ben je weer eens stukje sneller, maar is het wel altijd mooi om je te zien beuken. Veni, tijdens fietsen hing ik af en toe al met m'n tong uit m'n mond een beetje voorover te hangen, terwijl jij nog met rechte rug aan het koersen was, ik twijfel er niet aan dat jij binnenkort ook dat proefschrift afhebt! Stuur me er eentje op!

Even though it seems ages ago, I'm very glad I was able to start on B7, and getting to know the people there. Johan (zie je daar nog onvermoeibaar pipetteren), Floris (volste vertrouwen dat ze in R'dam blij met je zijn), Anirudh, was cool sharing paranimf duties, Guus (ook al bijna Dr!) Diede, Chong (excellent Dutch tv debut!), Klaas, Winny, Sid, Prasanth, Lorenza, Katrien, Marielle, Kathy, Sake (bedankt voor je USA tips) Lloedana&Valentina, the duo Ben&Pasi, Wouter, thanks for being (lab) buddies, sharing workdiscussion, reagents and beers. Patty, zelfs toen ik niet meer op B7 'woonde' kon ik nog altijd met allerlei dingen terecht die ik zelf niet wist te regelen, bedankt!

I had a lot of fun with the international PhD Conference committee, I'd say we go quite a wei back, Silvia, Roel, Gerjon, Caroline and last but certainly not least Henri. Thanks for the meetings, but even more thanks for the cool evenings! I have a lot of fond memories, and those I lost were due to overload. Silvia, special thanks to you for saving my life.

Then there is an entire collection of NKI riff raff I'm grateful for getting to know: Bert&Rogier (een van mijn favo NKI duo's), Kelly, Marit, Sander, Tao (I have high hopes that you become a crazy professor, I'm sure we'd all benefit), Rui, Gözde Ruud, Sjoerd, Gosia, Ilana (thanks for the encouragement!), Tada, Jens, and of course from the top floor: Lukas (cool we're sharing our defense date, are you also looking forward to it?!), Jackie S (ik heb nog steeds de hoop dat deze bijnaam aan gaat slaan), Joppe en natuurlijk Mumbles (Dude, vlieg een keer de oceaan over, lijkt me gezellig, vond het mooi dat we samen van Bos-bench naar NKI collega's "gegroeid" zijn). Thanks for all the beers, coffee, borrels and sharing failures as well as successes with me over time. Hope to continue seeing you on Pubmed/Facebook or even better, real life.

Lenny en Lauran, bedankt voor al jullie hulp! Ik heb altijd geprobeerd collega's duidelijk te maken hoeveel mazzel we hebben met jullie als ondersteuning!

Via Eef ben ik wel vaker getrakteerd op spontane gezellige avondjes waarin ik op jullie gezelligheid, Elke, Nynke, Tessa en Bianca kon rekenen. Fijn dat ik jullie zo cadeau kreeg, en al wonen we niet meer om de hoek, staat de deur nog altijd voor jullie open.

En sinds afstuderen zie ik jullie veel te weinig, Elena, Maui, Lisa en Bokkie, maar ik vind het wel echt tof dat we als we elkaar zien het dan altijd ook meteen weer gezellig is! Het duurt niet lang meer voor we allemaal niet meer in Utrecht wonen, maar zullen we wel reünies daar voortzetten?

Mannen van VV, fijn dat een biomedisch netwerk van semi-vrienden zo gemakkelijk te combineren is met gezelligheid, bier, weekendjes weg, Sinterkerst gedichten (mijn persoonlijke favoriet) en wat VVietsplezier. Hier was AiO lief en leed te delen gemakkelijk te delen, belachelijk te maken en te vergeten. Pro Viro! In het bijzonder Jorg, Niek, Frank de Tank, Tom, Dj Senergy, dank voor de slechte grappen en gezelligheid.

Dodo, ik heb het vaker gezegd, maar ik meen het als ik zeg dat ik niet bij zinnen was gebleven als ik niet op dinsdag om 18:30 op baan 3 alle frustratie er uit kon rammen, dus dank daarvoor, ook chill dat je me liet winnen als ik het nodig had ;) Jij succes en veel plezier met de dames onderhouden, als jullie weer aan stedentripjes beginnen hoor ik het wel! En bij sportcentrum Match moet ik natuurlijk ook Egbert en Rebecca bedanken, bedankt voor de gastvrijheid en het lekkere eten!

Heukie en Wietske, bedankt voor de oneindige stroom Herman-Finkers-waardige oneliners. Heukie, ik heb er heel veel respect voor van hoever je gekomen bent, en ik weet dan ook zeker dat je die nanobodies te pakken gaat krijgen, laat me weten als het lukt, dan drink ik erop! Los van werk, weet ik zeker dat jullie leuke en goede ouders gaan zijn!

Wat gaan jullie al lang mee, Bart, Erik, Jig, Gijs, Laurens en Koek. Ik weet niet of dat enige dagje gelletjes gieten, (of de nederlandse samenvatting in dit boekje) iets geholpen hebben met begrip voor biomedisch onderzoek, maar ik vind het top dat we elkaar na 18 jaar(+) nog altijd regelmatig zien. En ook als jullie er niks van begrepen hebben lijkt dat geen enkele belemmering om elkaar te begrijpen. Fijn dat ik af en toe de graai-bankiers, coöporate fatcats, ambtenaren en ons nationale treinstelsel zo dichtbij me heb om af te kraken ;) Ook mooi dat de aanhang tegenwoordig zo standvastig en geïntegreerd is! Ik hoop jullie aan de andere kant van de plas te zien, en kijk uit naar het voortzetten van jaarlijks kerstdiner als we weer terug zijn.

Peter, Wilma, Vera en Stefan, bedankt voor alle gastvrijheid en gezelligheid de afgelopen jaren, met verjaardagen en Kerst en wat al nog meer. Ik heb me altijd heel welkom

gevoeld in Giesbeek. Bedankt dat jullie Eef aan mij toevertrouwen voor een paar jaar in New York, misschien dat er toch nog wel een motor reisje langs de oostkust komt? Lijkt mij in ieder geval erg leuk!

Parentes, dank voor alles wat jullie me geleerd hebben, en voor alle ondersteuning. Ik heb heus wel door dat jullie me altijd flink verwend hebben, zowel met veel te veel lekker eten, als een te gekke plek om te wonen tijdens m'n studie en promotie. Zonde jullie had ik hier niet gestaan, maar zonder jullie steun was ik ook niet gekomen waar ik nu was. Flora, ouwe ass. Professor! Cool dat ik nu eindelijk ook dr. ben, ik vond je altijd al een goed voorbeeld, en dat ben je ook gebleven, tot in NY?! Broeder, dat jij de meest kick-ass Boekhout bent lijkt me wel duidelijk, ik vind het vet dat je zoveel passie hebt voor wat je doet, ook al kan ik niet altijd al je gedachten sprongen volgen, weet ik zeker dat het leger blij mag zijn met een kerel als jij in dienst, en ik met jou als broer.

Van wederhelft, verloofde, Dr. en zelfs vrouw, lieve Eef, inmiddels gaan we al heel wat jaren samen, en zonder jouw orde in mijn chaos weet ik vrijwel zeker dat dit boekje nu zou zijn geweest wat het nu geworden is. Het is zo fijn dat jij er voor me bent, of het nou is dat je alweer eten op tafel hebt getoverd, of dat je me aan het lachen maakt als ik er even klaar mee ben. Ik ben een enorme bofkont met jou, en heb ontzettend veel zin om samen het volgende avontuur aan te gaan, en weet zeker dat wat er ook gebeurt, jij er in ieder geval voor me zal zijn. Op naar New York!

CURRICULUM VITAE

Michiel was born on 24th of March in Leiden in 1985. He attended the 'Stedelijk Gymnasium' in Leiden, combining two science based profiles, and followed additional math courses. After high school he chose to study Biomedical Sciences in Utrecht in 2003, and became an active member of the study association, resulting in being chairman of the board from 2005-2006. After finishing his Bachelor he started the Master 'Cancer Genomics and Developmental Biology' in 2007, also at Utrecht University. He undertook a 9 months internship at the department of Physiological Chemistry in the lab of Hans Bos, under direct supervision of Martijn Gloerich, working on regulation of the protein Epac. He performed his second internship in Honolulu in the lab of Mark Martindale, characterizing expression of genes involved in neuronal development in the sea anemone *Nematostella Vectensis*, supervised by Heather Marlow. He obtained his Masters degree in 2010 and started his PhD the next month at the Netherlands Cancer Institute under supervision of Rob Wolthuis, and René Bernards. Here, he studied the cell cycle in human cells, more specifically the activity of the Anaphase Promoting Cyclosome/Complex, resulting in this thesis. He defends this work on September 14th 2015. Afterwards he will continue his scientific training as a post doc in the lab of Scott Keeney at Memorial Sloan Kettering in New York, studying meiosis in yeast.

LIST OF PUBLICATIONS

Boekhout M, Wolthuis R

Dynamic Instability of Nek2A in G2 Phase Requires APC/C^{Cdh1}

Under review

Bart Westendorp^{1,*}, Michiel Boekhout^{2*}, Annelotte P. Wondergem¹, Hendrika A Segeren¹, Elsbeth A. van Liere¹, Nesibu Awol Ababelgu¹, Imke Jansen¹, Rob Wolthuis^{2,3}, Alain de Bruin^{1,4,a}. (2015)

Feedback regulation between atypical E2Fs and APC/C^{Cdh1} controls the G1/S phase transition.

Under Review

Boekhout M, Wolthuis R(2015)

Nek2A destruction marks APC/C activation at the prophase-to-prometaphase transition by spindle-checkpoint restricted Cdc20.

Journal of Cell Science **128**:1639-53.

Clijsters L, van Zon W, Riet BT, Voets E, Boekhout M, Ogink J, Rumpf-Kienzl C, Wolthuis RM. (2014)

Inefficient degradation of cyclin B1 re-activates the spindle checkpoint right after chromatid disjunction.

Cell Cycle **13**:2370-8

Layden MJ, Boekhout M, Martindale MQ. (2012)

Nematostella vectensis achaete-scute homolog NvashA regulates embryonic ectodermal neurogenesis and represents an ancient component of the metazoan neural specification pathway.

Development **139**:1013-22

Marlow H, Roettinger E, Boekhout M, Martindale MQ. (2012)

Functional roles of Notch signaling in the cnidarian *Nematostella vectensis*.

Dev Biol 2012, **362**:295-308